PRELIMINARY DESIGN REVIEW

Volume I - Presentation and Design Description

ak Physics Experiment MAGNET SYSTEM

Magnet Preliminary Design and Manufacturing R&D

TOR PRELIMINARY DESIGN REVIEW
Presentation and Design Description

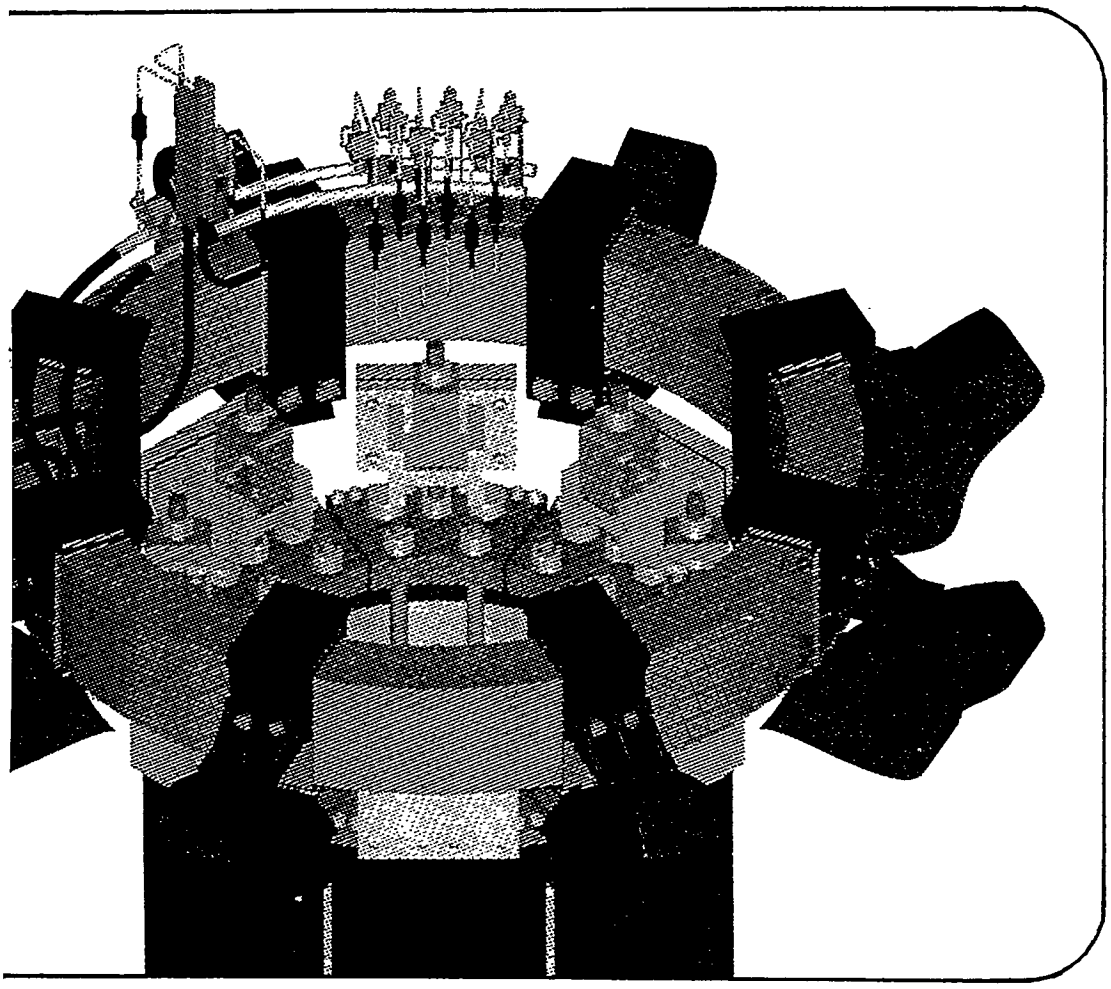

Tokamak Physics Experiment
TPX MAGNET SYSTEM
Poloidal Field Magnet Preliminary Design and Manufacturing R&D

Westinghouse
Northrop Grumman Corp.
Everson Electric Co.

DISTRIBUTION OF THIS DOCUMENT IS UNLIMITED

MASTER

ghouse ● Northrop Grumman Corp. ● Everson Electric Co.

UCRL-CR-121739

Tokamak Physics Experiment (TPX) Poloidal Field Magnet Final Report

LLNL Contact: Mark Jackson, Poloidal Field Technical Contract Manager

Westinghouse Electric Corporation : J. F. Roach, W. M. Urban, P. A. Sanger, D. R. Potter, R. J. Hillenbrand, G. Swartzback, H. A. Calvin, C. P. Molteni, M. P. Krefta, A. B. Corpuz, O. R. Christianson, T. Kupisewski, J. F. Lowry, C. G. Cesar, M. L. LaJeunesse, W. F. Hannan, P. G. McAuliffe, J. B. Hordabay, D. C. Johnson, R. K. Parman

Everson Electric
D. Hartman, G. Naumovich

Northrop Grumman Corporation
P. Walstrom, I. Clarkson, J. Schultheiss, A. Burger
Composite Technology Development, Inc.: J. B. Schultz, P. F. Fabian

September 22, 1995

Lawrence Livermore National Laboratory

This is an informal report intended primarily for internal or limited external distribution. The opinions and conclusions stated are those of the author and may or may not be those of the Laboratory.

Work performed under the auspices of the U.S. Department of Energy by the Lawrence Livermore National Laboratory under Contract W-7405-Eng-48.

Volume 1 - Presentation and Design Description

Table of Contents

CPDR Overview

- CPDR Agenda
- PF Magnet Team Overview

PF Magnet System

- PF Magnet System Requirements
- PF Magnet System Major Components
- PF Magnet System Interfaces
- Global Electromagnetics

Manufacturing R&D

- Helium Stub R&D Results
- Material Characteristics
  - 1 x 2 Results
  - 3 x 3 Results - Mechanical
  - 3 x 3 Results - Electrical
  - 5 x 5 Large Scale Verification

Westinghouse R&D

- Westinghouse Internally Funded Dummy Coil Program Lessons Learned

Central Solenoid

- Solenoid Overview
- EM and Preload
- Winding Configuration
- Electrical Insulation
- Coil Pack Structural Analysis
- EM Analysis of Joggles and Leads
- Transient Analysis of PF 2 & 5
- Preload Structure Design and CS Assy
- CS to TF Interface

Volume 1 - Presentation and Design Description

Table of Contents (continued)

PF 5 Ring Coil

Overview
Electromagnetics
Coil Pack Design
Assembly Design
Coil Pack Structural Analysis
PF 5 to TF Interface Design

PF 6/7 Ring Coil

Overview
Electromagnetics
Winding Configuration
Electrical Insulation Design
Coil Pack Structural Analysis
Case Design
PF 6/7 to TF Interface Design
PF 6/7 Thermal Analysis

Quality Assurance

B-Specification Verification
FMECA, Reliability Allocations
Material and Process Selection
Integrated Test Plan

Manufacturing

Manufacturing Plan
CS/PF 5
PF 6/7
TF Study

System Design Description, SDRL #15

Poloidal Field System, System Design Description, TPX-SDD-14

Volume 2 - PF Systems Engineering

Table of Contents

2.2.1.1 PF System Specification SDRL #17

TPX PF Magnet System Specification, TPX-SPEC-14-0001

2.2.2.1 Interface Control Documents SDRL #18

PF Magnet System to Tokamak Assembly Interface Document, TPX ICDP-1417

PF Magnet System to Single Point Ground Primary Interface Control Document, TPX-ICDP-1447

PF Magnet System to Cryogenic Equipment Primary Interface Control Document, TPX-ICDP-1472

PF Magnet System to Local I & C Secondary Interface Control Document, TPX-ICDS-1430-1450-01

PF Magnet System to Bus and Leads Secondary Interface Control Document, TPX-ICDS-1430-1460-01

PF Mounting Configuration Baseline on TPX-ICDP-1314-0001, 14-950814-WEC-MLaJeunesse-01

2.2.4 Configuration Item Specifications SDRL #20

TPX Central Solenoid Assembly Specification, TPX-SPEC-14-0002

PF 5 Magnet Specification, TPX-SPEC-14-0003

PF 6 & 7 Magnets Specification, TPX-SPEC-14-0004

TPX Winding System Specification, TPX-SPEC-14-0005

TPX Reaction System Specification, TPX-SPEC-14-0006

TPX Insulation and Impregnation System Specification, TPX-SPEC-14-007

Volume 2 - PF Systems Engineering

Table of Contents (continued)

2.2.5 Materials & Processes Selection, SDRL #21

TPX Poloidal Field Magnet System Materials and Processes Selection, TPX-14-950811-WEC-HCalvin-01

Development of Three-Dimensional Woven fiberglass Components for The TPX PF and TF Magnet Electrical Insulation Systems, TPX 14-950808-WEC-JLowry-01

2.2.6 FMECA, SDRL #23

TPX PF Magnet System Failure Modes, Effects, and Criticality Analysis, TPX-14-950705-WEC-HCalvin-01

2.3.12 Integrated Test Plan, SDRL #33, 45

PF Field Magnet System Integrated Test Plan, TPX-PLAN-14-001, 14-950810-WEC-DPotter-01

Volume 3 - Design And Analysis

Table of Contents

2.3.2 Electromagnetic Analysis, SDRL #29

Electromagnetic Analysis of TPX Poloidal Field Coils, TPX 14-950630-WEC-MKrefta-01

2.3.3.1 PF 1-5 Winding Pack Design, SDRL #30

TPX PF Winding Pack Insulation Design, TPX-14-950814-WEC-FRoach-01

PF Coil Dimensional Results Due to Thermal Contraction and Manufacturing Tolerances, 14-950807-WEC-MLaJeunesse-01

PF Magnet System Drawings, TPX-D-1431099

2.3.3.2 PF 6/7 Winding Pack Design, SDRL #30

TPX PF 6/7 Ring Coil Design, TPX 14-950817-WEC-PWalstrom-02

PF6 and PF7 Drawings , TPX-E-1431001

2.3.4 Structural Design & Analysis, SDRL #29

TPX Poloidal Field Magnets Central Solenoid Preload and Worst Coil Loads, TPX 14-950717-WEC-A Corpuz-01

TPX Central Solenoid Assembly Structural Analysis, TPX 14-950811-WEC-A Corpuz-02

TPX PF 1-4 Coil Pack Structural Analysis, TPX 14-950801-WEC-WHannon-01

Volume 3 - Design And Analysis

Table of Contents (continued)

2.3.4 Structural Design & Analysis, SDRL #29 (continued)

Structural Analysis of TPX PF 5 Coil Pack, TPX 14-950818-WEC-MKrefta-03

TPX PF 6 & 7 Coil Pack and Case Structural Analysis Report, TPX 14-950810-WEC-TSchultheiss-03

2.3.5 Thermal Design & Analysis, SDRL #29

Verification of Margin in PF 2 & 5 - Thermal Analysis of TPX Poloidal Field Coils, TPX 14-950731-WEC-OChristianson-02

Eddy-Current and Nuclear Heating in TPX PF 6 and 7 Ring Coils Cases, TPX 14-950815-WEC-PWalstrom-01

Nuclear Heat Rate Assumptions for Analysis of PF Coils, TPX 14-950403-WEC-DPotter-01

Feasibility of Cooling the Superconducting Outer Ring Coils Thermal Analysis of TPX Poloidal Field Coils, TPX-14-950721-WEC-TKupiszewski-01

2.3.6 Instrumentation & Control, SDRL #31

TPX Pulsed Coil System Instrumentation, TPX 14-950810-WEC-PWalstrom-01

Volume 4 - PF Manufacturing

Table of Contents

2.3.14 Integrated Magnet Plan, SDRL #36

PF Phase II Schedule
Tier 1 Fabrication Flowcharts

2.3.8 Coil Winding System, SDRL #22

Manufacturing Process Outline for Winding System for the TPX
Winding System Drawings

2.3.9 Coil Reaction System, SDRL #22

Process Plans for the PF Magnet Reaction

2.3.10 Coil Insulation & Impregnation, SDRL #22

Manufacturing Process Outline for Insulation System for the TPX
Insulation and Impregnation Drawings

2.3.11 Coil Assembly, SDRL #32

CS Coil Assembly Concept

2.2.8 Long Lead Materials, SDRL #25

Tokamak Physics Experiment Long Lead Material and Equipment

Volume 5 - Manufacturing R&D

Table of Contents

2.3.16.1 Insulation R&D, SDRL #12, 37

Material Characterization

Final Report on Shear Strength Under Compressive Load and Through Thickness Tension of TPX Insulating Materials, 14-950718-WEC-PSanger-01

1 x 2 Testing

TPX Insulation & Impregnation R&D - 1x2 Test Report, TPX 14-950630-WEC-FRoach-01

3x3 Testing

TPX Insulation & Impregnation R&D - 3 x 3 Test Report, Electrical Insulation, TPX 14-950630-WEC-FRoach-02

TPX 3x3 Insulation Mechanical Test Program, TPX 14-940719-WEC-JHillenbrand-02

5x5 Testing

TPX Magnet Insulation Large Scale Verification Test Program - TPX 14-950818-WEC-PSanger-01

2.3.16.2 Helium Stubs R&D, SDRL #12, 37

TPX Magnet Helium Stub Manufacturing R&D, TPX 14-950818-WEC-JHillenbrand-02

Topics

I. Introduction
II. PF Magnet Team Overview
III. PF Magnet System
IV. Manufacturing R&D
V. Westinghouse R&D
VI. Central Solenoid
VII. PF 5 Ring Coil
VIII. PF 6/7 Ring Coils
IX. Quality Assurance
X. Manufacturing

Agenda

Thursday Morning

I. Introduction (Deis, 10) 8:00

- A. Objective
- B. Agenda

II. PF Magnet Team Overview (Parman, 15) 8:15

- A. Preliminary Design team structure/roles
- B. Final Design team structure/roles
- C. Production team structure/roles

III. PF Magnet System (Elapsed: 50) 8:35

- A. System Overview (Calvin, 20)
  1. PF System Key Requirements
  2. PF System Major Components and General Arrangement
  3. Specification and Engineering Drawing Tree
  4. System Interfaces
- B. Global Electromagnetics (Krefta, 20)
- C. Chief Design and Fabrication Challenges (Potter, 10)

IV. Manufacturing R&D (Elapsed: 120) 9:45 (Break @ 9:30)

- A. Helium Stub Results (Hillenbrand, 30)
- B. Magnet Insulation Program (Sanger, 90)
  1. Overview (roadmap)
  2. Shear Compression Results
  3. Through Thickness Tension Results
  4. 1x2 Results
  5. 3x3 Results - Mechanical
  6. 3x3 Results - Electrical
  7. 5x5 Program

Agenda

Thursday Afternoon

V. Westinghouse R&D (Potter, 20) 1:00 (Lunch 12-1)

VI. Central Solenoid (Elapsed: 180) 1:25

A. Solenoid Overview (Corpuz, 10)
B. Electromagnetics and Preload (Corpuz, 20)
C. Coil Pack Design (Elapsed: 80)
   1. Winding configuration (Corpuz, 20)
   2. Electrical Insulation Design (Roach, 30)
   3. Coil Pack Structural Analysis (Sanger, 30)
D. EM Analysis of Joggles & Leads (Krefta, 20)
E. Verification of MIT Transient Thermal Analysis (Sanger, 15)
F. Assy and Preload Structure Design (Corpuz, 20)
G. CS to TF Interface Design (Corpuz, 15)

VII. PF 5 Ring Coil (Elapsed: 90) 3:30

A. Overview (Corpuz, 10)
B. Electromagnetics (Corpuz, 10)
C. Coil Pack Design (Corpuz, 5)
D. EM Analysis of Joggles & Leads (Corpuz, 0)
E. Thermal Analysis (Corpuz, 0)
F. Assy Design (Corpuz, 20)
G. Coil Pack Structural Analysis (Krefta, 25)
H. CS to TF Interface Design (Corpuz, 20)

Agenda

Friday Morning

VIII. PF 6/7 Ring Coils (Elapsed: 110) 8:00

- A. Overview (Walstrom, 10)
- B. Electromagnetics (Walstrom, 10)
- C. Coil Pack Design (Walstrom, 30)
  1. Winding configuration
  2. Electrical Insulation Design
  3. Coil Pack Structural Analysis
- D. Case Design (Walstrom, 20)
- E. PF 6/7 to TF Interface Design (Walstrom, 20)
- F. Thermal Analysis (Sanger, 20)

IX. Quality Assurance (Calvin, 30) 10:00

- A. B-Specification Verification Matrix
- B. FMECA, Reliability Allocations
- C. Materials and Process Selection
- D. Integrated Test Plan

X. Manufacturing (Elapsed: 150) 10:40

- A. Manufacturing Plans (McAuliffe, 30)
  1. Tier 1 Process Flow Charts
  2. Production Schedule
  3. Long-lead material assessment
- B. CS/PF 5 Tooling (Hartman, 60)
  1. CS/PF5 Tier 2 Process Flow Charts
  2. General Arrangement
  3. Major Components
  4. Everson Electric Facility

Agenda

Friday Afternoon

X. Manufacturing (continued) 1:15 (Lunch 12:15 - 1:15)

A. Integrated PF6/7 Fabrication Station (Burger, 30)
   1. PF 6/7 Tier 2 Process Flow Charts
   2. General Arrangement
   3. Major Components
   4. Northrup Grumman Facility

B. Toroidal Field Fabrication Study (McAuliffe, 30)
   1. TF Tier 2 Process Flow Charts
   2. General Arrangement
   3. Major Components
   4. Westinghouse Facility

XI. Committee Session (start at 2:15)

Section II

PF Magnet Team Overview

Russ Parman

The PF Magnet System Team

Westinghouse Electric Corporation

❑ Marine Division

- Overall Project Management
- Systems Engineering
  - Specifications
  - Interface Definition
  - FMECA
- Test Plans
- Integration of Tooling Designs & Manufacturing Plans
- Central Solenoid & PF5 Assembly Design & Drawing Preparation

❑ Science & Technology Center

- Coil Insulation/Impregnation R&D
- Helium Stub R&D
- PF System Analyses
  - Electromagnetic
  - Thermal
- CS and PF5 (Nb3Sn) Winding Pack Structural Analysis and Electrical Design/Analysis
- Systems Engineering Support

❑ Northrop-Grumman Aerospace

- PF6 & PF7 (NbTi) Coil Design & Analysis
- PF6/7 Drawing Preparation
- PF6 & PF7 Tooling Designs & Manufacturing Plans
- Systems Engineering Support

❑ Everson Electric Company

- Fabrication of Insulation R&D Samples
- CS and PF5 (Nb3Sn) Tooling Designs & Manufacturing Plans
- Systems Engineering Support

Final Design Team Structure / Roles

DRAFT

Magnet System Team

Westinghouse Electric Corporation

Marine Division

- Overall Project Management
- Systems Engineering
- Test Plans
- Manufacturing Development Tasks
- Central Solenoid & PF5 Assembly Design & Drawing Preparation
- TF Magnet System Design & Analysis
- Tooling Designs & Manufacturing Plans for TF Magnets

Science & Technology Center

- Manufacturing Development Tasks
- PF System Analyses
  - Electromagnetic
  - Thermal
- Electrical Design/Analysis of All Coils
- PF1-5 Winding Pack Structural Analysis
- Central Solenoid Structural Analysis
- Systems Engineering Support

Northrop-Grumman Aerospace

- PF6 & PF7 (NbTi) Coil Design/Analysis & Drawing Preparation
- PF6 & PF7 Tooling Designs & Manufacturing Plans
- Systems Engineering Support

Everson Electric Company

- CS Assembly & PF5 Coils Tooling Designs & Manufacturing Plans
- Systems Engineering Support

Fabrication Phase Team Structure / Roles

DRAFT

Magnet System Team

Westinghouse Electric Corporation

Marine Division

- Overall Project Management
- Systems Engineering
- Tooling Set-up & Check-out for TF
- TF Prototype Coil Fabrication & Testing Support
- Fabricate TF Magnet System
- Provide Technical Support to Central Solenoid & PF5 Fabrication Program

Science & Technology Center

- TF & PF Tooling Check-out Technical Support
- TF & PF Prototype Coil Testing Support
- Provide Overall Technical Support to TF & PF Fabrication Program

Northrop-Grumman Aerospace

- Tooling Set-up & Check-out for PF6 & PF7
- Fabricate PF6 & 7 Coils

Everson Electric Company

- Tooling Set-up & Check-out for PF1-4 & PF5 Coils
- PF Prototype Coil Fabrication
- Fabricate the Central Solenoid Coils & Assembly and PF5 Coils

System Overview

- Key Requirements
  - Ref. PF Magnet System Specification, TPX-SPEC-14-0001, Rev. 0
- Major Components
  - Ref. PF Magnet System Specification, TPX-SPEC-14-0001, Rev. 0
- Spec and Dwg Trees
  - Ref. TPX-D-1431099.SH001.P00 Draft
- System Interfaces
  - Ref. PF Magnet System Specification, TPX-SPEC-14-0001, Rev. 0

Essential Functions

- The Poloidal Field (PF) Magnet System provides the following essential functions:
  - Poloidal fields and flux changes necessary for plasma shaping and positioning, and discharge evolution.
  - Compensation for radial and vertical fields from the turn interconnecting the 16 TF Magnet System coils.

Functional Flow Block Diagram

tpx180b.sgw

FFBD flow follows the arrows. "And" gates ahead of parallel blocks ndicate all blocks in parallel must be completed before moving on. "Or" gates indicate a choice of paths. Each block must be completed before moving on. Small circles with nothing inside are connectors. Arrows of different size are for clarity only - no other significance.

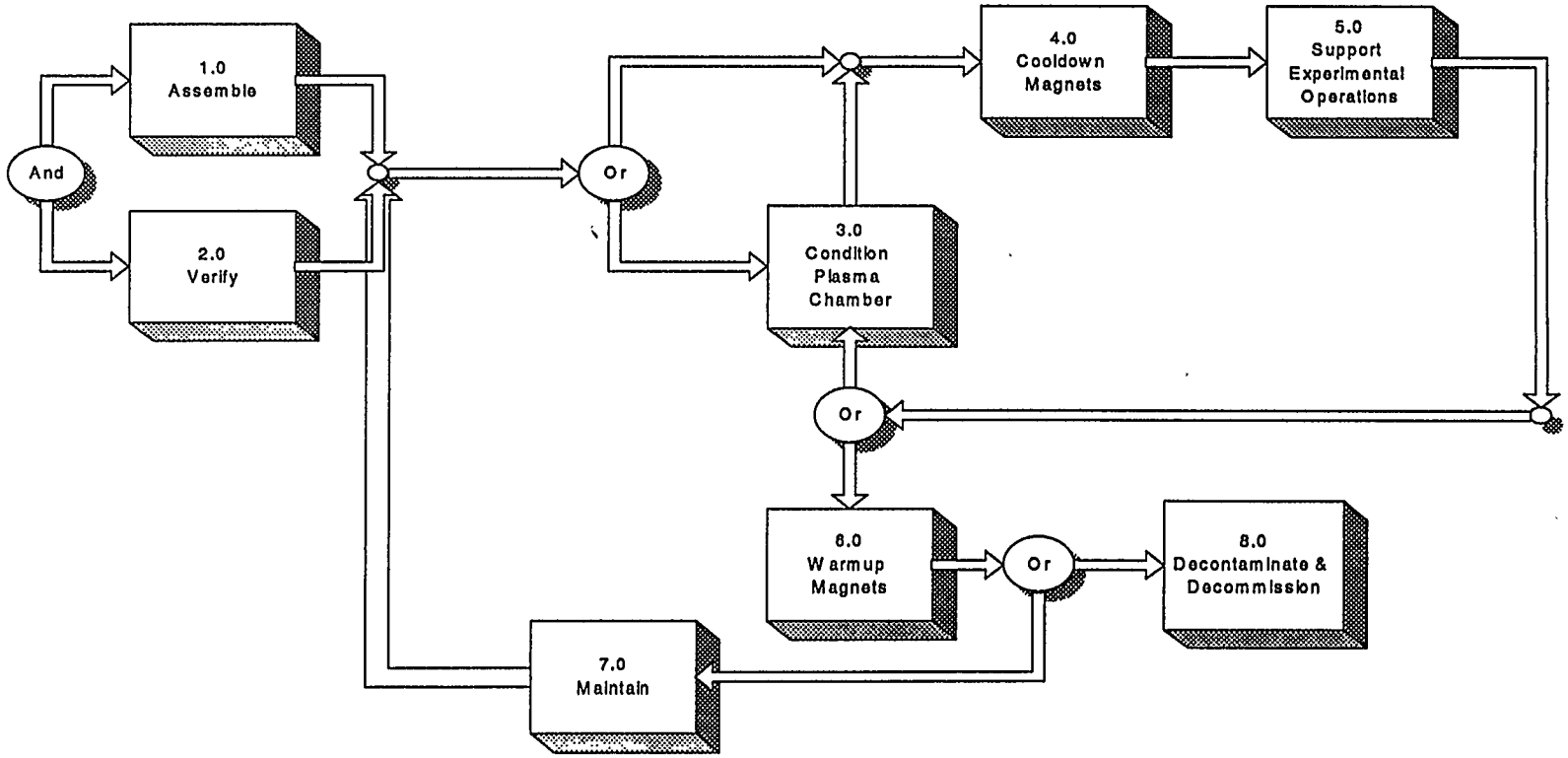

Functional Flow Block Diagram

FFBD flow follows the arrows. "And" gates ahead of parallel blocks ndicate all blocks in parallel must be completed before moving on. "Or" gates indicate a choice of paths. Each block must be completed before moving on. Small circles with nothing inside are connectors. Arrows of different size are for clarity only - no other significance.

tpx180b.sgw

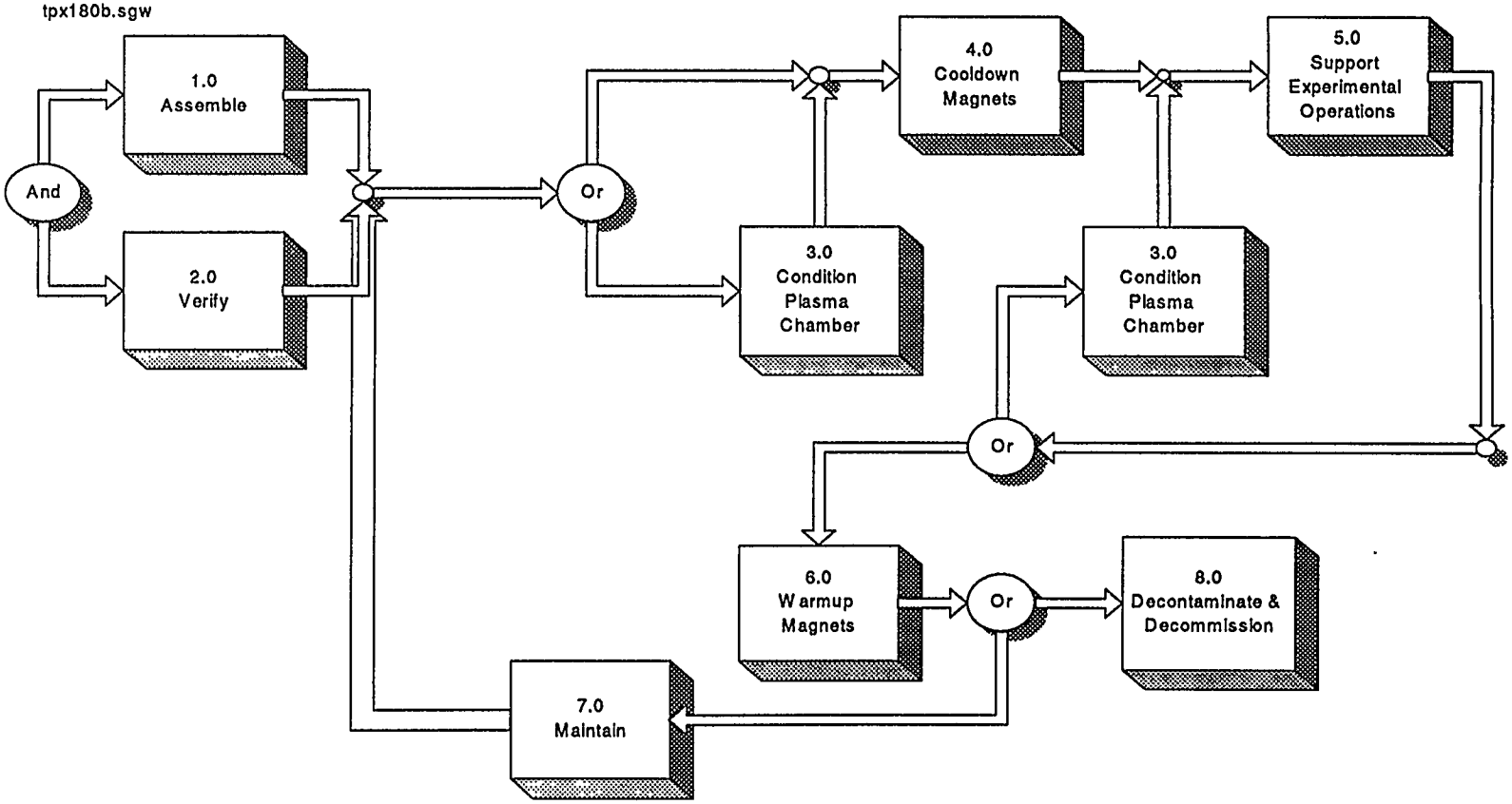

Major Components

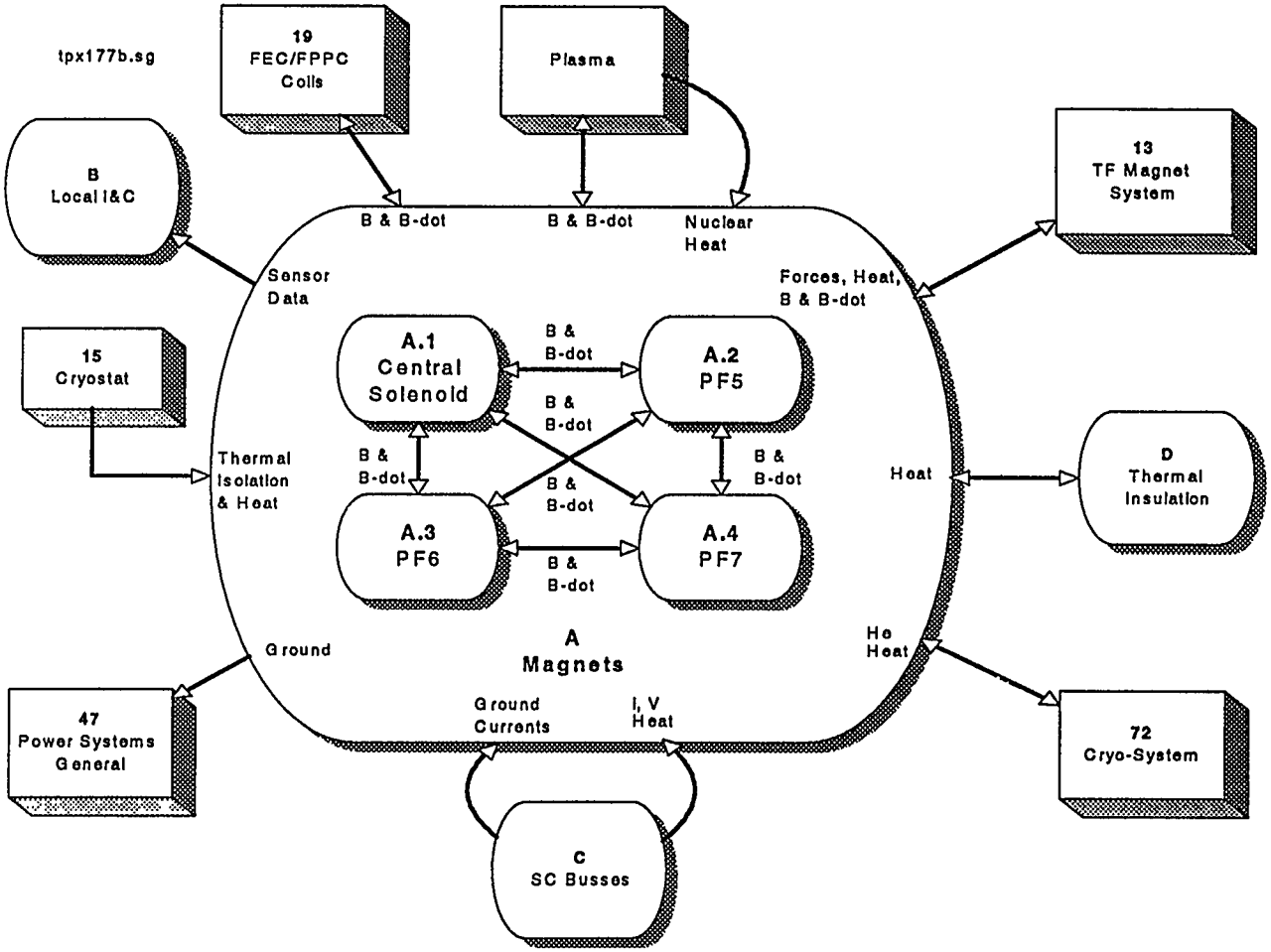

PF Magnet System & Environment

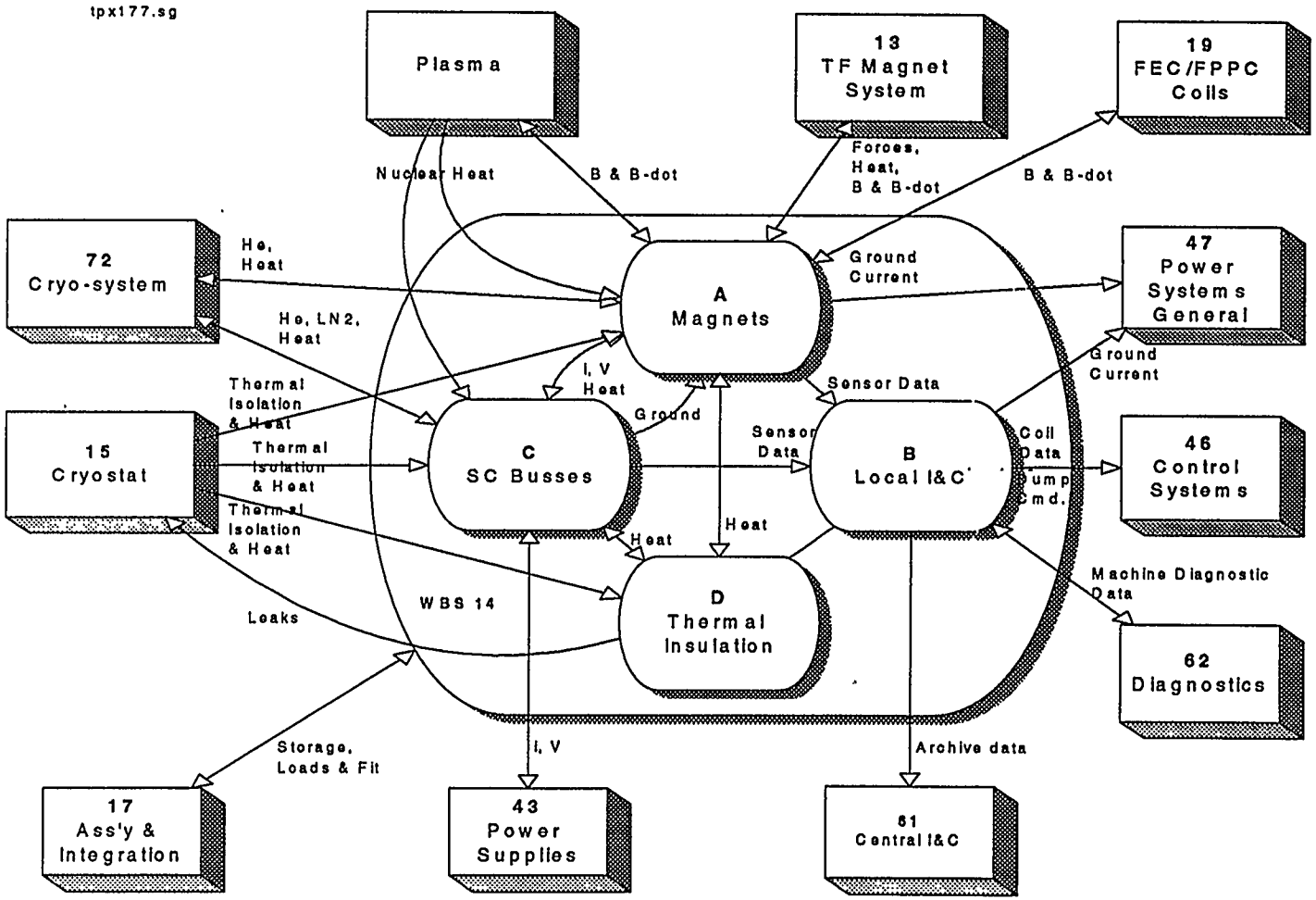

Specification Tree

tpx191b.s

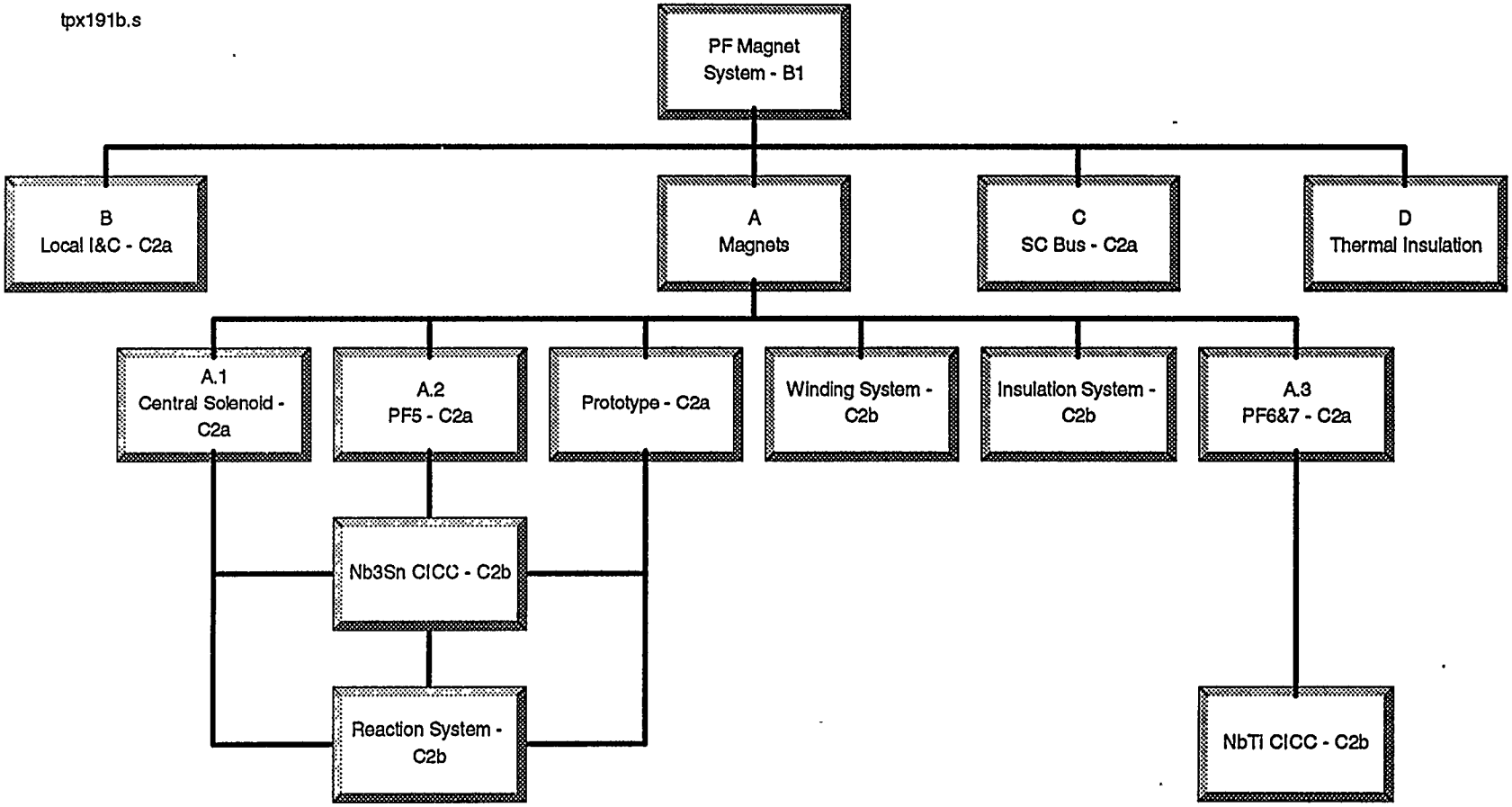

Drawing Tree (1)

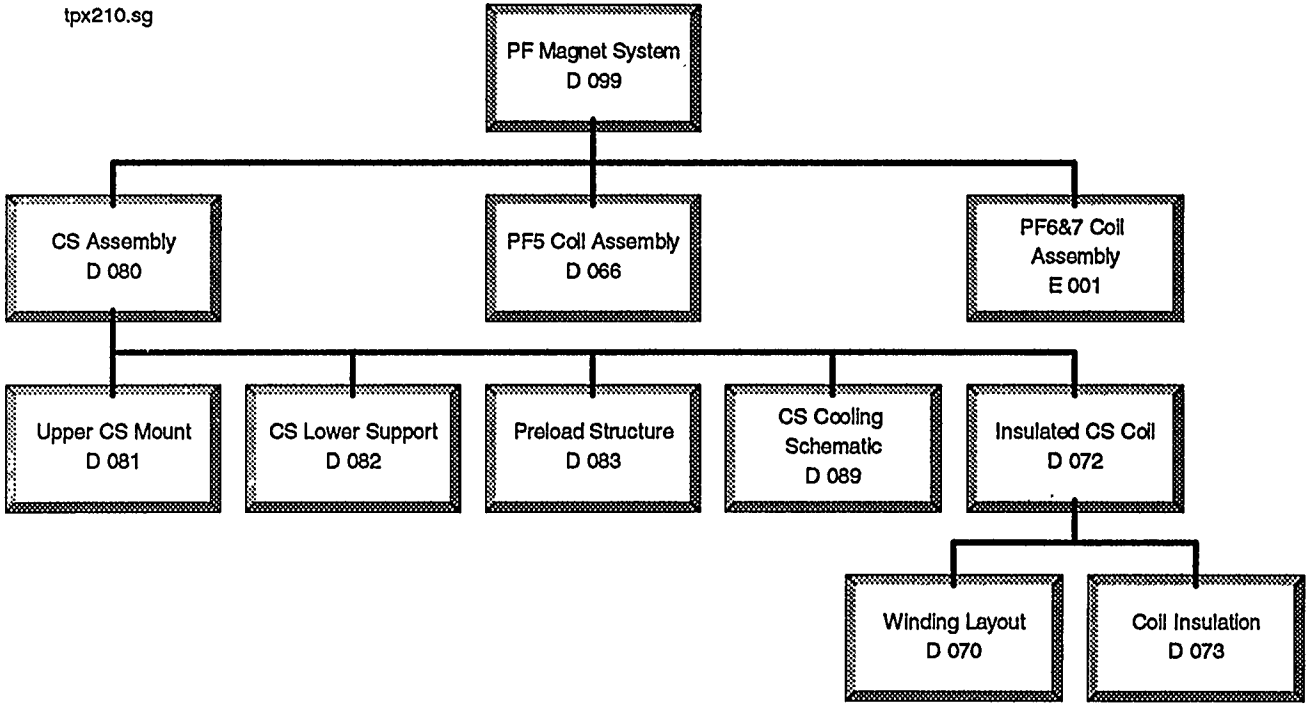

Drawing Tree (2)

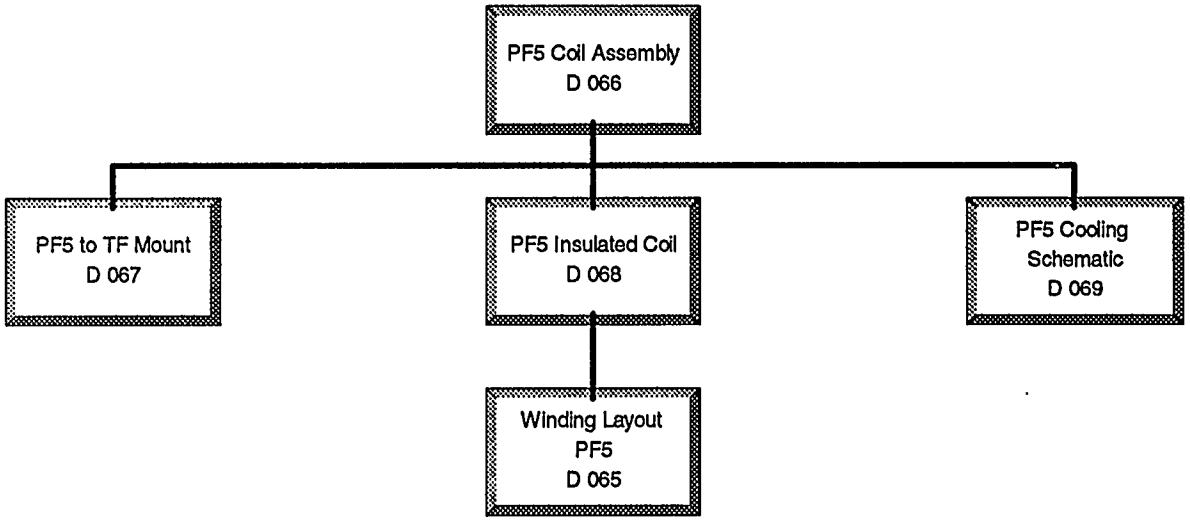

Drawing Tree (3)

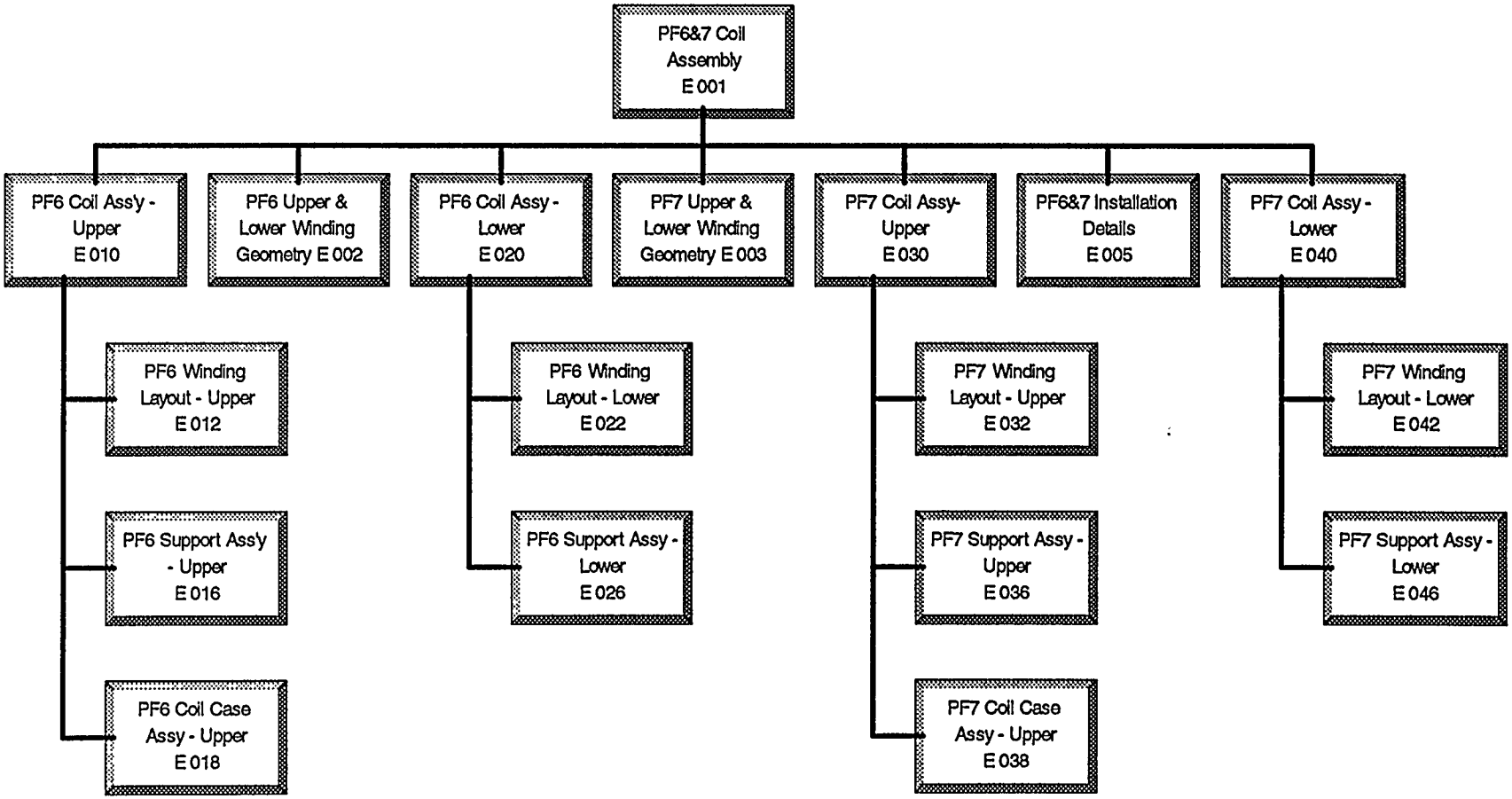

Section III - B

Global Electromagnetics

Electromagnetic Analysis

DRAFT

- Three-dimensional global model configuration
  - PF1 - PF7 upper and lower coils
  - TF1-16 coils
  - Plasma current
  - TF interconnects simulated as current ring
  - Upper / Lower internal control coils
- Magnetic field calculation using Ansys 5.0a Biot-Savart
  - PF coils, plasma, IC and TF interconnect modelled as rings with rectangular cross sections
  - TF coils modelled as combination of bars and arcs with rectangular cross section
- Analysis of HC scenario at t=9 sec

Electromagnetic Analysis

DRAFT

- Figure of 3-D global EM model attached
  - Global coordinate systems
  - Current flow conventions
- Figure of HC scenario Ampere-turns vs time attached
  - Presently analyzing current distributions at t=9 sec
- Figure of local fields for PF7-L coil attached
  - 22.5 degree span

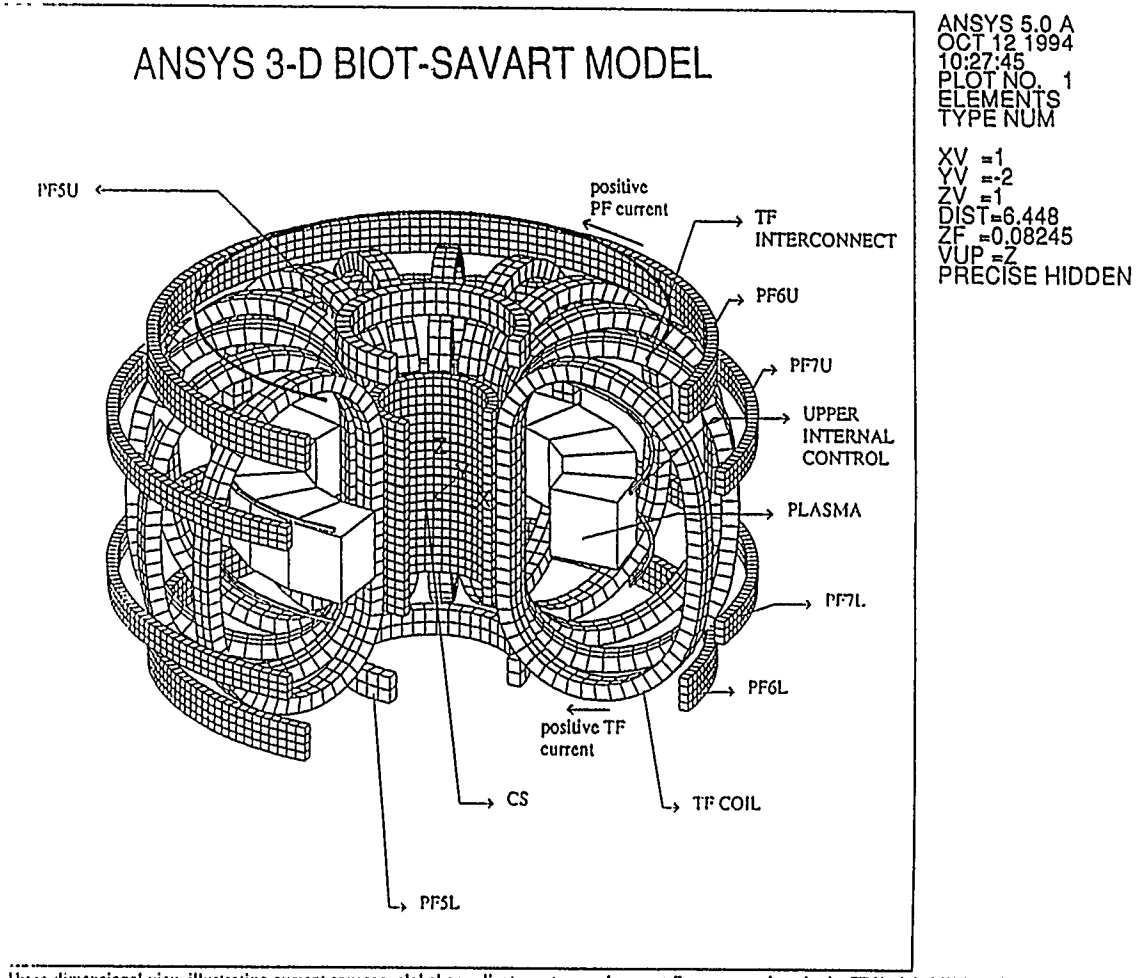

Three-dimensional view illustrating current sources, global coordinate system and current flow conventions in the TPX global EM model.

- HC scenario at t=9sec

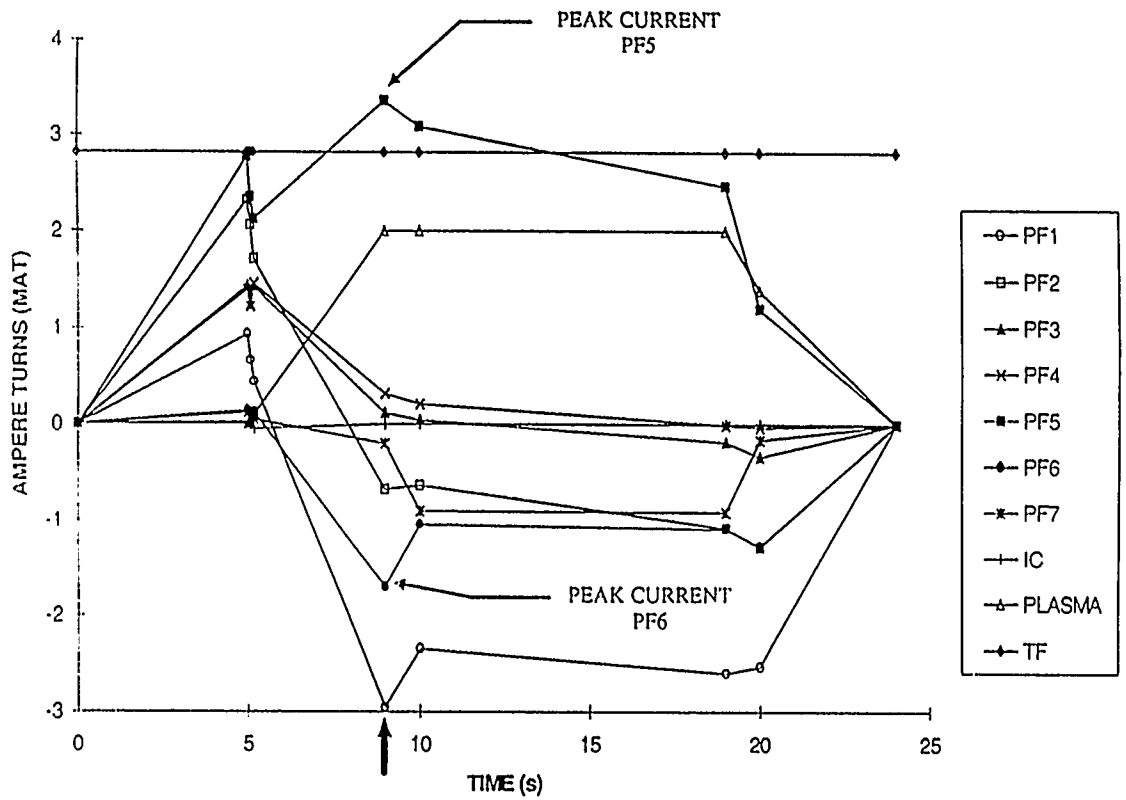

Figure 1 : System ampere-turns vs time for HC scenario.

Electromagnetic Analysis

DRAFT

- Magnetic field (i.e., IBI) distribution for PF7 lower
- HC scenario at t=9 sec.

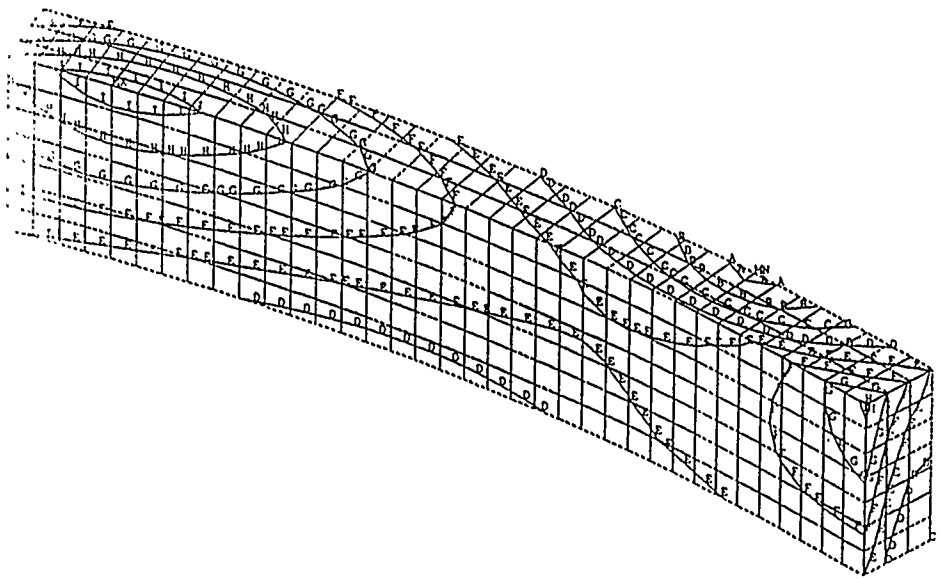

```
ANSYS 5.0 ,
OCT 17 1994
13:54:46
PLOT NO.   1
NODAL SOLUTION
STEP=1
SUB =1
TIME=1
BSUM      (AVG)
SMN =0.00752
SMX =1.041
A   =0.064915
B   =0.179704
C   =0.294494
D   =0.409284
E   =0.524073
F   =0.638863
G   =0.753652
H   =0.868442
I   =0.983231
```

PF 7L (C)

Electromagnetic Analysis

DRAFT

- Peak magnetic field for each of the **PF coils** at t=9 s of the HC scenario; *TF current set to zero*
  - Agreement is within 3 percent, except for PF6
  - Slightly lower W results probably due to:
    - observation grid fineness
    - calculation error (i.e., Biot-Savart integration error)

COIL	MIT/LLNL CALCULATION[1]	WESTINGHOUSE EM MODEL WITH I_{tf}=0
PF1U/PF1L (T)	5.071/5.071	4.982/4.982
PF2U/PF2L (T)	3.658/3.659	3.618/3.618
PF3U/PF3L (T)	2.107/2.116	2.073/2.073
PF4U/PF4L (T)	1.325/1.311	1.287/1.287
PF5U/PF5L (T)	4.738/4.734	4.634/4.634
PF6U/PF6L (T)	2.156/2.156	2.023/2.023
PF7U/PF7L (T)	0.457/0.457	0.444/0.444

- Peak magnetic field for the **TF coils** at t=9 s of the HC scenario; *PF current energized vs de-energized*
  - Discrepancies attributed to current representation
    - W model uses uniform current throughout rectangular cross section
    - MIT/LLNL uses filaments to represent each turn
  - W model shows peak located at top of straight leg with IPF=0 and at midplane with IPF≠0

COIL	MIT/LLNL CALCULATION[1]	WESTINGHOUSE EM MODEL
$TF_{Ipf=0}$ (T)	8.39	8.00
$TF_{Ipf\neq0}$ (T)	8.42	8.085

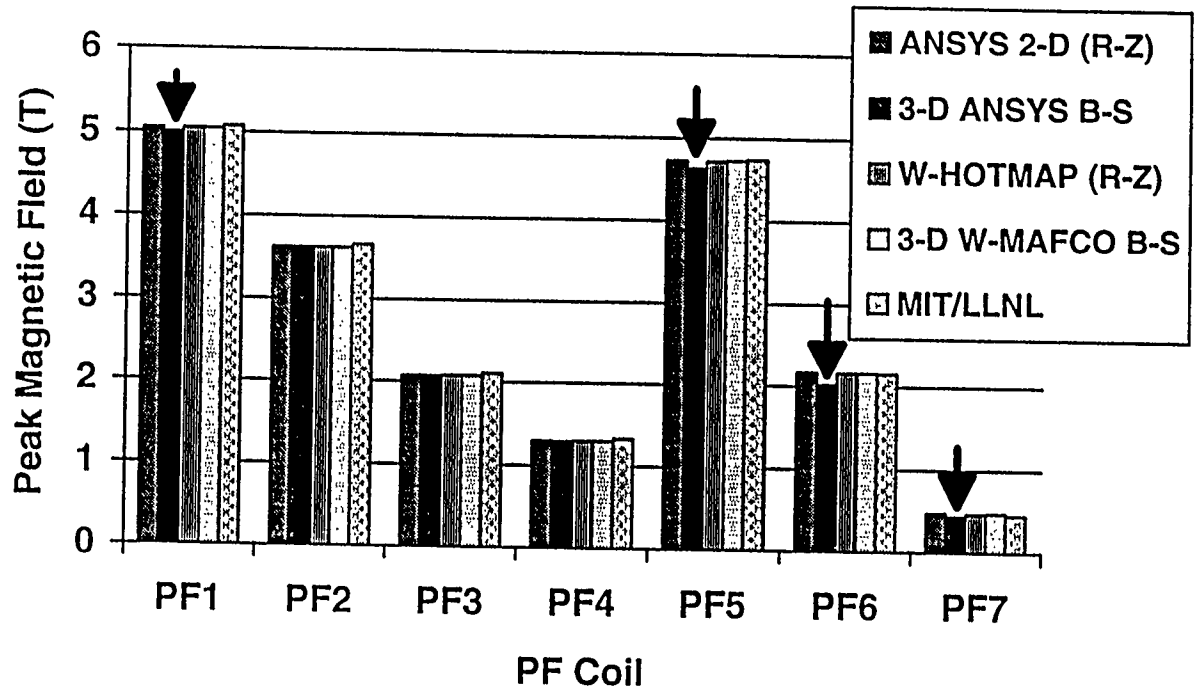

Figure 2.11 — Bar graph comparing value of peak magnetic field obtained in seven PF coils calculated using five different solution methods.

Electromagnetic Analysis

DRAFT

- Lorentz force calculations for PF5 and PF6 attached
- Results of calulations
  - TF field interaction evident for both PF5 and PF6 coils
    - Large variations in PF6 with TF energized
  - Period of force variation is 22.5 degs
  - Steady radial force component primarily due to self field of ring coil
  - Steady axial force due to interaction with other ring coils

- EM force components on PF5 upper and lower coils
- HC scenario at t=9 sec.

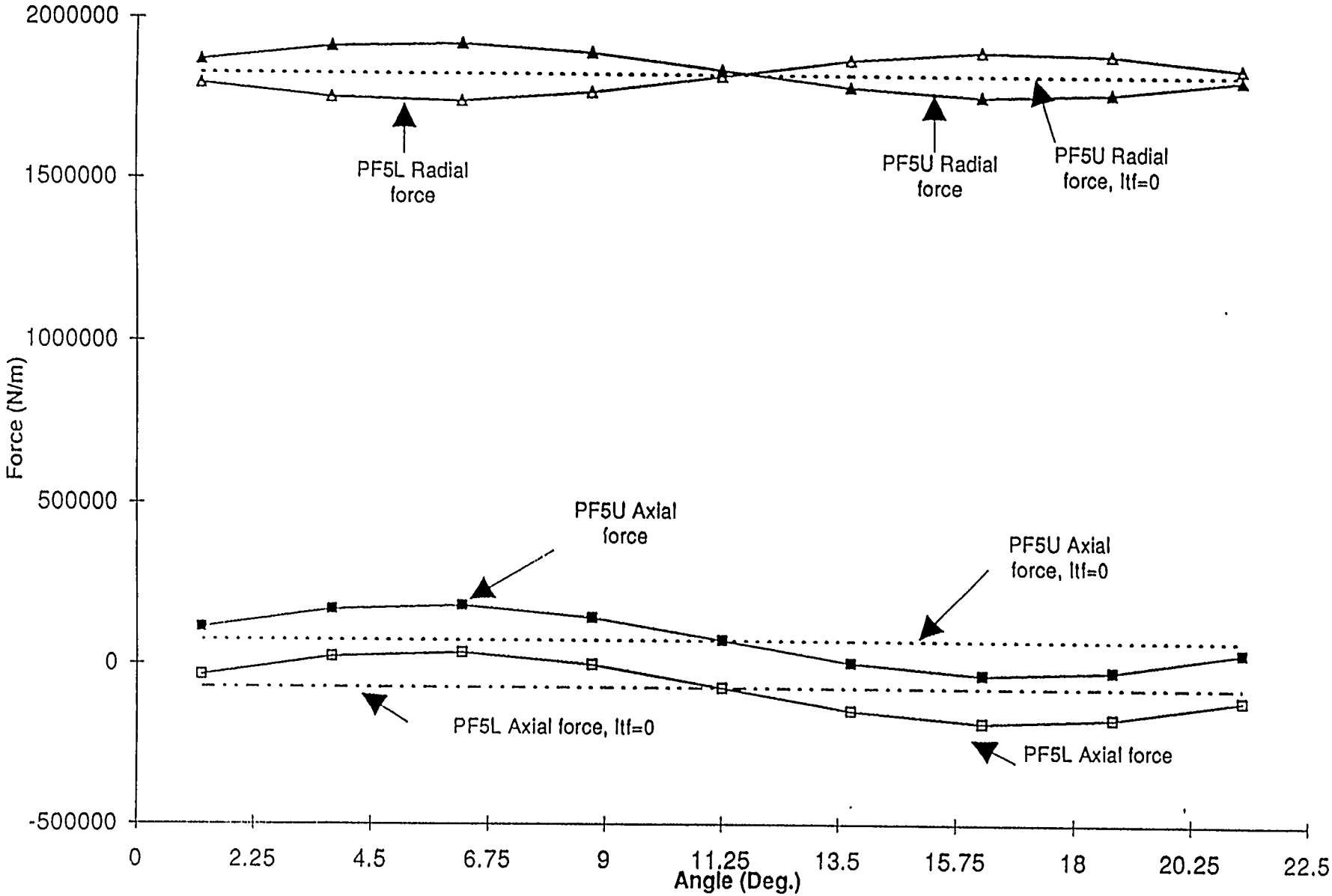

- EM force com[illegible]nts on PF6 upper and lower coils
- HC scenario at t=9 sec.

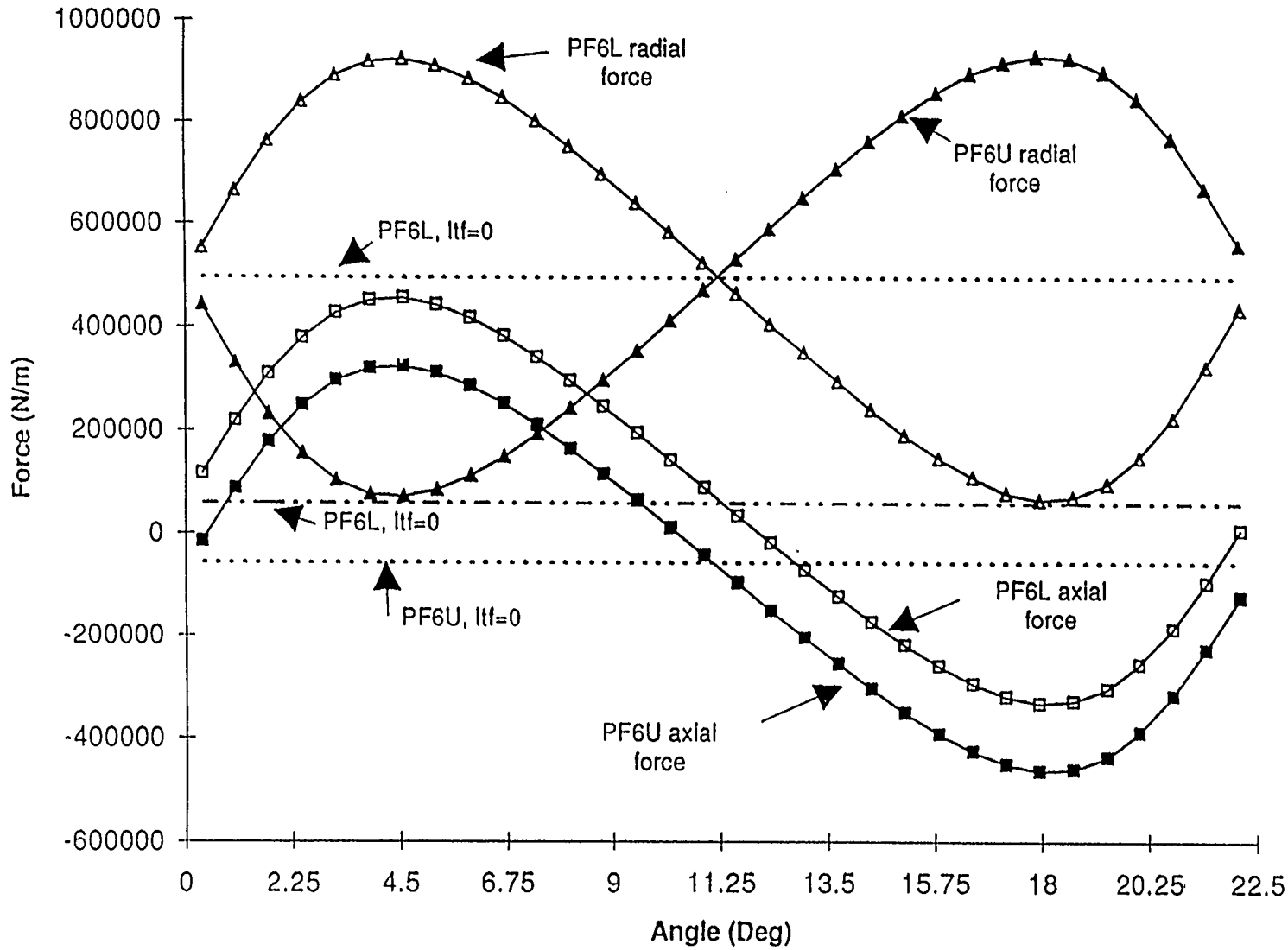

Electromagnetic Analysis

DRAFT

- Lorentz forces calculations for CS coils, PF1-4 attached
- Results of calculations
  - Radial and compressive forces as function of angular location
    - TF full excitation
  - Axial force primarily negative and compressing the stack
  - TF fields have little impact on force distribution
    - Axial and compression forces essential invariant with angular location
  - Net force on PF1-4 upper is 21.69 MN radial and 18.70 MN compressive
    - PF1 contributes greatest amount to net force at t=9 s

- EM radial and compressive force components on PF1-4 coils
- HC scenario at t=9 sec.

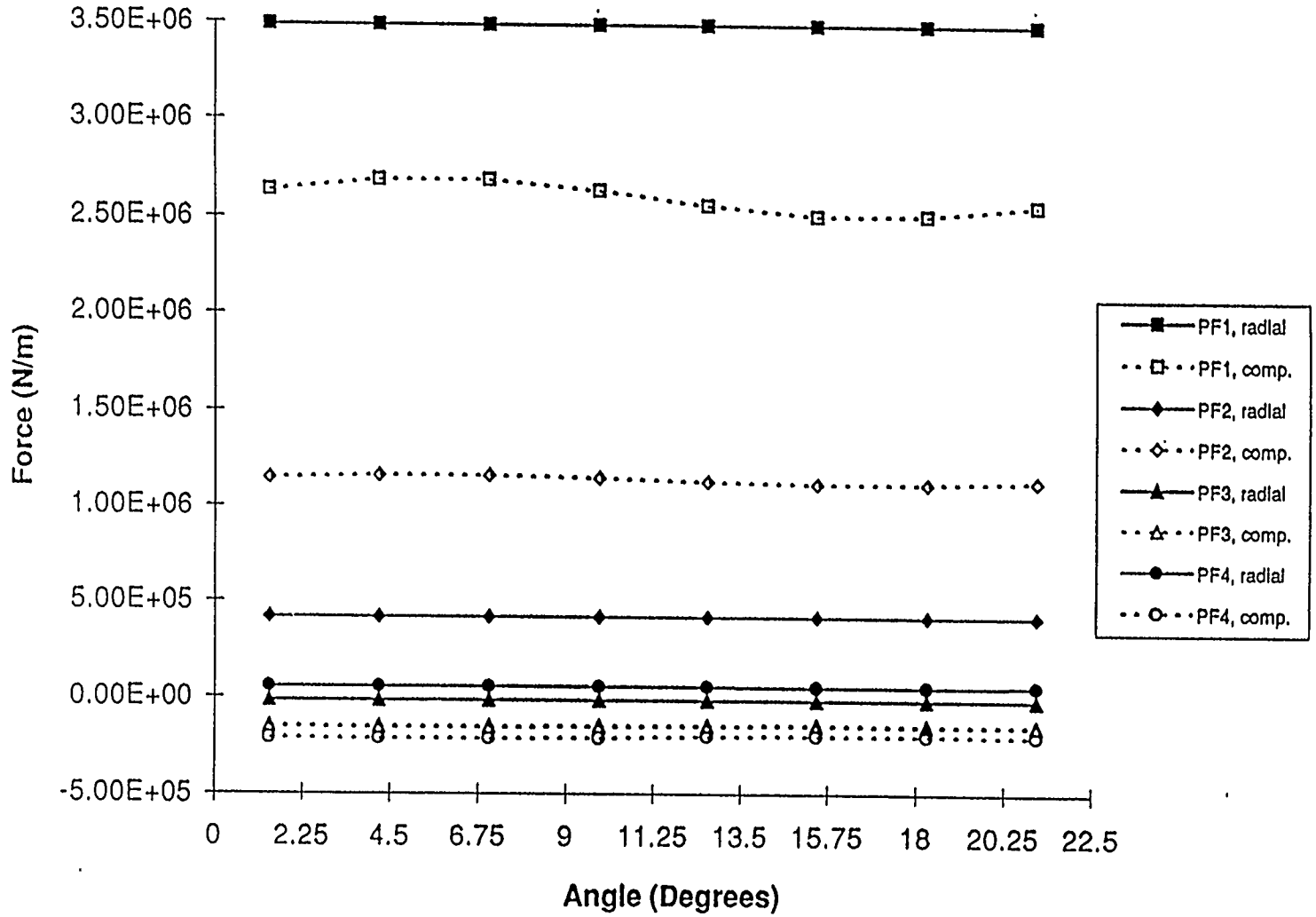

Figure 4 : Radial and compressive forces acting on PF1-4 upper coils plotted as a function of angular location. The case of full TF excitation is shown.

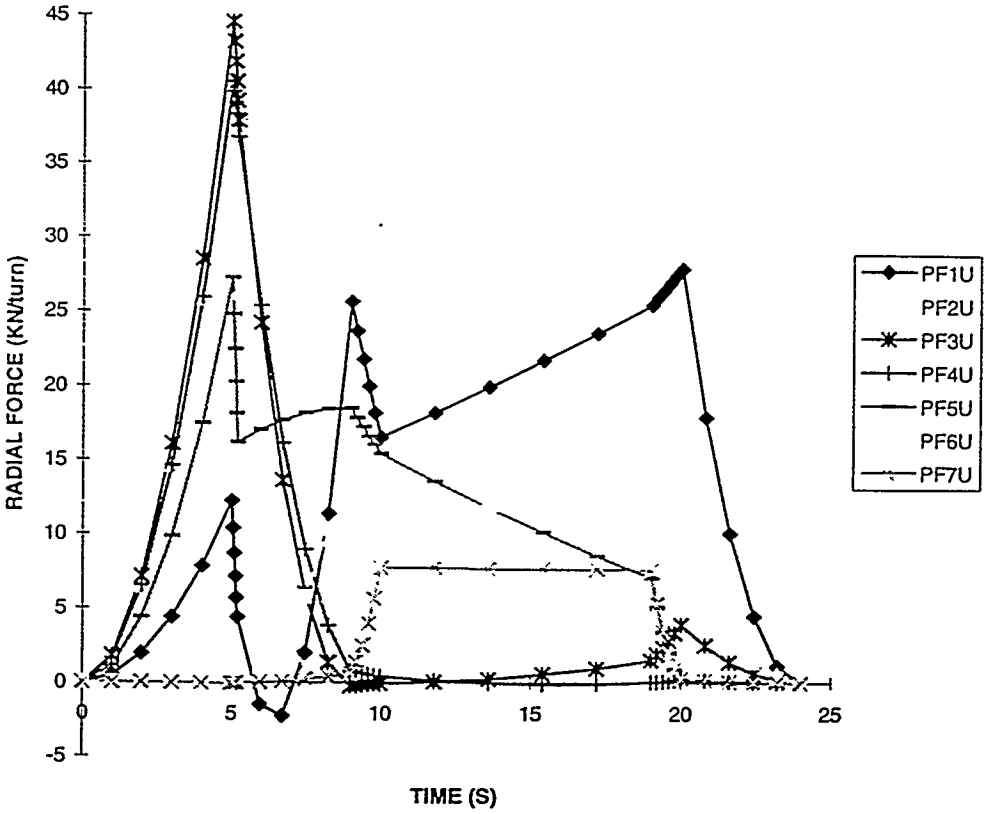

Figure 3.1 — Radial electromagnetic forces acting on PF coils 1-7 during HC scenario.

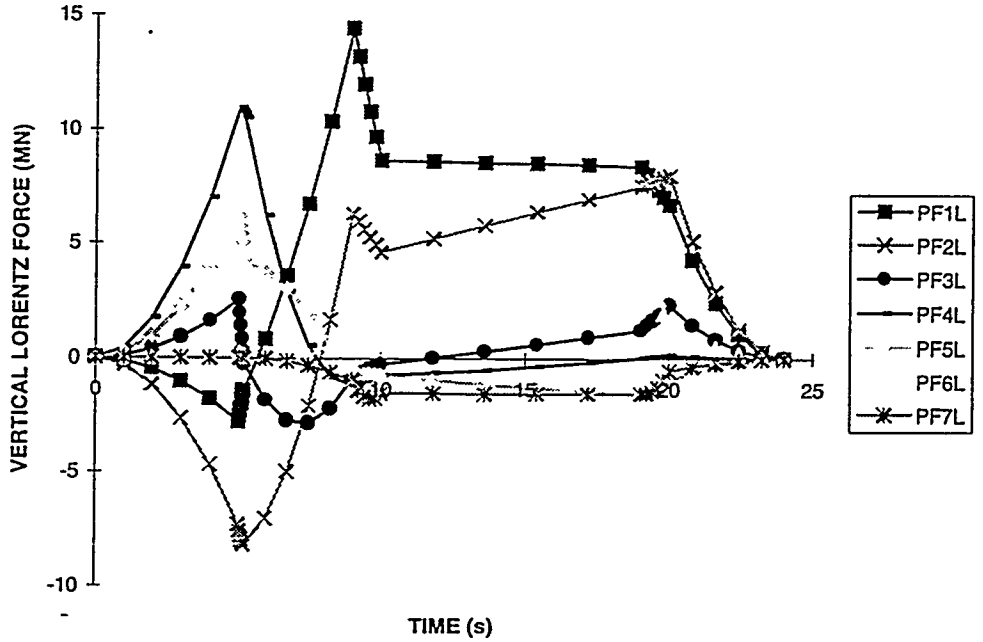

Figure 3.2 — Vertical electromagnetic forces acting on PF coils 1-7 during HC scenario.

Further Model Verification and 2-D Axisymmetric Model

- Comparison of 3-D model with 2-D axisymmetric models and MIT/LLNL steady force results for HC scenario at t=9 sec.

	VERTICAL FORCE (MN)			TENSION (MN)		
Coil	3-D ANSYS B-S	Axisymmetric FE	MIT/LLNL	3-D ANSYS B-S	Axisymmetric FE	MIT/LLNL
PF1U	-14.40	-14.41	-14.40	3.03	3.08	3.04
PF2U	-6.30	6.308	-6.32	0.370	0.369	0.36
PF3U	0.834	0.835	0.83	-0.015	-0.015	-0.013
PF4U	1.15	1.147	1.14	0.045	0.045	0.050
PF5U	0.61	0.616	0.51	2.37	2.353	2.42
PF6U	-1.406	-1.407	-1.42	1.88	1.871	1.81
PF7U	0.955	0.955	0.95	0.051	0.051	0.044

- Magnetic field (i.e. |B|) contour from 2-D axisymmetric solution
- HC scenario at t=9 sec.

Load step = 1 Iteration = 1

Neutral file = NEUTRAL_1

Variable = BMAG

Max. = 5.0364

Min. = 0.57977E-08

20 = 4.875

19 = 4.625

18 = 4.375

17 = 4.125

16 = 3.875

15 = 3.625

14 = 3.375

13 = 3.125

12 = 2.875

11 = 2.625

10 = 2.375

9 = 2.125

8 = 1.875

7 = 1.625

6 = 1.375

5 = 1.125

4 = 0.875

3 = 0.625

2 = 0.375

1 = 0.125

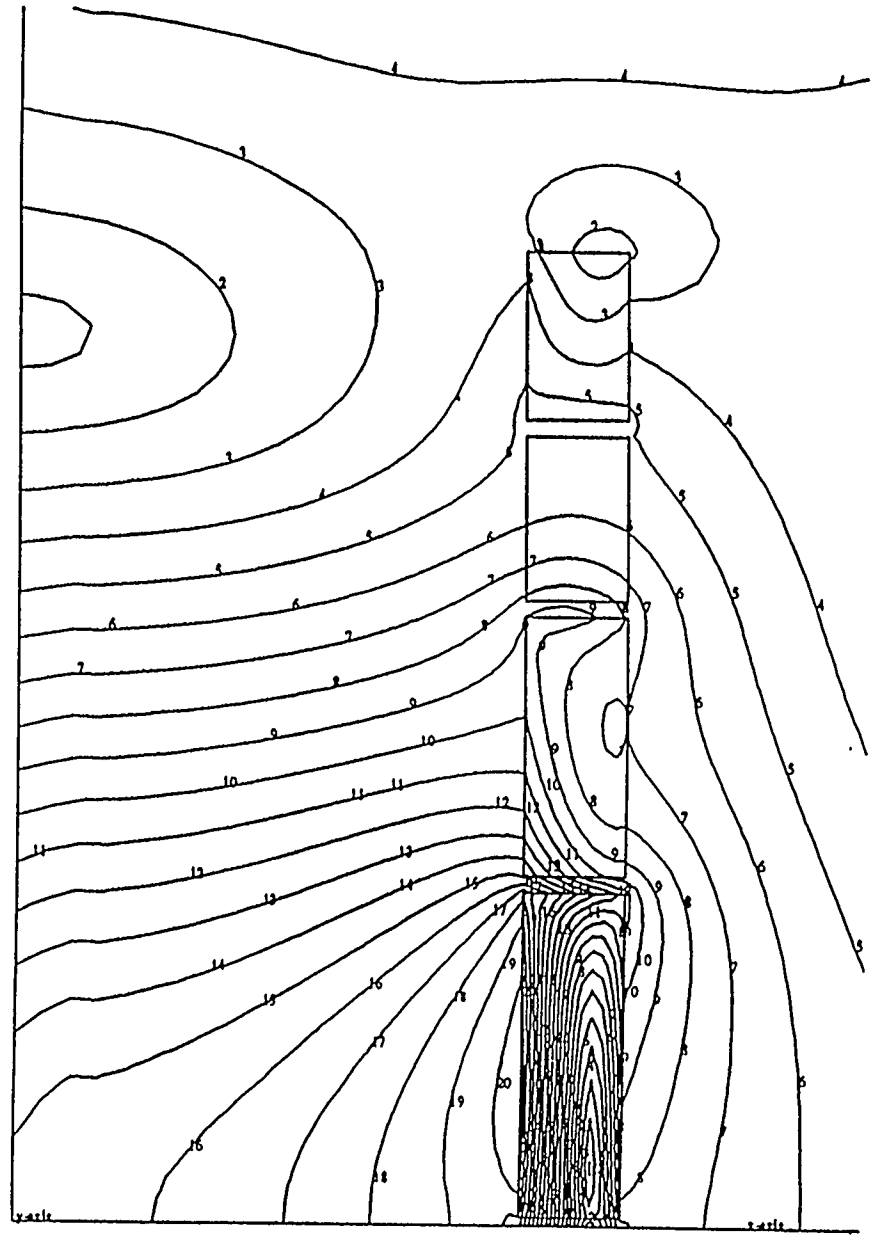

2D Axisymmetric

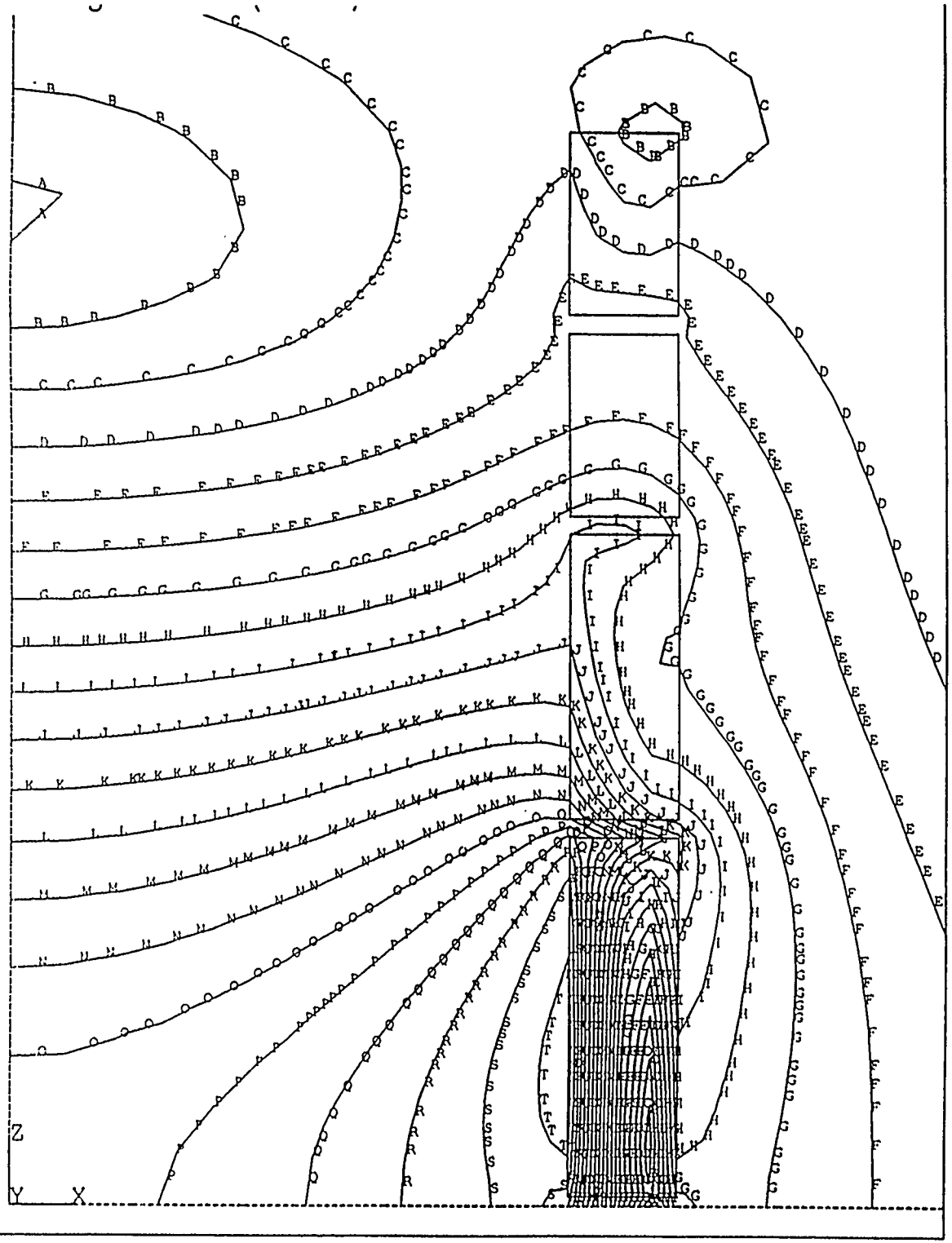

ANSYS 5.0
NOV 11 19
23:13:41
PLOT NO. 1
NODAL SOLUTION
STEP=1
SUB =1
TIME=1
BSUM (AVG)
SMN =0.001272
SMX =4.983
A =0.125
B =0.375
C =0.625
D =0.875
E =1.125
F =1.375
G =1.625
H =1.875
I =2.125
J =2.375
K =2.625
L =2.875
M =3.125
N =3.375
O =3.625
P =3.875
Q =4.125
R =4.375
S =4.625
T =4.875

ELEMENTS

HC scenario at t=9 sec

CONCLUSIONS

- A global model including TF coils, PF coils, internal control coils, plasma current, and TF interconnect hoop current has been fromed using ANSYS
- SOURC36 stranded bar and arc primitives are used to construct the current geometry & magnetic fields have been calculated using the Biot-Savart integration algorithim internal to the ANSYS code
- Lorentz forces have been evaluated in the post processor using a small set of ANSYS commands tailored for this purpose
- Forces results were in very good agreement (i.e. 2% or better) with University results with the exception of the radial force on PF5, which showed slightly lower radial forces, this discrepancy was tracked to a slight error in the radial build of PF5 in the University model
- In the case of magnetic field, local errors (up to 7%) were observed in the ANSYS model
  - These occurred on surfaces of the hoop coils where the Biot-Savart integration becomes particularly difficult due to singularities
  - ANSYS Inc. has been notified of the errors and indicated that they were working on refining their calculation at those locations
  - Since the peak field generally occurs on the inner surface of the hoop coils, the ANSYS generated results (for PF peak fields only) should be treated with caution
  - The error is very localized, thus it has very little effect on the body Lorentz forces

Section IV - A

Helium Stub R&D Results

Helium Stub performance criteria:

- Reliability of the overall design.
- Minimization of superconductor strand time temperature history.
- Leak Free mechanical performance of the stub.
- Inspectability of the penetration and joining.
- Automation Possible.
- Cost Effectiveness.

SELECTED CONFIGURATION

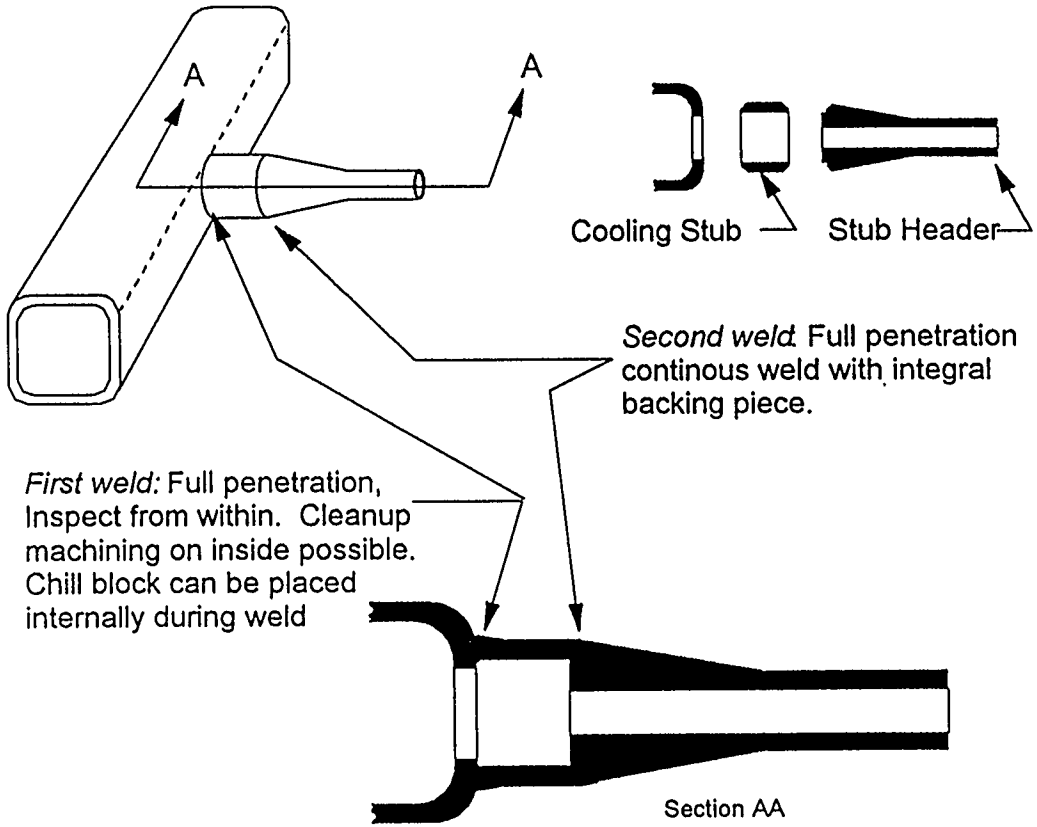

Figure 3.1 — Selected Approach.

. The techniques that were developed as follows:

- The shape of the helium cooling stub is circular and mated to a header piece.
- The height of the stub is short enough to allow for inside inspection of the weld using a borescope.
- The conduit is pieced with a Roto Broach tool leaving a very small burr (<0.1 mm)
- The foil which is wrapped around the cable is removed by a manual process using tweezers
- The weld is intermittant TIG welding using internal and external water cooled chills.
- The stub weld is inspected visually using a borescope.
- The ID of the stub is machined to remove 1.5 mm off the inside surface and eliminating any remaining areas of lack of penetration
- The stub weld is leak checked with a helium mass spectrometer leak detector
- The leak detection is speeded up using a plug with an O Ring seal in the pierced hole to isolate the cooling stub from the CIC conductor.
- The stub assembly is completed by a TIG weld between the header and the stub.

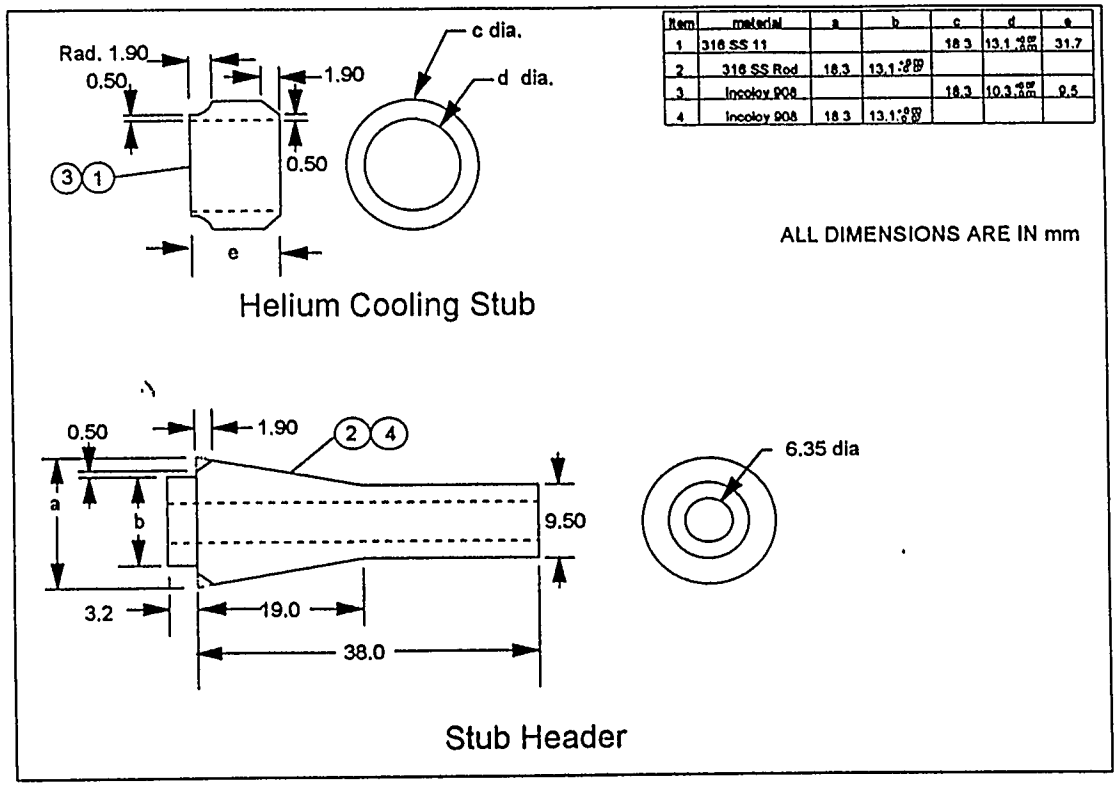

Item	material	a	b	c	d	e
1	316 SS 11			18.3	13.1	31.7
2	316 SS Rod	18.3	13.1			
3	Incoloy 908			18.3	10.3	9.5
4	Incoloy 908	18.3	13.1			

Figure 3.2 — Dimensions of helium cooling stub and header used for test.

OPTIONS EVALUATED FOR SHEATH PENETRATION

Table 4.1

Approach	Advantages	Disadvantages
Roto Bor/Broach	Pushes conductor away from cut (minimum risk to conductor) Final cut made dry (no cutting fluid)	Cutting fluid should be used for first part of cut, allowing for a cleanup procedure before completing the cut
Pressure Sensitive Drill		Requires feedback system
Hole Saw		Similar to Roto Bor but higher risk since conductor not displaced
Direct Machining		Removes more metal Requires cutting fluid
Weld to Plug and Withdraw		Difficult with high strength material
Chemical Etching		Hazardous chemicals in proximity to conductor

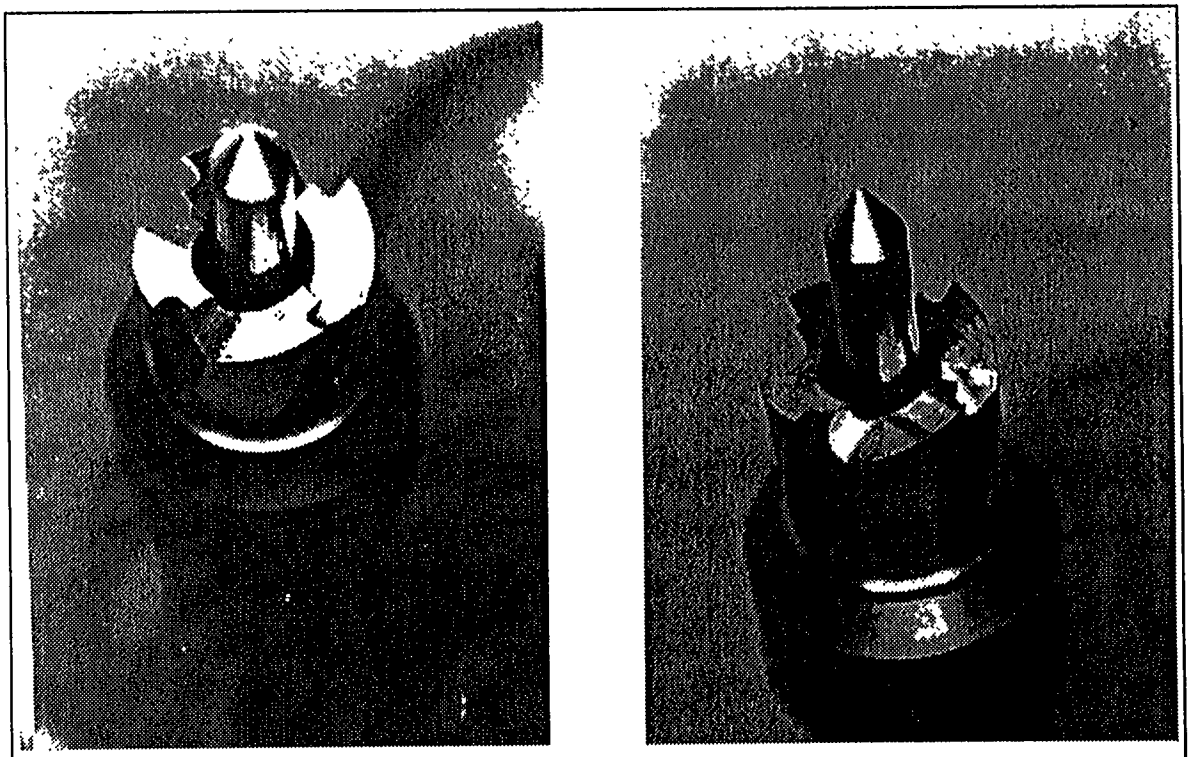

Figure 4-3 Picture of a Roto-Broach used for piercing the sheath.

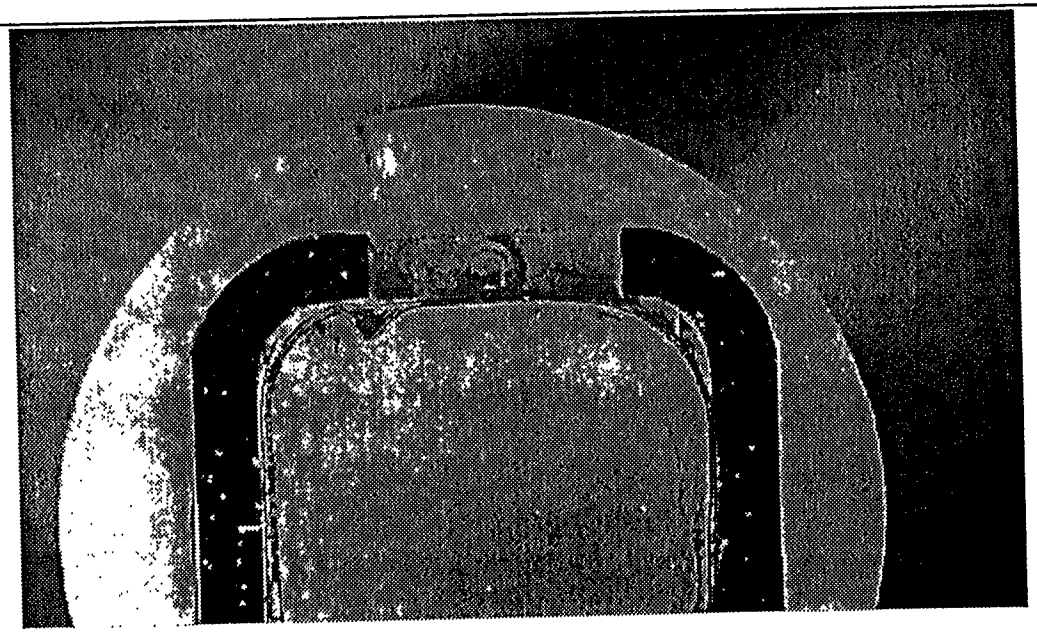

Figure 4-4 Micrograph of a conduit pierced with a new Roto Broach

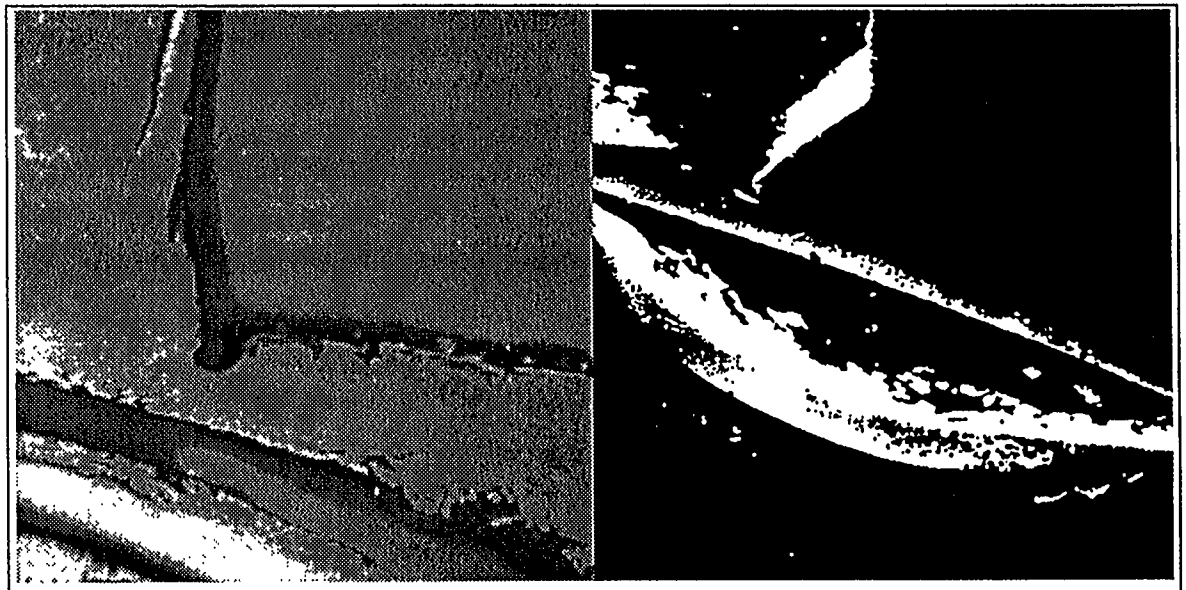

Figure 4-5 The residual burr left by a Roto-Broach after piercing an Incoloy 908 sheath

TEMPERATURE SENSITIVITY OF NbTi SUPERCONDUCTOR

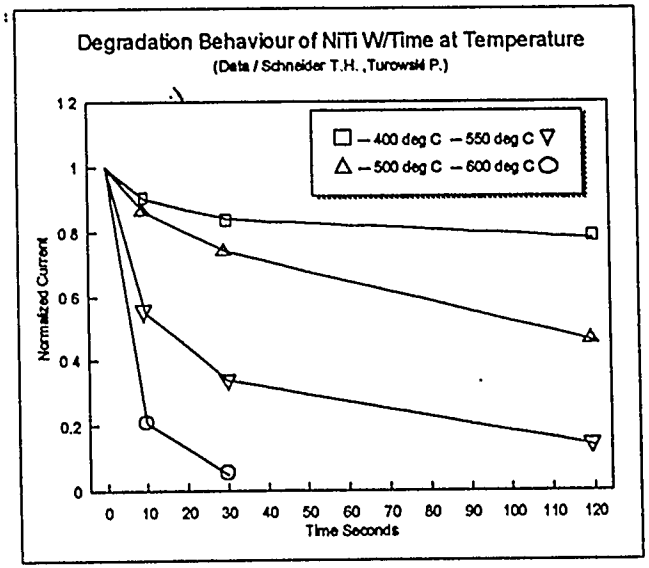

Figure 6.1 — Degradation behavior of NbTi.

The second source is compliance data from Supercon Inc. for TPX superconductor and is documented in 1141-950724-LLNL. The results are significantly better indicating that the superconductor tested for TPX is less susceptible to the thermal degradation than indicated by the Schneider data. Supercon Inc. data indicate no significant degradation at 500C at 30 seconds and minimal degradation at 600 C for 10 seconds.

Table 6.1 — Joining approaches considered for the helium stub to conduit.

Approaches	Advantages	Disadvantages
Automatic TIG Weld (Pulsed)	Equipment commercially available Continuous process Moderate heat input	Orbital weld head design/development required Weld process development required
Manual TIG Weld (Pulsed)	Equipment commercially available No weld head required Intermittent process - can stop and let cool	Weld process development required Intermittent welding could introduce porosity, leaks
Laser Weld (Pulsed)	Small heat-affected zone Equipment commercially available	Orbital weld head design/development required Precise joint fit-up and beam delivery required Process development required Very expensive equipment
Ultrasonic Welding	Equipment commercially available	Material next to ultrasonic tip must be thin Butt joints are a problem Temp. at interface may reach 0.35 to 0.5 of melt point of alloy
Friction Welding a) Inertia Welding b) Spin Welding	High temperatures but fairly localized	Large amount of upset Upset on inside of weld High equipment cost Probably requires post-machining
Flash Welding Upset Welding Percussion Welding		Interface reaches melting point/heat provided by electrical arc and/or resistance heating Wider heat pattern
Cold Welding		Only works with very ductile materials
EB Welding	Equipment commercially available Small heat-affected zone	Extensive development required High cost Non-vacuum EB requires head to be withi 3-5 cm of weld
Soldering		Flux required Low temperature solders have low strength
Brazing		Not recommended for 908 alloy (could b used with 316 alloys)
Epoxy		Poor strength, poor reliability

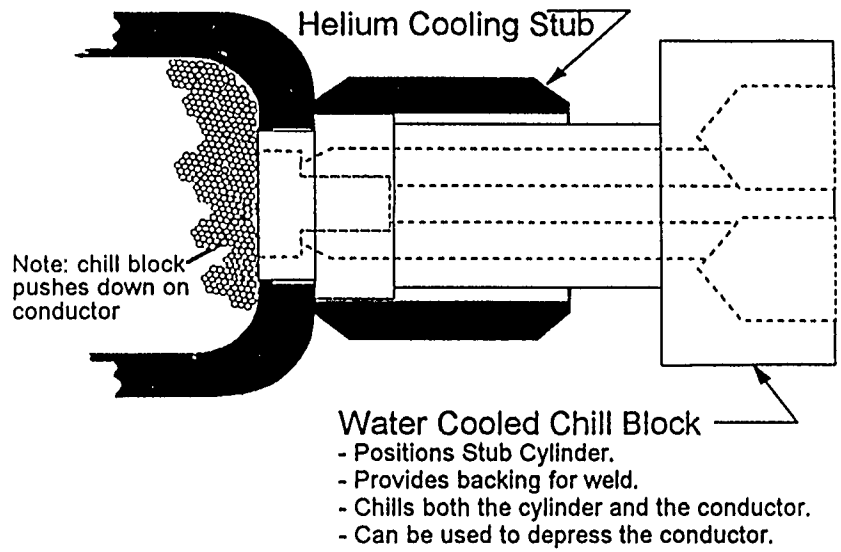

Figure 6.2 Conceptual Design of Internal Water Cooled Chill Block

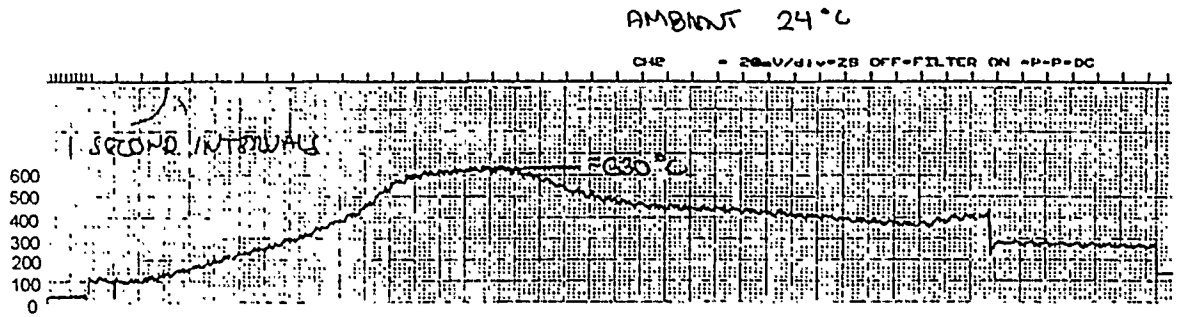

Figure 6.6 Typical Time Temperature History for T Welding Series

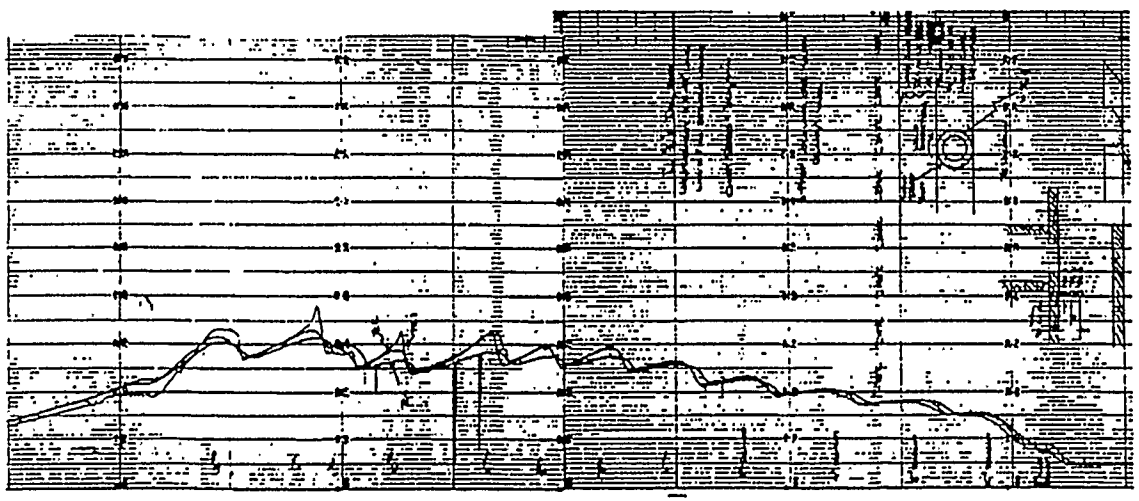

Figure 6.7 Weld Temperature Plot for Intermittant Welding

INTERMITTENT WELD PREPARATION & PROCESS

Weld Preparation

Initial Cleaning - Scotch Bright Pad, Alcohol Wipe
Interweld Cleaning - Wire Brush
Groove Design - J-Prep w/.0508mm land

Weld Process

Gas Tungsten Arc Weld, 70 Amps, 11.5 Volts
Single pass, intermittent, full penetration, overlapping weld
H2O Cooled Copper Chill 1.9 l / min 0°C
Filler - 0.9mm dia ER308L
Inert Gas - Argon 570 l / min.
Electrode - 1.6mm Dia., 2% Thoriated
Time delay between welds @ 1miniute
Weld Length @ .4.76mm (15 sec)
Internal Purge Gas - 280 l / hr. Argon

Figure 6-9 Typical weld bead profile of a helium cooling stub assembly (16X).

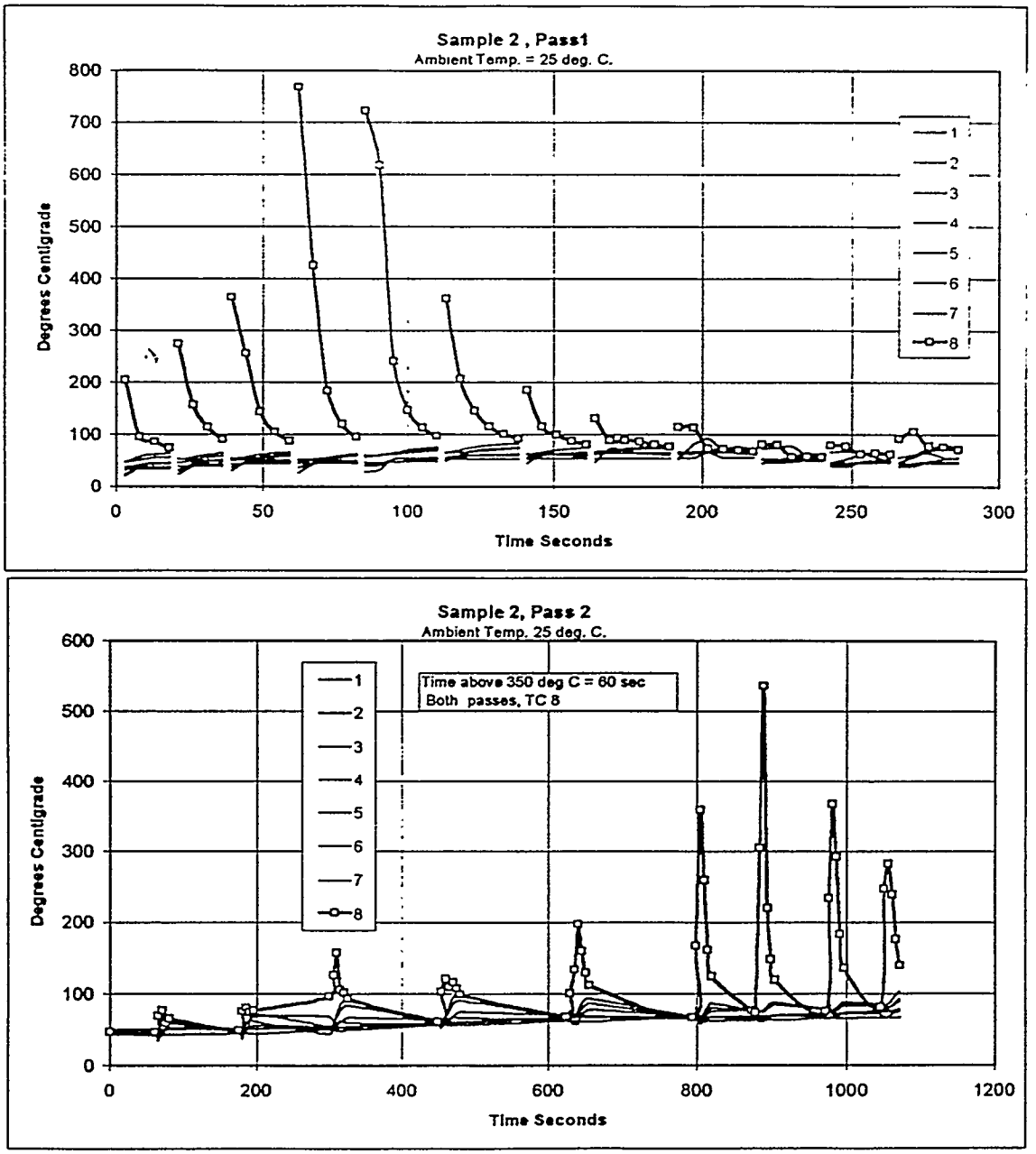

Figure 13. Temperature Recording of the Cable during the Welding of the 316LN Helium Cooling Stub with intermittant welding.

CONCLUSIONS

1. A partial penetration stub attachment weld was the most straight forward of all tests run to date.

2. Full penetration stub attachment welds were extremely difficult to achieve due to the sluggish weld pool characteristics of the 908.

3. Use of wider groove configurations and attachments to weld deposited buildups were not effective in improving the ability to achieve full penetration.

4. The partial penetration attachment allowed maximum cooling to be employed while significantly reducing the skills required to make the weld.

5. Maintaining low interpass temperatures was not difficult with low amperage segmented welds and water cooled chill blocks.

6. More effective cooling blocks to nest around the 908 square sheathing could further reduce the overall temperature cycles.

7.2 CRITICAL CURRENT SAMPLES

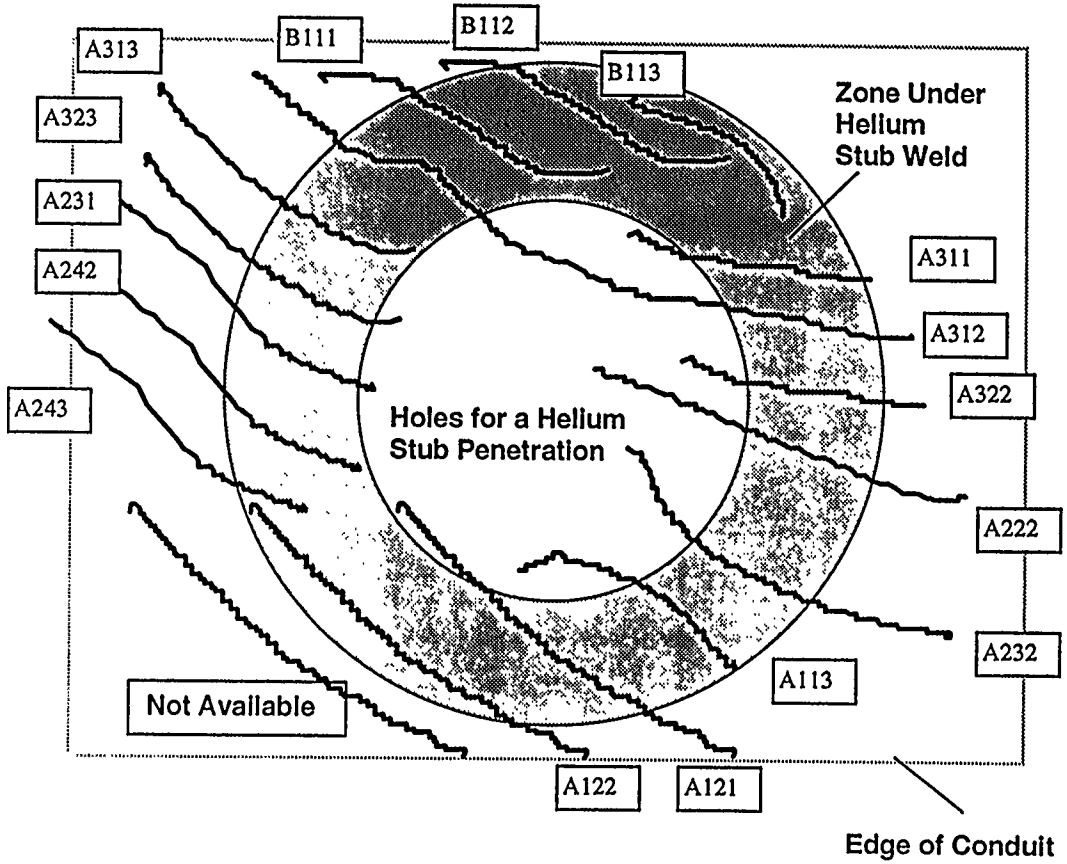

Figure 7-1 The location and layout of the strand for which the critical current was measured. The strand identifiers refer to the location in the cable starting with the largest subcable indicated by a letter. The view is from the top of the helium stub underneath the sheath.

Table 7-1 Measurement Of The Critical Current Of Strand Underneath The Stub Weld

Measured at Oxford
8/14/95

Loc #	Wire ID	Weld or not	Over twisted	Jc@7T	Jc@5T	Jc/Jco@7T	Jc/Jco@5T	Notes
1	B113	yes3	yes	0	0	0	0	open circui
2	A311	yes5	no	380	620	0.92	0.92	
3	A312	yes4&6	yes	0	0	0	0	broke durir mounting
4	A322	yes3	no	136	528	0.33	0.78	
5	A222	yes2	yes	0	0	0	0	open circui
6	A232	yes1	yes	0	0	0	0	open circui
7	A113	yes4	yes	0	0	0	0	open circui
8	A121	yes3	no	0	0	0	0	open circui
9	A122	yes2	yes	0	0	0	0	open circui
10	A243	yes11	no	410	672	0.99	1.00	
11	A242	yes10	no	410	672	0.99	1.00	
12	A231	yes9	no	390	644	0.94	0.95	
13	A323	yes8	no	59	330	0.14	0.49	
14	A313	yes7	no	340	560	0.82	0.83	
15	B111	yes 1	no	410	652	0.99	0.97	
16	B112	yes 2	no	412	664	1.00	0.98	
	B121	no	yes	410	672			
	B122	no	no	420	676			
	B123	no	no	410	672			
	A112	no	no	416	680			
	Control average			414	675			

OBSERVATIONS FROM I_c MEASUREMENTS

1. Four strands were measured as controls for the experiment. As can be seen, the variation is very small for the strands measured. Even the overtwisted strand yielded the expected critical current.

2. One strand, A312, broke in two pieces before being tested.

3. Six of the strands would not conduct current at all during the test. They acted as open circuits when cooled to 4.2K. This behavior suggests a fractured wire but no evidence of an obvious break could be found when examined after test

3. Of the remaining nine strands, seven performed adequately (the lowest was 82% of its original Ic). Notice that any degradation found was independent of field strength within the normally expected error bars.

4. The last two strands, A322 and A323, showed evidence of current degradation due to annealing of the NbTi. On these strands notice that the degradation at 7T was much greater than degradation at 5T. Annealing of the NbTi would be expected to affect the high field performance more strongly.

5. All of the strands for which the critical current could be measured were not over-twisted. All of the strands that were over-twisted exhibited the fractured behavior with no current flow.

. CONCLUSIONS

Minimization of heating during welding must continue. Intermittent welding offers significant temperature reduction over the standard process without apparent compromise to the leak tightness. Better use of the internal heat sink has the potential for further improvements. Improvements are isolation from the stub itself so as to better cool the cable and avoid being a conduit of heat from the weld to the cable.

Water cooling of the conduit, header and conductor with chill blocks lowers the time that the conductor is at significant temperature but does not significantly affect the peak temperature. The duration of the welding arc is primary variable in limiting the temperature of the superconductor.

Gas flow inside the conductor improves the weld penetration and provides important cooling of the cable.

Piercing of the sheath can be effectively accomplished using new, sharp tools. The Roto-broach is the preferred tool giving the smallest burr.

Optimization of the contact pressure from the Roto-broach must be optimized further to minimize burr while giving space between the cable and the sheath.

Machining of the inside of the cooling stub is required for the Incoloy908 to remove crack initiators due to the viscosity of the Incoloy 908 puddle. Implementation of that step to 316LN welding provides increased assurance of a strong and tough joint.

Section IV - B

Magnet Insulation R&D Program

Road Map to Resolution of Insulation Design

DRAFT

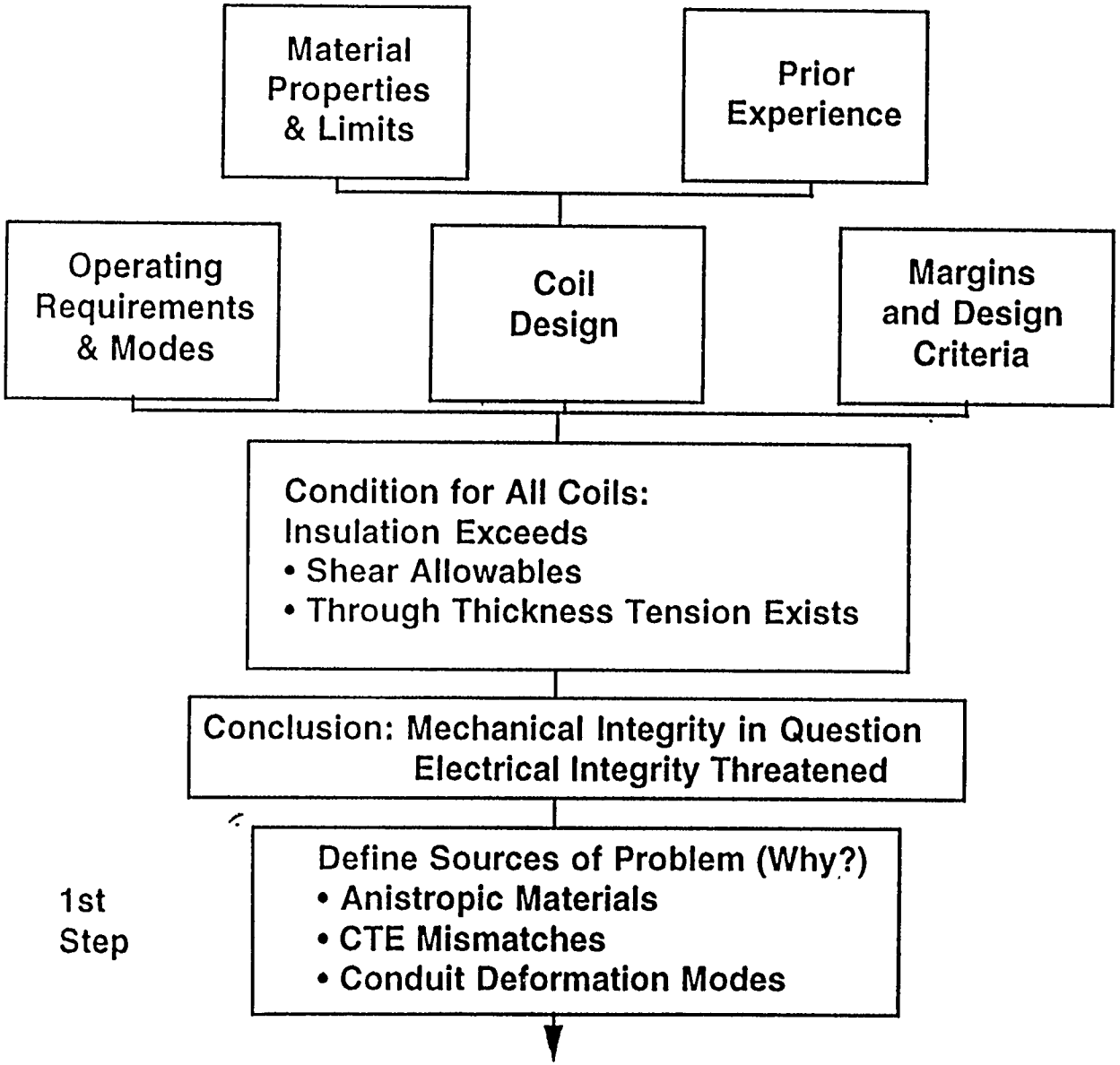

Statement of Problem

DRAFT

- A fully cooled and loaded TF and PF coils exhibits
  - Very high shear stresses 100 MPa in CS and 40 MPa in TF (particularly around the corners of the conduit)
  - Through thickness tension (greater than 50MPa) in the roving corner areas and between conduit sides
- These high stresses are attributed to the following:
  - The anisotropic properties of the baseline insulating matrix (qualitatively half of the problem)
  - Thermal contraction mismatch between the conduit and the matrix (third of the problem)
  - Concave deformation of the conduit side under load (sixth of the problem)

Winding Pack Structural Analysis

DRAFT

	Pass Shear Margin	Pass Normal Tensile Stress @ 1e6Pa	Pass Normal Tensile Stress @ 10e6Pa	Pass Normal Tensile Stress @ 20e6Pa	Pass Normal Tensile Stress @ 30e6Pa	Pass Normal Tensile Stress @ 40e6Pa	Pass Normal Tensile Stress @ 50e6Pa	Pass Tresca
Baseline, Rev'd Mat'l, Conduit Mat'l 908, Cooldown	XX	44	59	63	66	67	69	XX
Baseline, Rev'd Mat'l, Conduit Mat'l 908, cooldown And Preload (25.3MNt)	61	56	59	67	67	68	69	66
Baseline, Rev'd Mat'l, No Conduit, Cooldown	85	66	68	69	72	80	88	96
Isotropic Insulation Properties, Conduit Mat'l 908, Cooldown	100	49	68	88	99	100	100	100
Isotropic Insulation Properties, Conduit Mat'l 316LN, Cooldown	100	85	100	100	100	100	100	100
Isotropic Insulation Properties, Conduit Mat'l 316LN, Cooldown and Preload (27.1 MNt)	97	54	83	100	100	100	100	100
Percentage of the Model Area That Passes The Design Criteria								

Road Map to Resolution of Insulation Design

DRAFT

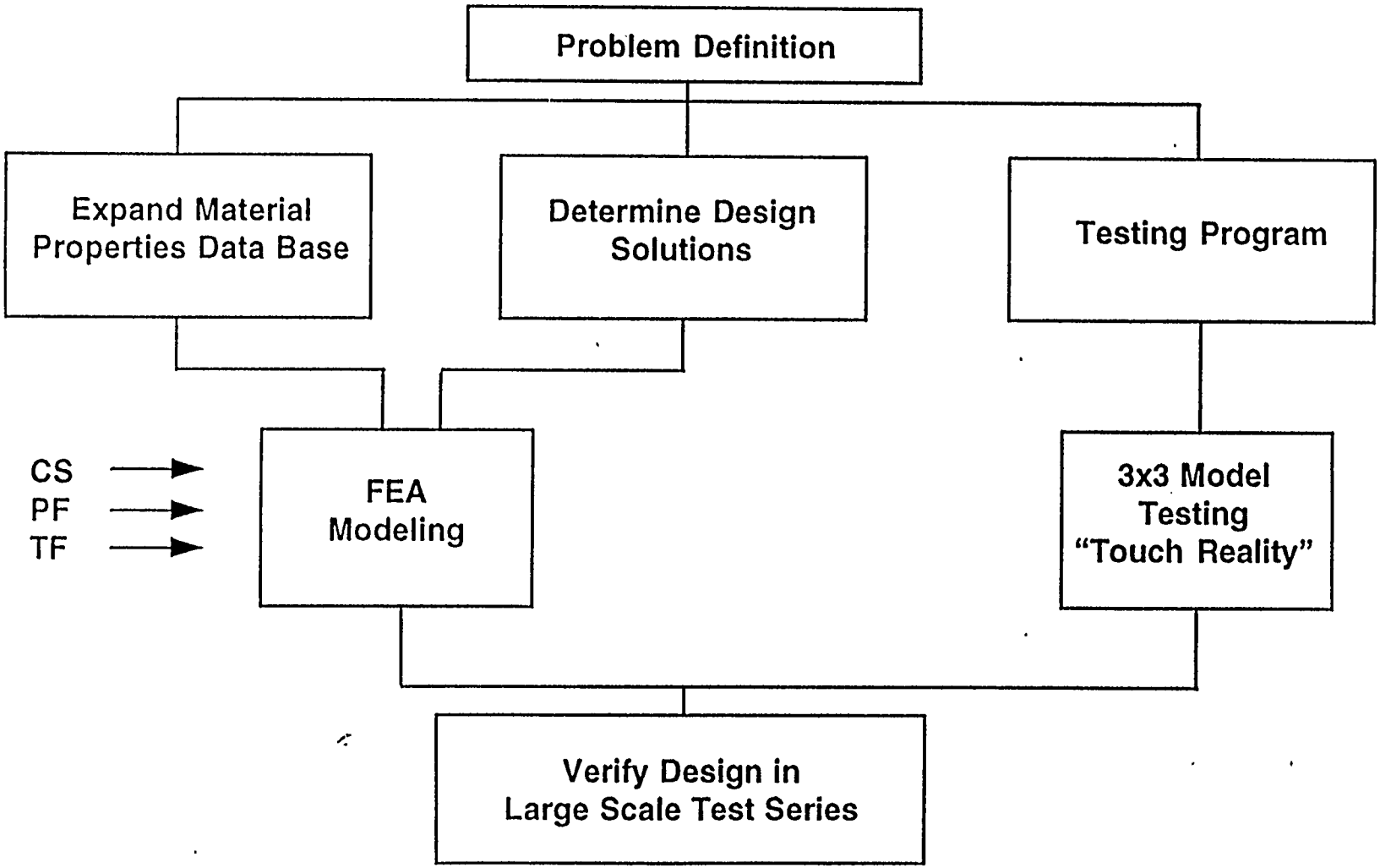

Road Map to Resolution of Insulation Design

DRAFT

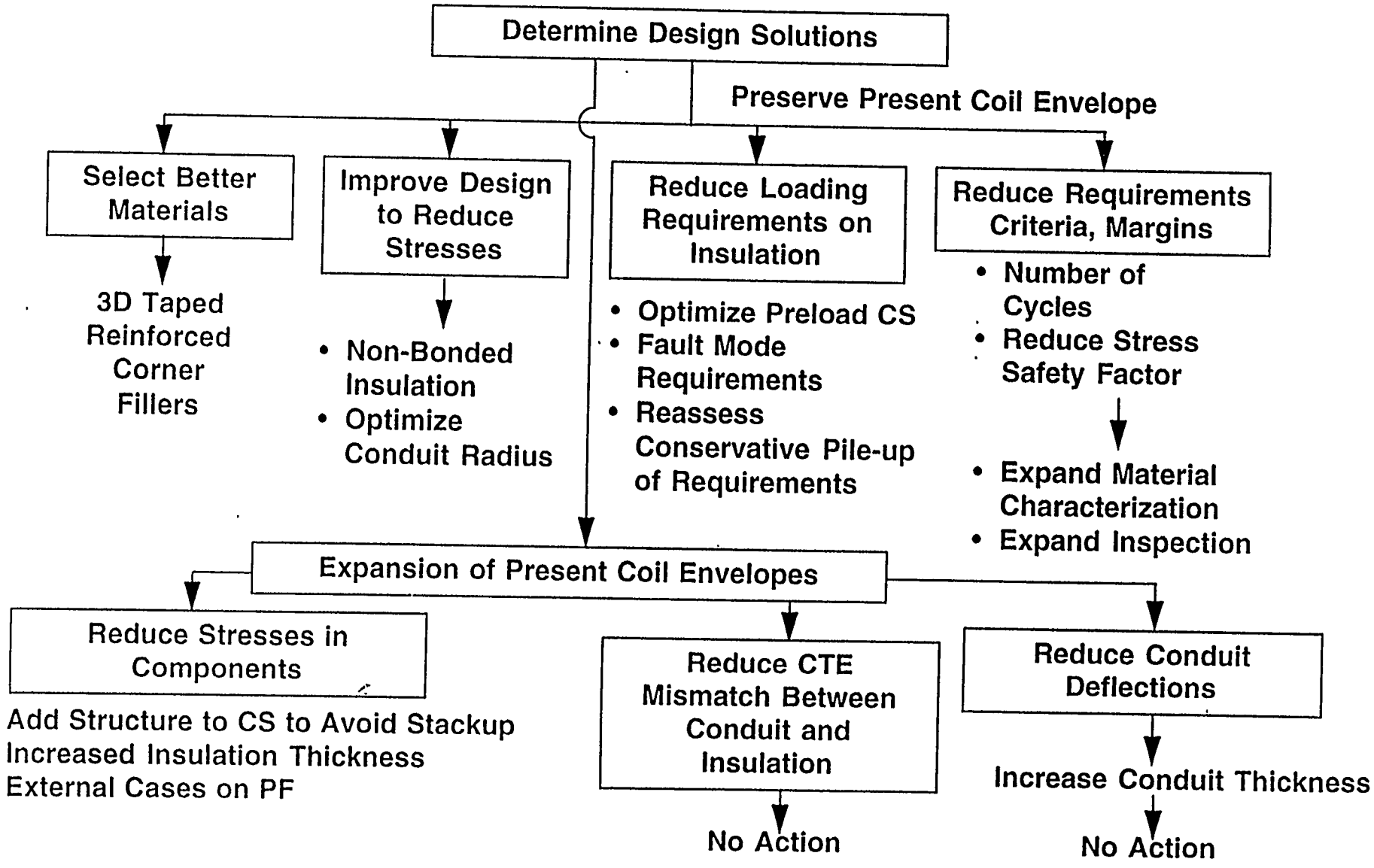

Road Map to Resolution of Insulation Design

DRAFT

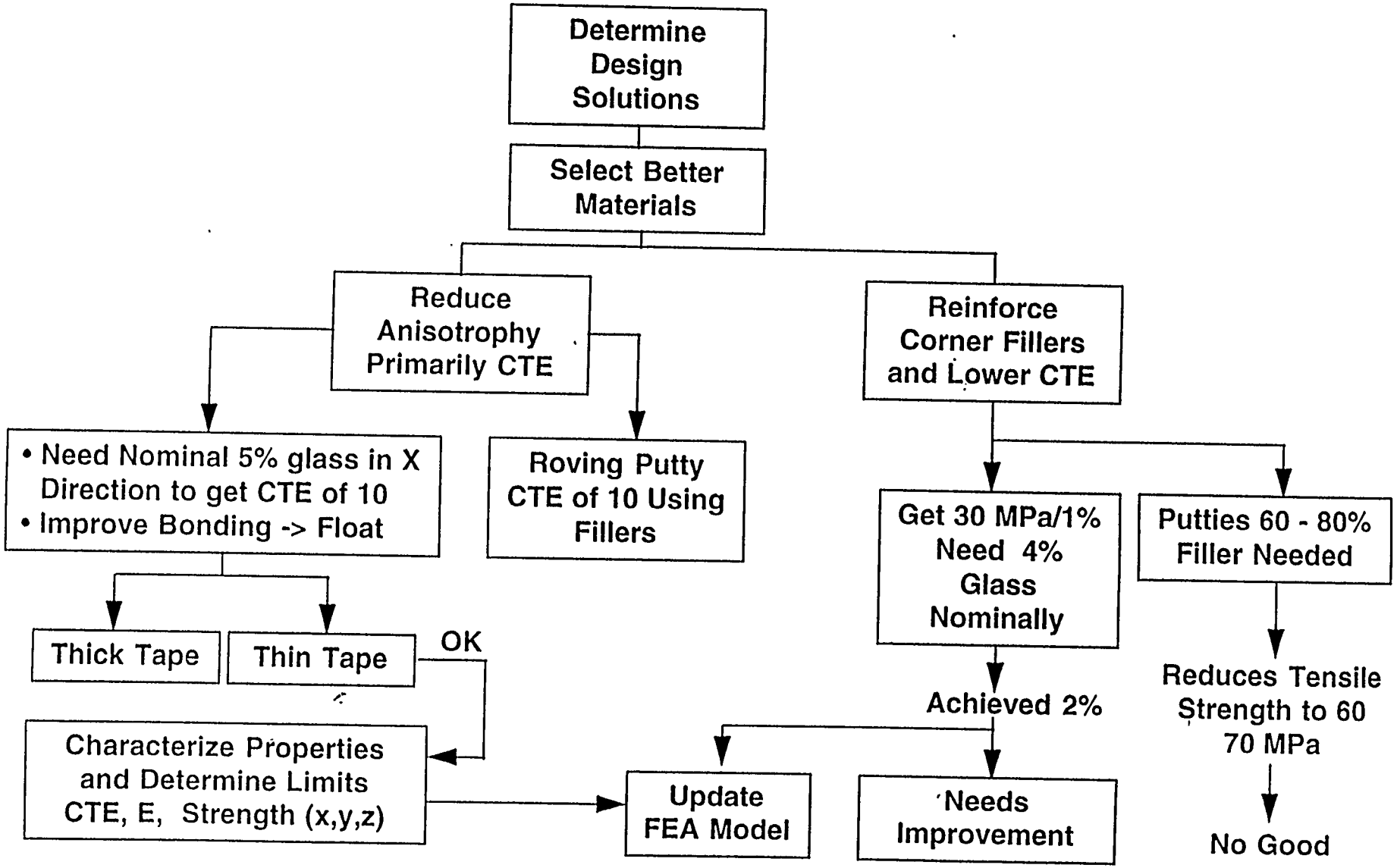

CONCLUSIONS

- Proposed Kapton optional insulation approaches performed electrically as well as or better than the CDR baseline based upon as received condition and limited thermal cycling under liquid nitrogen
- Shell 826 epoxy system performed poorer than the CTD-101K resin system for interleaved Kapton/glass insulation configurations
- Kapton/slip samples CA had the highest average break through stress at 25kV/mm with two 50% laps of 1 mil Kapton per conduit
- Option B-interleaved Kapton/dry glass, which is in principle fully bonded, performed well
- Kapton/slip options C and CA performed well electrically
- Hybrid cure approach using CTD-101K resin did not appear to work well as judged from sample cross sections which revealed lack of impregnation and full curing of the prepreg

1 X 2 INSULATION CONFIGURATIONS

DRAFT

Table 3.1 — Summary of insulation configurations as fabricated at Everson Electric for the 1x2 program.

SAMPLE TYPE	KAPTON WRAP (DuPont Type H, 0.051 mm thickness)	GLASS WRAP (TTI, S-2, 0.223 mm 4-Harness Satin Finish Weave)	BARRIER (G-10)	EPOXY SYSTEMS	CONDUIT
A- Baseline	None	2-50%	0.36 mm G-10 Sheet	CTD-101K & Shell 826	Incoloy 908
B- Kapton/ Dry Glass	Interleaved with S-2 glass 1-50% wraps	1-67% interleaved with Kapton on top	None	CTD-101K & Shell 826	Incoloy 908
C- Kapton Slip	2-50% wraps on conduit	2-50% overwraps	None	CTD-101K & Shell 826	Incoloy 908
CA- Adhesive Kapton Slip	2-50% counter wraped on conduit	1-50% & 1-Butt overwraps	None	CTD-101K	Incoloy 908 & 304LN
D- Kapton/ Prepreg	1-50% wrap centered on top of prepreg	1-50% ITER wet prepreg prototype, 0.229 mm	None	CTD-101K & CTD-112P (Prepreg resin)	Incoloy 908 & 304LN

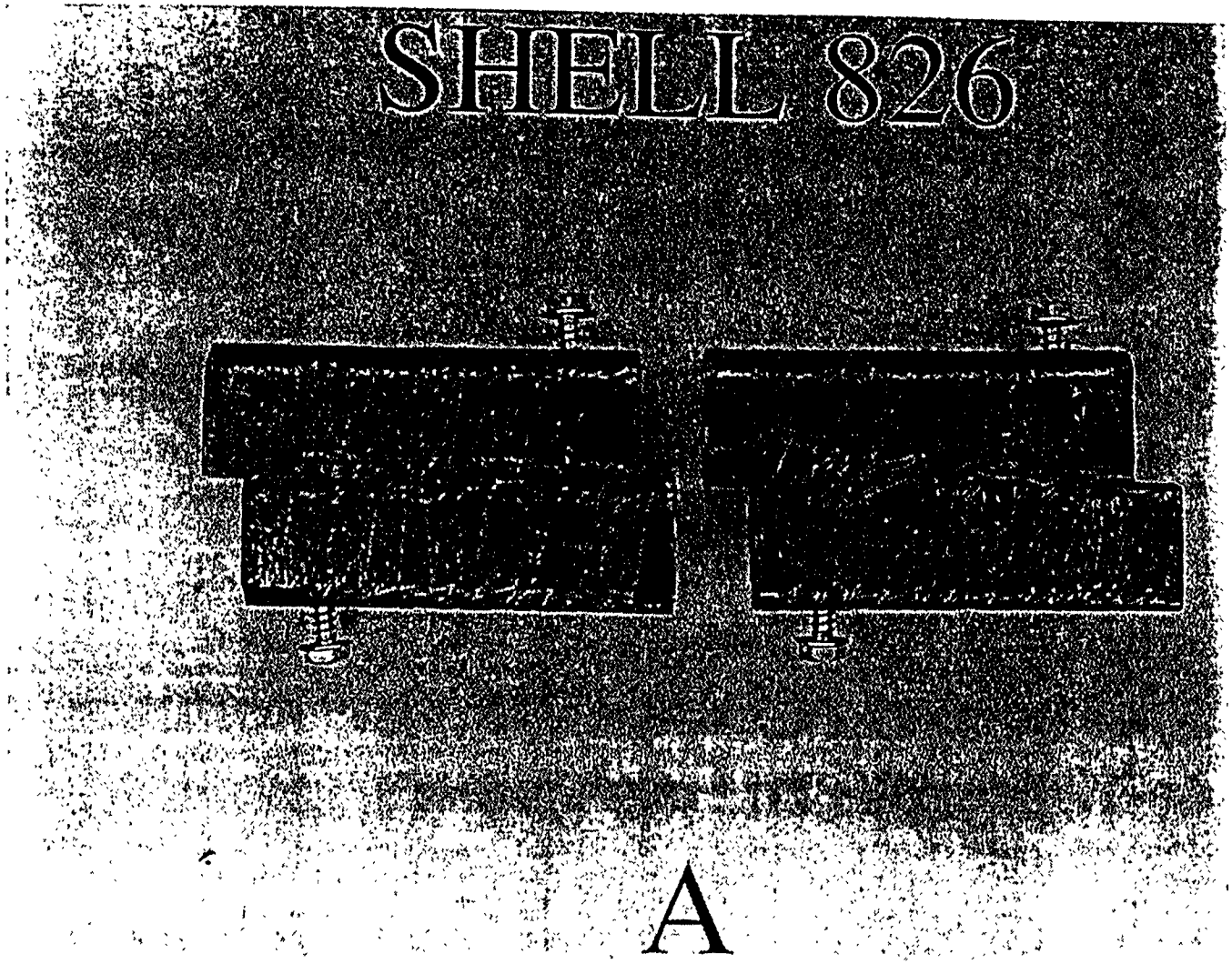

Figure 4.2 — Typical A-Baseline samples as received from Everson Electric with electrical lead posts screwed into top and bottom conduits.

1 X 2 Configurations & Test Plan

DRAFT

Table 5.1 — Summary of 1x2 configurations and test plan.

VPI BATCH	SAMPLE NUMBERS	CONDUIT MATERIAL	INSULATION SYSTEM Taping, Resin	THERMAL L-Nitrogen Shocks	TESTING Electrical(E) Sectioning(CS)
1	1,2	I-908(2)	A, CTD-101K	√	E, CS
1	1,2	I-908(2)	B, CTD-101K	√	E, CS
1	1,2	I-908(2)	C, CTD-101K	√	E, CS
2	1,2	I-908(2)	A, SHELL 826	√	E, CS
2	1,2	I-908(2)	B, SHELL 826	√	E, CS
2	1,2	I-908(2)	C, SHELL 826	√	E, CS
3	1,2,3	I-908(2) 304LN(1)	CA, CTD-101K	-	E,CS
3	1,2,3	I-908(2) 304LN(1)	D, CTD-101K	-	E, CS

1 X 2 Samples Hipot Testing

DRAFT

Table 5.9 — Failure Hipot testing in air for TPX 1x2 samples

SAMPLE NUMBER	INSULATION SPACING mm	HIPOT FAILURE VOLTAGE (40 kV max ; 50 μA Trip) kVdc		
		1 st Test	2 nd Test	3 rd Test
1-1A	1.880	-	-	-
1-2A	1.956	37.5 (E)	11.0 (E)	10.0 (E)
2-1A	2.007	38.5 (S,P)	-	-
2-2A	2.007	39.2 (I)	40 (WS)	-
Models A	Av Failure Stress	19.3 kV/mm		
1-1B	1.740	-	-	-
1-2B	1.588	38.0 (I)	38.5 (I)	38.5 (I)
2-1B	1.780	38.0 (E)	30.0 (E)	19.8 (I)
2-2B	1.690	36.7 (I)	32.7 (I)	36.0 (S,P)
Models B	Av Failure Stress	22.3 kV/mm		
1-1C	1.793	-	-	-
1-2C	1.830	38.0 (I)	37.8 (I)	40 (WS)
2-1C	1.868	38.5 (E)	18.0 (E)	16.0 (E)
2-2C	1.882	33.8 (E)	22.5 (E)	-
Models C	Av Failure Stress	19.8 kV/mm		
3-1D	1.562	-	-	-
3-2D	1.549	37.0 (S,P)	12.0 (S,P)	-
3-3D	1.579	34.0 (S,P)	6.0 (S,P)	-
Models D	Av.Failure Stress	22.7 kV/mm		
3-1CA	1.511	-	-	-
3-2CA	1.575	40 (WS)	-	-
3-3CA	1.575	39.0 (E)	-	-
Models CA	Av Failure Stress	25.1 kV/mm		

WS - Withstand
I - Internal fault
P - Puncture of turn insulation
S - External side fault
E - External end fault

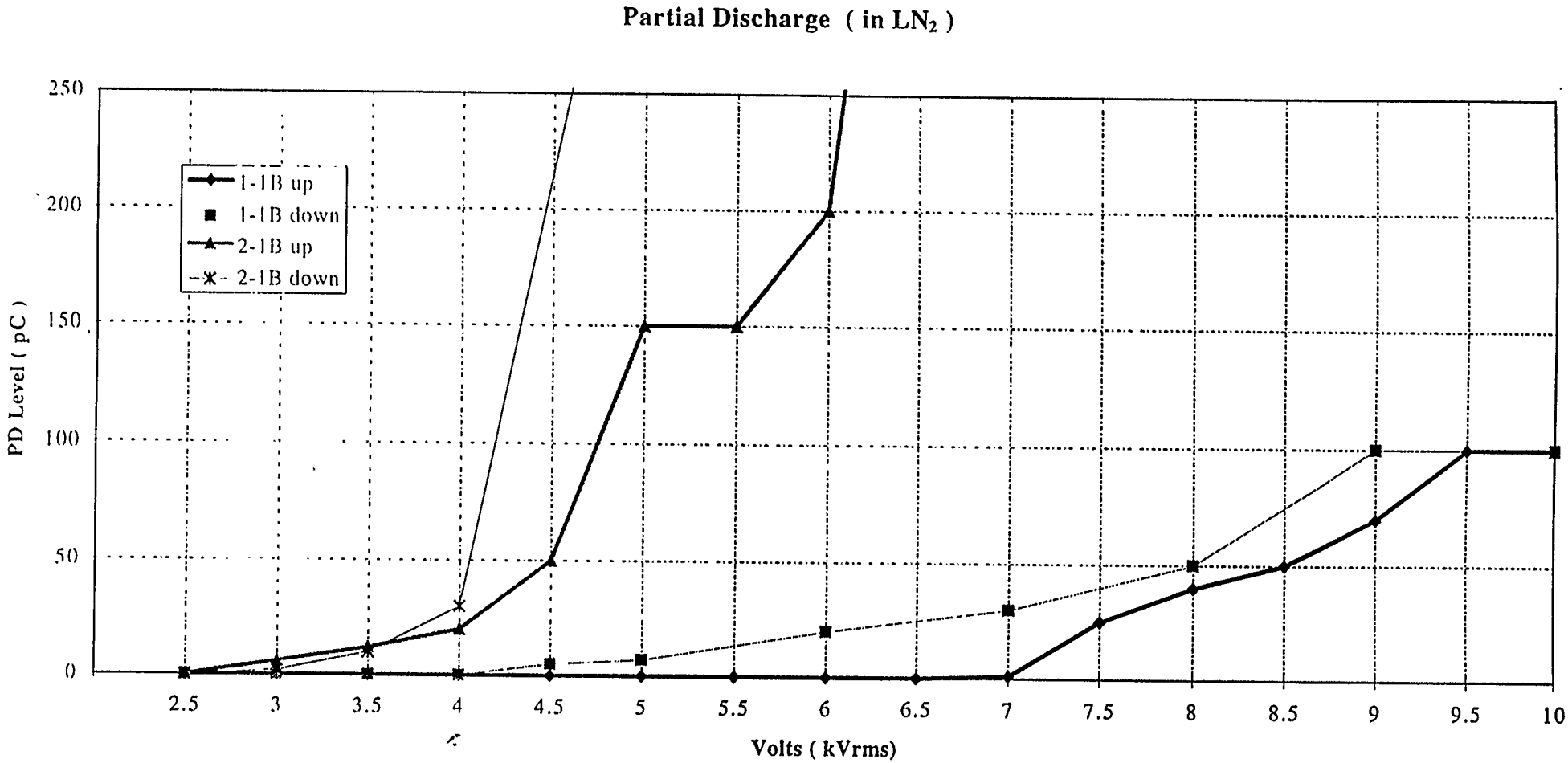

Figure 5.3 — Comparison of partial discharge for Shell 826 (1-) and CTD-101K (2-) 1B samples under liquid nitrogen after thermal cycling.

Road Map to Resolution of Insulation Design

DRAFT

3 X 3 Model Testing "Touch Reality"

- Validate FEA Modeling
- Assess Impact of Mechanical Damage on Electrical Integrity
- Provide Discriminators for Design Selection Electrical & Mechanical
- Evaluate Testing Techniques that Expose Weaknesses Leading to Large Scale Testing

To FEA Modeling

- Mechanical Conditioning that Exposes Weaknesses
- Significance and Role of Cracks
  - Micro-Cracks
  - Macro-Cracks

- 3X3 Sample Program (impact of electrical, mechanical and thermal stresses)
  - Matrix for six samples including baseline, araldite, kapton with adhesive
  - Full electrical testing at room temperature but with emphasis on partial discharge so that progressive deterioration can be seen
  - Subject to LN2 cold shock and retest at room temperature
  - Apply compressive and shear loads at LN2 and retest at room temperature
    - Cross head load and displacement for modulus measurement
  - Machine sample to provide
    - cross sections to polish and look for cracks
    - sample for composite shear measurement

3 X 3 Sample Configurations

DRAFT

Table 1 — 3x3 Coil Sample Configurations

Name Insulation System	Conduit Insulation System	Filler Material	Barriers Plate	Nominal Sample Length
Sample #1 CDR Baseline	2D S-glass Double thick	Glass Roving-Epoxy	G11- Micarta	150 mm (6 inches)
Sample #2 Option 1(e)-R Slip Plane Option	Kapton @ the conduit 2D weave overwrap	Glass Roving-Epoxy	None	250 mm (10 inches)
Sample #3 CDR Baseline w / Araldite	2D S-glass	Araldite Filled Epoxy (Low therm. expansion)	G11- Micarta	250 mm (10 inches)
Sample #4a Option 1(e) Interim Baseline	Kapton @ the conduit 3D weave overwrap	3D weave S-2 Glass	None	130 mm (5 inches)
SPARE Sample #4b Option 1(e) Interim Baseline	Kapton @ the conduit 3D weave overwrap	3D weave S-2 Glass	None	130 mm (5 inches)
Proposed Sample #5a Hybrid Prepreg	Kapton - Interleaved with 2D Glass Prepreg 3D weave Overwrap	3D weave S-2 Glass	None	130 mm (5 inches)
SPARE Sample #5b Hybrid Prepreg	Kapton - Interleaved with 2D Glass Prepreg 3D weave Overwrap	3D weave S-2 Glass	None	130 mm (5 inches)
Sample #6a Cigar Roll	3D weave S-2 Glass Overwrap	3D weave S-2 Glass	None	130 mm (5 inches)
SPARE Cigar Roll	3D weave S-2 Glass	3D weave S-2 Glass	None	130 mm (5 inches)

3 X 3 Test Set-up

DRAFT

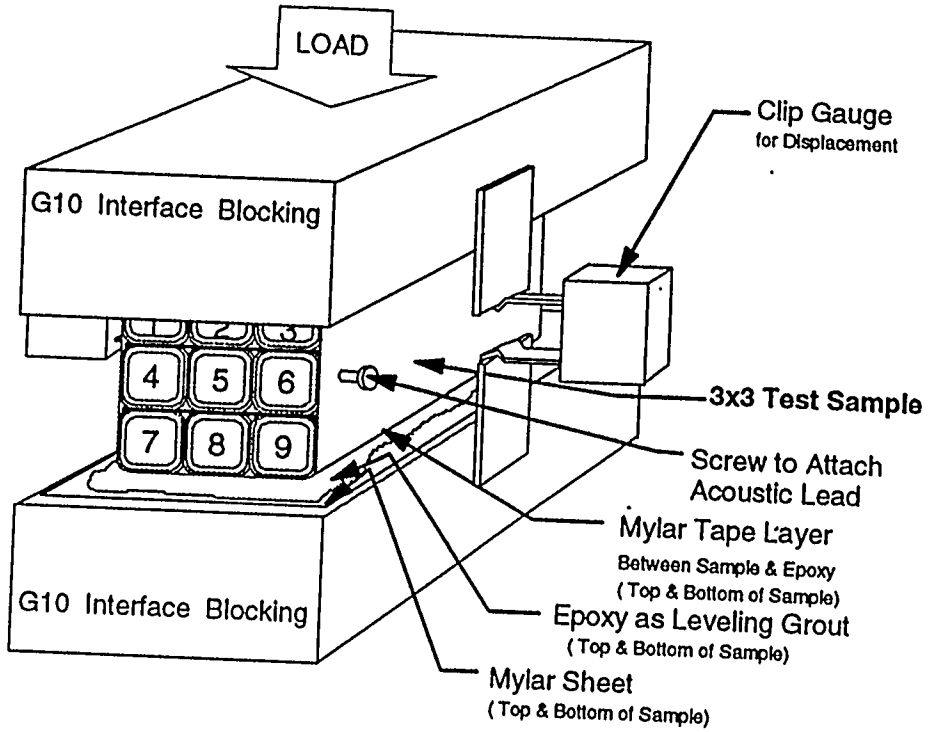

Figure 7 — 3x3 Sample Prepared for Testing

Typical 3 X 3 Test Sample

DRAFT

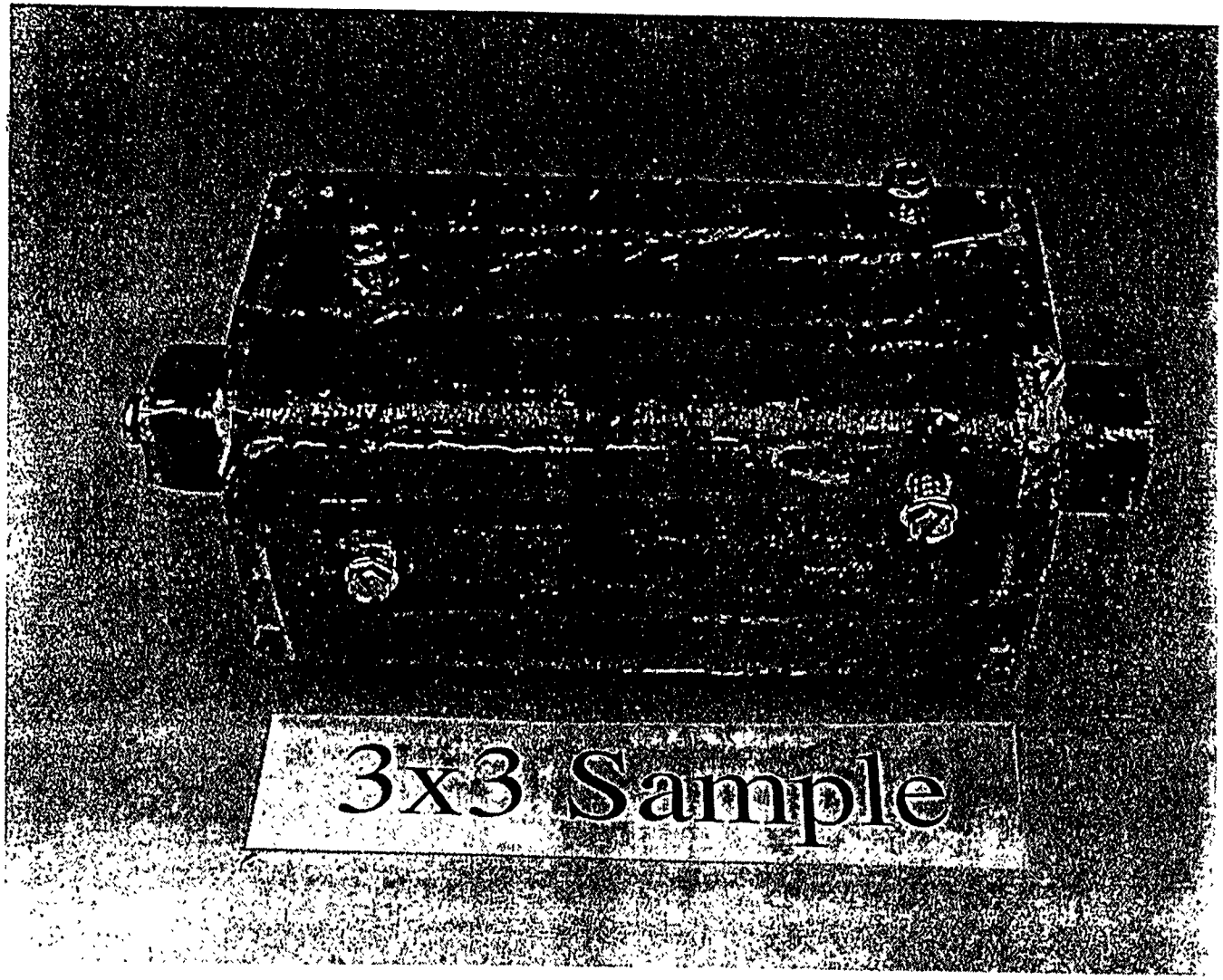

Figure 3 — Side View of a Typical 3x3 Sample

Table 6 — Comparative Finite Element Results 3x3 Vs. 6x10 Coil

Units = N/m²		CDR Baseline 6x10 coil		3x3 coil @ 42 MPa 15000 mech. cycles		3x3 coil @ 84 MPa Expected Failure	
		Laminar	Inter-Lam.	Laminar	Inter-Lam.	Laminar	Inter-Lam.
Conduit Wrap Insulation							
Cool down	Tension	60E+6	60E+6	20E+6	20E+6	Same as For 15000 cycles	
	Compression	-59E+6	-108E+6	-40E+6	-23E+6		
	Shear	-	69E+6	-	21E+6		
Cool Down & Vertical Id Plus EM Load for 6x10	Tension	88E+6	44E+6	27E+6	20E+6	53E+6	39E+6
	Compression	-90E+6	-142E+6	-90E+6	-108E+6	-177E+6	-217E+6
	Shear	-	96E+6	-	82E+6	-	157E+6
Cruciform Filler Material		Fiber Dir.	Inter-Fiber	Fiber Dir.	Inter-Fiber	Fiber Dir.	Inter-Fiber
Cool down	Tension	82E+6	150E+6	28E+6	78E+6	Same as For 15000 cycles	
	Compression	0	-107E+6	0	-30E+6		
	Shear	-	75E+6	-	26E+6		
Cool Down & Vertical Id Plus EM Load for 6x10	Tension	116E+6	136E+6	25E+6	100E+6	31E+6	114E+6
	Compression	0	-105E+6	0	-112E+6	-20E+6	-214E+6
	Shear	-	93E+6	-	24E+6	-	27E+6
Barrier Insulation Sheet		Laminar	Inter-Lam.	Laminar	Inter-Lam.	Laminar	Inter-Lam.
Cool down	Tension	61E+6	109E+6	26E+6	34E+6	Same as For 15000 cycles	
	Compression	-93E+6	109E+6	-54E+6	-30E+6		
	Shear	-	71E+6	-	1E+6		
Cool Down & Vertical Id Plus EM Load for 6x10	Tension	93E+6	91E+6	48E+6	17E+6	109E+6	34E+6
	Compression	-68E+6	-141E+6	000E+0	-131E+6	000E+0	-239E+6
	Shear	-	63E+6	-	997E+3	-	997E+3

3 X 3 Testing Sequence

DRAFT

Table 4 — 3x3 Testing Sequence

		Sample #1 CDR Baseline	Sample #2 Slip Plane Option	Sample #3 CDR Baseline W/ Araldite	Sample #4b Interim Baseline 3d Wrap& Rov	Sample #5a Hybrid Prepreg	Sample #6 Cigar Roll
1	Initial Electrical Tests	√	√	√	√	√	√
2	1->2 Cool Downs to 77K	√	√	√	√	√	√
3	7500 Compressive Load Cycles ①	28 ±14 MPa	28 ±14 MPa	28 ±14 MPa	28 ±14 MPa	28 ±14 MPa	28 ±14 MPa
4	Warm up to Room Temperature	√	↓	↓	↓	↓	↓
5	Electrical Tests	√	↓	↓	↓	↓	↓
6	Cool Down to 77K	√	▼	▼	▼	▼	▼
7	7500 Compressive Load Cycles	28 ±14 MPa	28 ±14 MPa	28 ±14 MPa	28 ±14 MPa	28 ±14 MPa	28 ±14 MPa
8	Warm up to Room Temperature	√	√	↓	√	√	√
9	Electrical Tests	√	√	↓	√	√	√ ⑤
10	*Sample Sectioned after 15000 cycles*	√	▼	↓	▼	▼	√ ⑥
11	Cool Down to 77K	√ ②	√	▼	√	√	√ ⑥
13	Mechanical Compressive Failure	87.2 MPa	73.8 MPa	76.4 MPa	85.9 MPa	86.2 MPa ③	62.9 MPa
14	Warm up to Room Temperature	√	√	√	√	√	√
15	Final Electrical Tests	▼	√	√	√		
16	*Sample Sectioned after "Mech. Failure"*	√	√	√	√	√	
17	Compressive Test to Distruction	89.9 Mpa ④					

① Nominal compressive pressure during test ±5%
② Sample was 150mm (6 in) long now sectioned piece is 75mm. long.
③ Sample buckled prematurely resulting in significant structural damage
④ Sample tested to buckling was about 38mm. long and had not previously been taken to "failu
⑤ Sample failed electrical testing
⑥ Testing continued on 57mm long section from the sample previously tested for 15000 cycles

3 X 3 Summary of Mechanical Results

DRAFT

Table 5 — Summary of Mechanical Results

3x3test wk4

24-May-95

		Sample #1 CDR Baseline	Sample #2 Slip Plane Option	Sample #3 CDR Baseline W/Araldite	Sample #4b Interim Baseline 3d Wrap& Rov	Sample #5a Hybrid Prepreg	Sample #6 Cigar Roll
Apparent Compressive Modul ①②							
Cycle 4	(Gpa)	9.6	7.9	9.7	8.1	9.7	9.1
Cycle 15000	(Gpa)	9.2	7.6	9.3	7.8	9.2	9.0
Percent decrease		3.5%	3.3%	3.8%	4.2%	5.8%	1.0%
Apparent Deformation ③							
Pressure Load	(Mpa)	44.7	41.3	41.8	42.6	42.7	42.6
Cycle 4	(cm)	0.034	0.038	0.031	0.038	0.031	0.034
Cycle 15000	(cm)	0.036	0.039	0.032	0.039	0.033	0.034
Mechanical Compressive Failure							
Cycle Number		15006	15038	15009	15021	15016	15005
Failure Pressure	(Mpa)	87.2	73.8	76.4	85.9		62.9
Def. at "Failure"	(cm)	0.071	0.089	0.069	0.089		0.086
Buckling Load	(Mpa)	89.9				86.2	
Def. at Buckling	(cm)	0.113				0.101	
Original Sample Dimensions:							
Length (Sample)	(mm)	152	254	254	127	127	127
Length (Conduit)	(mm)	137	252	252	122	122	122
Width	(mm)	74.0	71.6	70.9	72.5	71.8	71.8
Height	(mm)	74.6	71.6	71.5	72.6	71.7	71.2

1) Apparent Compressive Modulus = E = Load x height / (Loaded cross-section area x measured deformation)

2) Comparative apparent modulus (E) from finite element analysis (GPa) 10.8

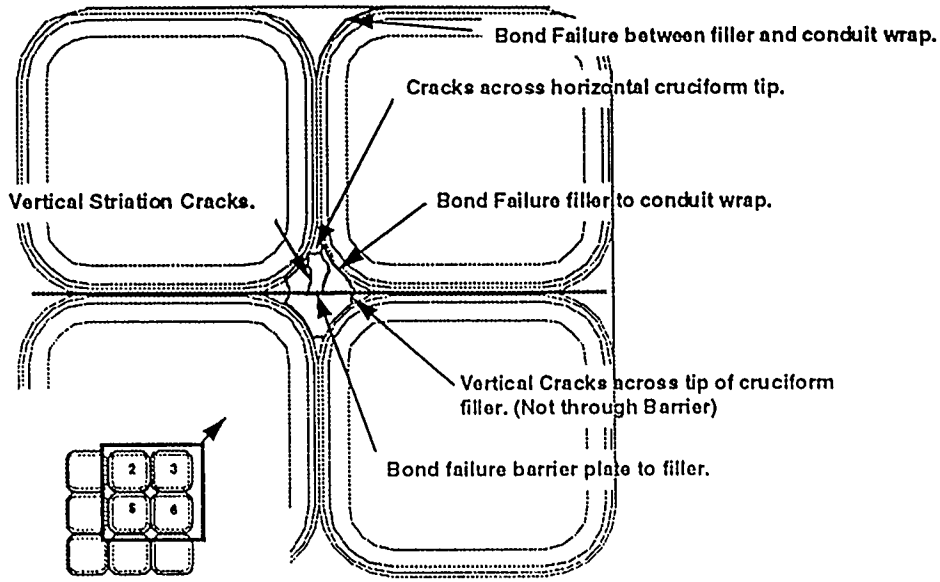

Figure 10 — Damage to Sample 1 After 15,000 Cycles

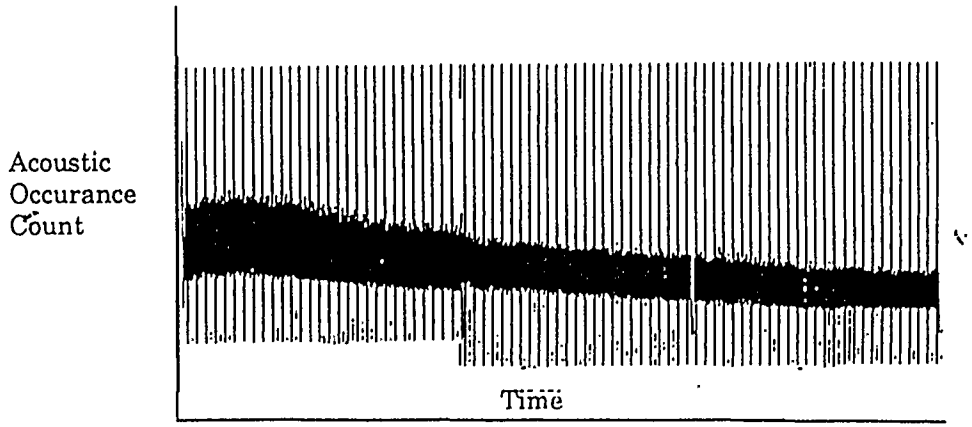

Figure 11 — Acoustic Emission During Cyclic Testing on Sample 1

3 X 3 - Disection of Sample #3

DRAFT

Figure 18 — Dissection of Sample 3 - CDR Baseline with Arolidite Filler

3 X 3 Mechanical Testing Conclusions

DRAFT

- CDR Baseline design performed without insulation failure at the 10kVdc Hipot level through 3 thermal and 15,000 mechanical cycles. Failed 20kVdc Hipot for all turn pairs except one
- The adhesive (XMPI) Kapton Slip Plane design had no turn failures at 20kVdc Hipot following 3 thermal and 15,000 mechanical cycles with minimum turn-to-turn withstand of 27kVdc
- Kapton/Slip Plane design had a withstand of at least 31kVdc for all turns after 2 thermal and 15,000 mechanical cycles. Following mechanical failure only one turn pair failed 20kVdc
- The Hybrid Prepreg/3-D design failed 20kVdc Hipot
- The all 3-D Cigar Roll design with 3-D woven cloth failed all turn pairs at 20kVdc Hipot following 2 thermal and 15,000 mechanical cycles

3 X 3 Electrical Testing Evolution

DRAFT

Table 2 — Electrical Testing Evolution and Matrix for 3x3 Models

MODEL	DIELECTRIC PROPERTIES			DC HIPOT AR/15,000/Failure				PARTIAL DISCHARGE To 10 kVrms in 0.5 kVrms steps Average & Peak pC			AC LIFE TEST Selected Turn Pairs at 10 kVrms for 1 hr 7.2 LC at 6 kVrms/mm
	C pF	Loss %	IR Ω	10 kVdc 5s	20 kVdc 15s	16 kVdc 60s	40 kVdc Withstand Maximum	All pairs	Selected pairs	Selected pairs & <2000 pC	Selected Turn Pairs
1-CDR Baseline	√	√	√	√				√			
3-CDR Baseline with Araldite	√	√	√			√	All pairs (1 Fault)		√		
2-Slip Plane Option	√	√	√		√	√	Only after cycling			√	
4B-Interim Baseline	√	√	√		√	√	All ext. pairs until two faults			√	√ After Failure
5A-Hybrid Prepreg	√	√	√		√	√	All ext. pairs until two faults			√	√ After 15,000 cycles
6A-3-D Cigar Roll	√	√	√		√	√	All ext. pairs until two faults				

3 X 3 60Hz Life Testing

DRAFT

Table 4. Summary of 1 Hour, 60 Hz Life Test for TPX 3x3 Models 4B, 5A and 6A

MODEL	TEST SEQUENCE	CONFIGURATION OF TEST LEADS		TEST VOLTAGE	PARTIAL DISCHARGE LEVELS		TEST DURATION		FAILED TURN PAIRS
		HV Turn	GD Turns	kVrms	pCav	pCpk	hrs	LC	
4B-Interim Baseline	After mech. failure	7	4 & 8	7.0	5.5	300 to 1500	1.0 Pass	7.2	Withstand
	After mech. failure	3	2 & 6	10.0	18.0	3000 to 6000	0.2 Fail	1.4	3-6 Short
5A-Hybrid Prepreg	After 15,000 cycles	5	All outside turns	10.0	35.0	1200 to 2400	0.5 Fail	3.6	5-2 Short
	After mech. failure (Model too damaged for life testing)	-	-	-	-	-	-	-	-
6A-3-D Cigar Roll	After 15,000 cycles								
	After mech. failure								

Table 5. Correlation of Failure Cracks and Hipot Failure for Model 3-CDR Baseline with Araldite Fillers

TURN PAIR	OBSERVED CRACK	WITHSTAND 16 kVdc, 1min TEST	FAILURE VOLTAGE kVdc	TYPE OF FAILURE
1-2 Turn-Turn	No	P	21 WS	Ext Leads
2-3 Turn-Turn	Yes	F	7	Internal
4-5 Turn-Turn	Yes	F	Short	(AR Test Fault)
5-6 Turn-Turn	Yes	F	7.5	Internal
7-8 Turn-Turn	Yes	F	6	Internal
8-9 Turn-Turn	Yes	F	9.5	Internal
1-4 Layer-Layer	No	P	19.5 WS	Ext Discharge
2-5 Layer-Layer	Yes	F	14.5	Internal
3-6 Layer-Layer	Yes	F	15.2	Internal
4-7 Layer-Layer	Yes	F	13	Internal
5-8 Layer-Layer	Yes	F	14.2	Internal
6-9 Layer-Layer	No	P	19.5	Internal

Measure Material Property & Limits

DRAFT

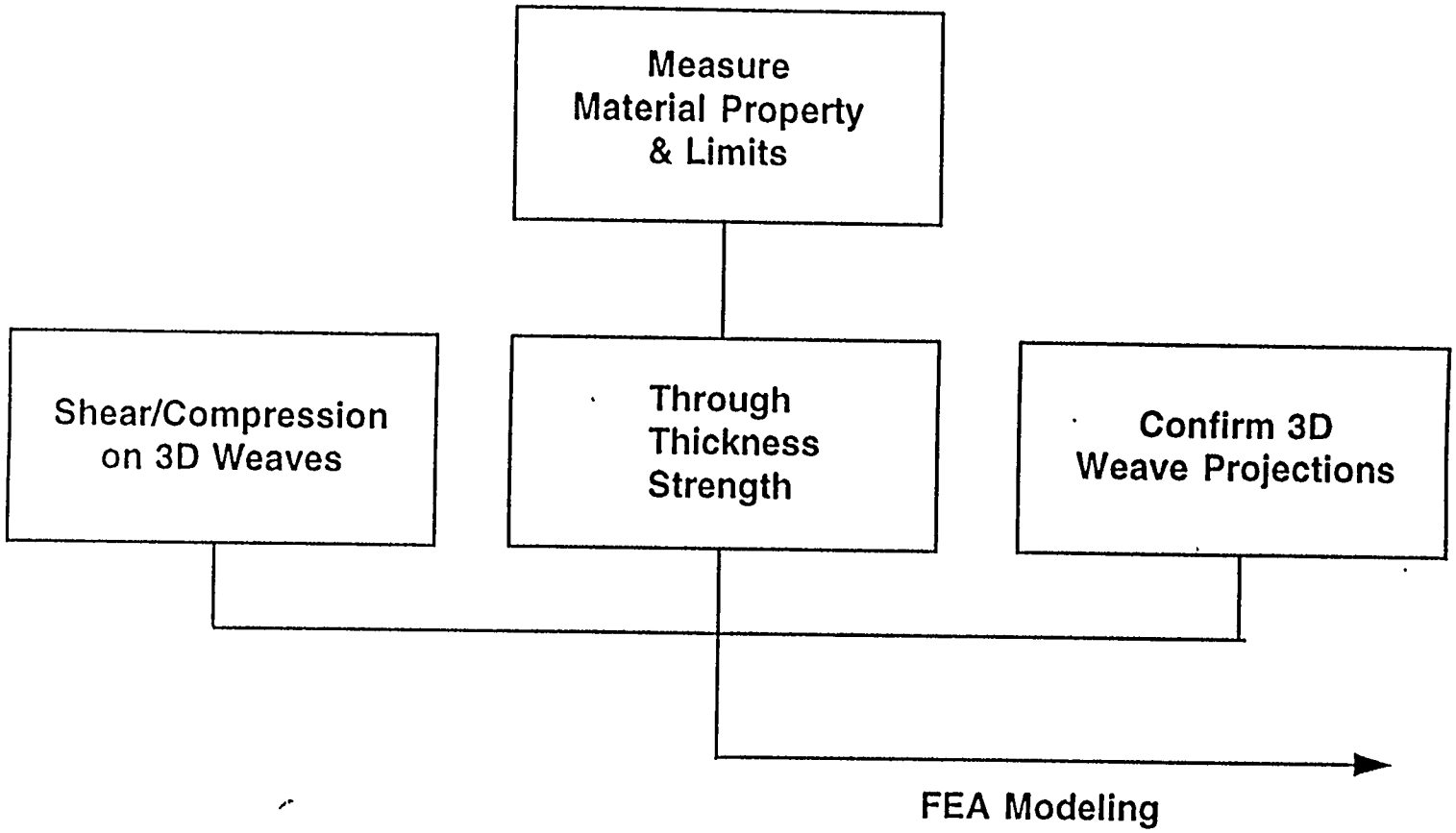

CTD Bond Strength Test Samples

DRAFT

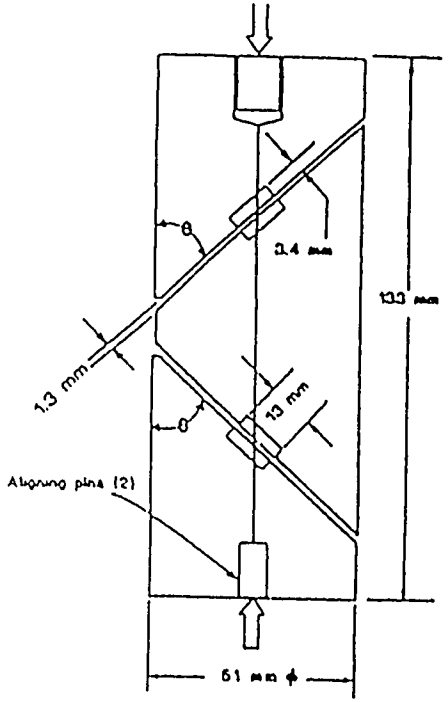

Figure 1 Test fixture used to simultaneously load 13 x 13 mm sandwich-type test specimens in shear and compression.

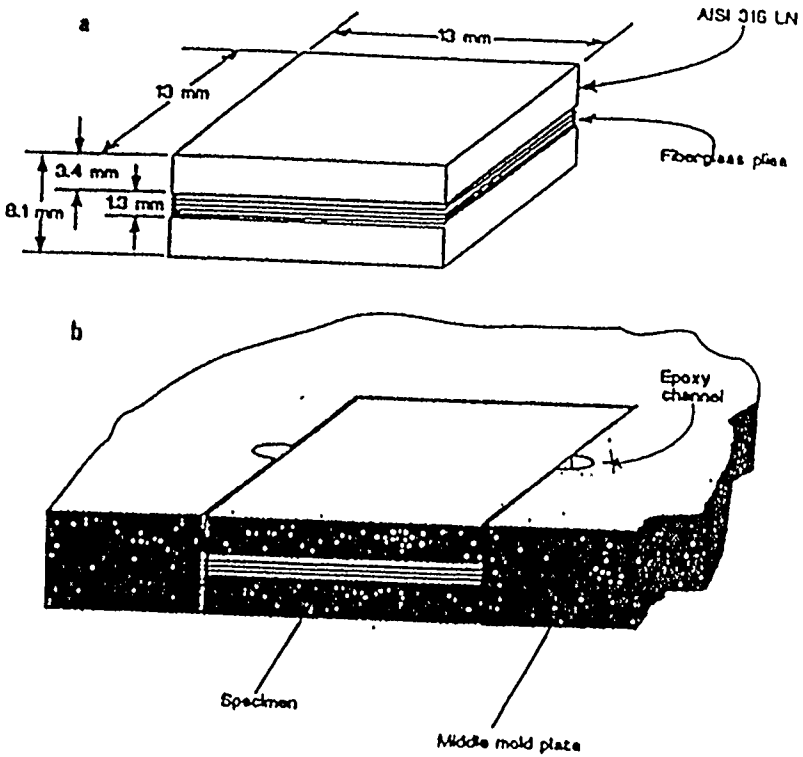

Figure 2 a. Test specimen (schematic).
b. Specimen in mold used for vacuum epoxy impregnation first stage cure. Upper and lower flat plates w channels for epoxy infiltration are not shown.

Bond Strength Test Matrix

DRAFT

Composite Insulation Systems (Rev 1, 12-07-94)

Resin System	Metallic Substrate	Barrier Material	Number of Samples	Shear/Compression Tests (3 ∠'s, 77 K)
Batch #1 CTD 101K	316 SS	Kapton	6	2 Samples each ∠
"	Incoloy 908	Kapton	6	2 Samples each ∠
"	Incoloy 908	G 10 or 11CR	4	2 Samples, 2 ∠'s
Batch #2 CTD-1PFS Prepreg with Shell 826 VPI	316 SS	Multiple Kapton / glass layers	6	2 Samples each ∠
Shell 826	Incoloy 908	Kapton	6	2 Samples each ∠
"	Incoloy 908	G 10 or 11CR	4	2 Samples, 2 ∠'s
Batch #3 CTD 112P Prepreg S-2 glass	Incoloy 908 & 316 SS	Multiple Kapton / glass layers	8 & 8	2 Samples each ∠ 2 in reserve 2 Samples each ∠ 2 in reserve
Batch #4 CTD 101K	Incoloy 908 & 316 SS	Multiple Kapton / glass layers	8 & 8	2 Samples each ∠ 2 in reserve 2 Samples each ∠ 2 in reserve
Batch #5 CTD 112P Prepreg with CTD 101K VPI	Incoloy 908 & 316 SS	Multiple Kapton / glass layers	8 & 8	2 Samples each ∠ 2 in reserve 2 Samples each ∠ 2 in reserve

TPX Shear/Compression Data Summary

	Chip Run	Resin System	Fabric Style	Metal	Barrier	Test Angle (°)	Shear Strength (MPa)	Std. Dev. (MPa)	Compr. Strength (MPa)	Std. Dev. (MPa)	Failure Mode	
1A	143A	CTD-101K	Satin	316	Kapton (1)	15	90.6	0.1	24.3	0.0	C/K	
						45	108.9	25.7	108.8	25.7	C/K	
						75	158.5		591.4		C/K	
1B	143B	CTD-101K	Satin	908	Kapton (1)	15	75.1	6.4	20.1	1.7	C/K,A/K	
						45	99.3	10.4	99.3	10.4	C/K	
						75	150.5		561.4		C/K	
1C	143C	CTD-101K	Satin	908	G10CR	15	28.6		7.7		A/M	1
						45	28.6		28.6		A/M	1
						75	255.4		952.8		C	
2A	145A	CTD-1PFS/ Shell 826	Satin	316	Kapton (4)	15	87.8	7.7	23.5	2.1	C/K	
						45	128.3	10.4	128.3	10.4	C/K	
						75	146.5		546.6		C/K	
2B	145B	Shell 826	Satin	908	Kapton (1)	15	99.0	3.5	26.5	0.9	C/K	
						45	158.0	3.8	158.0	3.8	C/K	
						75	183.8		685.7		C/K	
2C	145C	Shell 826	Satin	908	G10CR	15	0.0		0.0		A/M	1
						45	173.0		173.0		C	
						75	263.3		982.1		C	
3A	142A	CTD-112P	Satin	316	Kapton (4)	15	52.3	0.6	14.0	0.1	C/K	
						45	68.8	8.0	68.8	8.0	A/K,C/K	
						75	76.7		286.1		C/K	
3B	142B	CTD-112P	Satin	908	Kapton (4)	15	53.8	3.4	14.4	0.9	A/K	
						45	58.8	5.1	58.8	5.1	A/K	
						75	81.2		302.8		C/K	
		RETEST reserve specimens				**45**	**82.6**	**4.0**	**82.6**	**4.0**	C/K	
4A	141A	CTD-101K	Satin	316	Kapton (4)	15	50.7	7.2	13.6	1.9	C/K	
						45	88.2	41.6	88.1	41.6	A/K	2
						75	137.3		512.1		C/K	
4B	141B	CTD-101K	Satin	908	Kapton (4)	15	55.4	8.1	14.9	2.2	A/K	
						45	105.9	2.4	105.9	2.4	C/K	
						75	135.2		504.5		C/K	
		RETEST reserve specimens				**45**	**120.5**	**11.7**	**120.5**	**11.7**	C/K	
5A	144A	CTD-112P/ CTD-101K	Satin	316	Kapton (4)	15	70.9	0.8	19.0	0.2	A/K	
						45	139.9	1.3	139.8	1.3	A/K	
						75	137.6		513.2		C/K	
5B	144B	CTD-112P/ CTD-101K	Satin	908	Kapton (4)	15	80.7	6.9	21.6	1.8	C,C/K	
						45	133.0	4.5	133.0	4.5	C/K,A/K	
						75	133.7		498.7		A/K	
		RETEST reserve specimens				45	133.1	9.2	133.1	9.2	C/K,A/K	

Notes:

1. Adhesive failures at metal are highly unusual, and render data suspect.
2. One specimen failed low. Ignoring that data point, strength is 117 MPa.

TPX Shear/Compression Data Summary

	Chip Run	Resin System	Fabric Style	Metal	Barrier	Test Angle (°)	Shear Strength (MPa)	Std. Dev. (MPa)	Compr. Strength (MPa)	Std. Dev. (MPa)	Failure Mode
6A	160A	CTD-101K	Satin	316	Kapton (4)	15	59.2	10.4	15.9	2.8	A/K
						45	122.5	4.3	122.5	4.3	A/K, C/K
						75	131.4		490.0		C/K
6B	161A	CTD-112P/ CTD-101K	Satin	316	Kapton (4)	15	31.4	3.8	8.4	1.0	A/K
						45	102.5	4.7	102.5	4.7	C/K
						75	120.5		449.6		A/K
7A	159A	Shell 826	Satin	316	Kapton (4)	15	84.4	11.8	22.6	3.2	C/K, A/K
						45	144.0	6.3	144.0	6.3	C/K, A/K
						75	147.2		549.1		A/K
7B	162A	CTD-112P/ Shell 826	Satin	316	Kapton (4)	15	44.7	7.3	12.0	2.0	A/K
						45	106.2	11.2	106.2	11.2	C/K
						75	123.3		460.0		C/K
8A	160B	CTD-101K	Satin	316	G11CR(1)	15	104.1	16.5	27.9	4.4	C,G,AM
						45	180.9	3.3	180.9	3.3	C,C,G
						75	271.1		1011.3		C,G
8B	164A	CTD-101K	3-D weave	316	None	15	82.1	15.2	22.0	4.1	C, AM
						45	172.5	1.3	172.4	1.3	C, AM
						75	253.0		943.7		C
8C	164B	CTD-101K	Plain	316	Kapton (4)	15	8.5	2.1	2.3	0.6	A/K
						45	28.0	5.1	28.0	5.1	A/K
						75	132.5		494.2		A/K
9A	159B	Shell 826	Satin	316	G11CR(1)	15	110.2	20.1	29.5	5.4	C, C,G
						45	184.6	1.2	184.5	1.2	C
						75	252.8		943.1		C,G
9B	163A	Shell 826	3-D weave	316	None	15	63.7	9.1	17.1	2.4	C,AM
						45	173.4	3.2	173.4	3.2	C
						75	244.9		913.6		C
9C	163B	Shell 826	Plain	316	Kapton (4)	15	47.1	10.2	12.6	2.7	A/K
						45	111.4	7.8	111.4	7.8	A/K
						75	145.5		542.9		C/K
10A	165A	Shell 826	Satin	316	CTD-101G	15	87.8	22.3	23.5	6.0	B,AB,C,AM
						45	154.6	8.2	154.6	8.2	B
						75	226.6		845.2		B,C
10B	165B	Shell 826	Satin	316	AV 1580	15	64.7	4.6	17.3	1.2	B
						45	109.5	4.7	109.5	4.7	B
						75	196.3		732.2		B,C

Failure Modes:

A/M-Adhesive failure at the metal

A/K-Adhesive failure at the Kapton

C-Cohesive failure in the composite

C/K-Cohesive failure in the Kapton, tearing of the Kapton

C,AM-Failure located at metal interface; epoxy adhering to surface; some composite damage

A/B - Adhesive failure at the Barrier

B - Breakage/cohesive failure in the barrier

Conclusions of CTD Chip Tests

- Essentially no difference in bond strength between 316LN and Incoloy 908
- VPI improves prepreg properties (50-100%)
- Prepreg + VPI improves VPI at low compressive strength but essentially the same otherwise
- Shell 826 better than CTD101-K in single ply tests (20-60%)
- Multiple plys degrade shear strength
  - 26-45% at low compression
  - 10-15% at high compression
- Kapton/Prepreg plus VPI less than half the strength of glass Kapton layups
  - 37MPa at zero compression
- Plain weave fabric does not impregnate as well as satin weave

Specimen Configuration and Fabrication

Fabrication of through thickness tension specimens is nearly identical to fabrication of the shear/compression specimens described previously. The major difference is that the metal specimen parts are longer, and have a hole drilled in them to accommodate the tension clevises. The mold used for specimen fabrication is also thicker to accommodate the greater specimen length. Both prepreg and resin transfer molding fabrication techniques may be used with this specimen configuration. All insulation systems were fabricated to a nominal glass volume fraction of 0.50. The through thickness tension specimen is illustrated in the following sketch.

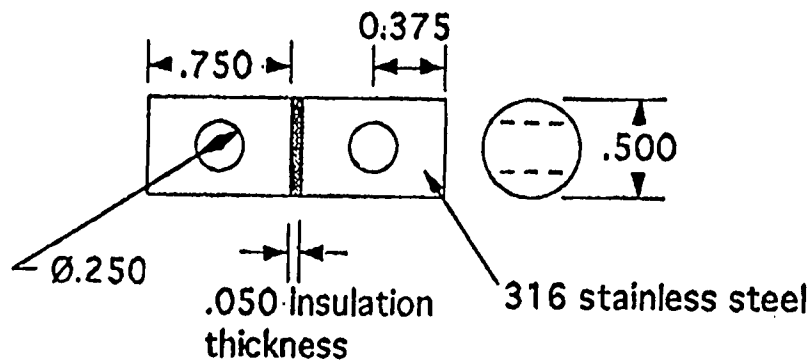

Insulation Through Thickness Tension Testing

DRAFT

TPX THROUGH THICKNESS TENSION DATA SUMMARY						
Run No.	Reinforcement	Resin System	Barrier	Strength Average (MPa)	Standard Deviation	Coefficient of Variation
TT1A	TTI 3-d weave	Shell 826	None	52.5	6.7	0.13
TT1B	6781 8-h	Shell 826	None	57.3	2.5	0.04
TT2A	6781 8-h	CTD-112P	Kapton 200HA	29.5	10.2	0.35
TT2B	6580 8-h	CTD-112PF	Kapton 200HA	37.7	9.6	0.25
TT2C	6781 8-h	CTD-112P	None	28.2	1.0	0.04
TT3A	6781 8-h	CTD-112P	Kapton 200HA	20.1	7.9	0.39
TT3B	6580 8-h	CTD-112PF	Kapton 200HA	27.5	9.1	0.33
TT3C	6781 8-h	CTD-112P	None	24.4	3.7	0.15
TT4A	TTI 3-d weave	Shell 826	None	46.4	6.7	0.14
TT4B	6781 8-h	Shell 826	None	63.1	8.1	0.13

Insulation Through Thickness Tension Testing

DRAFT

- Conclusions
  - Interlaminar tensile strengh is much higher than expected
    - nominally 50 MPa versus 10-15 MPa projected
  - Satin weave shows higher strength than 3D weave
    - attributed to less float and reduced ability to intermingle glass fibers
  - Prepreg plus Kapton exhibits much lower strength (50%)

Insulation Through Thickness Tension Testing

DRAFT

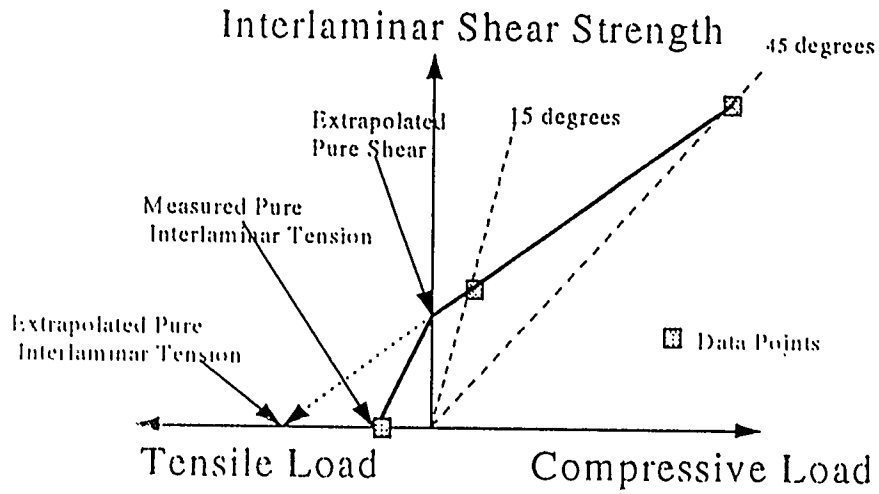

Composite Type	Pure Interlaminar Tension (MPa)	Pure Interlaminar Shear (MPa)	Compressive Slope
3D S2 glass tape	46	52	0.7
8 harness satin weave S2 glass tape	60	95	0.5

Large Scale Verification Test

Phillip Sanger

Road Map to Resolution of Insulation Design

DRAFT

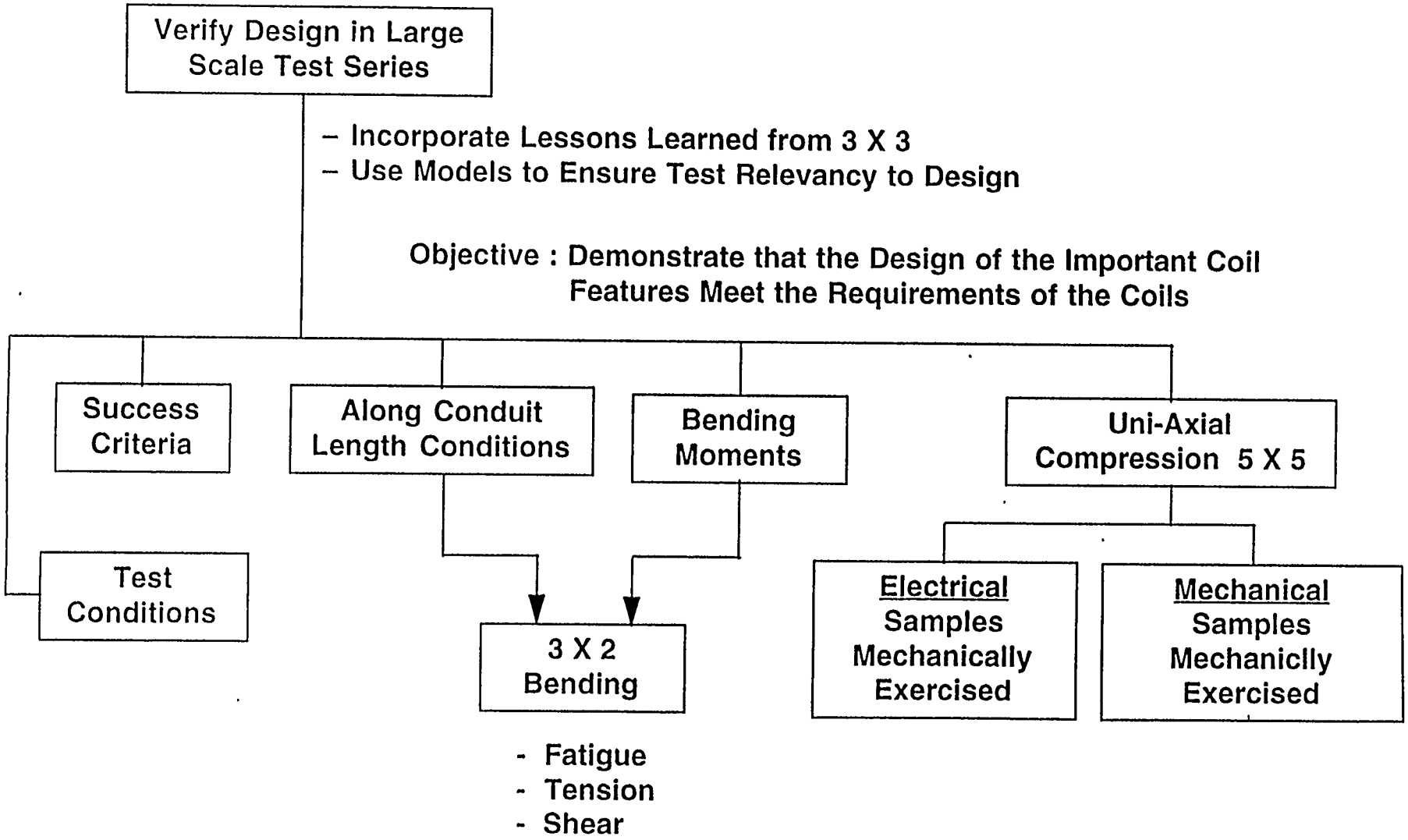

Objective

- Demonstrate by the **test** of a **representively sized** sample that the **preliminary insulation design** of the **important** coil features **meet** the **requirements** of the TPX coils

5 X 5 and 3 X 2 Test Arrangements

DRAFT

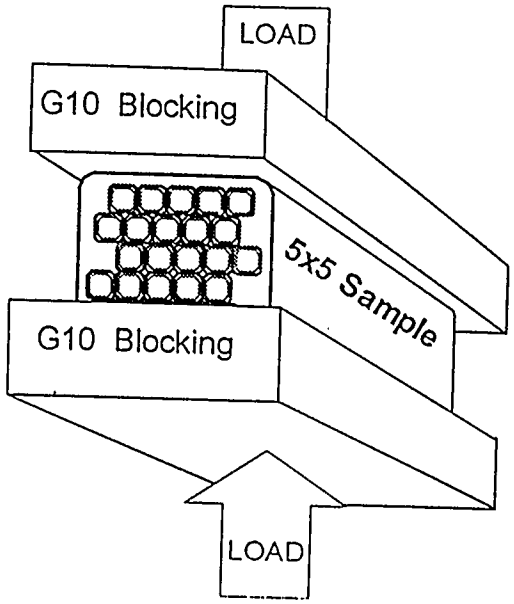

5x5 CS Coil CompressionTest

3 Point Bending Test

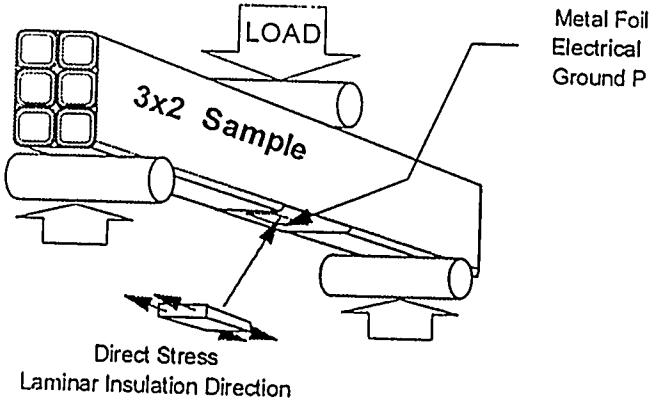

5x5 TF Coil CompressionTest

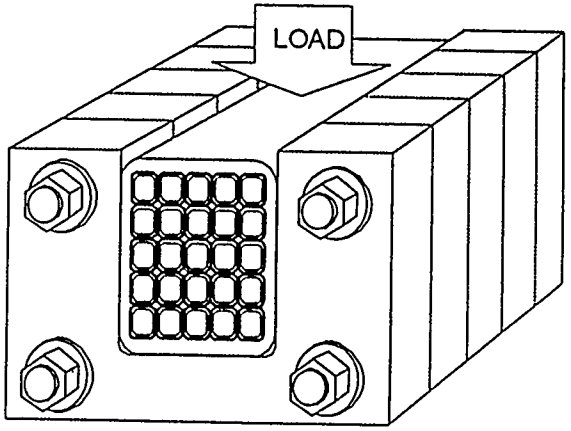

Figure 2-2 Schematic representation of the test loads.

Schematic of Test Program - Large Scale Testing

DRAFT

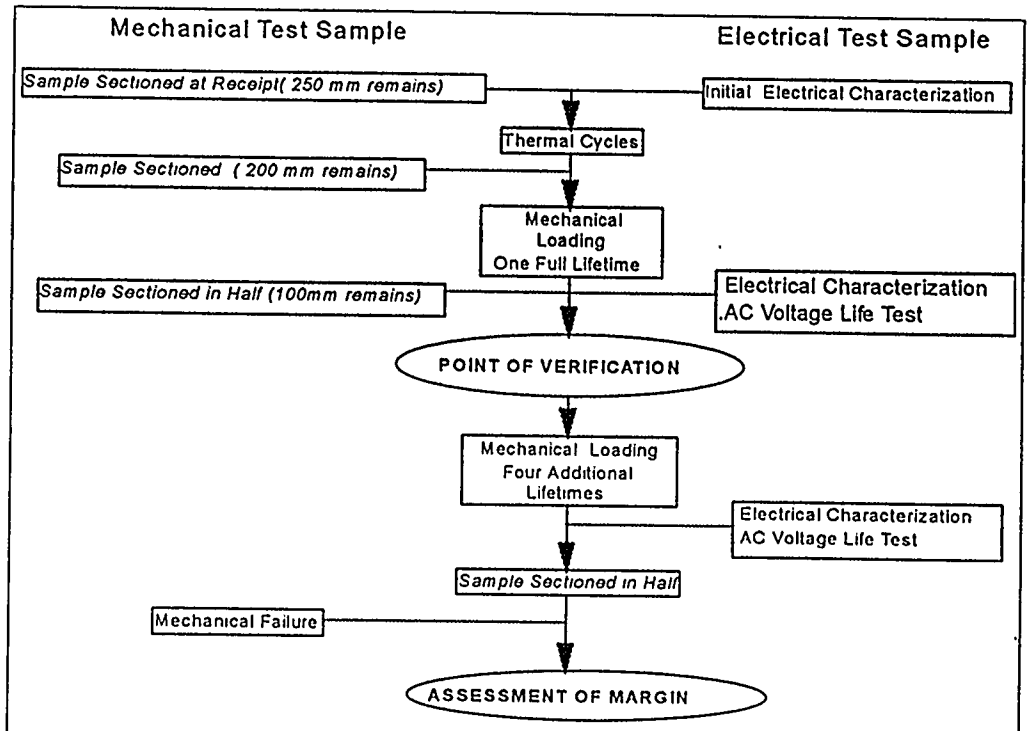

Figure 2-1Schematic representation of the test program.

Lessons Learned from 3 X 3 Testing

DRAFT

- Multiple samples are needed
  - i.e. combining electrical tests with mechanical testing require too much compromise
- Single axis compressive tests are not adequate to address all the important stresses
  - Tensile and shear stresses along the axis of conduit
  - Bending stresses
- Partial discharge testing is not sufficient to expose weaknesses and demonstrate design capability
  - Add 60 Cycle AC Life Testing
  - Ultimate breakdown Voltage

3 X 2 and 5 X 5 Electrical Acceptance Tests

DRAFT

- Recommended Acceptance Test Voltages
  - DC Test, 1 min voltage withstand, 50 microamp leakage current limit
  - AC Life Test, 15 min voltage endurance
  - AC LifeTest Stress Ratio = 1.414x(AC Test Voltage)/(Operating Voltage)

Table 3. Test Voltages for 3x2 & 5x5 Model Acceptance

INSULATION	OPERATING VOLTAGE Vmax	DC TEST VOLTAGE kVdc	AC LIFE TEST VOLTAGE kVrms	AC LIFE TEST STRESS RATIO
Turn-Turn	628 PF	10	6	13.5
Turn-Ground	7500 TF	16	-	-
Turn-Ground	4437 PF	-	10	3.2

Note: Test voltages same as recommended at at 05-03-95 TIM, Lynchburg, VA

Test Voltage Calculations

- Turn-Turn DC/AC Test Voltages (Driven by PF7 Coil)
  - *Peak Voltage* = (1.3x5.8)x628 = 4735 V
  - DC Test Voltage = 2x4735 + 1000 = 10,470 V = **10 kV, 1 min withstand**
  - AC Life Test = 10,470/1.7 = 6159 Vrms = **6 kVrms, 15 min duration**
- Turn-Ground DC Test Voltage (Driven by TF Line Lead)
  - Peak Voltage = 1.0x7500 V = 7500 V
  - DC Test Voltage = 2x7500 + 1000 = 16,000 V = **16 kV, 1 min withstand**
- Turn-Ground AC Test Voltage (Driven by PF5 Coil)
  - Peak Voltage = 1.8x4437 V = 7987 V
  - Equivalent DC Test Voltage = 2x7987 + 1000 = 16,973 V
  - AC Life Test = 16,973/1.7 = 9984 Vrms = **10 kVrms, 15 min duration**

3.2 ELECTRICAL:

1. The turn to turn insulation shall hold off 10 kV for 1 minute without arc discharge following a conditioning of 15 minutes at 6 kV rms.
2. The groundwall insulation shall hold off 16 kV for 1 minute without arc discharge between any turn and the ground plane following a conditioning of 15 minutes at 10 kV rms.

The above criteria will be tested with an instrument set to trip at a leakage current of 50 microamps.

3.1 MECHANICAL CRITERIA:

1. The force deflection curve of the sample shall not change by more than 10%.
2. No cracks extending completely across the glass/epoxy overwrap in the through thickness direction shall be allowed (see below for clarification of allowable cracks.)
3. No continuous in-plane delamination greater than the dimension of the insulation unit cell shall be observed (see sketches for further clarification).

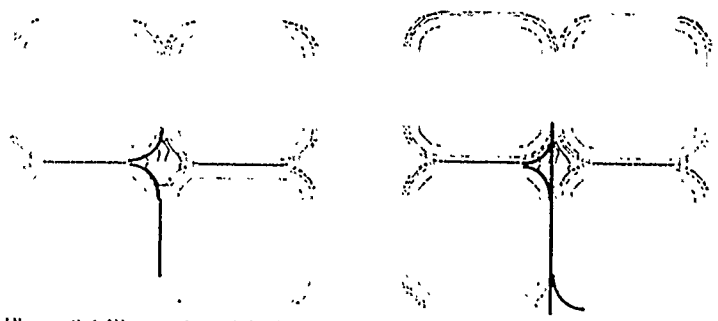

Figure 3-1 Illustration of the limiting cases for cracking in the unit cell of the winding pack represented by the 5x5 test samples

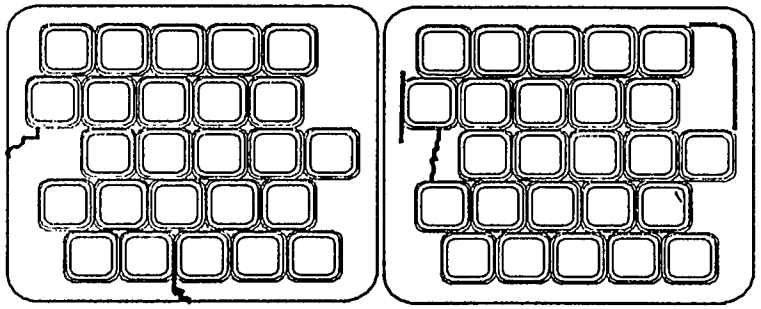

Figure 3-2 Illustration of both unacceptable (left) and acceptable (right) delaminations and cracking in the 5x5 sample used in the verification testing program

Comparison of Worst Case CS Coil Stress & Test Sample Stress

compare.xls

		A 5x5 Test Cooldown & 41MPa Press. Stress (MPa)	B 3x2 Test Cooldown & 90kN Force Stress (MPa)	C PDR Baseline Max Vert Comp & Cl Dn GT to 4K PF1 Lower, Eq16 Stress (MPa)	Comparison (A or B) / C
Turn Wrap	Interlaminar Compression	-127	-	-85.1	149%
	Interlaminar Tension	18.1	-	19.6	92%
	Laminar Compression	-253	-	-307	82%
	Laminar Tension	322	-	307	105%
	Cir. Laminar Tension	-	285	183	156%
	Interlaminar Shear	-92.6	-	-76.8	121%
Cruciform Filler Material	Compression	-95.4	-	-65.7	145%
	Tension	273	-	229	119%
	Circumfrential Tension	-	-	87.3	-
	Shear	77.7	-	70.9	110%
Conduit	SINT	988		744	133%
Transition Piece	Interlaminar Compression	-32.4	-	-33.8	96%
	Interlaminar Tension	164	-	297	55%
	Laminar Compression	-234	-	-184	127%
	Laminar Tension	11.7	-	236	5%
	Interlaminar Shear	39.9	-	87.8	45%
Ground Wall	Interlaminar Compression	-219	-	-242	90%
	Interlaminar Tension	35.2	-	80.3	44%
	Laminar Compression	-177	-	-303	58%
	Laminar Tension	135	-	145	93%
	Interlaminar Shear	80.4	-	134	60%

5 X 5 vs. Worst Case TF Coil Stresses Comparison

DRAFT

Table 4-7Comparison of Worst Case TF Coil Stress and 5x5 Test Sample

Stress Comparisons: Detailed Equatorial Model with Energized Coil to 5 x 5 Mockup Test Article under 36 MPa Pressure (Provided by B&W)					
	Sx (In Plane)	Sy (Thru-thick)	Sxy	Sz	Sint
Equatorial Model					
Conduit	-701 144	-85 20	<1	81 320	760
Kapton Layer	-198 66	-150 20	10	-167 5	
3D Overwrap	-301 254	-150 23	80	-51 167	
Corner Fill	-212 160	-260 60	75	1 100	
5X5 Model					
Conduit	-470 2.5	-66 1.3	<1	95 236	570
Kapton Layer	-106 42	-200 5	13	-122 10	
3D Overwrap	-160 208	-190 14	75	-150 160	
Corner Fill	-187 150	-169 73	74	-0.1 94	

* Stresses in MPa

Large Scale Verification Testing Program & Sequence

DRAFT

Table 7-1 Verification Testing Program & Sequence

5xtstseq wk4

		5x5 CS Coil Sample #A1 300mm	5x5 CS Coil Sample #A2 150mm	5x5 TF Coil Sample #B1 300mm	5x5 TF Coil Sample #B2 150mm	3x2 TF & PS Coil Sample #C1 300mm	3x2 TF & PS Coil Sample #C2 300mm
	Sample Sectioned at Reciept(250 mm remains)	√	no	√	no	no	no
1	Initial Electrical Characterization ①	no	√	no	√	√	√
2	Thermal Cycles RT to 77K	20 Cycles	20 Cycles	20 Cycle	20 Cycles	20 Cycles	20 Cycle
3	*Sample Sectioned (200 mm remains)*	√	no	√	no	no	no
4	Mechanical Loading @ 77K One Full Lifetime	31000 Cycles 14 to 41 MPA Compression	31000 Cycles 14 to 41 MPA Compression	6000 Cycl 0 to 36 MI ◀ Comp with side restraint ▶	6000 Cycles 0 to 36 MPA	31000 Cycles 0 to 90 kN 3Pt. Bending	31000 Cy 0 to 90 3Pt. Bendin
5	Electrical Characterization @ R.T. ①	no	√	no	√	√	√
6	AC Voltage Life Test @ R.T. ②	no	√	no	√	√	no
7	*Sample Sectioned in Half (100mm remains)*	√	no	√	no	√ ③	no
	POINT OF VERIFICATION	Testing Done Beyond this point is for information not verification					
8	Mechanical Loading @ 77K Four Additional Lifetimes	124000 Cycles 14 to 41 MPA Compression	124000 Cycles 14 to 41 MPA Compression	24000 Cycles 0 to 36 MPA ◀ Comp with side restraint ▶	24000 Cycles 0 to 36 MPA		124000 Cycle 60 ± 30 kN Bending
9	Electrical Characterization ①	no	√	no	√		√
10	AC Voltage Life Test	no	√	no	√		√ ③
11	*Sample Sectioned in Half*	*50 mm remains*	√	*50 mm remains*	√		√
12	Mechanical Failure	?? MPA		?? MPA			

Held In Reserve

Held In Reserve

① Turn to turn capacitance, partial discharge up to 10 KV, breakdown or 40 KV and Turn to ground capacitance, partial discharge up to 10 KV, breakdown

② 60 Cycle AC Voltage insulation life testing for 15 minutes at 10 KV.

③ Foil break down tests at 10 KV DC.

5 X 5 Sample Preparation

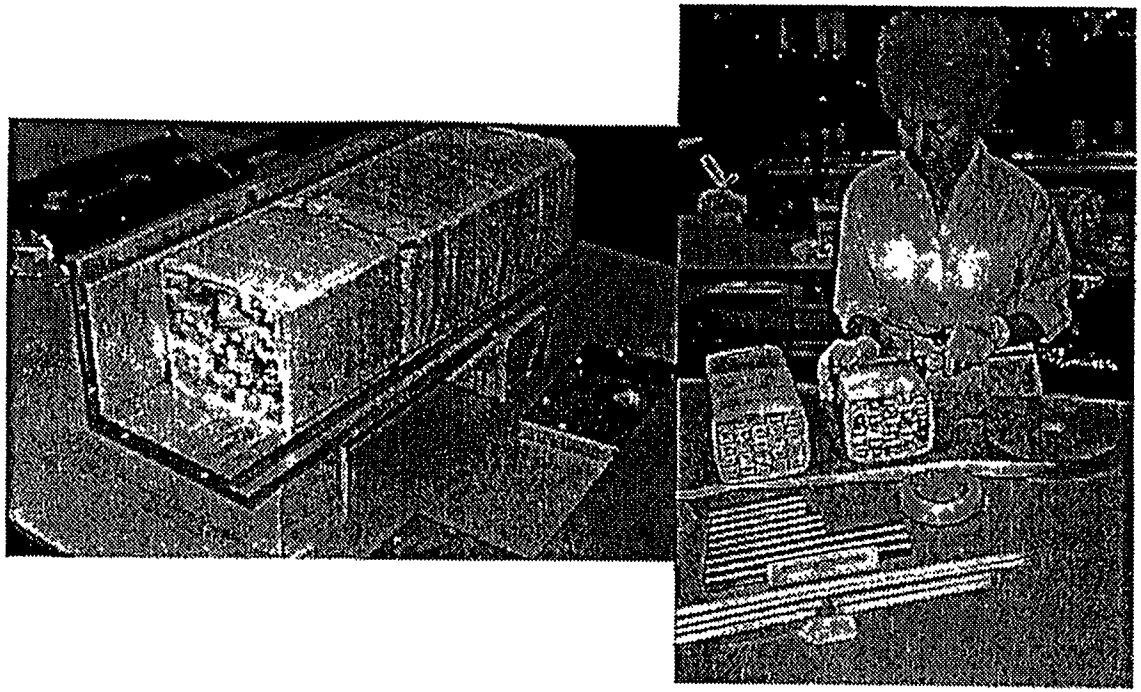

Figure 6-3 Insulated B1 and B2 5x5 samples and partial installation in mold.

3 X 2 and 5 X 5 Sample Configurations

DRAFT

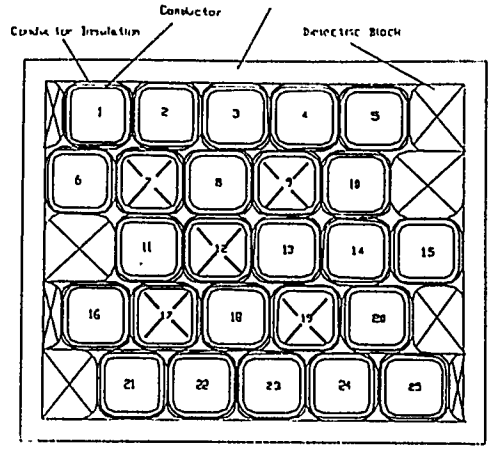

5x5 PF Sample A2

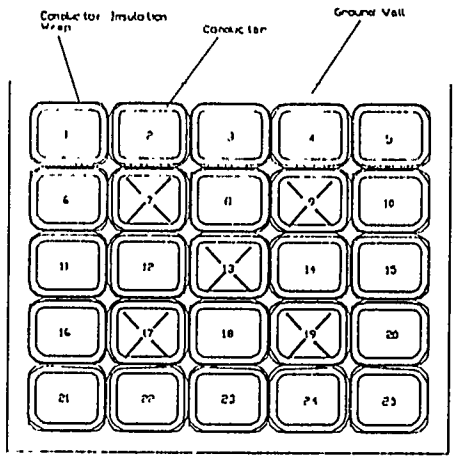

5x5 TF Sample B2

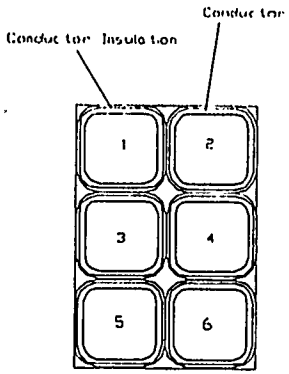

3x2 CS Sample C2

Figure 6-1Cross sectional configurations of 3x2 and 5x5 samples showing extended conductors (marked with an "X") and identification of conductors for insulation testing.

5 X 5 Test Set-up

DRAFT

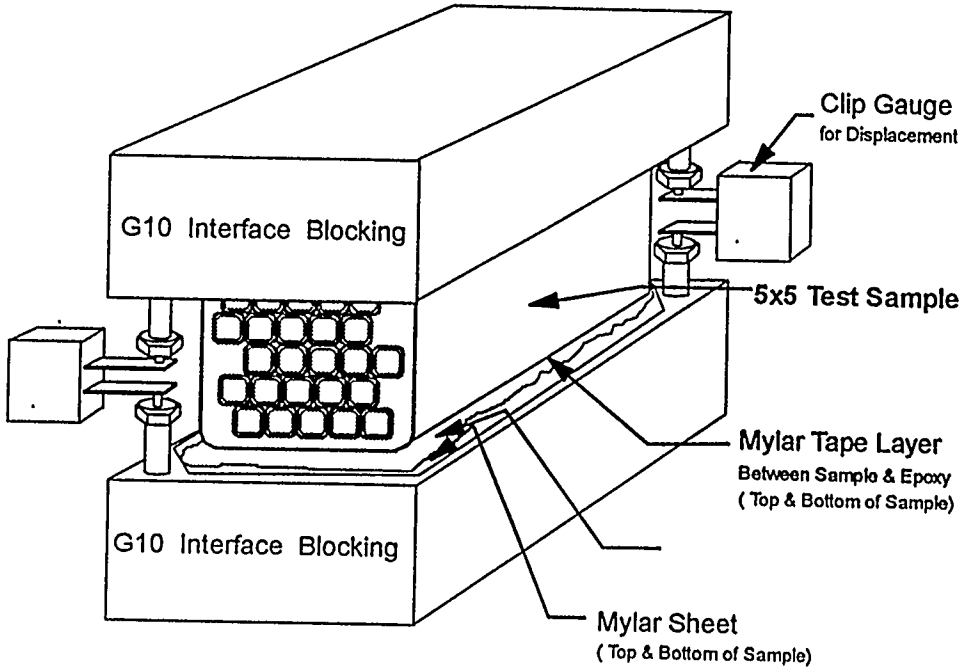

Figure 7-4 CS 5x5 Sample Prepared for Testing

Cross Section of CS 5 X 5 Sample

DRAFT

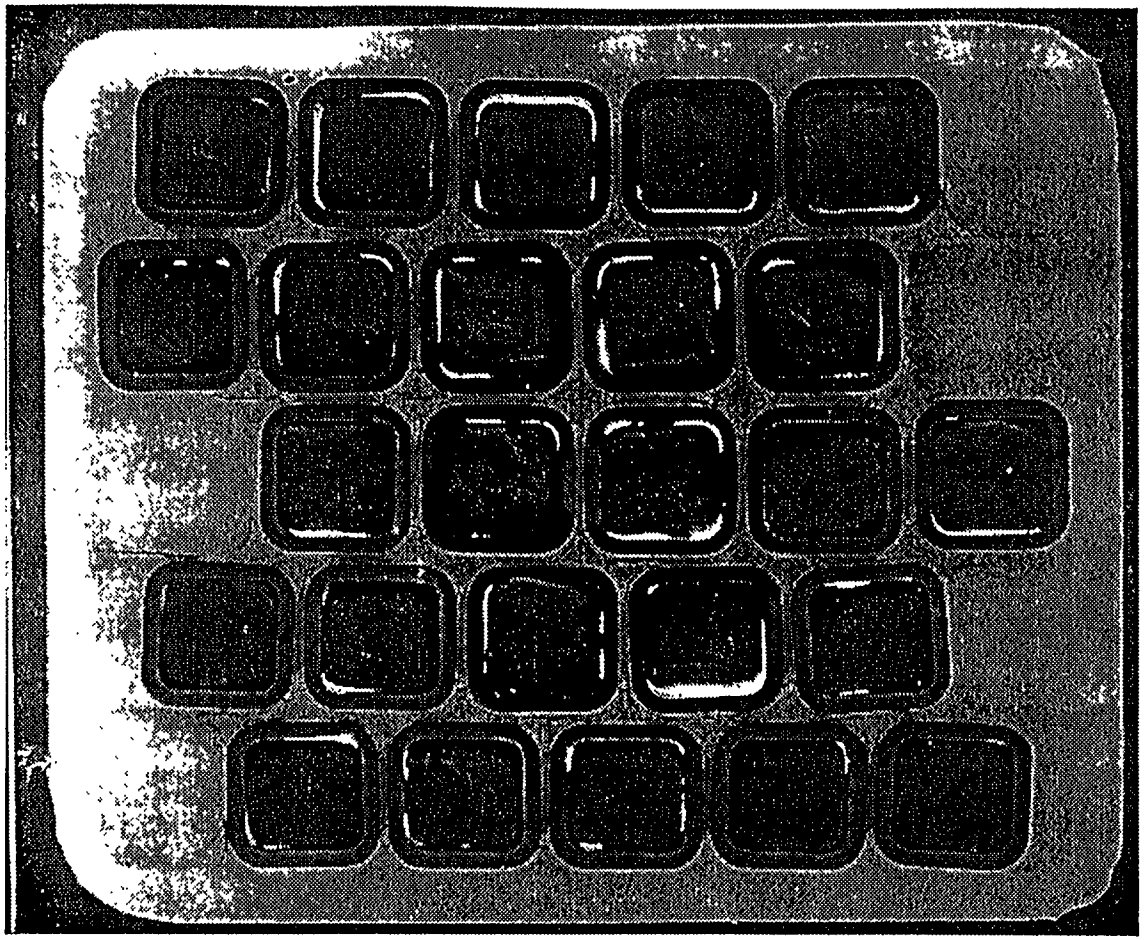

Figure 7-2 Sample A1 - Section 1 - As Manufactured

CS 5 X 5 Sample Cross Section After Thermal Cycles

DRAFT

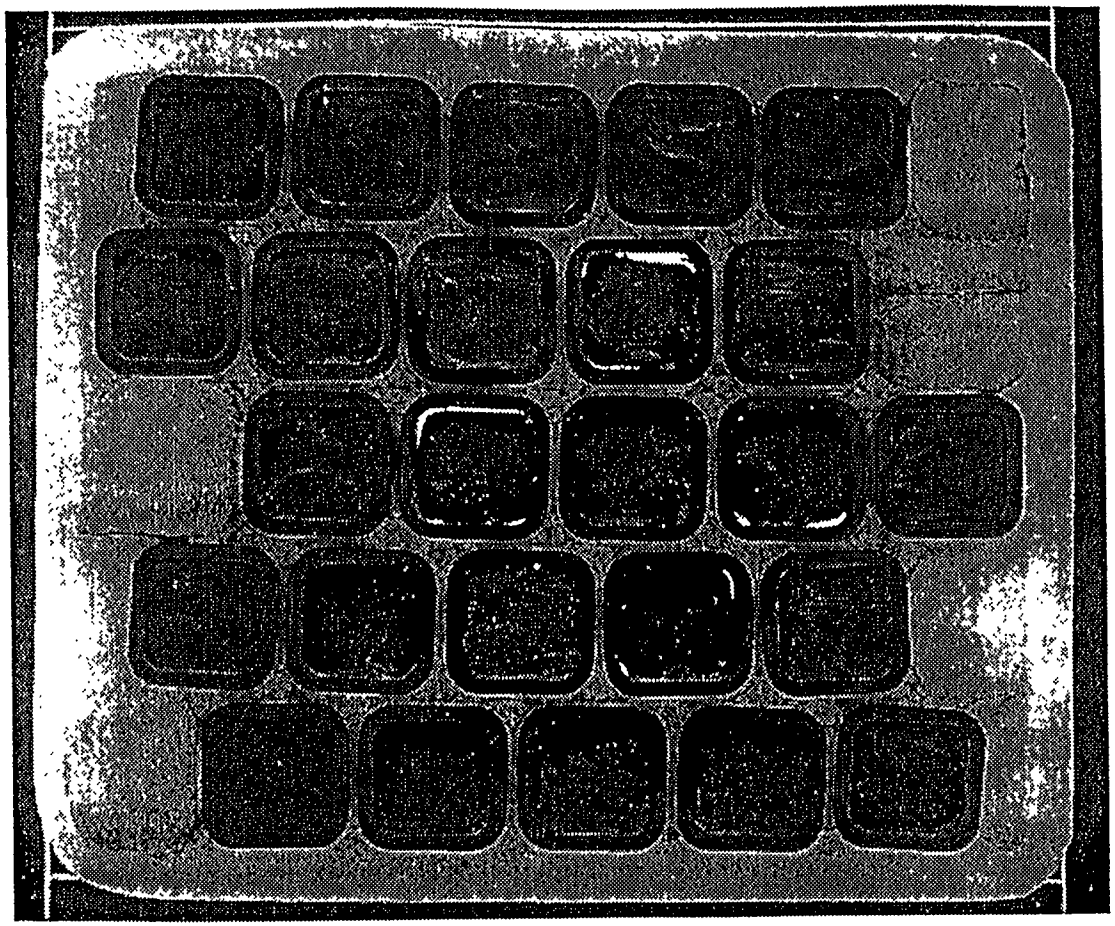

Figure 7-3 Sample A1 - Section 2 - After 19 Thermal Cycles.

CS 5 X 5 Sample Cross Section After Load Cycles

DRAFT

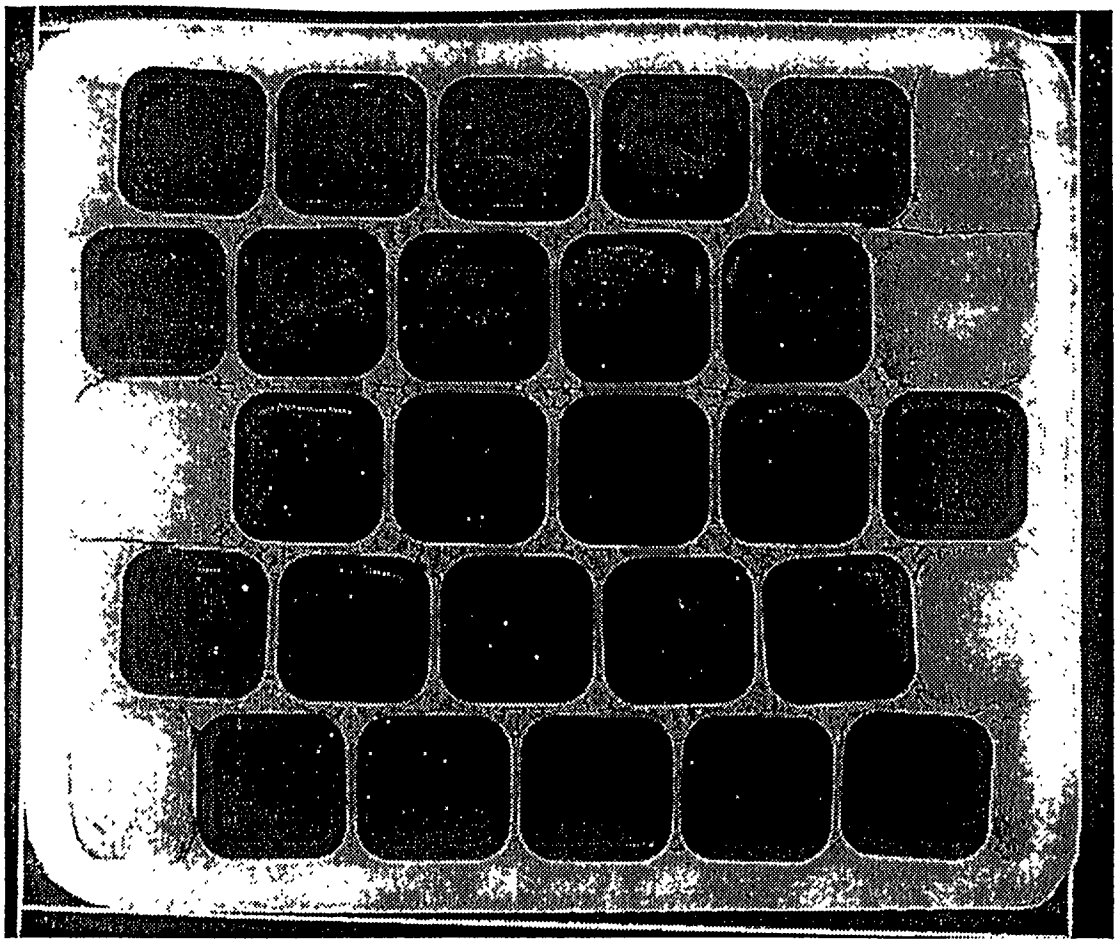

Figure 7-9 Sample A1 - Section 3 - After 31000 Compressive Load Cycles.

5 X 5 Sample Characterization of Cracking

DRAFT

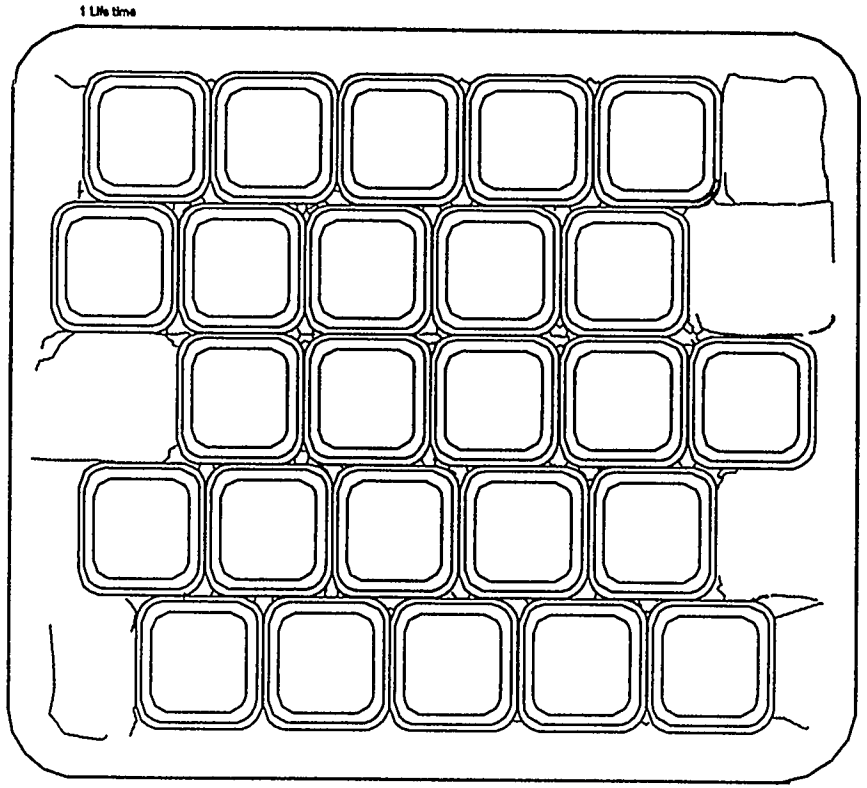

Figure 7-10 Characterization of cracking in - sample A1 - section 3 The cracking present does not violate the rules set forth in section 3 and the structure appear to remain mechanically robust. Figure 7.10 is intended to characterize the cracking observed from the section A1-3.

5 X 5 Sample After 155,000 Load Cycles

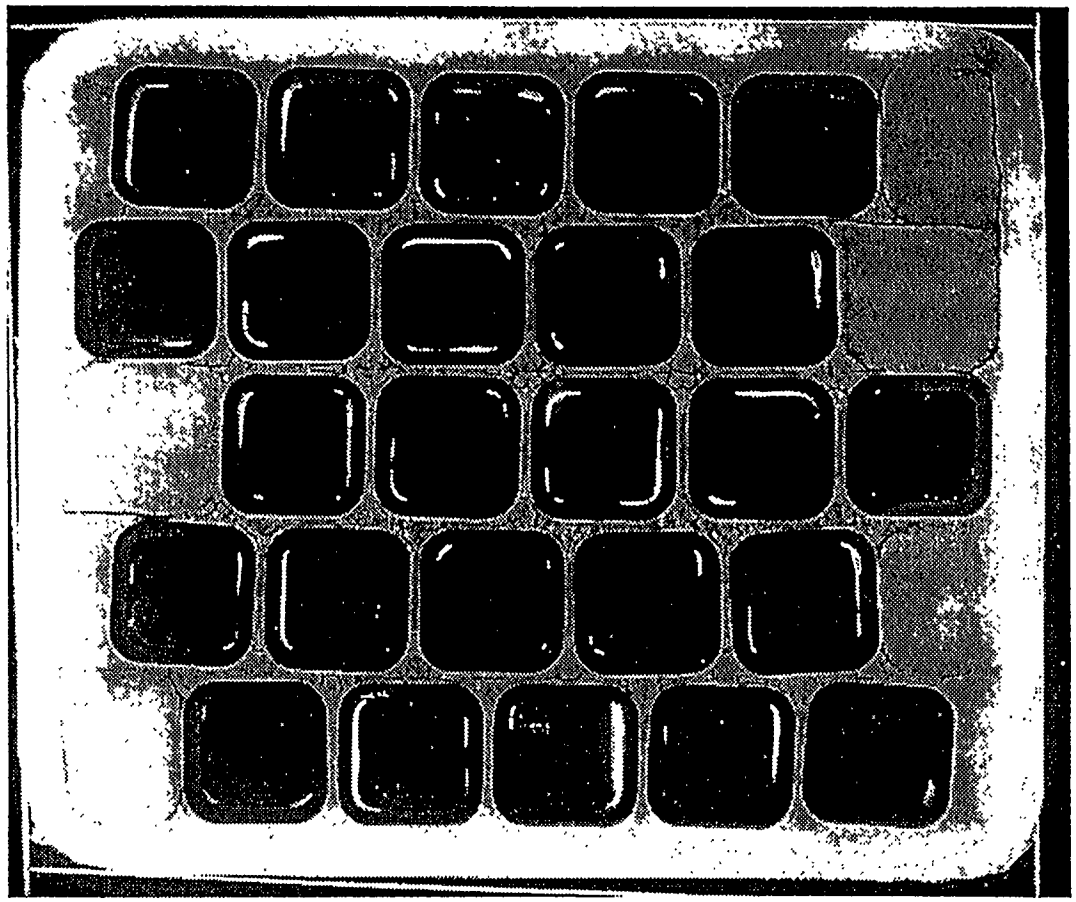

Figure 7-11 Sample A1 - Section 4 - After 155000 Compressive Load Cycles.

5 X 5 Sample After Compressive Failure

DRAFT

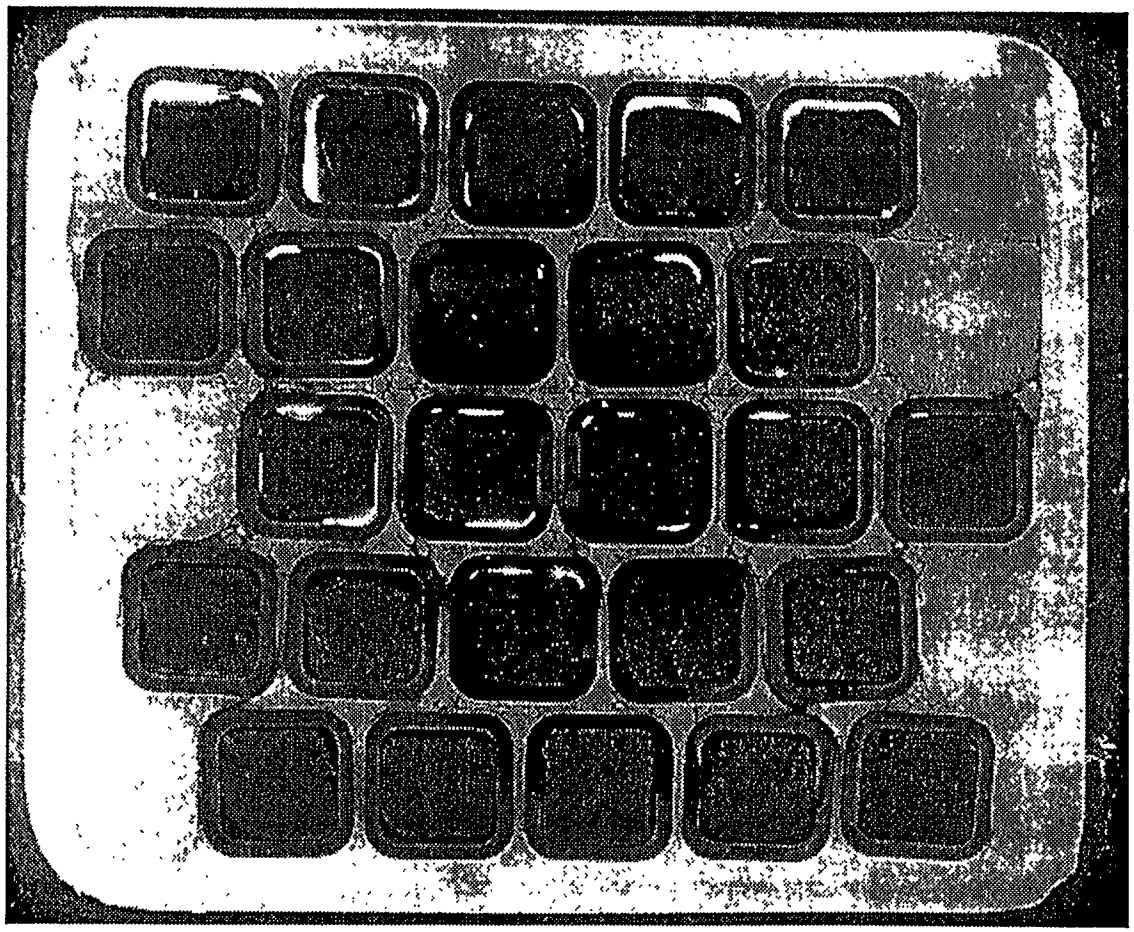

Figure 7-13 Sample A1 - Section 5 - After Compressive Failure

Characterization of Cracking in 5 X 5 Sample

DRAFT

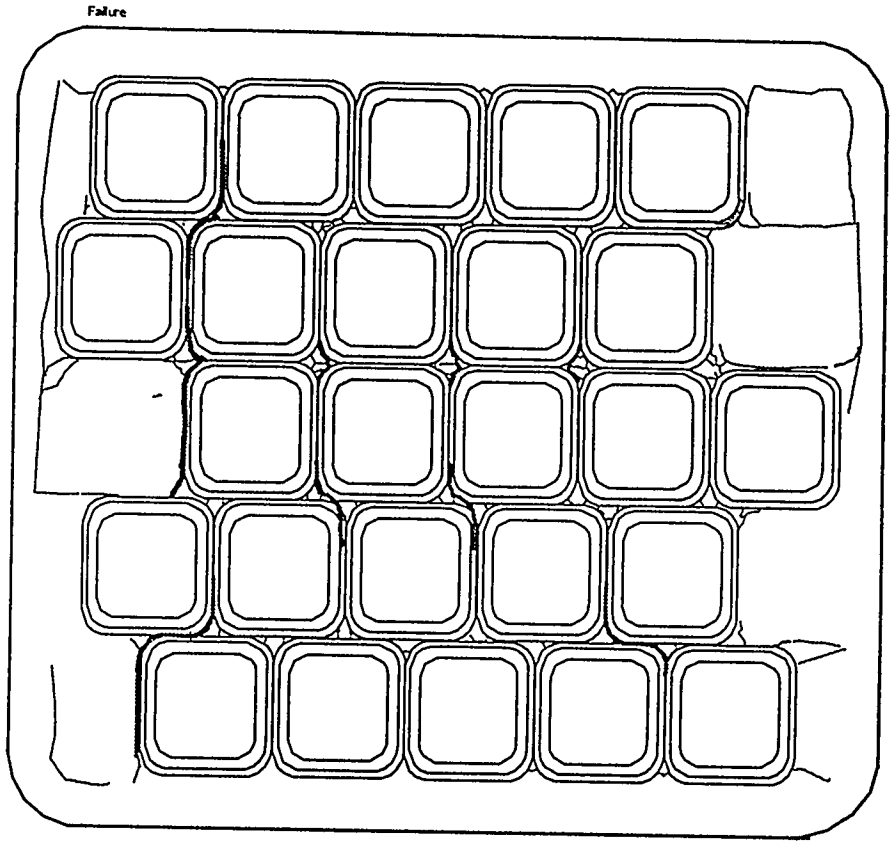

Figure 7-14 Characterization of cracking in - sample A1 - section 5

Modulus & Change in Modulus fo CS 5 X 5 Sample

DRAFT

Table 7-3 Modulus and Chance in Modulus for the CS 5x5 Coil Sample

CS 5X5 Stiffness Tabulation

	SAMPLE A1				SAMPLE A2		
Number of Cycles	Sample Length	Elastic Modulus GPa	% Decrease in Elastic Modulus	Cumulative % Decrease in Elastic Modulus	Elastic Modulus GPa	% Decrease in Elastic Modulus	Cumulative % Decrease in Elastic Modulus
3 *	8	4.2					
5	8	7.5	-80.1%		6.9		
11000	8	7.5	0.0%	0.0%	6.9	0.6%	0.6%
31000	8	7.5	0.0%	0.0%	6.9	-1.2%	-0.6%
41000	4	7.2	3.6%	3.6%	6.4	7.1%	6.6%
124000	4	7.1	2.3%	5.9%	6.2	3.1%	9.7%
155000	4	6.9	2.0%	7.9%	6.3	-1.1%	8.6%

* Data at Room Temperature

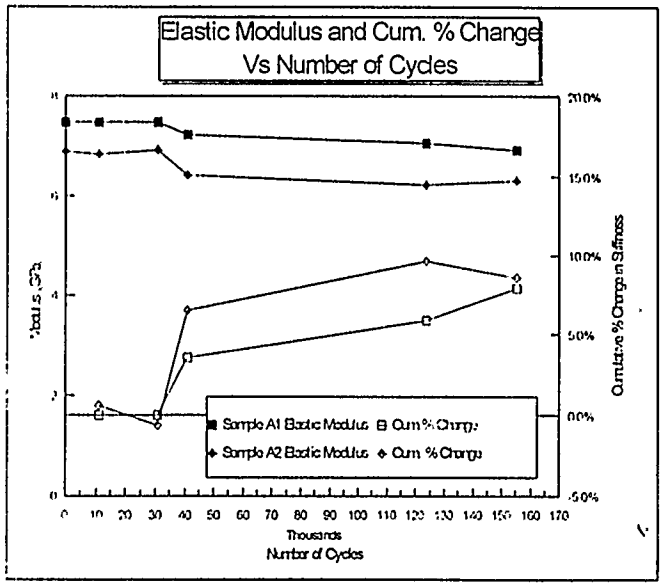

Figure 7-8 Modulus and Chance in Modulus for the CS 5x5 Coil Sample

CS 5 X 5 - Modulud vs. Max. Load Previous Cycle

DRAFT

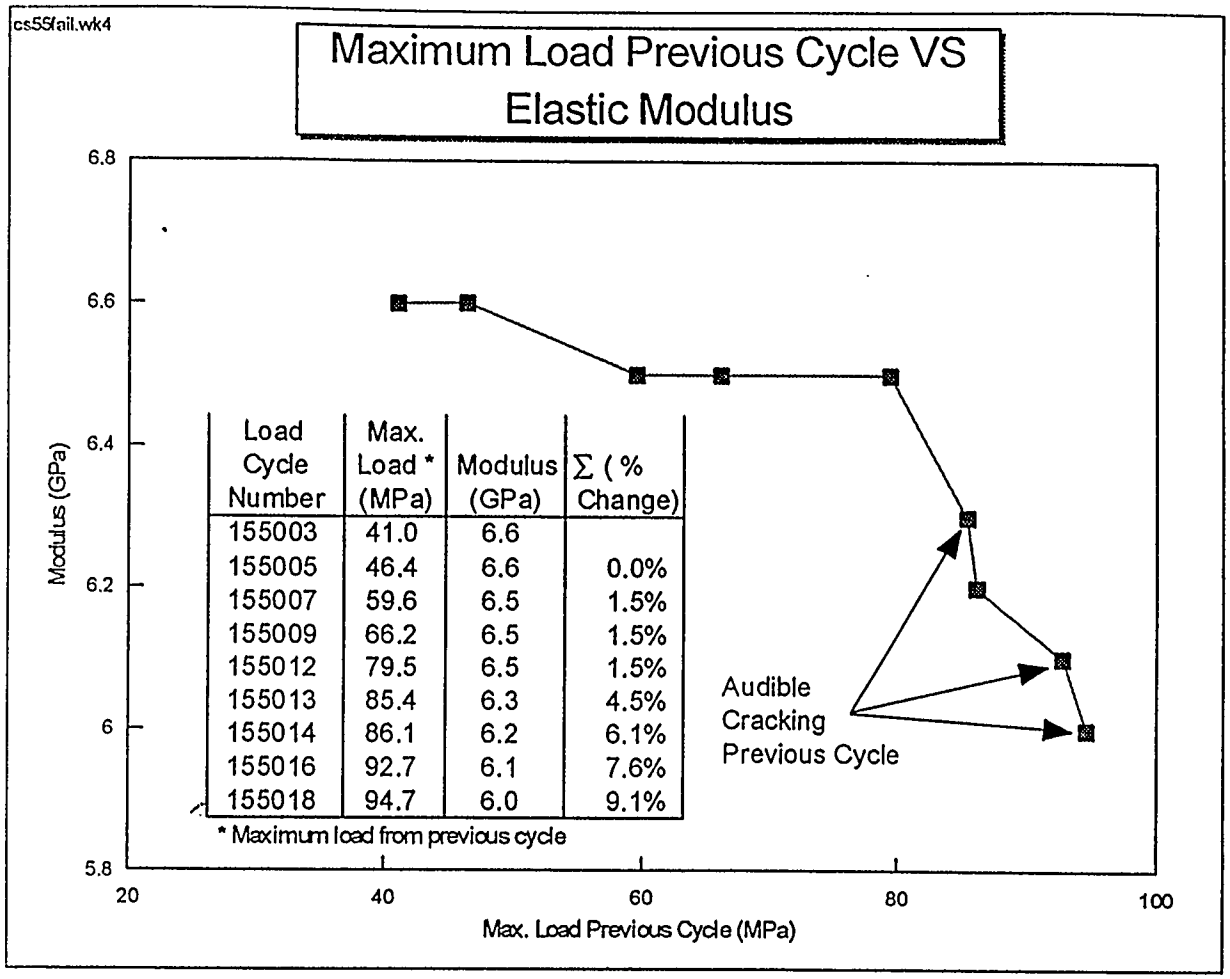

Load Cycle Number	Max. Load * (MPa)	Modulus (GPa)	Σ (% Change)
155003	41.0	6.6	
155005	46.4	6.6	0.0%
155007	59.6	6.5	1.5%
155009	66.2	6.5	1.5%
155012	79.5	6.5	1.5%
155013	85.4	6.3	4.5%
155014	86.1	6.2	6.1%
155016	92.7	6.1	7.6%
155018	94.7	6.0	9.1%

* Maximum load from previous cycle

Figure 7-12 Maximum Load Previous Cycle VS Elastic Modulus

5 X 5 TF Sample Configuration & Stiffness

DRAFT

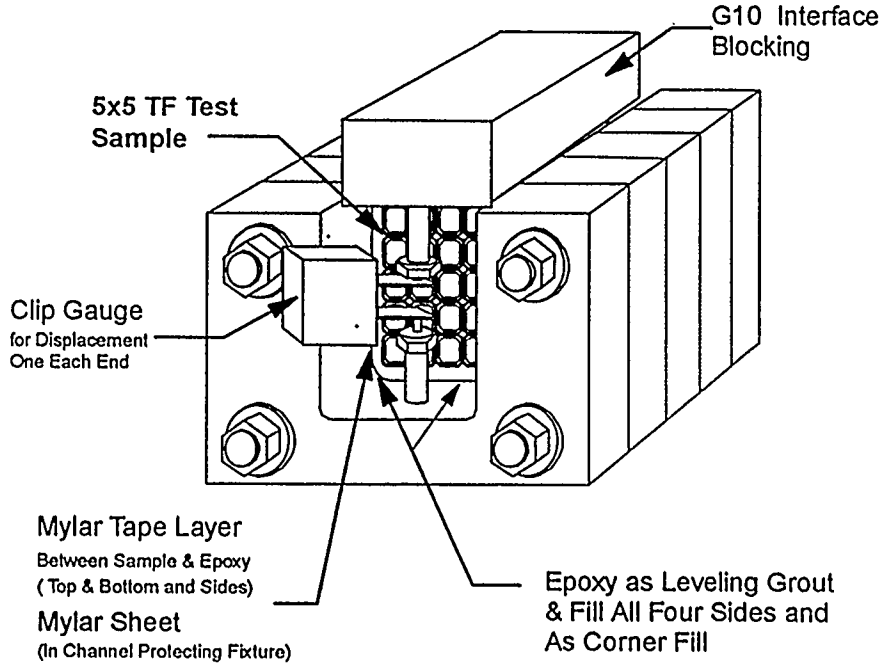

Figure 7-15 TF 5x5 Sample Prepared for Testing

Table 7-5 Stiffness From Compressive Tests of TF 5x5 Coil

TF 5X5 Stiffness Tabulation

Number of Cycles	Stiffness from 1.6 MPa			
	Sample Length	Elastic Modulus GPa	% Decrease in Elastic Modulus	Total % Decrease in Elastic Modulus
20	6	7.7		
6000	6	7.1	8.7%	8.7%
6001	6	7.4	-5.0%	4.2%
31000	6	7.9	-6.7%	-2.2%
Tangent @ Max Load	6	10.0	-26.8%	

3X2 Calculations and Test Results

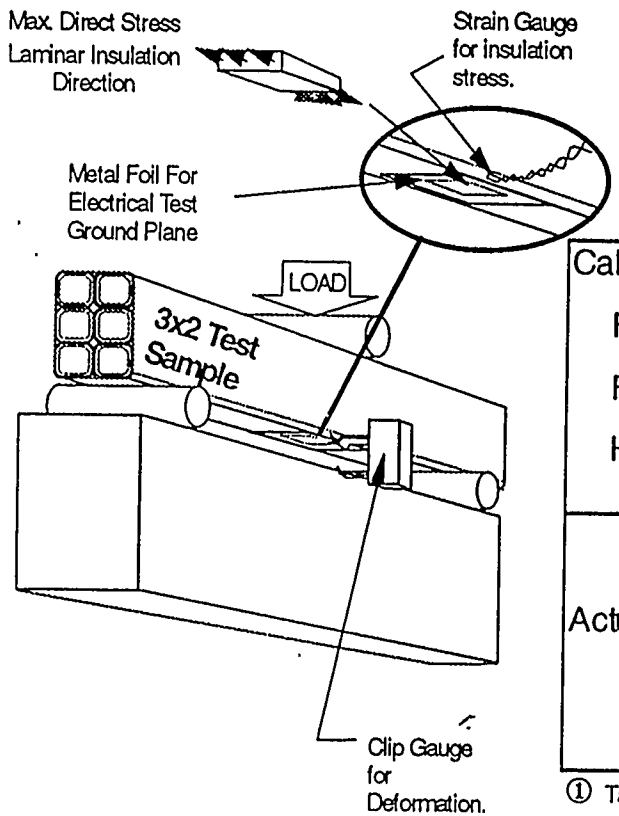

	Load kN	Deflection mm	Stiffness kN / mm	Conduit Wrap Laminar (Z) Ins Stress ①
Calculations:				MPA
FEA Analysis (Non Bonded)	106	2.2mm(.088")	47.4	285
FEA Analysis (Bonded)	369	1.2mm(.048")	300	362
Hand Calc. (Non Bonded)	79	1.6	49.4	220
Actual LN2 Tests	Applied Load	Measured Deflection		Per Strain Gauge E=25e9 Pa
Test Series 1	89	1.0	91.0	53.1
Test Series 2	127	1.5	83.9	64.4

① Target stress is 220 MPa. based on 120% of 183 MPa PDR Baseline Max Vert. Compression

Large Scale Tests - Groundplane Foil Electrode

DRAFT

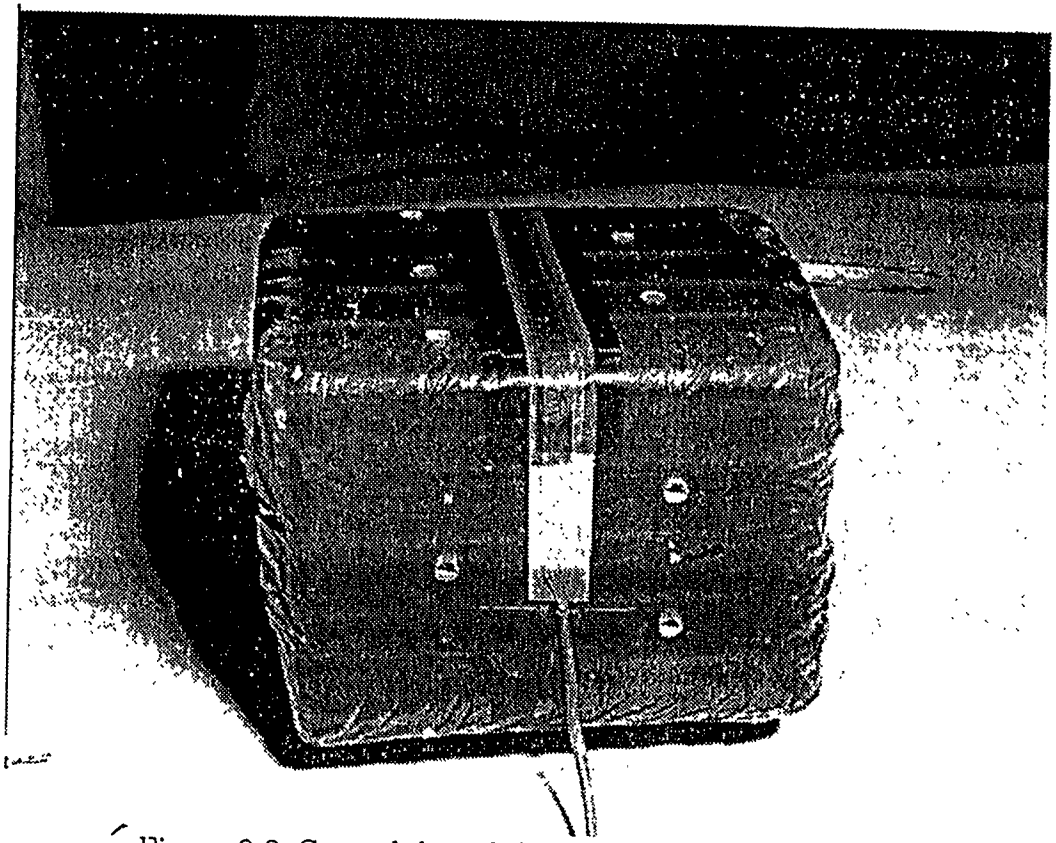

Figure 8-2 Groundplane foil electrode on 5x5 sample B2.

Hipot Failures After Mechanical Testing

DRAFT

Table 8-4Hipot Failure of A2 and B2 Samples after all Mechanical Testing

SAMPLE	CONNECTIONS		HIPOT FAILURE (50 μA)	FAILURE MODE
	HV	GD	kV	
A2	7	2,11,16	21	EXTERNAL LEAD
	9	4,13,8	25	EXTERNAL END
	2	1,3	32	INTERNAL END
	4	3,5	31	INTERNAL END
	8	3,12	28	EXTERNAL END
	1	6	33	INTERNAL END
	FOIL	ALL	40	WITHSTAND
B2	13	8,14,12	27	EXTERNAL LEAD
	7	2,8,6,12	24	EXTERNAL LEAD
	9	4,10,14,8	27	INTERNAL END
	4	3,5	33	INTERNAL END
	2	1,3	26	INTERNAL END
	6	1,11	30	INTERNAL END
	10	15,5	26	EXTERNAL END
	8	3	26	INTERNAL END
	12	11	27	INTERNAL END
	14	15	24	INTERNAL END
	FOIL	ALL	32	EXTERNAL FOIL EDGE

Summary of High Voltage Test Results

DRAFT

Table 8-3 Summary of High Voltage Test Results for Selected Connections
(Where: AR=As received; EMT=End of Mechanical Testing)

SAMPLE	CONNECTIONS		HIPOT 10 kV, 50 µA		PEAK PARTIAL DISCHARGE, pC 6 kVrms		AC LIFE 6 kVrms, 15 min	GROUNDWALL HIPOT 16 kV	
	HV	GD	AR	EMT	AR	EMT	EMT	AR	EMT
A2	18	ALL	P	P	3200	4000	P	-	-
	8	ALL	P	P	3000	3000	P	-	-
	FOIL	ALL	-	-	125	800	P 10kVrms	P	P
B2	13	8,12, 14,18	P	P	1200	2000	P	-	-
	7	2,6,8, 12	P	P	800	1000	P	-	-
	FOIL	ALL	-	-	NT	2600	P 10kVrms	P	P
C2	1	2 or	P	P	-	-	-	NA	NA
	4	3	P	P	-	-	-		
	6 or	2, 3, or 6	P	P	-	-	-		
	3	5	P4kV	P4kV	-	-			
	FOIL	1,2	-	-	120	2500	P 3kV		
	FOIL	5,6	-	-	200	700	-		
	1,3,5	2,4,6	-	-	-	-	-		
	3,4	1,2, 5,6					P		

Cracks

- No cracks appear to penetrate into the glass epoxy coil over wrap (outer ground wall) or extend into the glass epoxy conduit over wrap (conduit wall insulation).
  - Satisfies the mechanical acceptance criteria #2.
- Most of the cracks appear to be localized in the filler or criciform area and they do not extend between the conduits beyond the filler area and none approach the unit cell limit.
  - Satisfies the mechanical acceptance criteria #3
- All of the observed cracking is well inside that allowed by the acceptance criteria
  - Therefore, the CS models pass all of the acceptance criteria regarding crack size & location. Beyond acceptance at 31,000 cycles the samples pass the crack criteria after 5 lifetimes of mechanical compressive loading

Mechanical Strength

- No criteria was established for mechanical strength, however, test results show that after exposure to 5 lifetimes of compressive load cycles the coil can withstand approximately two times the peak operating load before significant damage will occur and can withstand 225% of operating load before limits are reached

Mechanical Stiffness - Modulus

- Criteria - measured decrease in modulus shall be less than 10% after one lifetime
  - 31,000 cycles for the CS sample
  - 6,000 cycles for the TF sample
- CS model test data indicates that an 8% loss in modulus after 5 lifetimes, or 155,000 cycles
  - CS model passes the acceptance criteria at both 1 and 5 life times
- TF model test data indicates that an 8% loss in modulus occurs over the first 6,000 cycles with little or no reduction indicated in the following 24,000 cycles
  - TF model passes the acceptance criteria at both 1 and 5 life times

Electrical Acceptance

- The 3X2 C2 sample and 5X5 A2 & B2 samples passed all Hipot, partial discharge, and AC life cycle electrical acceptance criteria in both the as received condition as well as after completion of all thermal and mechanical cyclic load testing
  - The samples met all criteria without electrical failure of any kind, including electrical lead and/or model end conductor faults
  - The 5X5 models had residual Hipot capability of > 20kV for all turn pairs and > 32kV for the groundwall insulation as determined in Hipot failure testing following completion of all mechanical testing at the end of the program

Large Scale Tests - Overall Conclusions

DRAFT

- *Based on mechanical and electrical testing , the selected insulation system is adequate to meet the rigors of the worst case loading conditions for the life time of the coil and indications are that the CS coil which is thought to have the worst case loading has a margin in excess of 5 on life and 2 on mechanical load*

TPX Magnet System Development

Westinghouse Internally Funded Dummy Coil Program

• Dave Potter

Status

- Dummy conductor received 4/24/95.
- Winding trials complete - excellent correlation between control and free radius.
- Transition and lead benders complete, bend trials successful
- Dummy Coil wound - 5 non-conforming regions
  - 4 flat spots 10" long
  - 1 multi-flat region 30"
- VPI mold in fabrication
- Insulation material orders placed
- Corner preform tooling complete and at Techniweave

Transition and Lead Benders

- **Transition bend trials on 3 foot pieces of conductor**
  - Transition on the order of 0.7 rather than 0.942 inch
  - Recut top and bottom dies, achieved our target transition height to within 0.030 inch
- **Lead bend trials on 3 foot pieced of conductor**
  - Produced 8.5"R
  - Resultant angle was 105° at full stroke and dimpled the conductor wall
  - Minor adjustments and a shorter stroke resulted in a bend angle of 89.7° and no dimples

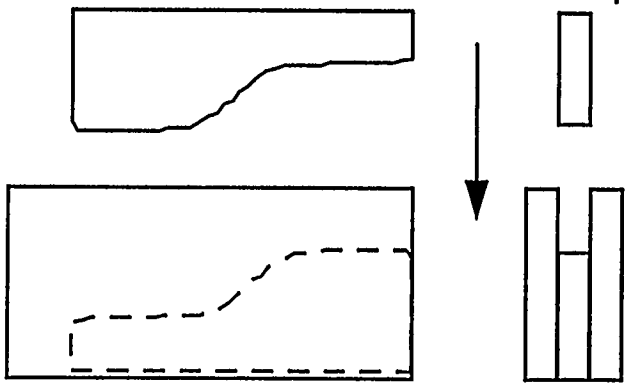

Transition Bender

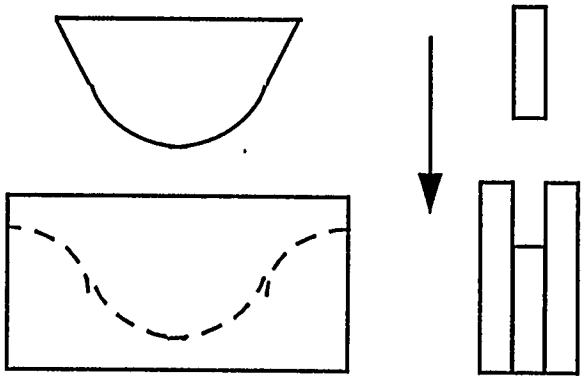

Lead Bender

Corner Filler Tooling

Non-Conforming Areas

- Anomaly description
  - First anomaly was on the 2nd turn of the first pancake - resulted in a local "flat-spot"
    - Region measures about 10" long and appears to have a radius of closer to 60" rather than the desired 30"
    - Resultant gap of 0.2" rather than the 0.064
  - Second through forth anomalies occured on layers 2-3 and had the same characteristics as the first
  - On the 4th layer, 4th turn, a complex anomaly occurred that is some combination of over or under bent regions.
    - Region measures 30 + inches in arc length and has 3 0.2 inch gaps on the ID and 2 on the outside
- Repair
  - Use lead bender to "bump" flat region. The 0.200 gap improved to 0.06 - 0.100 inch.

Non-Conforming Areas

- **Hypotheses**
  - Contoller or roll former errorred
  - Local region was harder and thus higher yield
  - Weld location
  - Barber pole
  - Receiving table momentarily stopped/slowed (caused similar problem in wind trials)
- **Investigation**
  - Hardness Tests
  - Metallurgical Tests
  - Process review
  - Dissection

Non-Conforming Areas

- Conclusions
  - 4 Small spots => Hardness correlation
    - Barber pole pitch variation = orbital straightener
  - 1 Larger region => Take-up table inconsistency

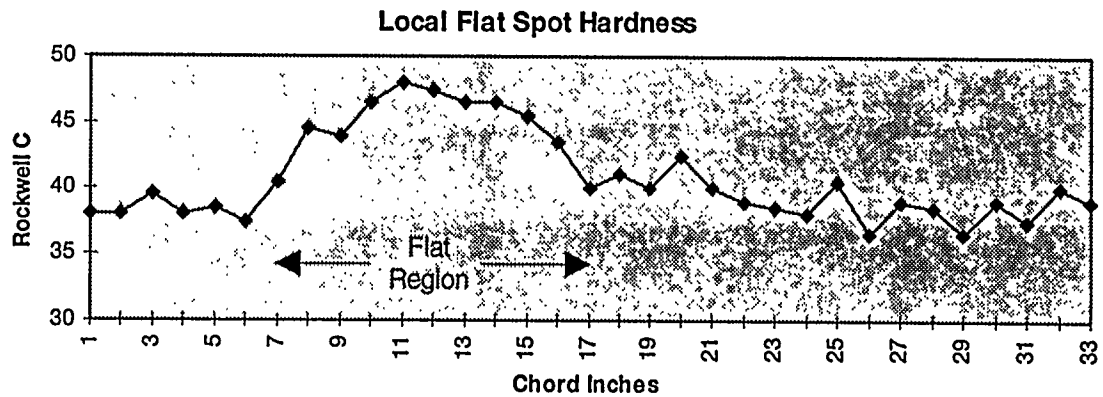

Dummy Coil Photos

View of 0° From Centerline

Underside at 0°

Insulation Application

- Insulation application ongoing
  - Kapton & Overwrap expected complete 9/1
  - Ground wall, ground plane expected complete 9/8
  - VPI week of 9/11

1

PF6 Cooldown 293K - 4K

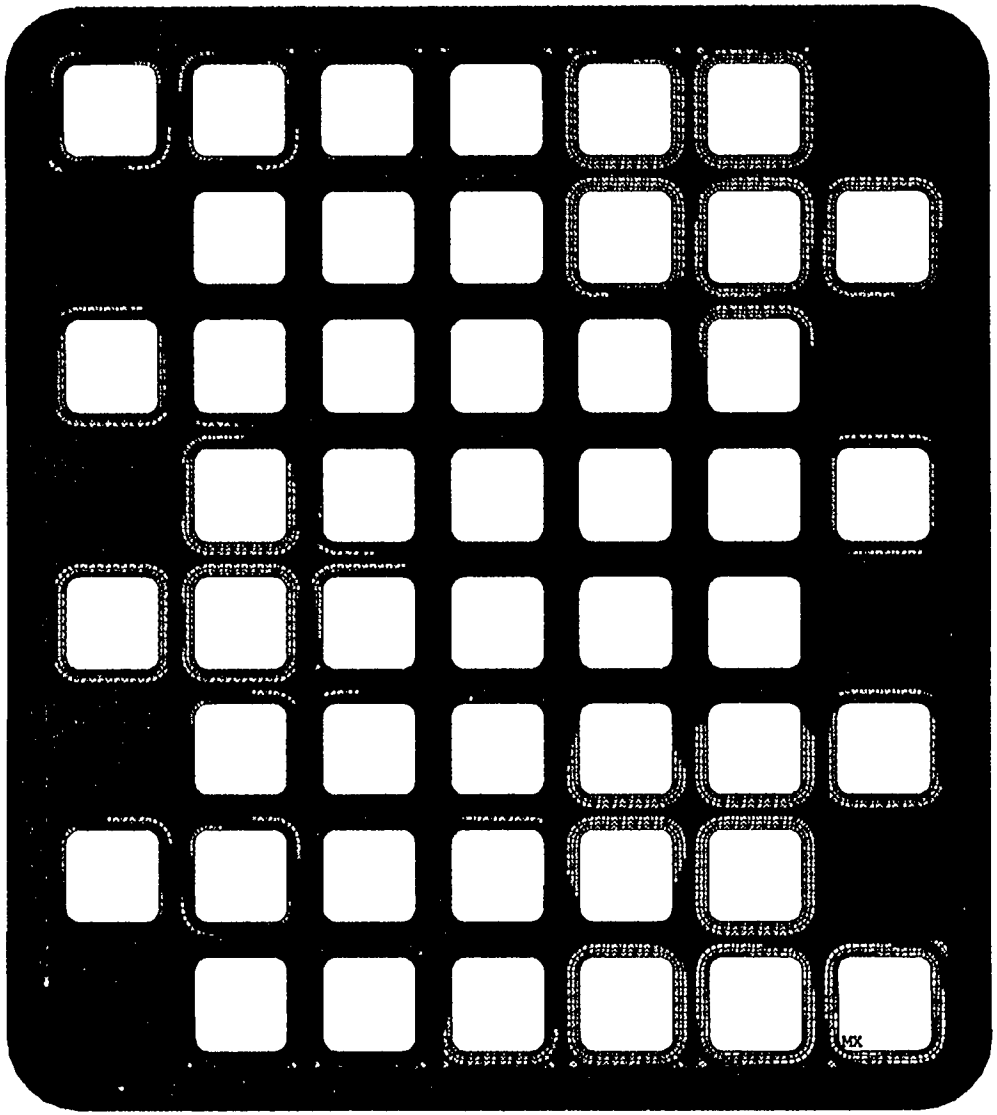

Hoop Stress In Winding Pack

ANSYS 5.1
AUG 15 1995
08:12:35
PLOT NO. 1
NODAL SOLUTION
STEP=3
SUB =1
TIME=3
SZ (AVG)
RSYS=SOLU
DMX =0.00306
SMN =-44.409
SMX =61.368

-44.409
-32.656
-20.903
-9.15
2.603
14.356
26.109
37.862
49.615
61.368

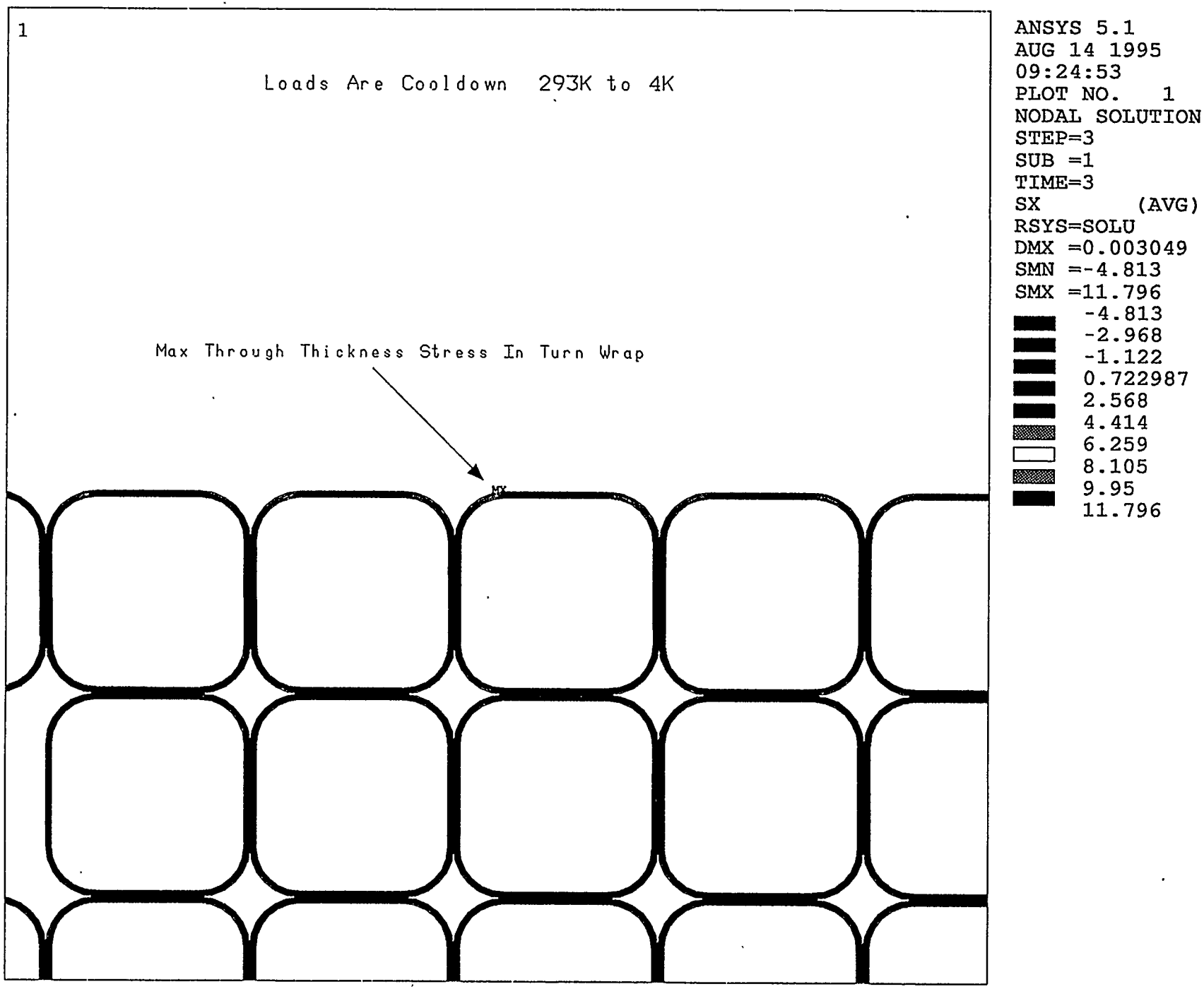
1
Loads Are Cooldown 293K to 4K
Max Through Thickness Stress In Turn Wrap
MX
ANSYS 5.1
AUG 14 1995
09:24:53
PLOT NO. 1
NODAL SOLUTION
STEP=3
SUB =1
TIME=3
SX (AVG)
RSYS=SOLU
DMX =0.003049
SMN =-4.813
SMX =11.796
-4.813
-2.968
-1.122
0.722987
2.568
4.414
6.259
8.105
9.95
11.796

Solenoid Overview

- Key Requirements
  - EM Loads
  - CS-TF Differential Motion (Thermal Contraction)
  - Space and Packaging Constraints
- Assembly Drawing

Solenoid Overview - Assembly Drawing

- CS delivered with coils, preload structure, and cooling system completely assembled
- Upper and lower mounts supplied as kits

Electromagnetics & Preload - Worst EM Forces

- Cooldown Cases
  - Room temperature preload: ~9.4 MN at CS center
  - Room temp. preload; structure and coils at 4K: ~14.8 MN at CS center
- Worst Electromagnetic Force Cases
  - Max separation force: used to determine required preload
  - Max vertical body force: ~3.7 MN upward on CS
  - Max compressive force: ~32.5 MN at CS center
  - Max radial normal
  - Max radial fault

  } Worst Coil Cases
- ANSYS 2D axisymmetric structural model provides input to detailed coil pack models

Electromagnetics & Preload - Structural Model

- ANSYS 2D axisymmetric model
- Smeared coil properties
- Input forces per coil
- Coil-to-coil interface does not slip

[figure of model]

SUMMARY OF WORST CASE EM LOADING ON PF COILS

MAXIMUM RADIAL AND VERTICAL LOADS

Body EM Loads on the Central Solenoid

both the radial and vertical compressive components of force throughout the HC

evaluation of the forces are determined on a spread sheet by simply substituting the PF current levels. The force coefficients have been verified by comparing with the University supplied body forces for the twenty-three static equilibria. The concept has applied to the alternating force component from interactions with the TF system and the internal compressive forces due to a turn interacting with its self field.

Table 3.5 — Peak internal radial forces (MN/(m^2-radian)) acting on each PF coil during 23 normal operating equilibria.

	PREBLIP	BLIP	SOF	SOB	EOB	EOF	SOF	SOB	0.4, 5.0	0.5, 2.2	0.7, 0.0	1.2, 0.0	1.2, 5.0	0.4, 5.0	0.5, 2.2	0.7,0.0	1.2, 0.0	1.2, 5.0	0.4, 7.0	0.4, 5.0	0.7, 0.0	1.5, 0.0	1.5, 7.0	MAX	MAX DENSITY
	1	2	3	4	5	6	7	8	9	10	11	12	13	14	15	16	17	18	19	20	21	22	23	MN/(m^2-radian)	MN/m^3
PF1U	10.82	2.41	108 13	68.19	83 63	79 37	0 04	1.76	25.71	66.63	113.62	112.72	65.48	27.64	76.94	111.38	79.06	40.44	9.95	13.62	50.95	38.02	2.26	113.62	140.27
PF1L	10.82	2.41	108.13	68 19	83 63	79 37	0 04	1.76	25.71	66.63	113.62	112.72	65.48	27.64	76.94	111.38	79.06	40.44	9.95	13.62	50.95	38.02	2.26	113.62	140 27
PF2U	96.72	52.82	8.30	7.26	20.96	29.63	10.92	2.49	97.30	70.92	7.86	3.94	1.46	102.65	61.61	10.15	1.05	0.87	79.08	70.50	4.54	8.03	4.10	102.65	126.72
PF2L	96.72	52.82	8 30	7 26	20.96	29.63	10.92	2.49	97.30	70.92	7.86	3.94	1.46	102.65	61.61	10.15	1.05	0.87	79.08	70.50	4.54	8.03	4.10	102.65	126.72
PF3U	92.25	90.35	0 58	0 07	1.52	4.94	29.30	21.50	44.71	21.99	0.81	22.94	4.79	18.82	3.38	4.23	0.89	1.69	40.38	34.38	0.13	17.46	5.67	92.25	113.90
PF3L	92.25	90.35	0.58	0 07	1.52	4.94	29.30	21.50	44.71	21.99	0.81	22.94	4.79	43.04	23.19	1.39	6.19	0.65	40.38	34.38	0.13	17.46	5.67	92.25	113.90
PF4U	86.98	94.31	4.48	2.02	0.00	0 05	46.59	45.24	26.63	10.10	5.15	32.32	5.21	1.38	0.05	8.40	3.70	3.23	25.28	21.25	1.59	20.77	7.69	94.31	116.43
PF4L	86.98	94.31	4.48	2.02	0.00	0.05	46.59	45.24	26.63	10.10	5.15	32.32	5.21	29.95	11.27	0.21	11.09	2.93	25.28	21.25	1.59	20.77	7.69	94.31	116.43
PF5U	148.09	86.74	216.34	183.68	117.27	28.21	52.35	58.84	222.71	178.72	218.93	184.16	163.88	65.27	43.89	69.09	89.46	37.50	152.07	135.53	86.17	60.06	151.10	222.71	183.61
PF5L	148.09	86.74	216.34	183.68	117.27	28.21	52.35	58.84	222.71	178.72	218.93	184.16	163.88	237.37	201.85	224.82	131.98	152.39	152.07	135.53	86.17	60.06	151.10	237.37	195.69
PF6U	0.78	0.53	176.77	67.78	73.60	99.74	3.21	1.52	334.49	318.09	189.05	17.71	30.69	221.66	217.78	133.20	0.84	1.06	196.31	210.13	83.83	0.31	0.01	334.49	88.99
PF6L	1.28	0.95	170.32	63 81	69.46	94.91	4.15	2.18	325.60	309.42	182.38	15.71	28.04	323.93	323.38	207.28	20.97	20.48	189.51	203.09	79.41	0.64	0.02	325.60	86.63
PF7U	1.81	0.28	5.12	102.79	104.84	3.21	14.94	17.37	9.15	0.41	2.71	107.38	201.78	16.17	1.93	3.58	109.95	200.83	46.39	14.17	1.21	75.96	196.09	201.78	46.96
PF7L	1.81	0.28	5.12	102.79	104.84	3.21	14.94	17.37	9.15	0.41	2.71	107.38	201.78	16.17	1.93	3.58	109.95	200.83	46.39	14.17	1.21	75.96	196.09	201.78	46.96

Table 3.6 — Peak internal vertical forces (MN/(m^2-radian)) acting on each PF coil during 23 normal operating equilibria.

	PREBLIP	BLIP	SOF	SOB	EOB	EOF	SOF	SOB	04, 5.0	0.5, 2.2	0.7, 0.0	1.2, 0.0	1.2, 5.0	0.4, 5.0	0.5, 2.2	0.7,0.0	1.2, 0.0	1.2, 5.0	0.4, 7.0	0.4, 5.0	0.7, 0.0	1.5, 0.0	1.5, 7.0	MAX	MAX DENSITY
	1	2	3	4	5	6	7	8	9	10	11	12	13	14	15	16	17	18	19	20	21	22	23	MN/(m^2-radian)	MN/m^3
PF1U	11.78	2.63	117.72	74.24	91.05	86.41	0.05	1.92	27.99	72.54	123.70	122.72	71.29	30.09	83.77	121.26	86.07	44.03	10.84	14.83	55.47	41.39	2.46	123.70	152.71
PF1L	11 78	2.63	117.72	74 24	91 05	86.41	0 05	1 92	27.99	72 54	123.70	122.72	71.29	30.09	83.77	121.26	86.07	44 03	10.84	14.83	55.47	41.39	2.46	123.70	152.71
PF2U	105.85	57.81	9.08	7.94	22.94	32.43	11.95	2.73	106.49	77.62	8.61	4.31	1.60	112.34	67.42	11.11	1.15	0.95	86.55	77.15	4.96	8.79	4.48	112.34	138.69
PF2L	105.85	57.81	9.08	7.94	22.94	32.43	11.95	2.73	106.49	77 62	8.61	4.31	1.60	112.34	67.42	11.11	1.15	0.95	86.55	77.15	4.96	8.79	4.48	112.34	138.69
PF3U	89.11	87.27	0.56	0 07	1.47	4.77	28 30	20.77	43.18	21.24	0.79	22.15	4.63	18.18	3.26	4.08	0.86	1.63	39.00	33.21	0.12	16.87	5.48	89.11	110.01
PF3L	89.11	87.27	0.56	0.07	1.47	4.77	28.30	20.77	43.18	21.24	0.79	22.15	4.63	41.57	22.40	1.35	5.98	0.63	39.00	33.21	0.12	16.87	5.48	89.11	110.01
PF4U	84.02	91.09	4 32	1.95	0 00	0.04	45.00	43.70	25.72	9.75	4.97	31.21	5.03	1.33	0.05	8.12	3.57	3.12	24.42	20.53	1.53	20.06	7.43	91.09	112.46
PF4L	84.02	91.09	4.32	1.95	0 00	0.04	45.00	43.70	25.72	9.75	4.97	31.21	5.03	28.93	10.88	0.20	10.71	2.83	24.42	20.53	1.53	20.06	7.43	91.09	112.46
PF5U	154.23	90.34	225.30	191.30	122.13	29.38	54.52	61.28	231.95	186.12	228.00	191.79	170.68	67.98	45.71	71.95	93.17	39.06	158.37	141.15	89.74	62.55	157.36	231.95	191.22
PF5L	154.23	90.34	225.30	191.30	122.13	29.38	54.52	61.28	231.95	186.12	228.00	191.79	170.68	247.21	210.22	234.14	137.45	158.71	158.37	141.15	89.74	62.55	157.36	247.21	203.80
PF6U	0.87	0.59	195.88	75.11	81.56	110.52	3.56	1.68	370.65	352.48	209.49	19.63	34.01	245.62	241.32	147.60	0.93	1.18	217.53	232.84	92.90	0.34	0.01	370.65	98.62
PF6L	1.41	1.05	188.74	70.71	76.97	105.17	4.60	2.41	360.80	342.87	202.10	17.41	31.07	358.95	358.34	229.69	23.24	22.70	210.00	225.05	88.00	0.71	0.02	360.80	96.00
PF7U	1.93	0.30	5.47	109.75	111.94	3.43	15.95	18.54	9.77	0.44	2.90	114.65	215.45	17.27	2.06	3.83	117.40	214.43	49.53	15.13	1.29	81.11	209.38	215.45	50.14
PF7L	1.93	0.30	5.47	109.75	111.94	3.43	15.95	18.54	9.77	0.44	2.90	114.65	215.45	17.27	2.06	3.83	117.40	214.43	49.53	15.13	1.29	81.11	209.38	215.45	50.14

3-15

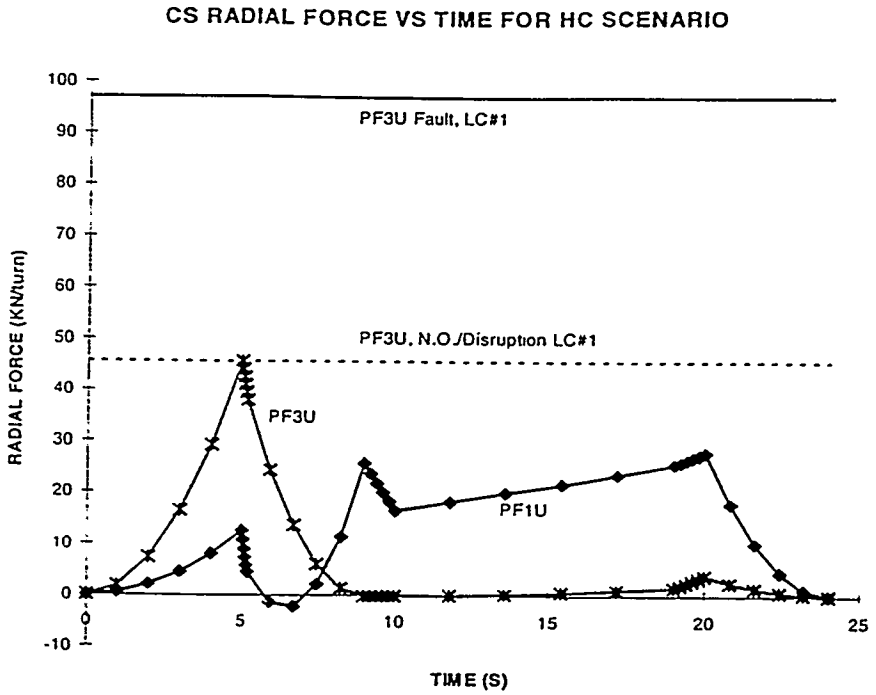

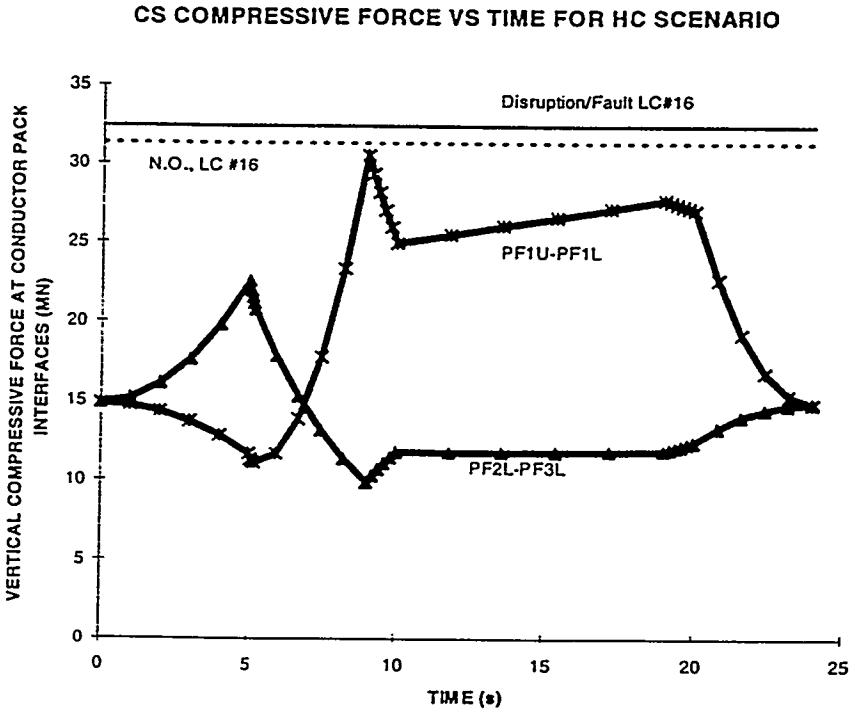

Figure 4.1 — Maximum Radial and vertical compressive forces acting on the CS. The radial forces are of electromagnetic origin. The vertical compressive forces include prestress and cooldown effects in addition to electromagnetic forces.

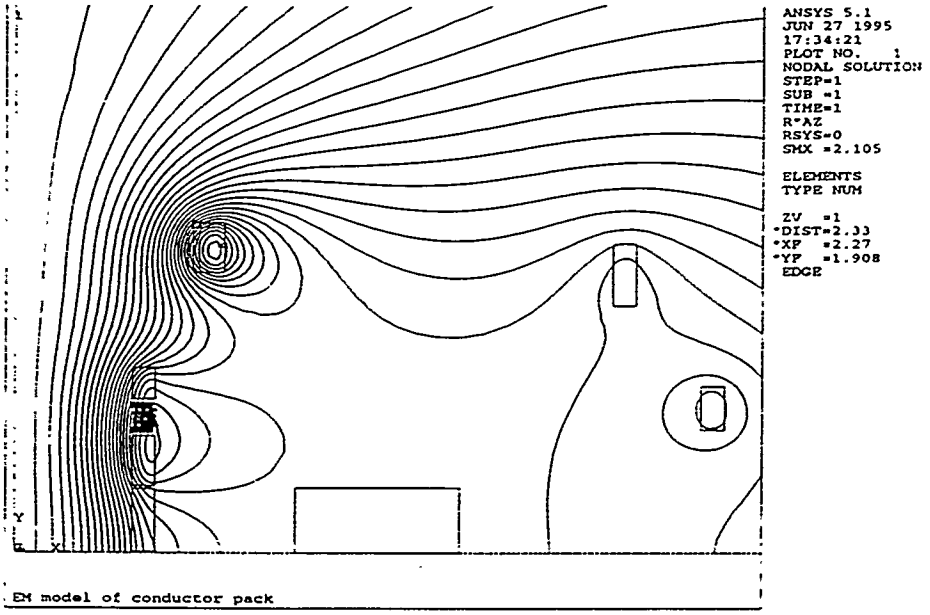

Figure 4.5 — Contours of magnetic flux for equilibria #1 (t=5 s of HC scenario) obtained using an axisymmetric ANSYS model of the PF conductors. The 60 individual turns in conductor PF3U has been modeled in detail.

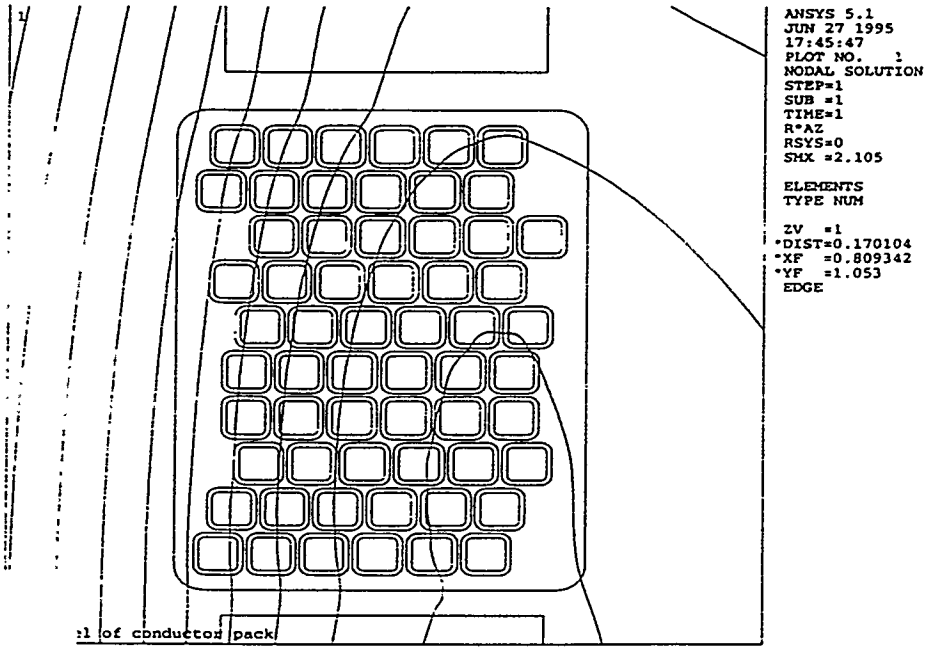

Figure 4.6 — Blowup of magnetic flux lines throughout coil pack PF3 for equilibria #1 (t=5 s of HC scenario). The effects of the incoloy magnetization have been neglected in the case shown.

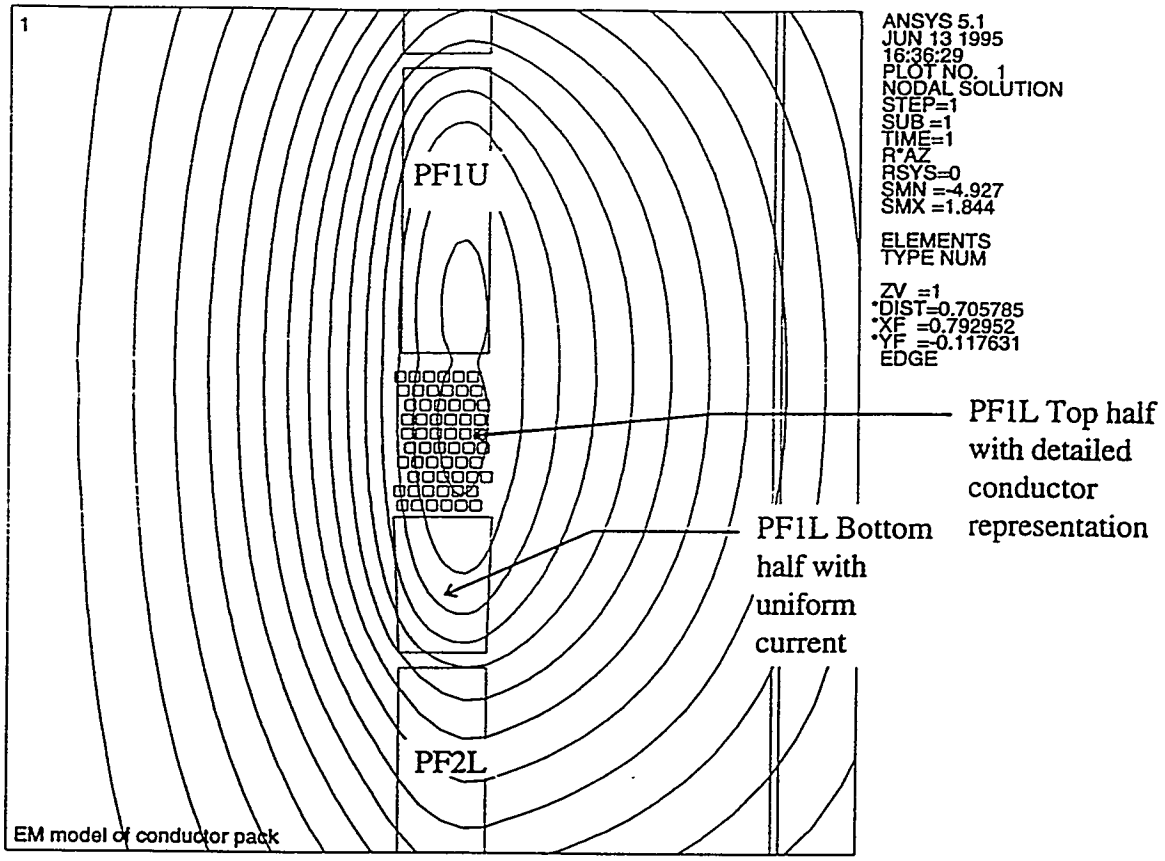

Figure 4.19 — Blowup of the magnetic flux lines in the vicinity of conductor pack PF1L.

Table 4.1 — Summary of worst case CS coil loadings to be analyzed using detailed conductor pack models.

Case Description		Radial EM Body Force[a] (kN/turn)	Vertical EM Body Force[a] (MN)	Upper/Lower Coil End Normal Force[b] (MN)	Upper/Lower Coil End Tangential Force[b] (MN)
PF3U Radial	Fault following Equilibria #1	97.0	-0.073	-14.29/14.40	-4.36/-4.25
PF3U Radial	Normal Operating Equilibria #1	45.6	-3.37	-19.18/22.5	0.19/-0.01
PF3U with PF2 Shear	Normal Operating Equilibria#1	45.6	-3.37	-19.18/22.5	0.01/-1.39
PF1L Compres-sive	Normal Operating Equilibria#16	28.5	13.5	-31.33/17.95	-0.02/-0.95

[a] Lorentz force acting on single conductor pack only
[b] Based on structural analysis of entire central solenoid

THE IMPACT OF INCOLOY MAGNETIZATION ON PEAK FIELD.

Table 4.4 — Peak magnetic field throughout conductor pack PF3 for equilibria #1.

ANALYSIS	PEAK MAGNETIC FIELD
MIT/LLNL	5.82
Refined without conduit	5.929
Refined with conduit Magnetization	5.948

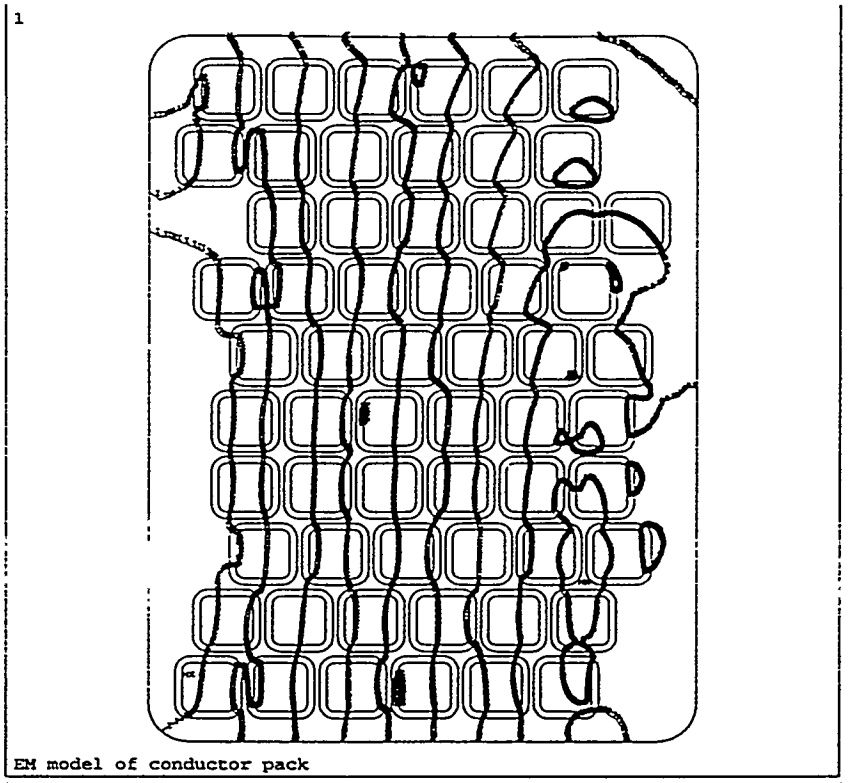

conduit magnetization ignored

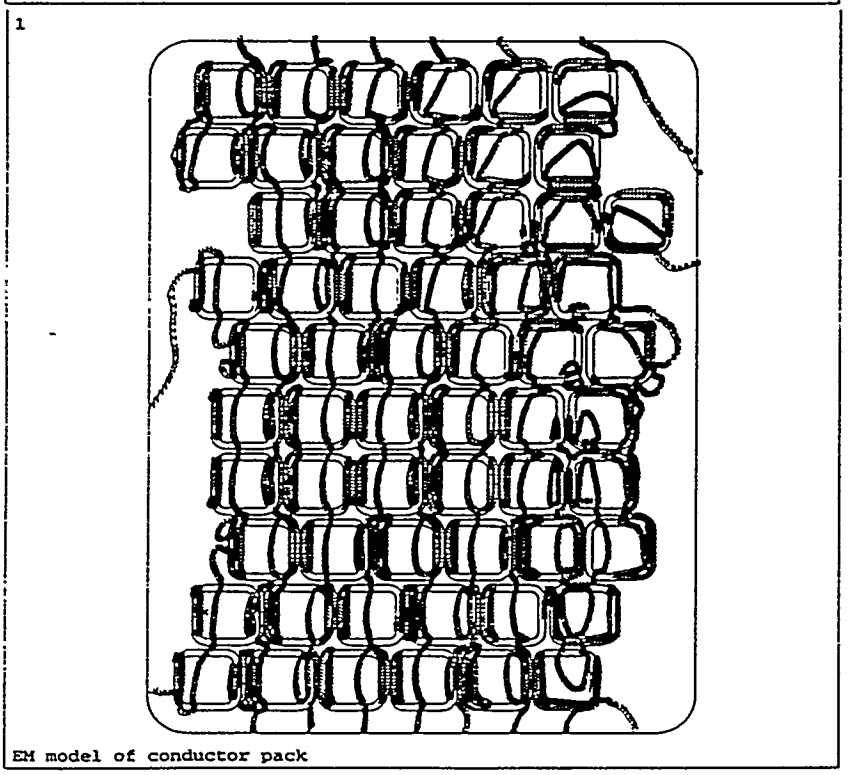

conduit magnetization included

Figure 4.7 — Contours of constant magnetic field magnitude throughout coil pack PF3 for equilibria #1 (t=5 s of HC scenario).

Electromagnetic body forces acting on conductor pack PF3 calculated using Maxwell stress and Lorentz body force methods. The cases of including and neglecting the magnetic properties of the incoloy conduit are shown.

	Without Incoloy Magnetization		With Incoloy Magnetization	
	Radial Force (MN)	Vertical Force (MN)	Radial Force (MN)	Vertical Force (MN)
Lorentz (JxB)	2.774	-3.662	2.791	-3.561
Maxwell Stress	2.640	-3.638	2.591	-3.769
MIT/LLNL	2.74	-3.34	-	-

Electromagnetics & Preload - Preload Derivation

- Maximum separation load case used to determine preload
- Preload is a combination of
  - Room temperature prestrain
  - Differential contraction during cooldown (determined in cooldown analysis)
- Overall goal is minimization or elimination of tension in the insulation
  - Analysis groundrule is to eliminate any separation force between coils

Coil Pack Design- Winding Configuration

- Spiral Wound with Joggles located at leads
- Helium stubs located adjacent to leads
- Lead spur

[Drawings]

Coil Pack Design - Insulation System Design

- Conductor Pack
  - CICC insulation (Kapton & 3D glass)
  - Fillers (corner & transition)
  - Ground Wall (ground wrap + ground plane screen + outer wrap)
- Ground plane
  - Individually wrapped leads and coil pack
  - Ground plane breaks
- Projections (overlapping drapes & molded Kapton)
  - Helium stubs; Lead spurs
- VPI to prepreg transitions (continuous Kapton & grd plane)
  - Leads; Joints (molded inserts)

(drawings)

Section VII - G

Coil Pack Structural Analysis

FEA MODELING PARAMETERS

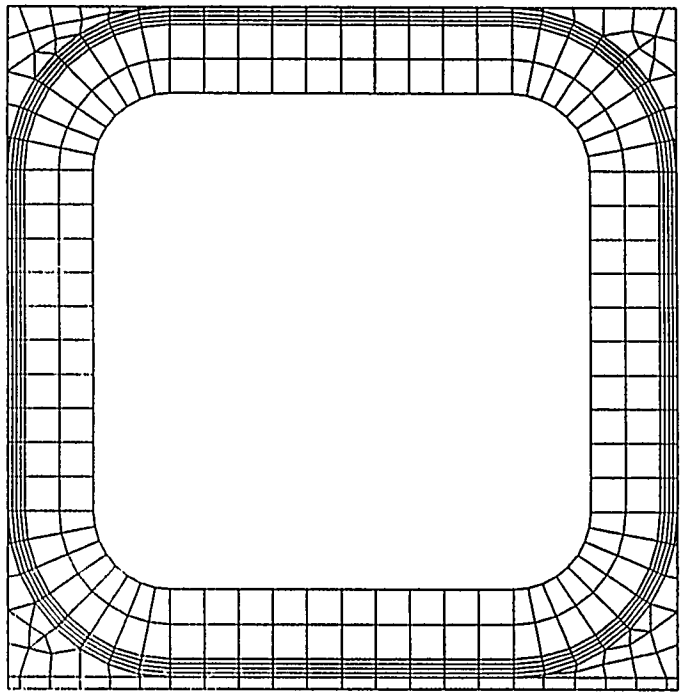

Figure 2-1 — Modeling mesh and the conduit, wrap, and roving pattern of a single conductor used to build the CS CDR FEM Model.

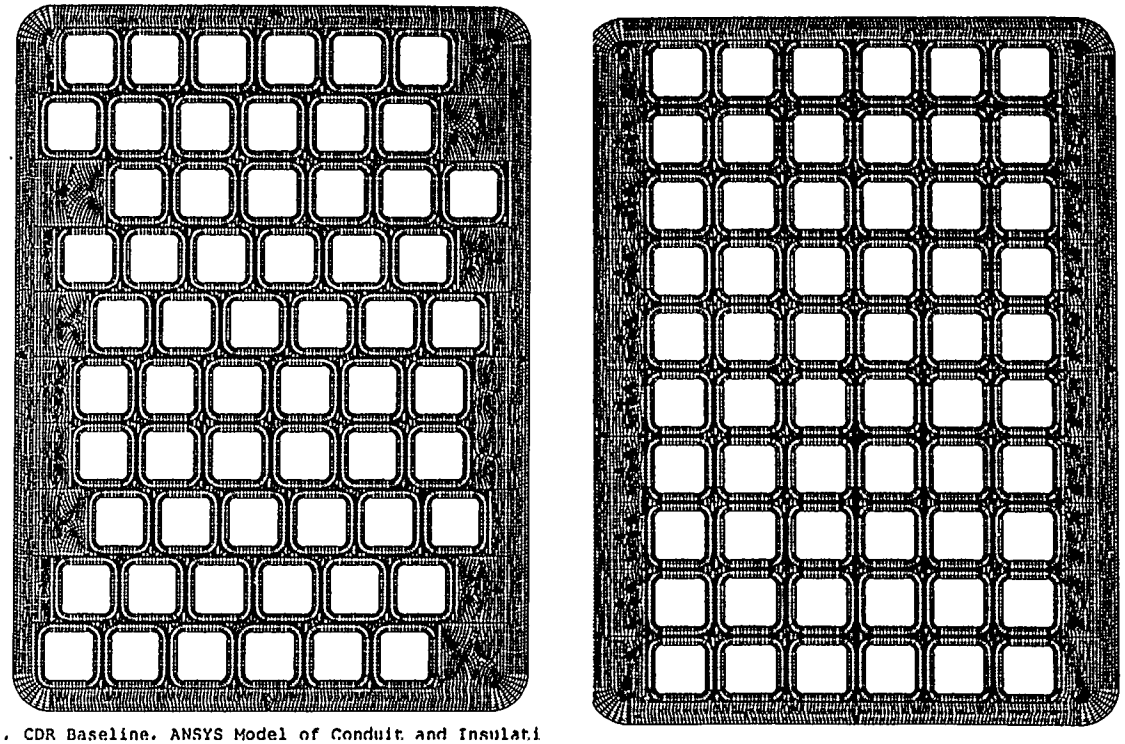

Figure 2.2 The ANSYS Model used to describe the CS Aligned and Staggered Coil Construction

Table 3-1 TPX CPDR Material Property Data Base (4K) for use in Finite Element Modeling
(Superscripts are refer to references)

Material	E_x [GPa]	E_y [GPa]	E_z [GPa]	α_x [μ/K]	α_y [μ/K]	α_z [μ/K]	G_{xy} [GPa]	G_{xz} [GPa]	G_{yz} [GPa]	υ_{xy}	υ_{xz}	υ_{yz}
316LN SS	207[16]	207[16]	207[16]	10.4[16]	10.4[16]	10.3[1]	81[2]	81[2]	81[2]	0.282[2]	0.282[2]	0.282[2]
Incoloy 908	185[1]	185[1]	185[1]	5.92[16]	5.92[16]	5.92[16]	71[2]	71[2]	71[2]	0.299[2]	0.299[2]	0.299[2]
Conduit Wrap	19.7[1]	29.6[1]	29.6[1]	19.9[1]	6.7[1]	6.7[1]	7.6[3]	7.6[3]	10.7[3]	0.26[4]	0.26[4]	0.26[4]
Ground Wrap	19.7[1]	29.6[1]	29.6[1]	19.9[1]	6.7[1]	6.7[1]	7.6[3]	7.6[3]	10.7[3]	0.26[4]	0.26[4]	0.26[4]
Roving Corner Fill	19.7[1]	19.7[1]	29.6[1]	19.9[1]	19.9[1]	6.7[1]	7.6[4]	7.6[4]	7.6[4]	0.26[4]	0.26[4]	0.26[4]
HP Laminate (G11)	24.0[1]	35.0[16]	37.0[16]	24.9[1]	8.3[1]	8.3[1]	8.2[16]	9.7[16]	11.6[3]	0.26[4]	0.25(zx)	0.26[3]
Resin	8.0[16]	8.0[16]	8.0[16]	40[1]	40[1]	40[1]	2.9[16]	2.9[16]	2.9[16]	0.4[16]	0.4(zx)	0.4[16]
3D Weave (See notes 14,15)	23	32	25	19.2	8.25	16.2	8 (yx)	8	8 Av.zy&yz	0.26	0.37 (zx)	0.35(zy) 0.25(yz)
3D Corner Fill (See notes 14,15)	22	25	31	20.3	16.2	7.56	8.5[11]	9 (zx)	8 Av.zy&yz	0.26	0.38 (zx)	0.23(zy) 0.36(yz)
Araldite at 296K	18[8]	18[8]	18[8]	10[8]	10[8]	10[8]	6.9[5]	6.9[5]	6.9[5]	0.3	0.3	0.3
Kapton	4.8[12]	5.5[12]	5.5[12]	43.2[13]	13.0[10]	15.8[10]	0.37[10]	0.37[10]	0.37[10]	0.34[9]	0.34	0.34
SC Cable	0.6[7]	0.6[7]	60[7]	7.24[7]	7.24[7]	7.24[7]	0.23[5]	0.23[5]	0.23[5]	0.3[4]	0.3[4]	0.3[4]

Table 3-2 The net normal and the net radial forces that develop in the 2D global smeared model

	Surface Normal Force (MN) Global Model	Surface Normal Force (MN) Detailed Model	Surface Traction Force (MN) Global Model	Surface Traction Force (MN) Detailed Model
PF3U Radial Fault following LC #1	-14.29/14.40	-14.19/14.26	-4.36/-4.25	-4.76/-5.28
PF3U Radial NormalOperating LC #1	-19.18/22.5	-18.33/-22	0.19/-0.01	0/0
PF3U With PF2 Shear Normal Operating LC #1	-19.18/22.5	-18.56/22.22	0.01/-1.39	0/-1.43
PF1L Compressive Normal Operating LC #16	-31.33/17.95	-30.06/16.68	-0.02/-0.95	0/0

		FEA Load Case #8 Max Vert Compression (MPa)	FEA Load Case #4 Max. Rad. Oper.W /shear (MPa)	Max Rad. Oper. W O /Shear (MPa)	FEA Load Case #5 Max Radial Fault (MPa)	Effects of Cooldown		FEA Load Case #7 11MNt Vert ld cldwn GT to 4K (MPa)
						Cooldown GT to4K (MPa)	Cooldown GT to RT (MPa)	
Conduit	SX	-583	-481	-463	-882	-382	-127	-311
		479	380	361	756	229	76.4	265
	SY	-749	-619	-609	-892	-291	-97.2	-398
		354	301	290	460	204	67.9	210
	SZ	-186	-112	-68.8	-51.3	-238	-79.3	-224
		215	226	251	520	-5.66	-1.89	-1.39
	SXY	-289	-184	-180	-378	-133	-44.2	-156
		216	241	228	402	122	40.5	168
	SINT	740	612	602	941	375	125	389
Kapton	SX	-94.1	-70.6	-73.9	-137	-45.2	-15.1	-43.7
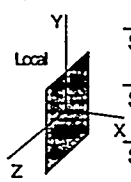		12.3	10.8	9.57	17.4	7.24	2.41	7.92
	SY	-40.7	-26.5	-26.9	-79	-14.4	-4.8	-16.1
		61.3	58	56.4	65.6	59.3	19.8	54.6
	SZ	-3.62	5.99	6.54	-25.7	10.8	3.61	5.36
		41.5	42.4	43.9	51.1	43	14.3	36.2
	SXY	-2.75	-1.99	-2.09	-3.38	-1.53	-0.51	-1.41
		2.71	2.19	2.18	4.48	1.56	0.52	1.31
Conduit Wrap	SX	-84.8	-71.1	-71.5	-123	-37.4	-12.5	-46.9
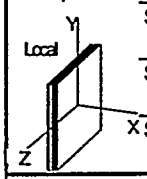		19.5	21.8	22.2	29	28.1	9.36	25.8
	SY	-306	-232	-234	-483	-145	-48.4	-116
		307	293	272	366	241	80.4	260
	SZ	40.5	65	-69.4	-19.7	59.2	19.7	64.2
		184	190	189	203	166	55.3	163
	SXY	-76.3	-75.7	-76	-79.5	-60.7	-20.2	-63
		79.9	68.9	69.4	54.4	62.2	20.7	65.2
Roving	SX	-65.5	-53.5	-54	-88.7	-25.2	-8.41	-36.2
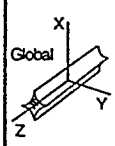		131	149	149	135	216	71.8	168
	SY	-37.5	-32.7	-32.7	-51.8	-33.9	-11.3	-28.4
		229	214	211	226	173	57.5	186
	SZ	9.64	19.3	19.9	30.9	-10.8	-3.61	-7.25
		87.1	95.6	97	117	84.1	28	67.7
	SXY	-70.9	-61.7	-58.2	-74.8	-58.6	-19.5	-53.3
		61.8	69.8	70.3	84.1	74.7	24.9	63.6
Spacer Block	SX	-33.8	-27.7	-27.7	-55.9	-24.6	-8.21	-26.1
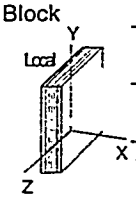		298	265	276	223	225	74.9	244
	SY	-183	-132	-140	-286	-90.9	-30.3	-106
		49.2	37.2	31.2	58.5	94.1	31.4	40.8
	SZ	65.6	85.7	90.1	16.7	82.3	27.4	76.3
		236	228	238	201	192	64.1	199
	SXY	-91.8	-76.5	-77	-71.6	-67.7	-22.6	-76.7
		83	93.7	87.7	74.4	72.1	24	82.7
Ground Wrap	SX	-242	-183	-190	-279	-13.1	-4.38	-101
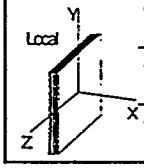		95.2	56.1	55.1	42.7	49.1	16.4	52.4
	SY	-303	-236	-247	-308	-124	-41.5	-179
		145	109	116	118	80.1	26.7	97
	SZ	-130	-86.3	-88.6	-119	-36.5	-12.2	-77.1
		49.8	54.7	56.9	67	20.3	6.77	27.1
	SXY	-107	-99.8	-106	-152	-38.2	-12.7	-63.3
	-	134	87.3	82.8	109	26.8	8.93	52.4

Table 3-3 - FEA Maximum Stress Result Summary for the CS Coil Assembly

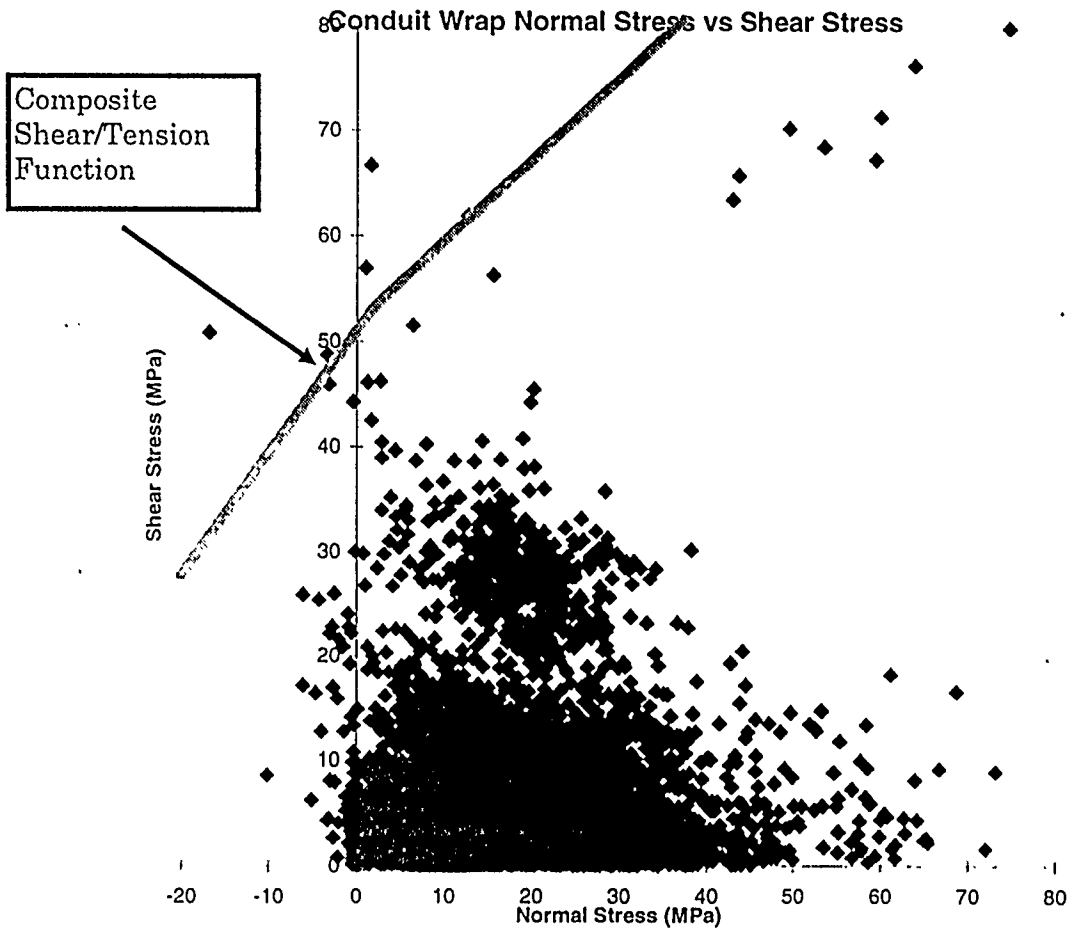

Figure 4.3 Scatter Plot of all elments ~~cantioning~~ conduit wrap

Contain

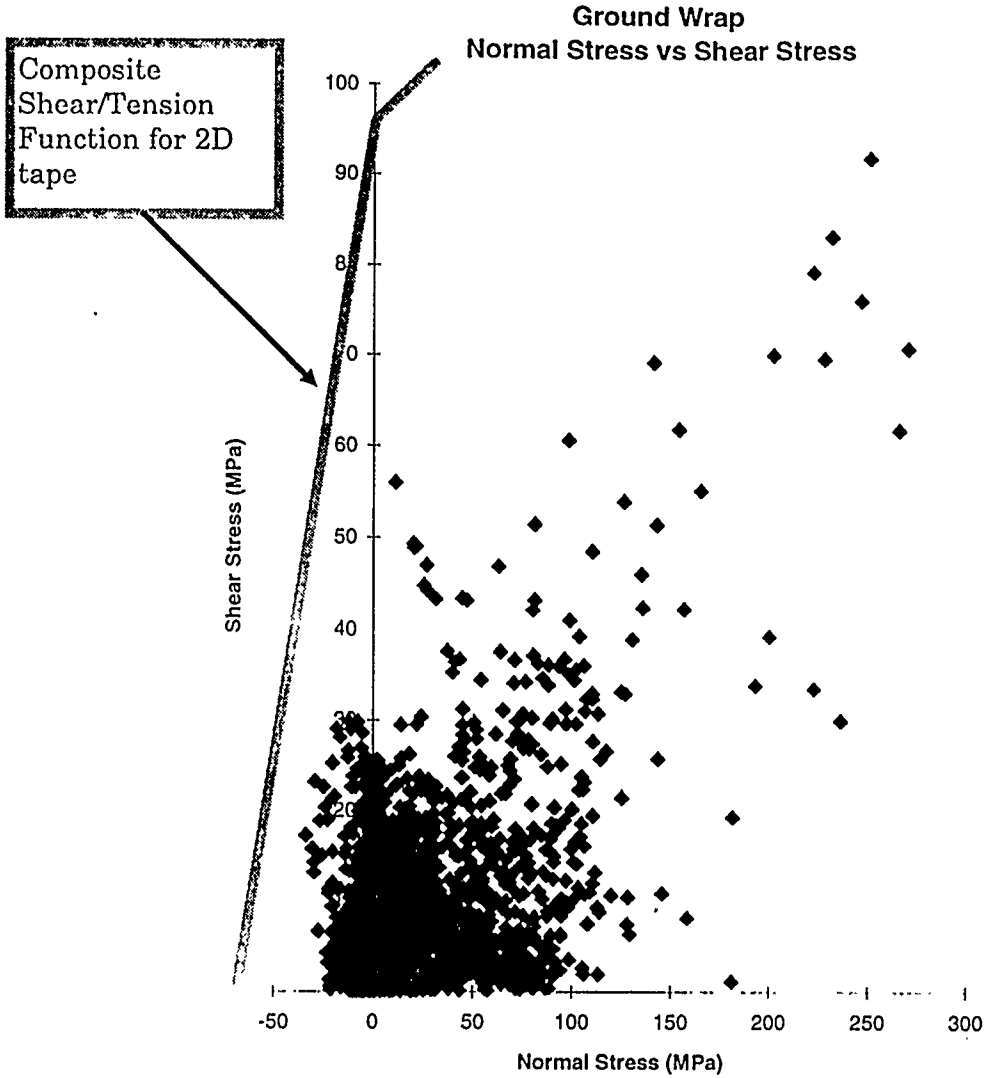

Figure 4.4 Scatter Plot of all elments cantioning Ground Wall INsulation.

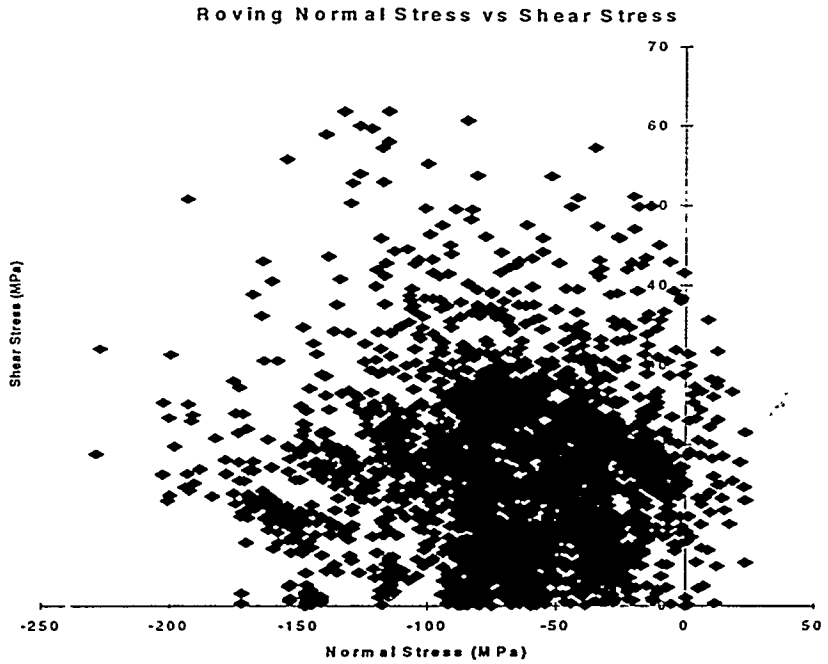

Figure 4.5 Scatter Plot of the Shear and Tensile Stresses of the Corner Filler

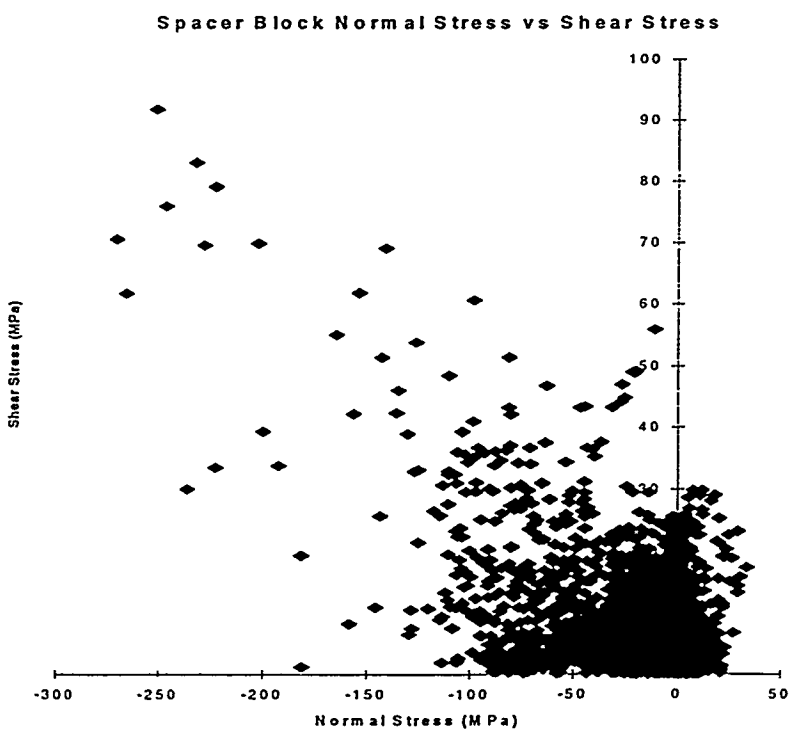

Figure 4.6 Scatter Plot of the Shear and Tensile Stresses in the Spacer Blocks

CONCLUSION

1. 99.87% of the conduit wrap passes the design criteria
2. 100% of the ground wall insulation passes the design criteria.
3. The corner fillers are still under very high combined tensile and shear stress with only 36% passing the criteria.
4. 90% of the transition pieces/spacer blocks pass the criteria

It is clear that the structural design of the CS coils cannot meet by analysis the allowables as defined in the TPX Design Criteria. However the design criteria provides for *Verification by Testing* in section I-4.1.4.4 "Stress Limits for Insulating Materials". The Large Scale Insulation Verification Test Program was designed to verify the design of the CS coil structural with the exception that irradiated materials were not available and the irradiation of a sample large enough to perform an adequate test was problematic.

AREAS OF FURTHER IMPROVEMENT

1. The transition pieces or spacer blocks are subjected to combined shear and tensile forces from thermal mismatches and property anisotropy. Reinforcement and further design refinements can improve this condition.

2. The corner fillers are highly stressed in tension and shear. The R &D program placed glass fibers in the through thickness direction but only achieved approximately 5% glass content. The same approach should be continued with a more radical shift in glass orientation from the 5% to approximately 30% in each direction. The filler pieces become essentially through-thickness glass held together with longitudinal fibers instead of the present longitudinal bundles of glass held together with glass threads. The weaving process and configuration would remain the same. This shift in glass orientation simultaneously reducing the thermal contraction and decreasing the modulus.

Section VI - D

EM Analysis of Joggles & Leads

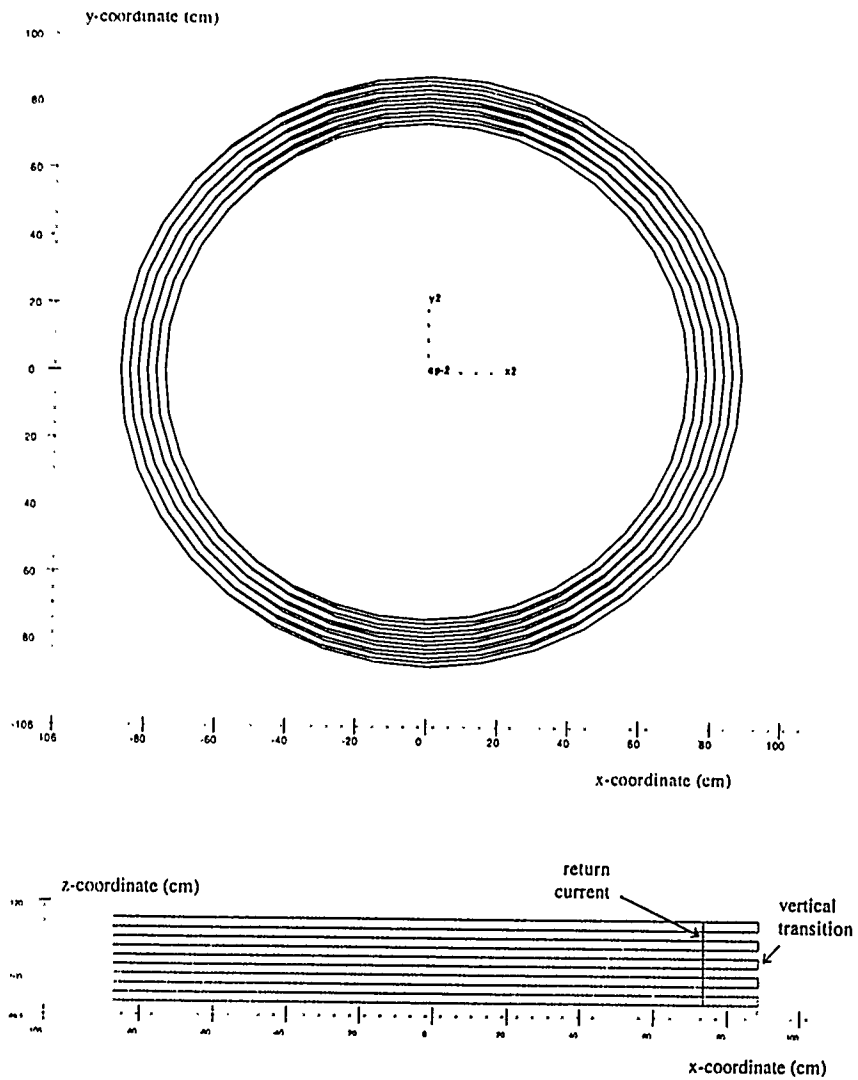

Figure 5.1 — Orthogonal views illustrating two layer spiral winding configuration with 6 turns per layer.

EM Analysis of Joggles & Leads

DRAFT

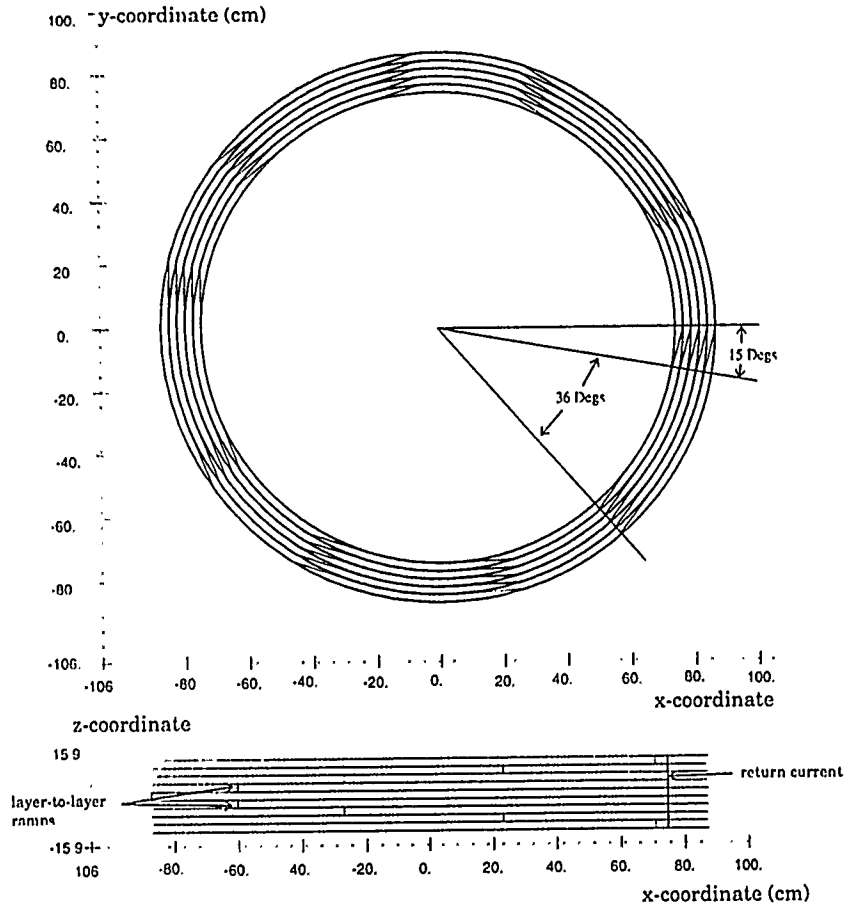

Figure 5.2 — Orthogonal views illustrating 10 layer, constant radius/jog winding configuration with 15 degree crossover interval and 36 degree retarded clocking.

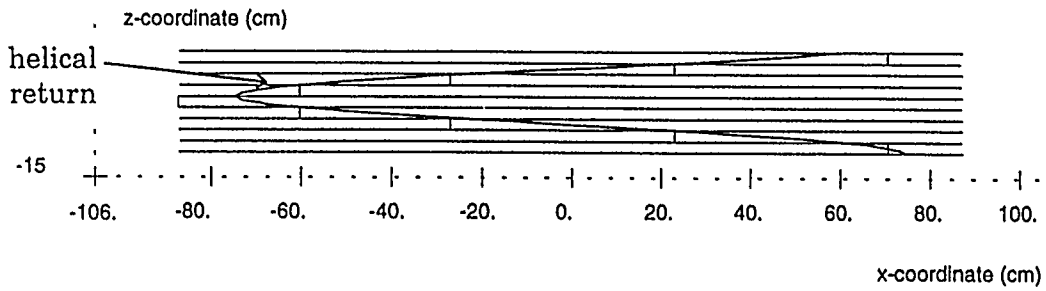

Figure 5.3 — Helical return path used to compensate for the layer-to-layer ramps.

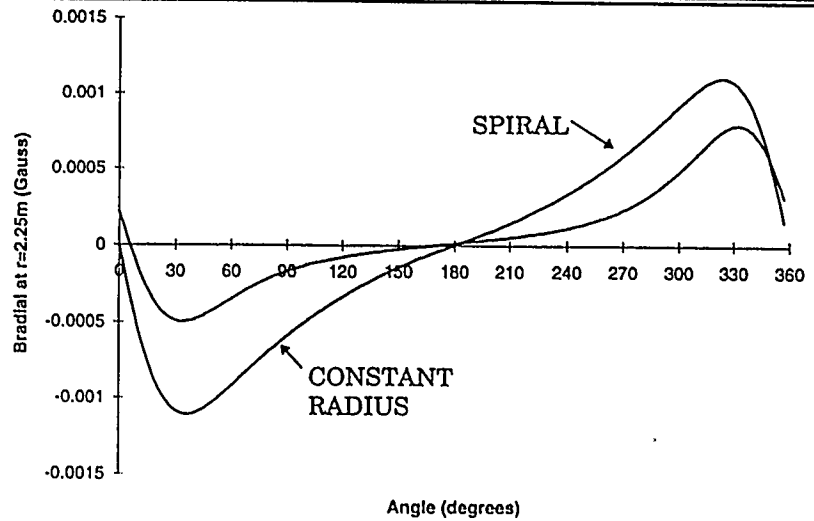

Figure 5.4 — Comparison between radial field perturbations for 60 turn spiral and constant radius coil configurations. The radial transition interval for the constant radius/jog configuration is degrees.

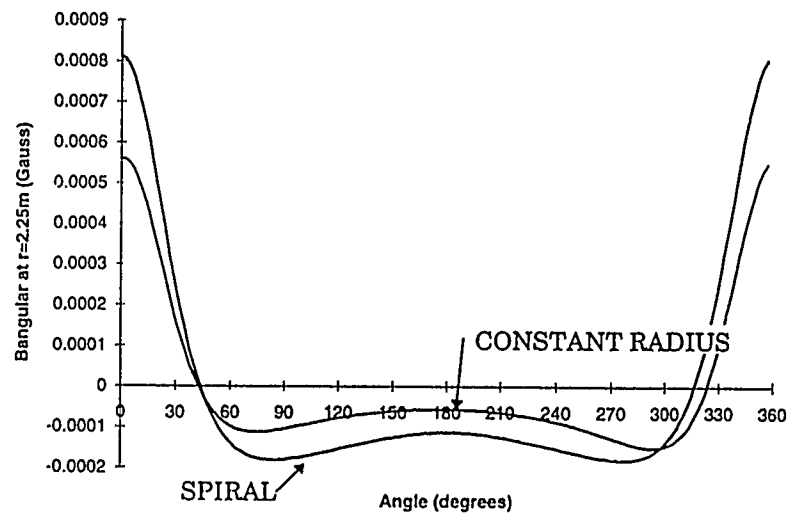

Figure 5.5 — Comparison between angular field perturbations for 60 turn spiral and constant radius coil configurations. The radial transition interval for the constant radius/jog configuration is 30 degrees.

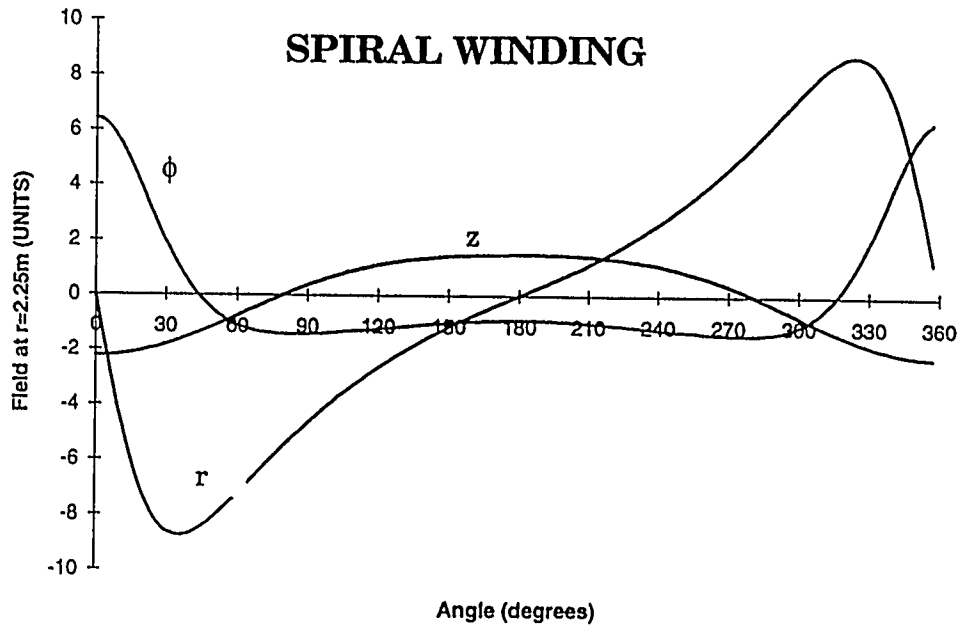

Figure 5.8 — Magnetic field errors for a co-located 60 turn spiral configuration with a vertical return lead.

EM Analysis of Joggles & Leads

DRAFT

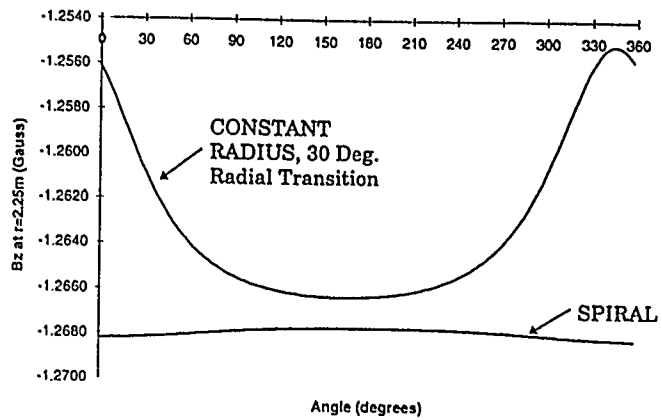

Figure 5.6 — Comparison between vertical field perturbations for 60 turn spiral and constant radius coil configurations. The radial transition interval for the constant radius/jog configuration is 30 degrees.

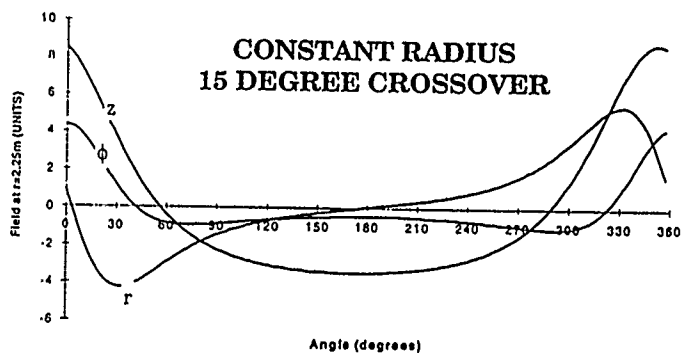

Figure 5.7 — Magnetic field errors for a constant radius/jog configuration with 15 degree radial transition interval and vertical return lead.

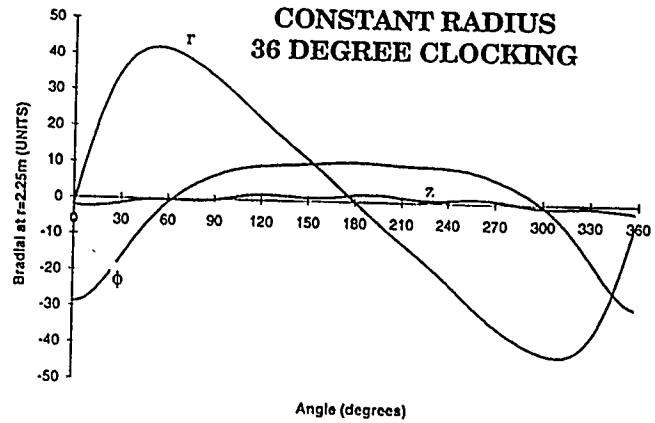

Figure 5.10 — Magnetic field errors for a constant radius/jog configuration with 36 degree clocking and 15 degree radial transitions.

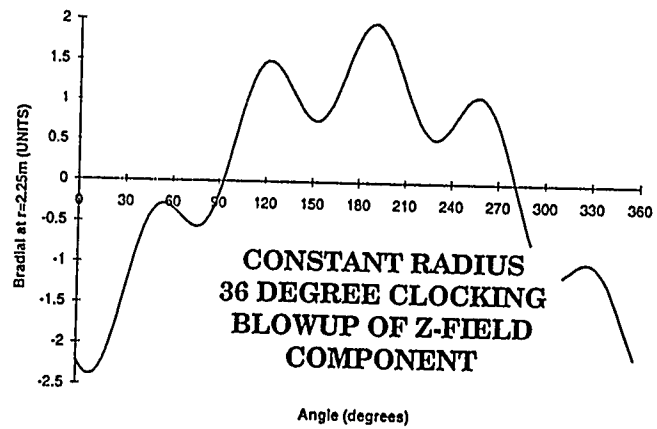

Figure 5.11 — Blowup of vertical magnetic field error for a constant radius/jog configuration with 36 degree clocking and 15 degree radial transitions.

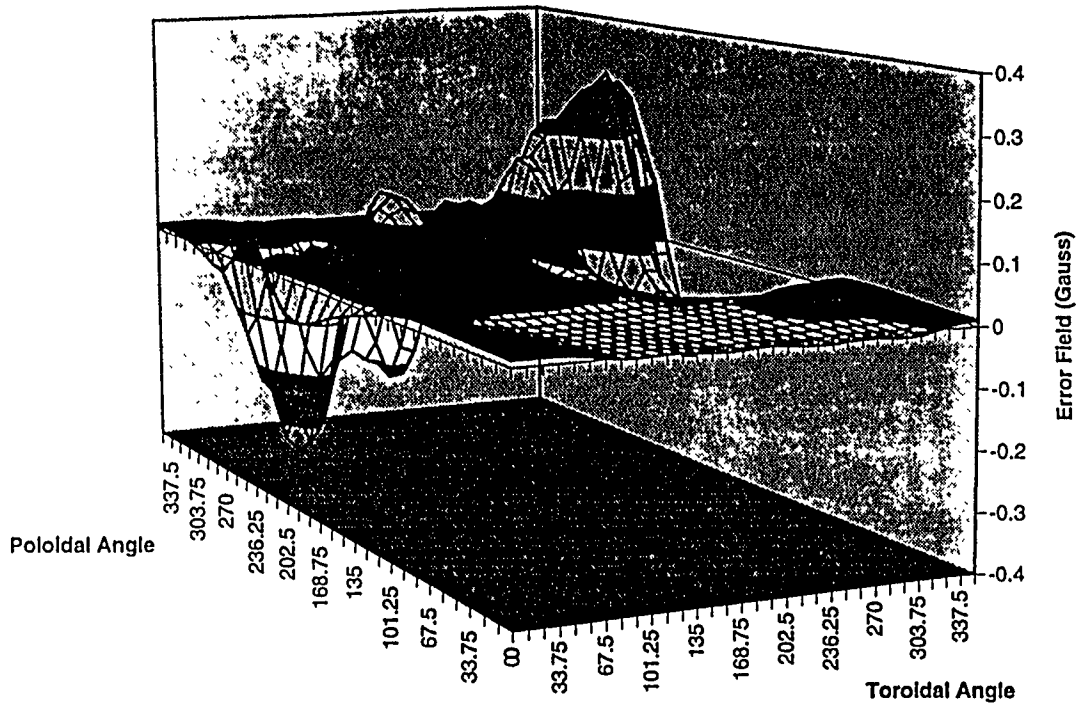

Figure 5.18 — Developed plot of the non-axisymmetric magnetic field on the "dee-shaped" plasma surface for coil PF5U with a uniformly clocked (i.e., -36 degree) constant radius/jog type winding and a compensating helical return lead.

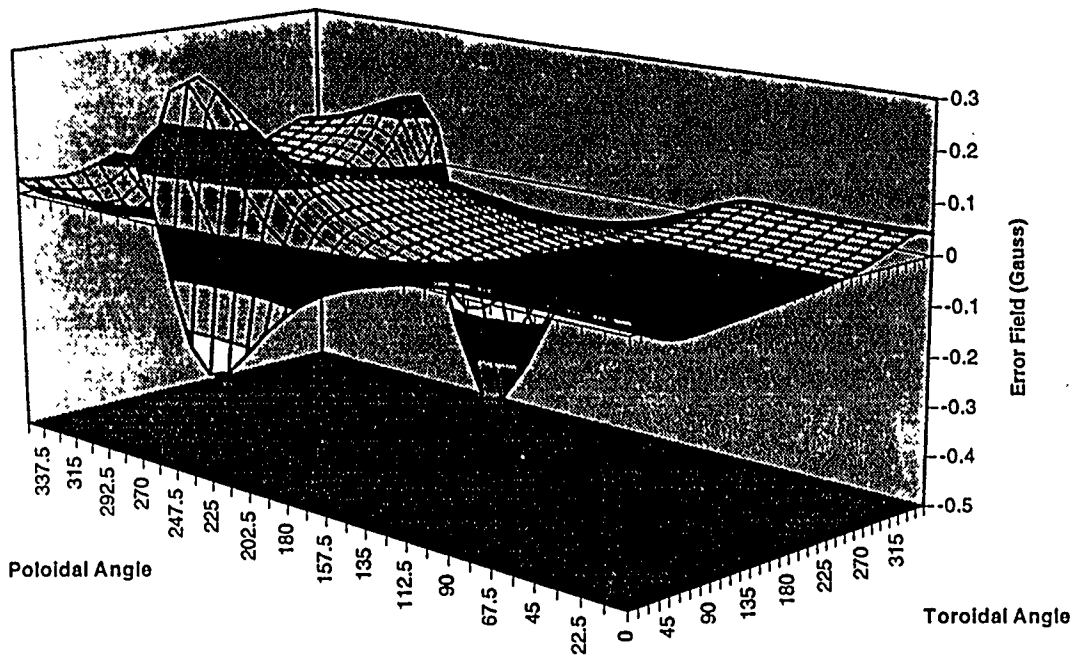

Figure 5.16 — Developed plot of the non-axisymmetric magnetic field on the "dee-shaped" plasma surface for coil PF5U with a co-located constant radius/jog type winding with 10 degree radial transitions and a vertical return lead.

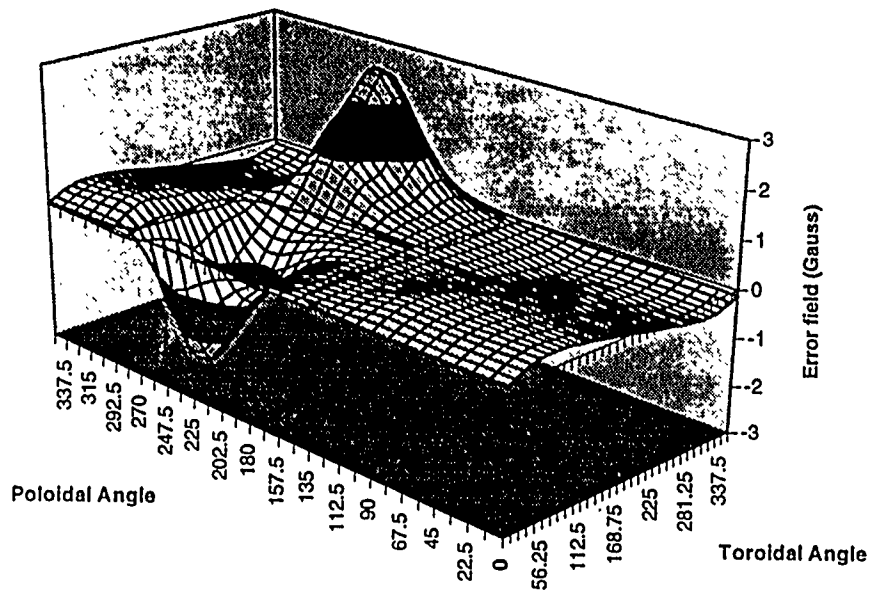

Figure 5.17 — Developed plot of the non-axisymmetric magnetic field on the "dee-shaped" plasma surface for coil PF5U with a uniformly clocked (i.e., -36 degree) constant radius/jog type winding and a vertical return lead.

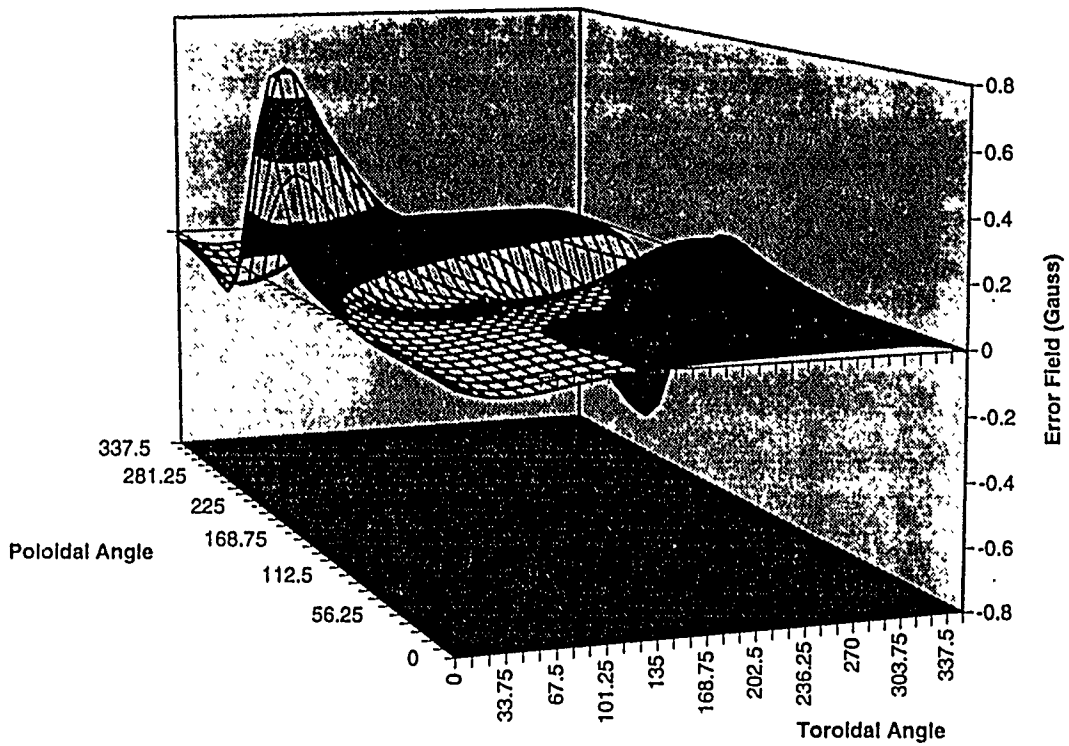

Figure 5.15 — Developed plot of the non-axisymmetric magnetic field on the "dee-shaped" plasma surface for coil PF5U with a co-located spiral type winding and a vertical return lead.

Table 5.2 — Magnitude of the critical right helical field modes produced by four different PF5 coil designs. The coefficients are expressed as parts per 10^4 relative to 4T.

	n=1				n=2		
	m=1	m=2	m=3	m=4	m=3	m=4	m=5
System Requirement	< 2.000	< 1.000	< 1.000	< 1.000	< 4.000	< 4.000	< 4.000
PF5U Spiral, co-located	0.0197	0.0194	0.0139	0.0094	0.0068	0.0041	0.0027
PF5U constant radius/jog co-located	0.0077	0.0039	0.0019	0.0011	0.0020	0.0010	0.0004
PF5U constant radius with -36 deg. clocking	0.0962	0.0639	0.0436	0.0269	0.0177	0.0109	0.0059
PF5U constant radius, -36 deg. clocking, helical return	0.0079	0.0092	0.0062	0.0044	0.0029	0.0019	0.0011

CONCLUSIONS

- It has been shown that constant radius/jog designs with a radial transition interval greater than 15 degrees produces more field error than a spiral type design
- Additionally, layer-to-layer clocking arrangements without vertical current compensation produce a significant level of field error
- It is demonstrated that a helical return lead can be configured to compensate for the layer-to-layer clocking so that the resulting field errors are reduced by an order of magnitude
- The level of field error from a poorly designed (as judged from the viewpoint of field errors) coil are of the same magnitude as that from a gross 3 mm horizontal coil misalignment
  - This implies that field errors inherent to the coil design can be a significant contributor to the total field error
- A co-located vertical transition, spiral type coil design is being proposed for the PF coils
  - This design has been analyzed for the case of PF3 and shown to produce acceptavble levels of field error on the plasma surface

Section VI - E

Verification of MIT Transient Thermal Analysis

Verification of Margin in PF 2&5

- Objective: Verify MIT calculation of margin in PF coils
- Temperature rise will be calculated with Quencher
- Temperature margin is found comparing conductor operating point to the superconductor critical surface

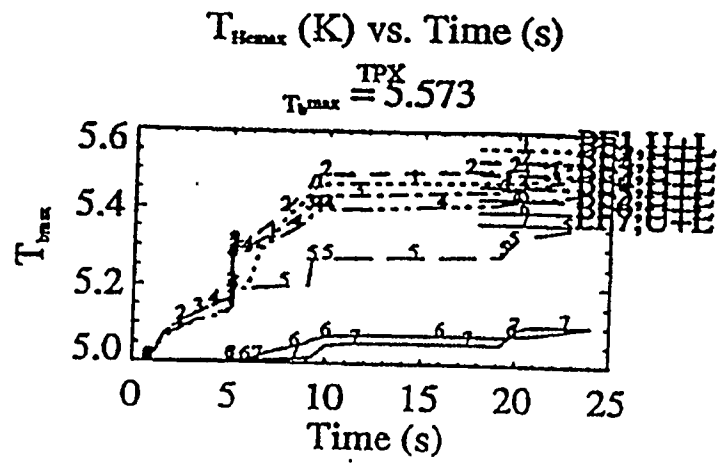

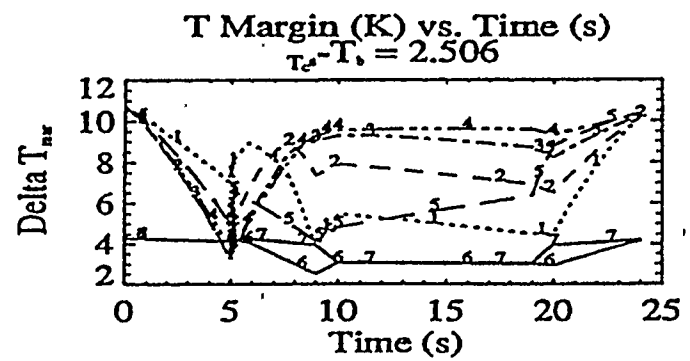

MIT Calculated AC Losses

Losses are less than previously reported

Energy Deposited in PF 2&5

HC Scenario - One Double Pancake

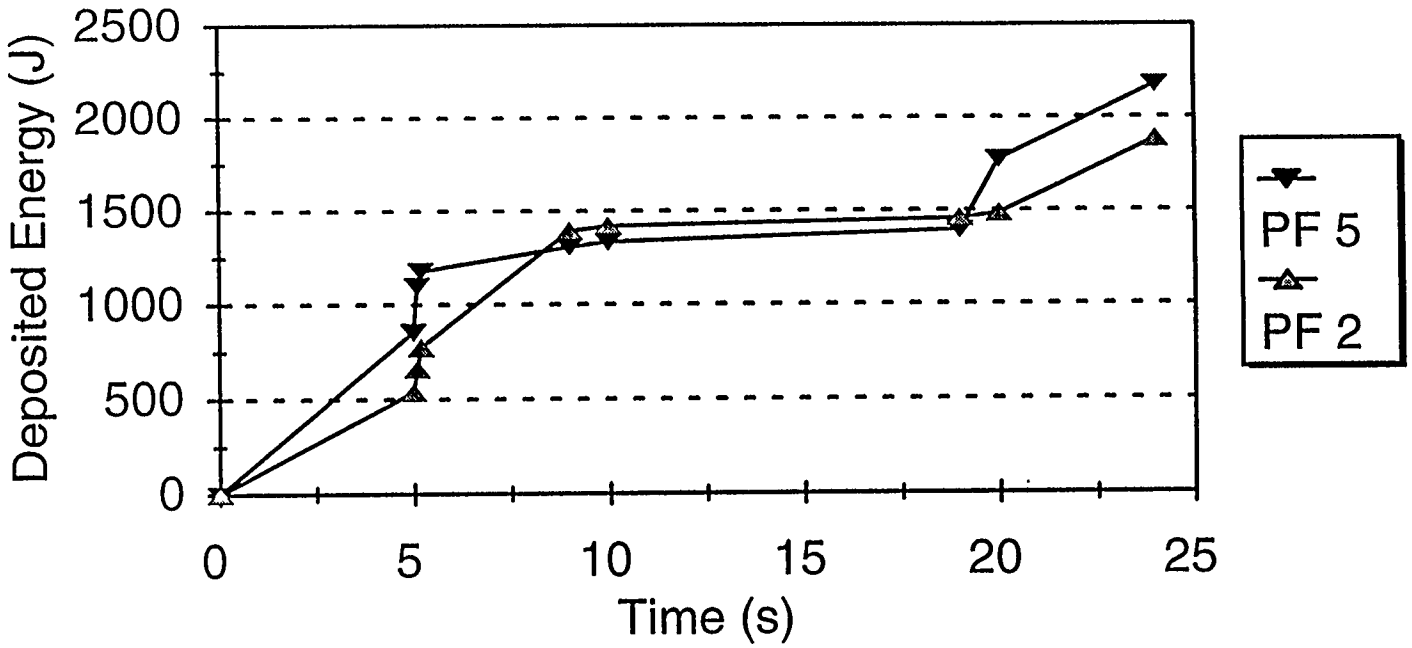

Temperature Rise and Margin

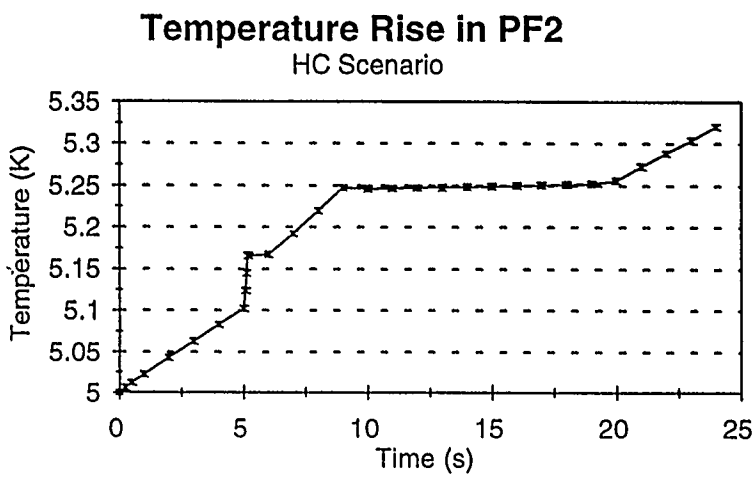

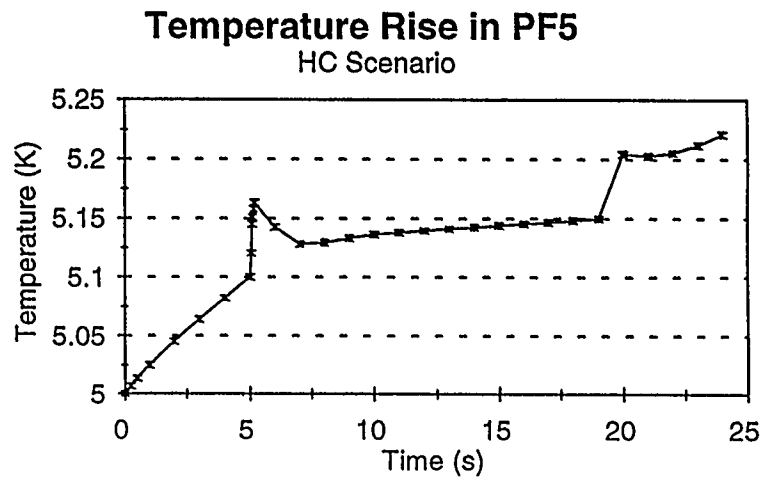

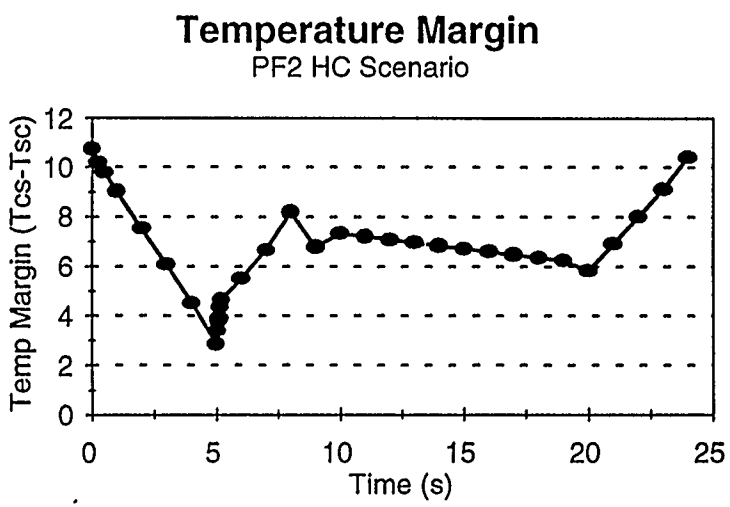

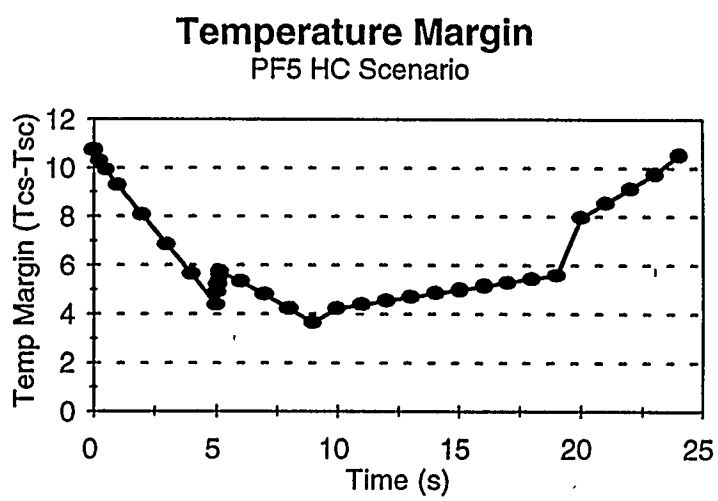

Flow Reversal

- For large heating, the temperature and pressure rise causing flow reversal. This appears as a negative mass flow.
- Flow is re-established at about 10 seconds when the heating decreases.

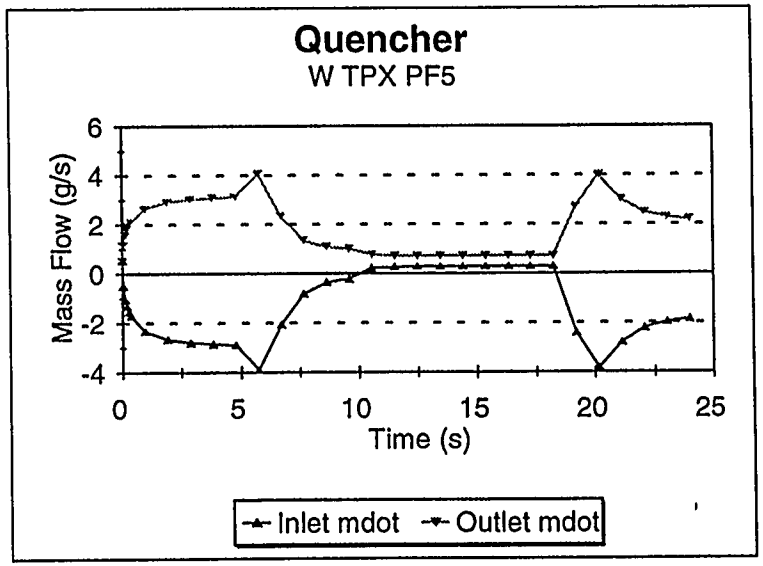

Racheting

- The dwell time to prevent ratcheting is estimated with Quencher by simulating the cooling front propagation.
- The cooling front propagates at 0.05 m/s in PF2.
- Dwell time of 20 minutes will prevent ratcheting in coil PF2, and 40 minutes in PF5 assuming the same cooling front propagation velocity.

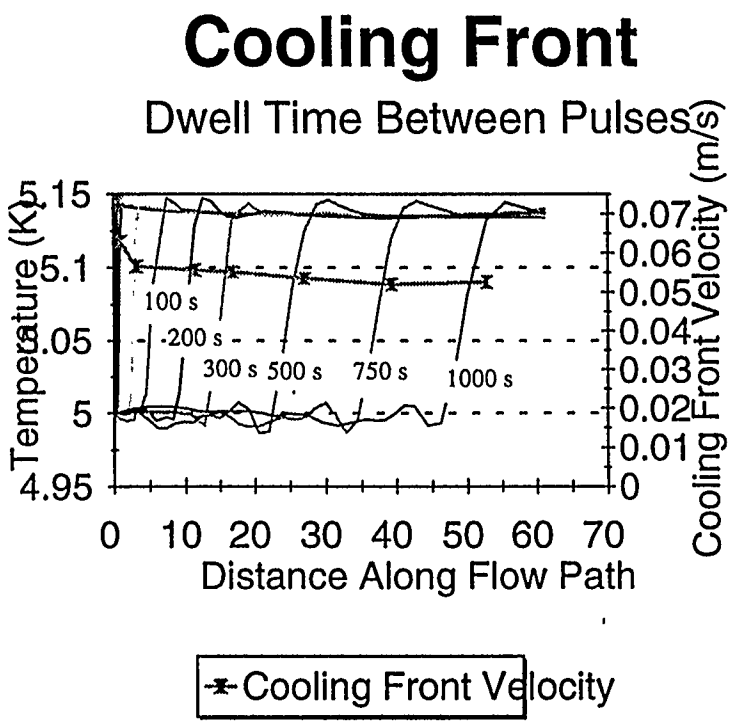

CONCLUSIONS

- Agreement with MIT calculations (slightly lower temperature rise due to lower AC losses)
- Conductors meet margin and headroom requirements during HC scenario
- Flow reversal occurs during the initial heating and final heating parts of the HC scenario. Flow is re-established when the heating decreases at about 10 seconds.
- Dwell times of 20 and 40 minutes will prevent ratcheting in coils PF2 and PF5, respectively.

Assembly and Preload Structure

- Preload structure design
- Coils assembled into structure & preloaded
  - Coil centers aligned to structure center
- Cooling system separately subassembled
- Cooling system assembled to coil/structure assembly
- Instrumentation (table)

[Drawings]

CS to TF Interface Design - Lower Mount

- TF interface locations are mapped
  - Interfacing shear pin bushings are drilled at assembly
- Lower mounts are installed prior to lowering the main CS assembly
- Installed precisely to act as guide pins mating with V-blocks
  - Easier to locate the guide pins exactly than to manipulate the total CS
- Act as temporary vertical supports prior to upper mount installation
  - Allows crane removal to facilitate upper mount installation

[Drawings]

CS to TF Interface Design - Upper Mount

- Use shear pin bushings (drilled at assembly) and shims (+/- 1/2")
- Allow use of stud tensioners to apply even loading to the CS hanger rods

[Drawings]

VII. PF 5 Ring Coil

A. B. Corpuz

Overview

- Key Requirements
  - EM Loads
  - Thermal Contraction
  - Space and Packaging Constraints
- Assembly Drawing

Electromagnetics

- Worst EM Loads
  - Vertical 7.23 MN
  - Radial 6.32 MN

Coil Pack Design

- 8 X 16 Spiral Wound With Co-located Transition and Lead Areas
- Electrical Insulation Design similar to CS

Assembly Design

- Helium and lead routing and support
- Instrumentation (table)

[drawings]

PF5 to TF Interface Design

- Vertical EM Loads are Design Drivers
- Mount Configuration
  - Fixed Supports in the Vertical Direction
  - Sliding Interface Within Mount Hardware
  - Fixed Radial Interface with TF Structure

PF5 Upper Installation Concept

- Coils are Fiducialized (Mapped) at Factory To Determine Current Center
- Map the TF Supports
- Pre-assemble Mounting Brackets, Instrumentation, and He Manifolds on Coil Prior to Shipping to Site
- Assemble Appropriate Shims at Each TF Support
- Install Coil Assembly on Shimmed TF Support
- Verify Alignment
- Adjust Mounting Bracket Shims as Needed, and Install Pins and Fasteners

PF5 Lower Installation Concept

- Coils are Fiducialized (Mapped) at Factory To Determine Current Center
- Pre-assemble Mounting Brackets, Instrumentation, and He Manifolds on Coil Prior to Shipping to Site
- Lower Coil Assembly and Temporarily Support on Cryostat Base
- Install TF Structure; Map the TF Supports
- Assemble Appropriate Shims at Each TF Support
- Raise Coil Assembly onto TF Support& Verify Alignment
- Adjust Mounting Bracket Shims As Needed, and Install Pins and Fasteners

ANSYS THREE-DIMENSIONAL PF5 STRUCTURAL MODEL

GEOMETRY DESCRIPTION

A three-dimensional finite element model of conductor pack PF5 was created using ANSYS structural solid elements STIF45 and point-to-point contact elements STIF52. The entire array of 128 turns was modeled throughout a 45 degree angular span at the ends of which the coil is supported in the vertical direction.

A matrix of 8 radial by 16 vertical cells is formed to represent the 128 turns of PF5. The mean radial and vertical location of this coil pack was taken to be 1.213 m and 2.35 m, respectively.

Table 2-1 - Dimensions used in the PF5 structural model for a single turn in the conductor pack.

DIMENSION	LENGTH (mm)
Cable width	17.47
Inside conduit corner radius	2.692
3-D wrap build	0.813
Overall cell size	23.93 by 23.93

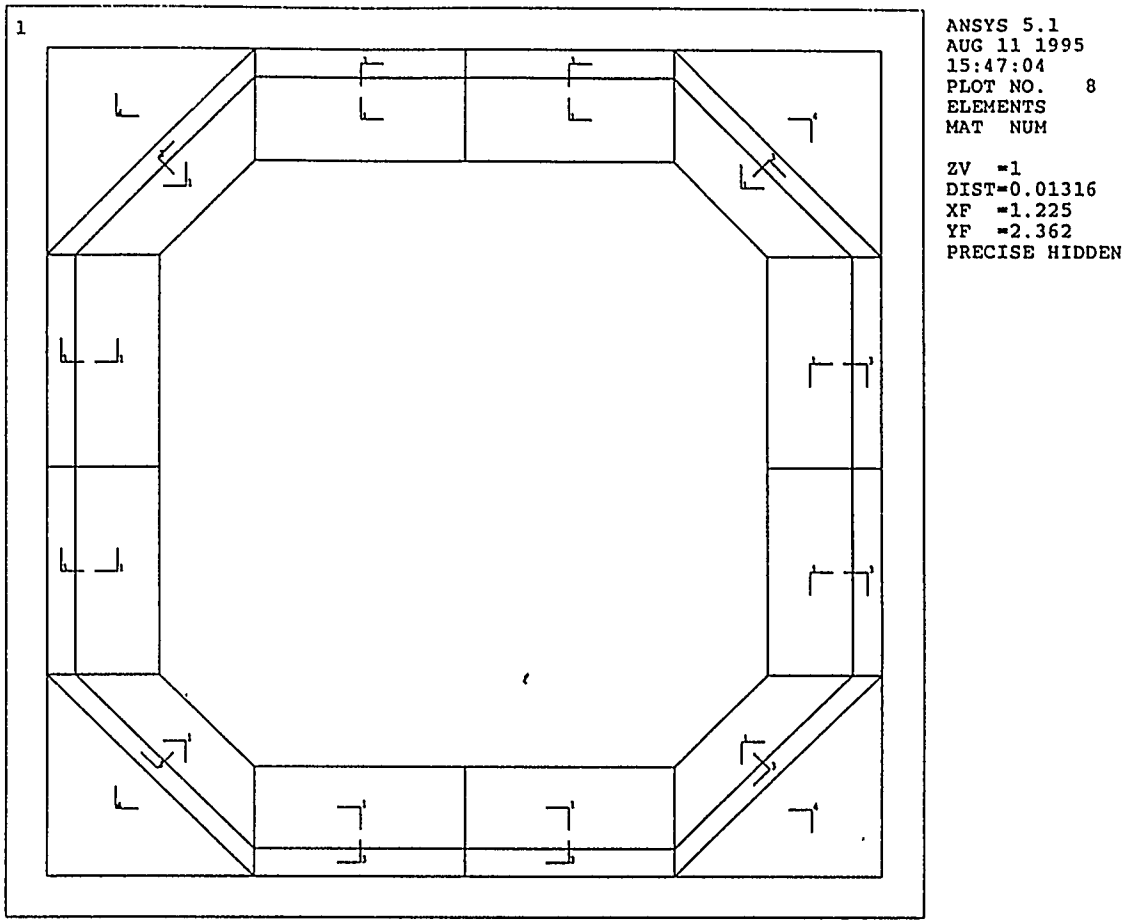

Figure 2-2Cross section showing principle directions associated with finite elements in the conduit, three-dimensional wrap and roving corner fill regions of the conductor pack.

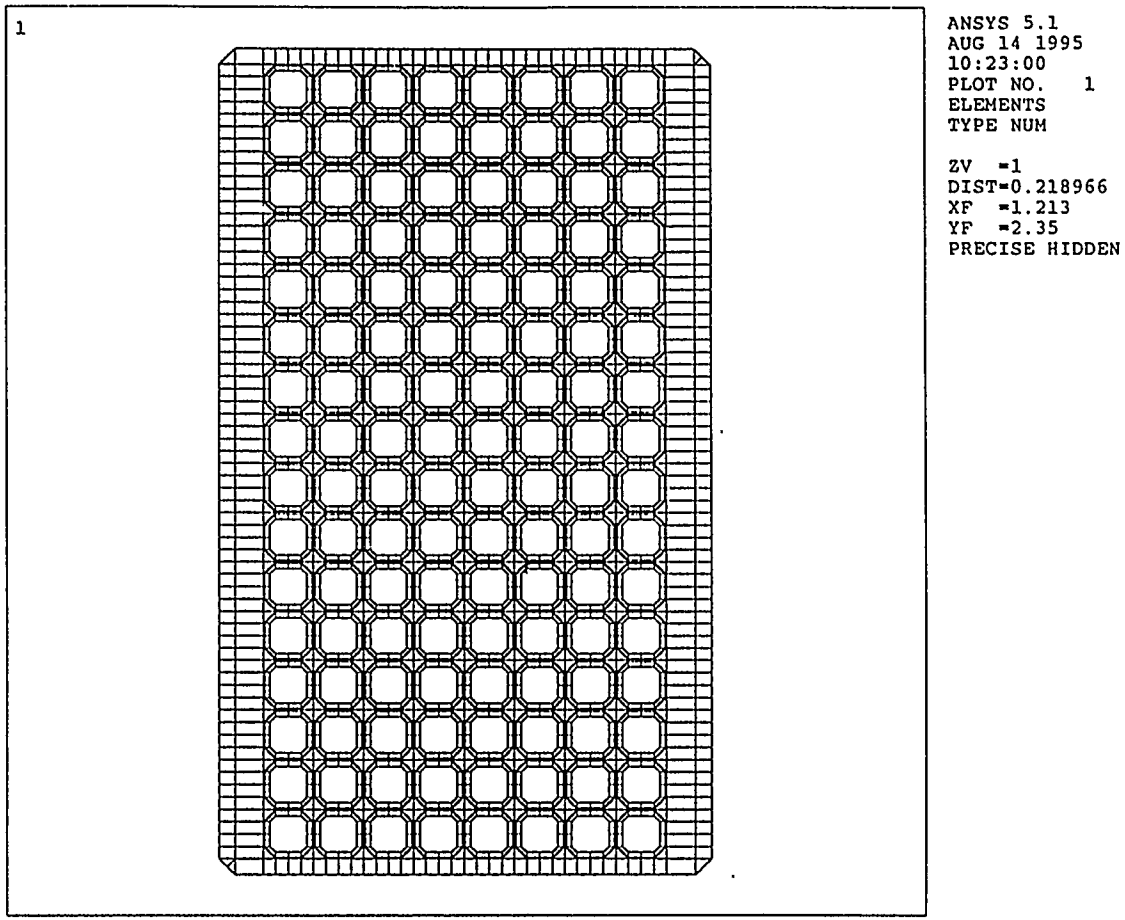

Figure 2-3Cross-sectional cut of PF5 finite element mesh showing build-up of conductor pack from 128 turns and surrounding filler material and ground wrap insulation.

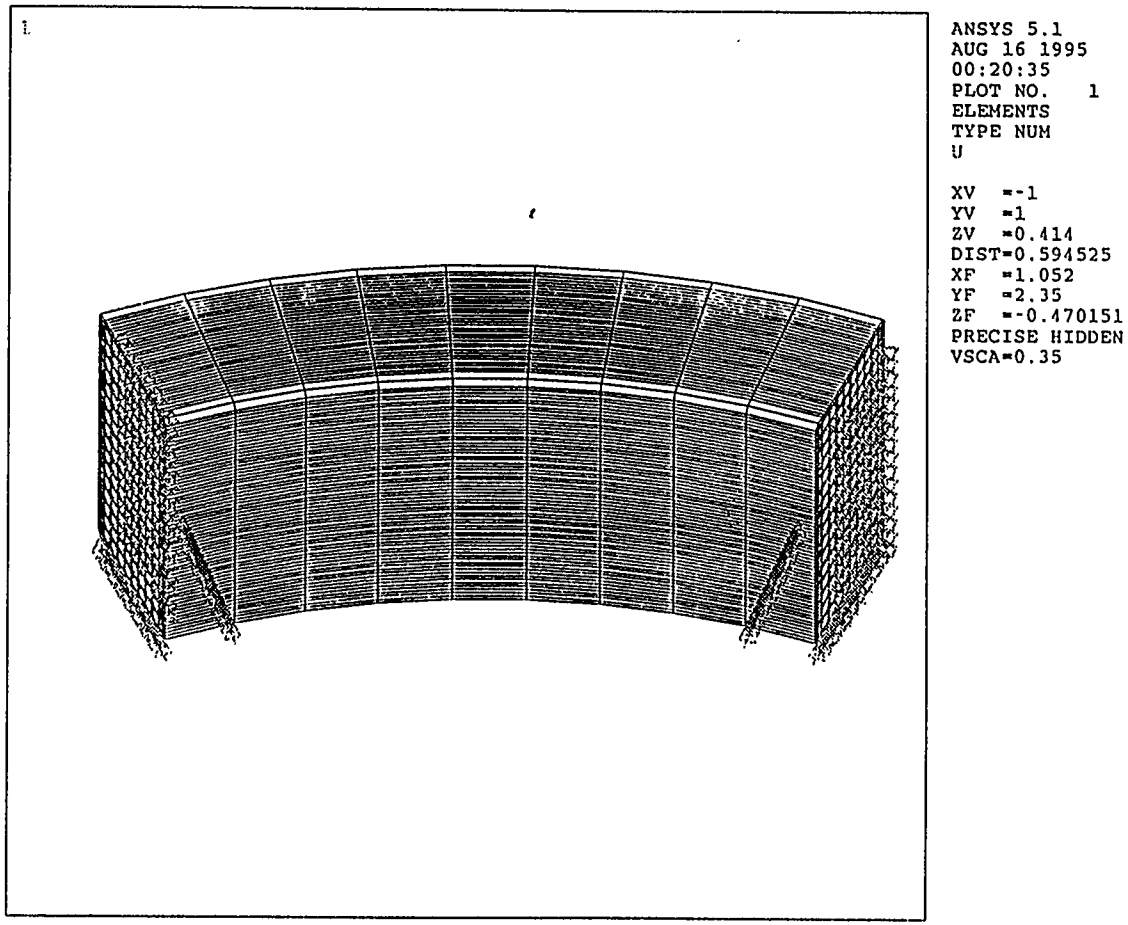

Figure 2-1Three-dimensional view of PF5 structural model illustrating 45 degree section of coil being modeled and vertical and angular constraints applied to the conductor pack.

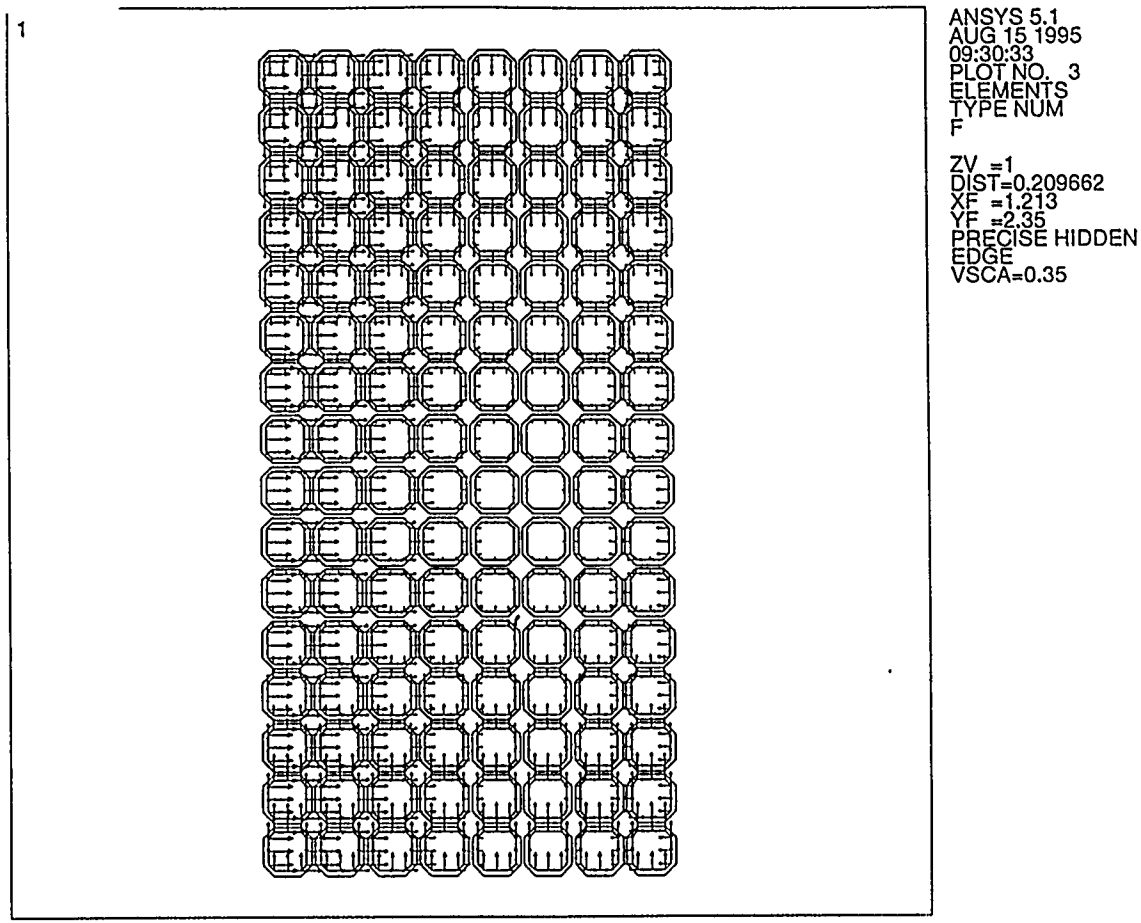

Figure 2-6 Electromagnetic force distribution throughout PF5U cross section during equilibria #1 at a location directly above a TF support..

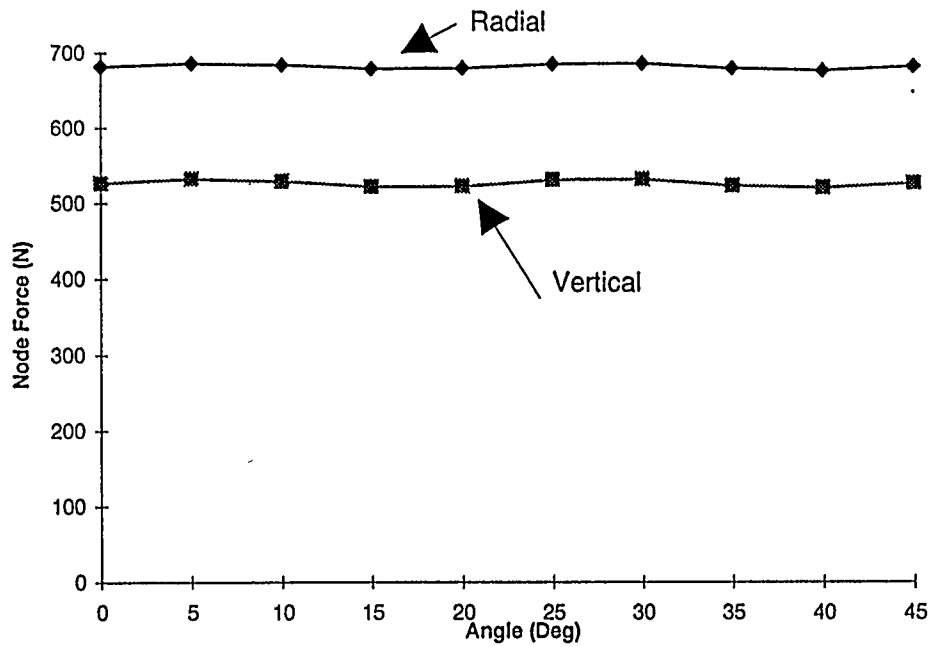

Figure 2-7 Electromagnetic force variation along PF5U conductor path due to interaction of PF5 current with TF generated magnetic fields. A node associated with the innermost lower turn in the PF5U conductor pack is shown in this plot

Table 2-2 Material properties and orientations assumed in PF5 structural model

Material ID	Material Type	E_x (GPa)	E_y (GPa)	E_z (GPa)	α_x(μ/K)	α_y(μ/K)	α_z(μ/K)	G_{xy} (GPa)	G_{xz} (GPa)	G_{yz} (GPa)	υ_{xy}	υ_{xz}	υ_{yz}
1	Incoloy	185	185	185	5.92	5.92	5.92	71	71	71	.299	.299	.299
3	3-D weave thin tape	32	23	25	8.25	19.2	16.2	8.0	8.0	8.0	.186	.34	.34
4	3-D corner fill	22	25	31	20.3	16.2	7.56	8.5	9.0	8.0	.26	.38	.23
8	3-D weave filler blocks	23	32	25	19.6	8.25	16.2	8.0	8.0	8.0	.26	.37	.25
9	Ground wrap	19.7	29.6	29.6	19.9	6.7	6.7	7.6	7.6	10.7	.26	.26	.26

Material ID	ORIENTATION
1	Not an issue - material is isotropic
3	x is along wrap direction, y is through thickness, z is along conductor direction (i.e., angular)
4	x is vertical, y is radial, z is along conductor direction (i.e., angular)
8	x is radial, y is vertical, z is along conductor direction (i.e., angular)
9	x is through thickness, y is along wrap direction, z is along conductor direction (i.e., angular)

. a 125 K cooldown from glass transition temperature plus a 290 K cooldown from ambient to cryogenic operating temperature (i.e., 4K).

2.3 BOUNDARY CONDITIONS AND LOADINGS

The boundary conditions placed on the PF5 model include periodicity constraints in the form of coupled degrees of freedom and angular and vertical displacement constraints.

a 45 degree section is required for the analysis.

The periodicity is enforced by coupling the deflections (i.e., U_r, U_ϕ, U_z) throughout the coil pack

(i.e., $U(\phi)=U(\phi\pm45)$ for any node).

, some form of hoop constraints must be applied to restrict the coil pack and conduits from spinning about the vertical axis. Therefore, a single node associated with each of the 128 conduits along with a single node in the insulation region of the conductor pack is fixed in its angular degree of freedom (i.e., U_ϕ,=0).

COIL PACK DEFORMATIONS

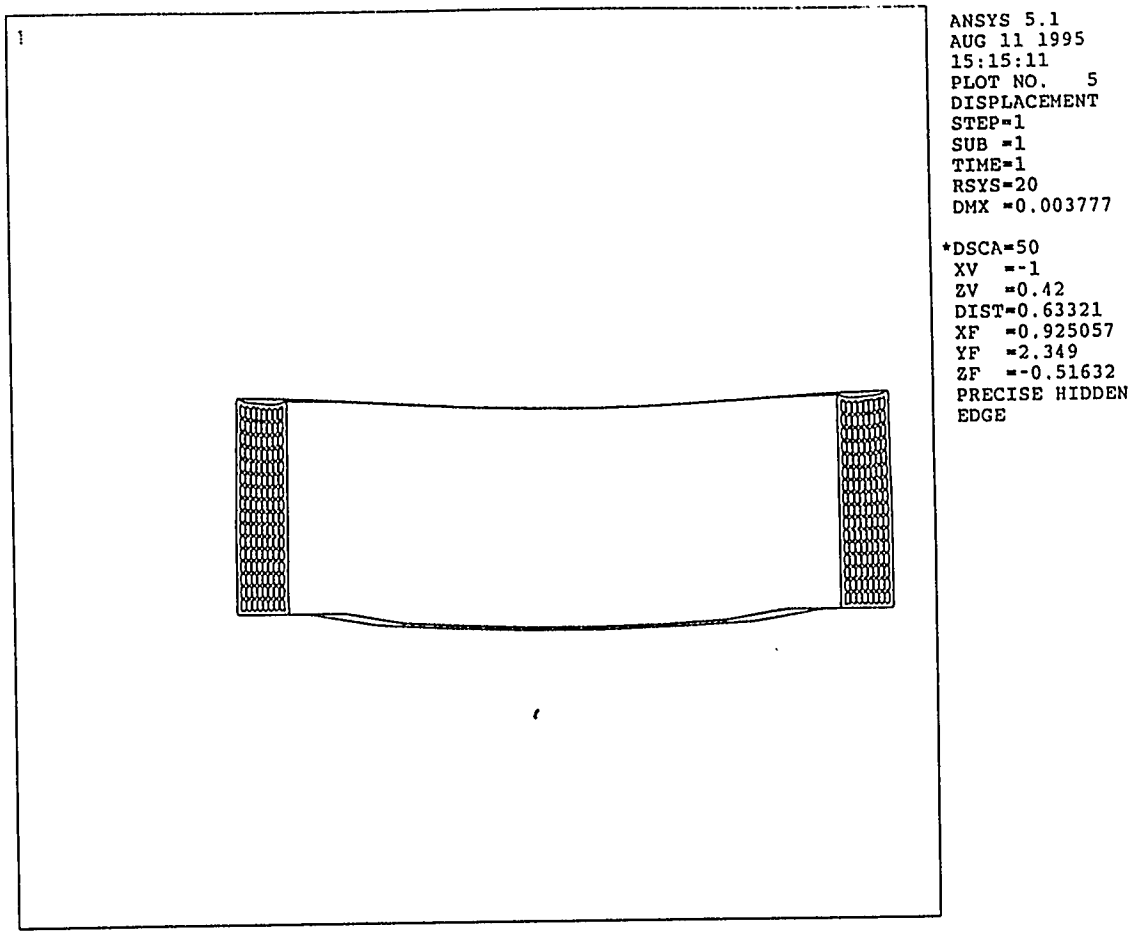

Figure 3-2 Side view of deformed PF5 coil illustrating sag between vertical support points due to downward vertical Lorentz loading.

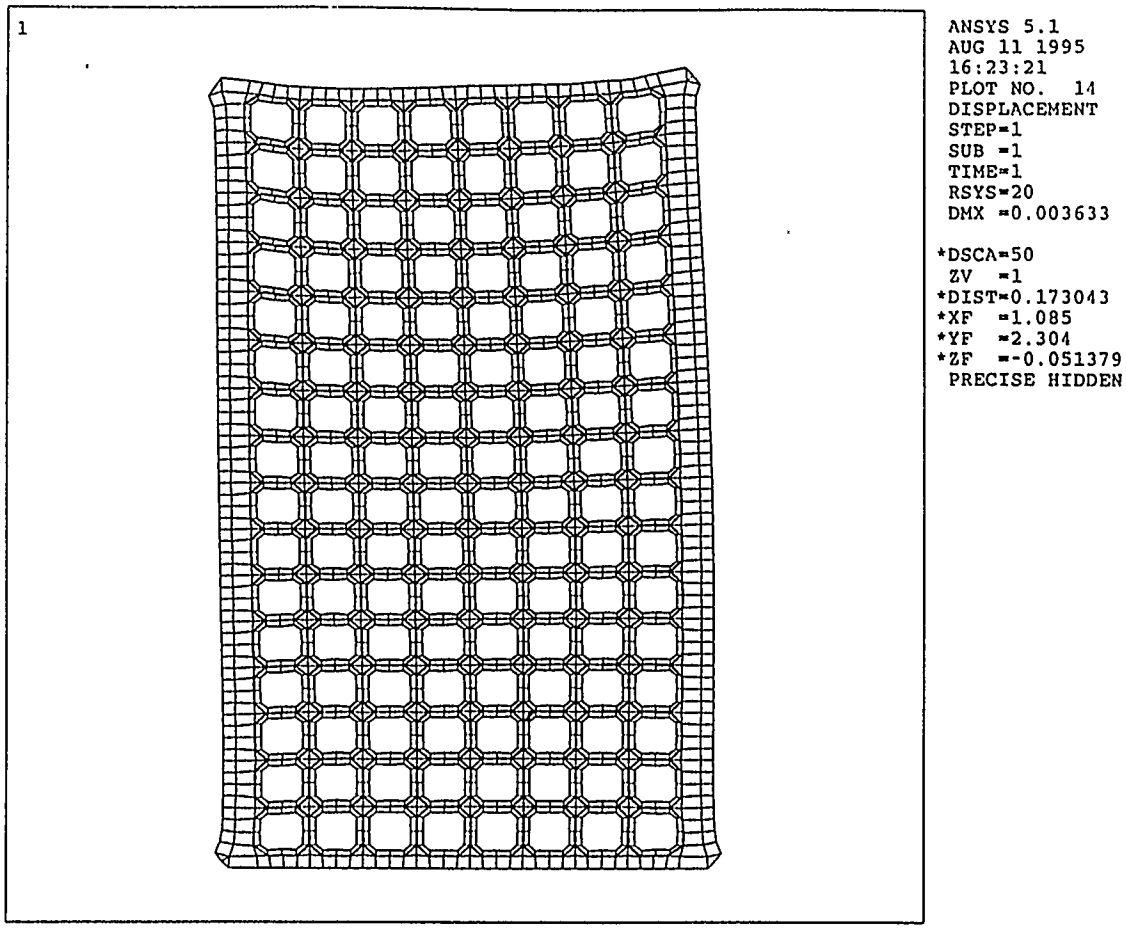

Figure 3-3 Cross section of PF5 conductor pack directly above TF support point illustrating deformed shape of pack due to cooldown and Lorentz force loading.

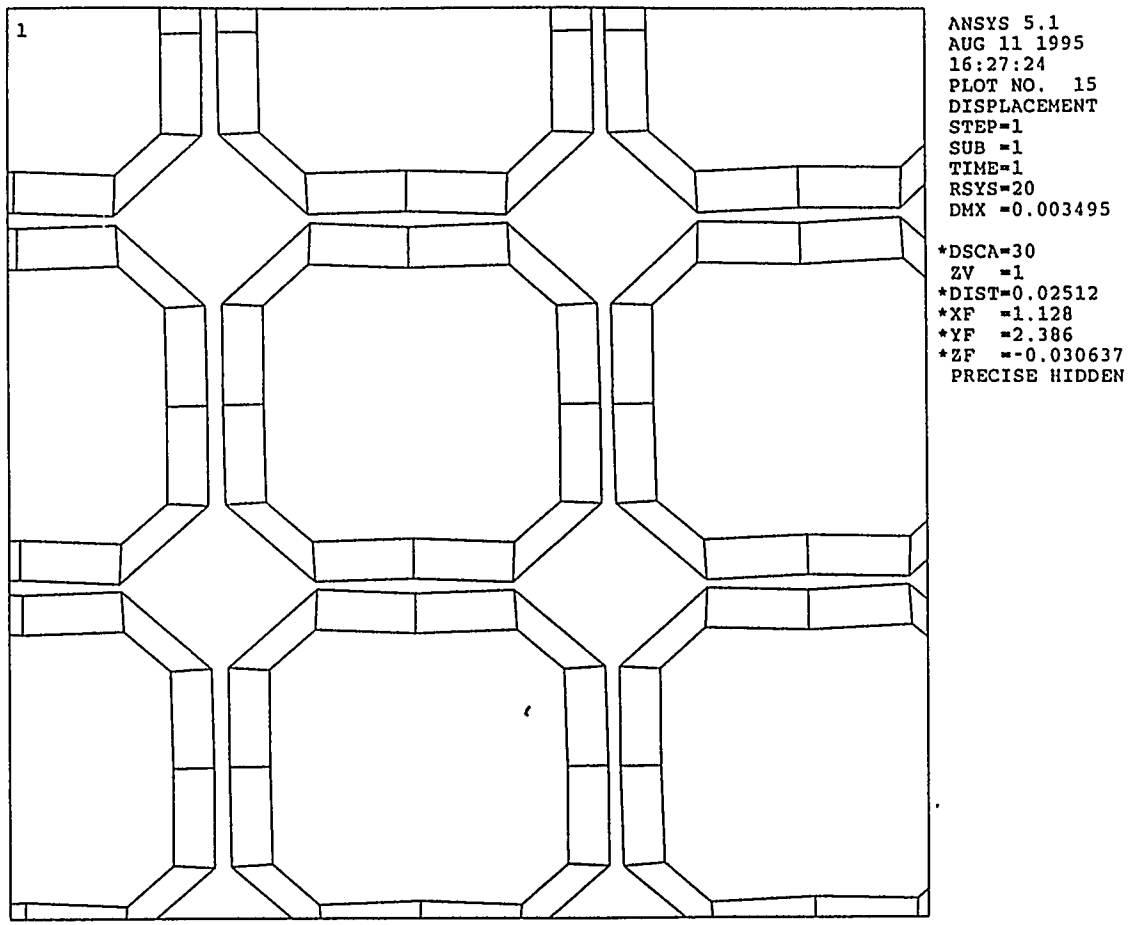

Figure 3-4 Blowup of conduit elements showing deformation which is evident even with the coarse model.

Table 3-1-Summary of maximum and minimum stress components throughout the PF5 conductor pack.

		Three-Dimensional Model Cooldown and Lorentz Loads (MPa)	Axisymmetric Model Cooldown and Lorentz loads (MPa)
Conduit	SX	-248	-188
		197	130
	SY	-65.4	-213
		171	96.1
	SZ	-327	-26
		174	120
	SXY	-62.5	-117
		127	117
	SINT	369	238
3-D Weave Thin Tape 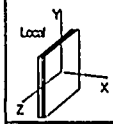	SX	-88	-92
		55.8	30.5
	SY	-106	-87.5
		154	147
	SZ	75.1	86
		170	165
	SXY	-54.8	-21
		50.2	21
Roving 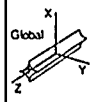	SX	11.4	30.8
		111	108
	SY	25.4	31.8
		90.7*	91.9
	SZ	33.5	52.2
		102	90.5
	SXY	-38.6	-39
		36.3	39.7
Spacer Block 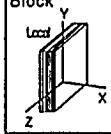	SX	-18.6	-11
		132	120
	SY	-86.4	-44
		89.5	63
	SZ	87.4	103
		194	175
	SXY	-15.8	-11.7
		15.3	10.6
Ground Wrap 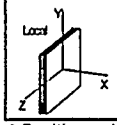	SX	-77.8	-19
		53.3	41
	SY	-106	-1.02
		24	27.5
	SZ	-25.3	-14.8
		48.7	36.2
	SXY	-24.2	-19.7
		26.4	19.9

* Positive values signify tension & negative numbers indicate compression.
Material properties reflect CPDR baseline properties.

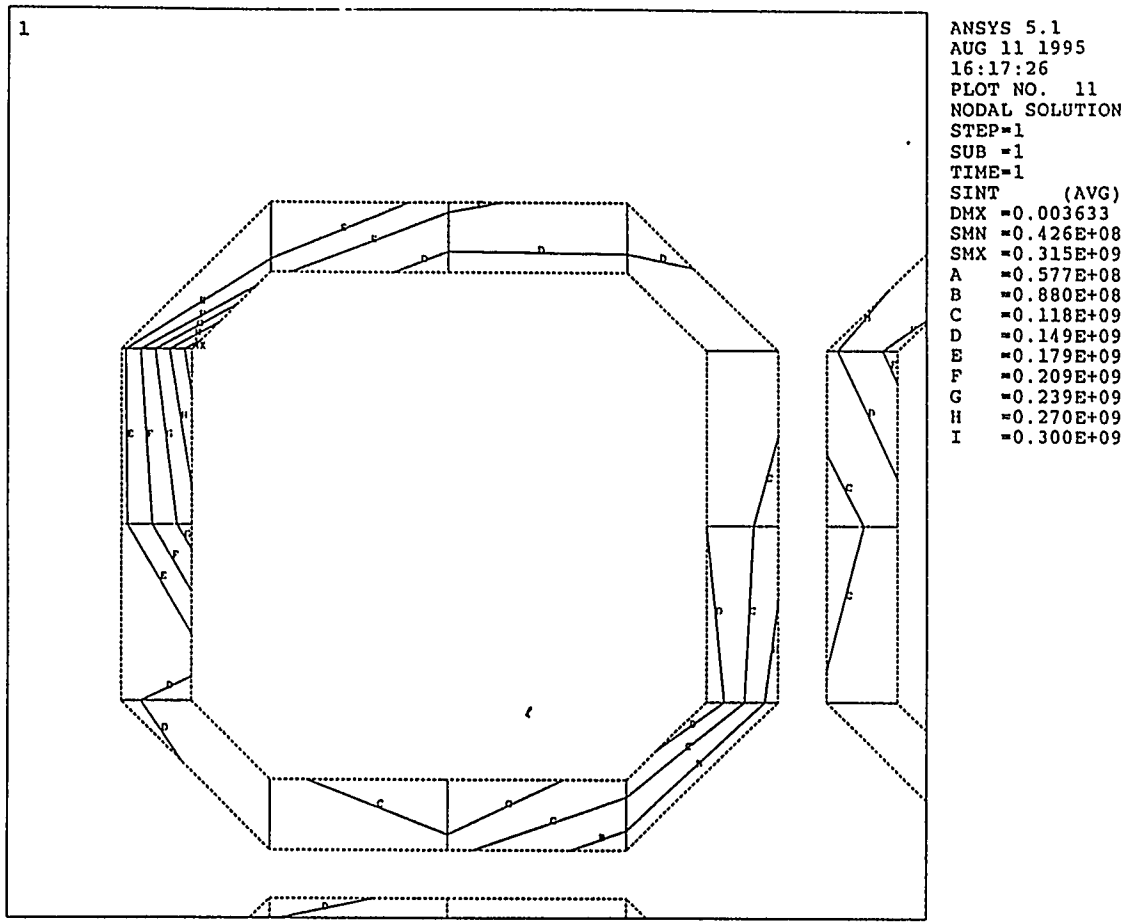

Figure 3-6 Blowup of stress intensity distribution in uppermost left conduit of PF5 conductor pack.

DISCUSSION OF RESULTS

1. A limited amount of bending occurs as a result of the discrete support points based on the deformation plots.
2. The electromagnetic force variations along the path of the conductor are very small in PF5. Further, deformations as a result of these forces cannot even be observed in the results.
3. A large internal compressive force exists in PF5 due to the interaction of the PF5 current and its self field.
4. Surprisingly, a large change in the conduit stresses (see Table 3.2) is observed in the 3-D model indicating the conduit plays a major role in limiting the bending, rather than the insulation.
5. Credence is given to the 3-D solution since the effects of bending can be observed by examining differences in hoop stress (SZ) between axisymmetric and 3-D solutions. For each material in the coil, the spread in the hoop stress (i.e., max-min) is larger in the 3-D as would be expected.
6. Overall, the stresses in the insulation system appear lower for PF5U than in the CS. One exception is the 3-D weave thin tape through thickness stress which is 55.8 MPa for the PF5 model. Perhaps a refined model of this region would be appropriate.
7. The conduit stresses are substantially lower in PF5U compared with the CS, even with the bending effects included.

PF6/7 Ring Coils

Outline

A. Overview

B. Magnetic Loads

C. Winding Pack Design

D. Winding Pack and Coil Case Stresses

E. Coil Case Design, Coolant and Current Supply, and Instrumentation

F. Eddy-Current Heating of Case

G. Interface to TF Coils

Figure showing TPX machine cross-section with PF and TF coils

PF 6/7 Overview

- PF6 and PF7 coils occur in pairs placed symmetrically above and below the machine midplane.

- PF6U is essentially identical to PF6L, and PF7U essentially identical to PF7L.

- Act in concert with the other PF coils to provide the desired flux changes and time-varying field pattern in the plasma volume for plasma shaping, position control, and discharge evolution.

- Also act to compensate effective ring currents from the TF coils and TF current interconnects.

- Differ from other PF coils and TF coils in that they have NbTi, not Nb_3Sn superconductor, 316LN instead of Incoloy conduit.

- Axial and radial magnetic loads vary considerably with azimuthal angle.

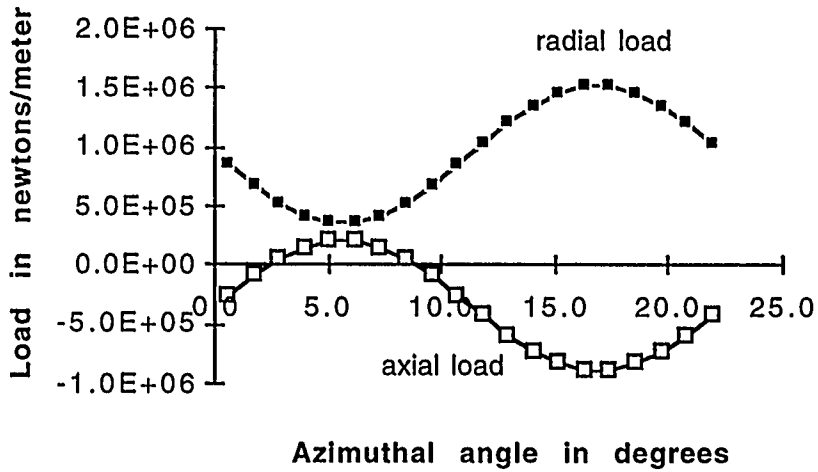

Azimuthal variation of axial and radial loads* over one sixteenth of the circumference of PF6.

*PF currents of equilibrium condition 9 of Radovinski's memo of March 27, 1995, with the plasma current set to zero.

Overview (cont.)

- The azimuthally varying component of the radial and axial loads arises from the interaction of the PF6 and 7 currents with the axial and radial components, respectively, of the ripple fields from the discrete toroidal field coils.

- The only other PF coils with significant force ripple are the two PF5 coils, and their ripple component is much less than that in the PF6 and 7 coils.

- The net magnetic and gravity loads on the PF6 and 7 coils are supported by mounts on the sixteen toroidal field (TF) coils. That is, each of PF6U, PF6L, PF7U, and PF7L is supported at sixteen points along its circumference.

- These supports react only vertical loads (either positive or negative) and, to some degree, moments around rays that pass radially from the machine axis through the coil mounts, but allow free movement in the remaining four degrees of freedom.

- In the present design, a stainless-steel coil case is provided in order to guarantee adequate stiffness and structural integrity over the entire high-cycle operating lifetime of the machine.

Overview (cont.)

- Wound with fully reacted, insulated conductor.

- The allowable helium temperature rise for a given helium inlet temperature in the PF6 and PF7 conductor conduits is less than that in the Nb_3Sn PF coils. This is an issue of major concern.

- The winding pack configuration of PF6 and 7 is similar in concept to that of the other PF coils, with Kapton-wrapped conduits covered with fiberglass cloth that is vacuum impregnated with epoxy to form a solid structure. There is no ground screen, because there is a stainless steel coil case.

- The radial build of both PF6 and PF7 is 6 turns

- The axial builds of PF6 and PF7 are 20 and 14 turns, respectively.

Figure showing winding pack cross-section with coil case

Overview (cont.)

- In order to maximize the number of helium inlets and outlets, the coils are wound in flat spirals or pancakes (sometimes also referred to as layers), each with six turns. The pancakes are connected at the inner and outer radii with joggles.

- Helium inlets and outlets are located at the outer radius of the windings between double pancakes. Additional inlets and outlets ocuur at lead terminations and splices.

- Two conductor splices are needed in PF6 and one conductor splice in PF7. These splices are made outside of the coil case. The same basic joint that is used to make the connection between the lead-in and lead-out conductors and the current supply busses is also used to make the intermediate splice joints.

Assembly drawing showing PF6U and PF7U, together with their attachment to the TF coil system. Helium manifolding is also shown.

B. Electromagnetics

(Schultheiss) Summary of EM forces. Worst case loads (bending, launch vs. centering, etc.) Mention thermal stresses.

Winding Pack Design

1. Winding Configuration

2. Electrical Insulation Design

Winding Configuration

- Pancake (layer) winding minimizes the length of the cooling channels and facilitates manufacturing.

- Inlet and outlet fluid connections can be made at the outside radius of the pancakes.

- Both electrical current lead connections can be made at the outer radius.

- In principle, cooling channel lengths can be further reduced by adding helium stubs at the inner radius of the coil. The major difficulty in adding these coolant connections is the restricted space at the inner radius of the coils.

- Helium stubs are distributed on the outer radius of the coils and are staggered in the axial (vertical) direction in order to maintain enough separation between them to accommodate the insulating fluid connections and inlet and outlet manifolding.

- Turns have constant radius for 270° of the circumference and ramp up over a 90° arc.

4-6 dwgs showing turn layout and cross sections.

Winding Configuration (cont.)

- Joggles between pancakes occupy 22.5 ° of arc and are placed in a row at the same azimuthal angle.

- No lead spur is required in PF 6 and 7, because the coil case resists radial forces.

2-4 dwgs showing side view of joggles

Electrical Insulation Design

• The basic winding pack insulation scheme is the same as that in all of the PF coils. The major difference is that the insulation is applied during winding, rather than after winding and reaction, as in PF1 through PF5.

– Conduit insulation:

2 layers of unbonded polyimide tape, 0.001 in. thick and 1 in. wide, 50% half-lapped.
2 layers of 1 in. wide fiberglass 3-D weave tape, each with an as-wound thickness of 0.014 in.

-Winding pack ground wall insulation:

13-14 layers of half-lapped, 3 in. wide, 0.022 in. thick fiberglass tape.

-This basic insulation scheme is brought some distance out of the coil case wherever penetrations are made for leads and helium stubs.

Electrical Insulation Design (cont.)

- The voids formed by the turn-to-turn transitions and joggles are filled with specially formed fiberglass transition fillers with a cross section of approximately 1 in. by 1 in. These pieces are built up of many layers of 3-D-weave fiberglass tape and are designed to maximize the through-thickness glass fiber content.

- Cutouts in the coil case for current leads and splice joints are reinforced with bolted covers that carry loads around the cutouts and that also fill in all of the cutout area except for clearance for insulation around the conduit.

- During the epoxy impregnation process, temporary VPI (vacuum impregnation) molds are placed around the leads and helium stubs. They allow the epoxy impregnation to be continued for a distance of a few inches outside of the coil case.

- There is no separate ground screen layer inside the case. A ground screen covers the electrical-lead and helium-stub insulation outside of the coil case. It is brought down to the coil case and attached electrically to the coil case around the leads so that the case, together with the screen, forms a continuous ground envelope around any parts of the coil that can reach high voltage during a fast coil discharge.

Electrical Insulation Design (cont.)

- Past the impregnated length, insulation is field-applied by first scarfing back the insulation and then applying polyimide film and epoxy-pre-impregnated fiberglass. The ground screen is also applied in this process. The ground screen is covered with a layer of prepreg epoxy-fiberglass in order to protect it from mechanical damage.

- Field-applied insulation is a feature common to all of the electrical leads within the cryostat, both on the coil sides of the joints and on the supply side, a standardized process specification will be developed in the final design phase of the project.

- The combined ground envelope is connected to the machine ground at one point, so that no closed loops that could couple inductively to the PF coil system are present.

- After wrapping the with polyimide tape and the standard two layers of fiberglass, custom trimmed polyimide and fiberglass insulation pieces are packed around the helium stubs and lead-in and lead-out conduits.

D. Winding Pack and Coil Case Stresses

1. (Schultheiss) Includes thermal (cooldown stresses) and magnetic loads. Compare no case vs. with case stresses in conduit, interlaminar shear, etc. (table) Interlaminer shear model? Can one use a simple conversion factor to relate interlaminar shear stress to smeared-property shear stress? etc. etc.

Justification for Coil Case

The decision to include a coil case in the design of PF6 and 7 was made by balancing a number of considerations, some of which favored a coil case, and some that favored no case. They are summarized in the following:

Reasons for having a coil case

1. A case of sufficient strength guarantees the structural integrity of the coil and greatly reduces the stresses in the winding-pack insulation.

–If the coil has no case, bending stresses due to the ripple component of the axial and radial loads must be carried mostly by the web of epoxy-fiberglass formed by the conduit insulation and ground wall insulation.

–The exact distribution of stresses and the high-cycle fatigue behavior and failure modes of this complicated web structure cannot be predicted with complete confidence; in addition, resin-poor and resin-rich regions may occur in actual production and make the local epoxy-fiberglass properties less than the ideal ones.

2. A case provides a stable and convenient structure for mounting to the TF coil support structure.

3. A case provides a stable, flat reference surface for alignment fiducials.

Reasons for having a coil case (cont.)

4. A case eliminates the need for lead spurs in the lead terminations and intermediate splices.

5. A case acts as a neutron shield, thereby reducing the neutron heating of the winding pack and increasing the margin between the current-sharing temperature and the helium coolant temperature (provided that additional cooling is supplied to the coil case). In the final design phase, adding higher-temperature neutron shielding should also be considered.

6. A case eliminates the need for a separate vacuum impregnation mold, since the coil windings are potted into the coil case.

7. A case provides a convenient structure from which to support leads, flow meters, helium lines and insulating breaks, etc.

Reasons for not having a coil case

1. A case adds to the expense of the PF coil system. The cost of the coil case is only partly offset by eliminating the cost of the vacuum impregnation mold, since one vacuum impregnation mold can serve for two coils, and the coil case is made of stainless steel instead of carbon steel and has shear pins, bolts, etc. that are not required for the vacuum impregnation mold.

2. A case increases the total load on the 5K cryogenic system because the total neutron heating of the windings plus case is greater than the heating of the windings without a case. In addition, significant eddy-current heating of the case due to changing magnetic fields from the PF coils occurs.

3. A case increases the volume occupied by the PF6 and 7 coils and reduces system clearances in some places.

4. A case increases the weight of the PF coil system and increases the size of the gravity support columns, their heat leak, etc.

E. Coil Case Design, Coolant and Current Supply, and Instrumentation

1. Mechanical design description (Clarkson)
2. Supporting stress analysis=Shear flow (2 components), normal force along bolt/shear pin line (Shultheiss)
3. Helium coolant lines, insulating breaks,, electrical lead routing, (Clarkson)

Instrumentation

- For monitoring and controlling cooldown and normal operation, and to detect quenches.

- Instrumentation includes

flowmeters
absolute pressure sensors
temperature sensors
strain gauges, etc.

- Installation includes mounting sensors, routing and protection of lead wires for these sensors, including voltage tap wires, which are critical for quench detection.

- Many sensors are under development and final dimensions and installation details are not presently available. Exact numbers and type of sensors will be specified in the final design phase.

PF6&7 Sensors

Sensor	*Number*	*Location*	*Remarks*
Strain Gages	48	Mounts, PF6U	16 mounts x 3/mount
	18	Mounts, PF6&7L, PF7U	2 mounts x 3/mount x 3
	12	Coils (3 per coil)	Measure hoop/bending stress
Internal Fiber Optic Temperature Sensors	2 Fibers x (2 magnet terminations +4 splice ends) x 2 magnets +2 Fibers x (2 magnet terminations +2 splice ends)x 2 magnets = 40 sensors	Co-wound, exiting at the magnet terminations and conductor splices.	Inside CICC
Voltage Taps external	2 pairs (one redundant pair) per joint x (2 magnet terminations +2 splices) x 2 magnets +2 pairs per joint x (2 magnet terminations +1 splice)x 2 magnets = 28 sensors (twisted pairs)	Across magnet terminations and splice joints	Monitors voltage drop across joint

Voltage Taps Co-wound (Non-Inductive)	6 sensors(twisted pairs) x (2 terminations+4 splice ends) x 2 magnets+ 6 sensors(twisted pairs) x (2 terminations+2 splice ends) x 2 magnets = 120 sensors (twisted pairs)	@ Magnet terminations and conductor splices	Inside CICC
Flowmeters	PF6 11 x 2 = 22 PF7 8 x 2 = 16 TOTAL = 38	@ all double-pancake helium inlet & outlet lines (& terminations)	
Pressure Transducers	2	Inlet / Outlet manifolds	
Temperature Sensors (CGR or Cernox)	PF6 6 x 2 = 12 PF7 4 x 2 = 8	@ pancake (& termination) He outlet lines	
	2	@ He inlet manifold	
	48+18+12 = 78 TOTAL = 98	@ each strain gage location	
Hall Probes	1 x 4 magnets = 4	@ centerline of I.D. for each magnet	

Voltage Taps

- Are the primary quench-detection sensor.

- Co-wound coaxial cables inside CICC to minimize inductive pickup. The differential voltage between the sheath and center wire is the raw quench signal.

- Six coaxes extracted at lead terminations and conductor splices. Detailed procedure for the connections under development.

- Coaxial cables made up of a center wire insulated with S-glass braid and surrounded by a copper braided sheath and coaxial stainless-steel sheath.

- As the coaxes leave the conductor cable, a transition will be made to a single cable with six insulated inner conductors, surrounded by a single conducting sheath.
- If better noise performance is required, use of 12 individual twisted pairs inside a sheath could be considerd.

- The outer sheath will be surrounded by solid high-voltage insulation, a grounded sheath, and an outer insulation layer.

Copy of Joel Schultz's July TIM figure of lead termination- coax extraction

Voltage Taps (cont.)

- One possible backup appproach to internal voltage taps is to co-wind a Kapton-insulated metal ribbon with the conduit. The signal-to-noise performance of this would not be as good as that of the internal coax, but would be much better than that of conventional taps.

- Voltage taps across all conductor joints for monitoring joint voltage drops will also be installed. These are installed in redundant pairs with separate high-voltage cabling.

Fiber-Optics Temperature Sensors

- Measures average temperature change along fiber.
- Terminated with mirror surface on end inside conduit.
- Minimal high-voltage problems- no high-voltage cables, connectors, feedthroughs, isolation amplifiers, etc.
- Requires cryogenic optical connectors and feedthroughs.

Flowmeters and Pressure Measurements

- For secondary quench detection and monitoring cooldown and opertating helium flows.

- A final flowmeter approach has not yet been selected.

- Venturi tubes with differential pressure (DP) gauges have been used for precision liquid helium flow measurement.

- Problem with finding a cold DP transducer that operates in a high magnetic field.

- Time delay in running capillary tubes to a warm DP transducer.

- Dynamic range problem with Venturi + DP measusrement because the differential pressure varies as the square of the mass flow rate.

- Other possible flowrate (velocity) sensors with a linear response.

- One absolute pressure pressure transducer will be installed on the inlet manifold of each coil and one on the outlet manifold.

Temperature Sensors

- For monitoring helium and structure temperatures during cooldown and operation.

- One or two temperature sensors on the inlet manifolds and at least one sensor on each outlet (helium stub or lead termination) will be used.

- The installations will be "wet" (i.e., the sensor and some length of lead wires will be immersed in the helium) to ensure accurate readings. This requires use of a multipin liquid helium/vacuum feedthrough with a high pressure rating.

- Recommend a combination of a germanium resistance thermometer (GRT) and a carbon glass resistance thermometer (CGRT) to allow *in situ* calibration of CGRTs.
- Need other thermometers for cooldown– e.g., platinum resistance thermometers.

- Need to monitor coil case and support temperatures during cooldown. A relatively inexpensive approach that covers the most critical portion of the cooldown cycle (300-50K) with adequate accuracy is to use type E (chromel-constantan) thermocouples.

Strain Gauges and Displacement Transducers

- Strain gauges will be mounted on the coil case and structural supports (grounded structures only).

- As in the LCP, these will be installed in active/dummy compensating pairs, and read out with ac carrier amplifires to eliminate spurious thermal voltages.

- Recommend the use of displacement transducers to monitor the position of the coils with respect to the TF mounts is recommended, since this information cannot be obtained directly from strain measurements.

- A moving-coil differential transformer (MCDT) that behaves in much the same as the LVDT, but has no ferromagnetic parts, was developed and used sucessfully in the LCP program in Oak Ridge for displacement measurements on the superconducting test coils inside the LCP magnet test cryostat.

5. Support of leads and other components (Clarkson)

Eddy-Current Heating of the Case

- Significant heat load due to eddy currrent heating of the case.

- Eddy current heating in the PF6 and 7 coil cases was calculated in the full-penetration limit. This approximation is conservative in that it overestimates the heating.

- Justified by the fact that the classical skin depth in stainless steel at the frequencies of interest (less than tens of Hz) is much greater than the case thickness.

- The primary eddy-current loop in the coil is blocked by an insulating break. The eddy-current pattern, except near the insulating breaks where the currrents flow across the top and bottom of the case, is composed of currents that flow around the major circumference.

- The current density in a cross section of the case away from the breaks is negative in some areas and positive in others, with a total average current density of zero.

  - Treat the problem in 2-D. Case curvature was neglected and the coil was treated as an infinitely long rectangular current-carrying buss.

Eddy-Current Heating of the Case (cont.)

- The changing magnetic field that drives eddy currents is dominated in PF6 and 7 by the self-field of the respective coils. The eddy-current power density is highest around the four case corners and is greater in PF6 than in PF7, with a peak-to-average ratio of about three to one.

- Eddy-current heating was computed for the 24-second HC scenario.

- The cycle-averaged eddy-current case heating was calculated to be 85 W in PF6 and 35 W in PF7. These figures should be compared with typical nuclear heating averages of 77 W for the PF6 case and 254 W for PF7.

- A more detailed treatment of the problem would include a search of the proposed scenarios for the one with the maximum time-averaged square of *dI/dt,* and include the thermal transients in the case and helium streams.

- A realistic model of the heat transfer from the case through the insulation system, conduit wall, and foil wrap to the helium stream inside the conduits is needed to compute the margin between the current-sharing temperature and helium temperature in the conduit as function of time and position in the winding pack.

Eddy-Current Heating of the Case (cont.)

- With such a model, the flow rate, temperature, and distribution of the case coolant stream required to accomodate the worst-case scenario of simultaneous eddy-current and nuclear heating can then be determined.

G. Interface to TF coils

1. Loads and design constraints (Clarkson, Schultheiss, Walstrom)
2. Design Description (Clarkson)
3. Installation (Clarkson, Burger)

Installing Fiducials and Finding the Magnetic Center

- Before installation in TPX, the magnetic field of the coil, energized as a single separate magnet, will be characterized by magnetic field measurements at points that are referenced to a set of fiducial points fixed in the coil case.

- Fiducial holes, sized for holding removable targets for computerized-theodolite optical alignment, will be drilled in the top and bottom of the coil case at 8 points on the top, and 8 points on the bottom cover of coil case, halfway azimuthally between the TF mounts and at the mean winding radius. The holes will be (typically) 1/8 in. wide and 1/4 in. deep.

- The radial position and height of the nominal winding-pack centroid is independent of azimuthal angle in the present coil design. However, the effective width of the winding pack does vary with angle.

Installing Fiducials and Finding the Magnetic Center (cont.)

- Energize coil to 500A at room temperature intermittently and cool continuously with dry instrument air.

- This level of current in PF6 gives a peak field of over 600 gauss (0.06 T), which is high enough for precision Hall-probe field measurements.

- Measure field around minor case circumference at 16 locations on circumference

- The effective winding pack width and centroid at each azimuthal angle will be determined by fitting the magnetic field data with a simplified winding-pack current-distribution model.

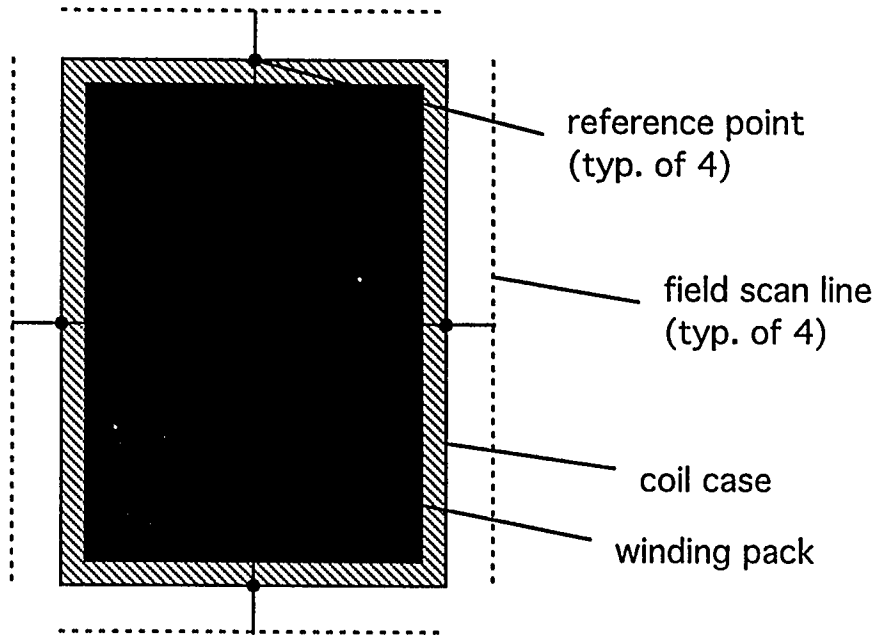

Magnetic center characterization concept

b. Shim sizing (Clarkson)

c. Assembly Sequence and Special Fixtures (Clarkson, Burger, Peterson)

PF6/PF7 Structural Analysis

- Thermal Model and Thermal Stresses
- Slip-Plane Considerations
- Magnetic Loads
- Structural Configurations
- Results And Comparisons
- Issues
- Recommendation

1

PF6/PF7 Thermal Cooldown Model

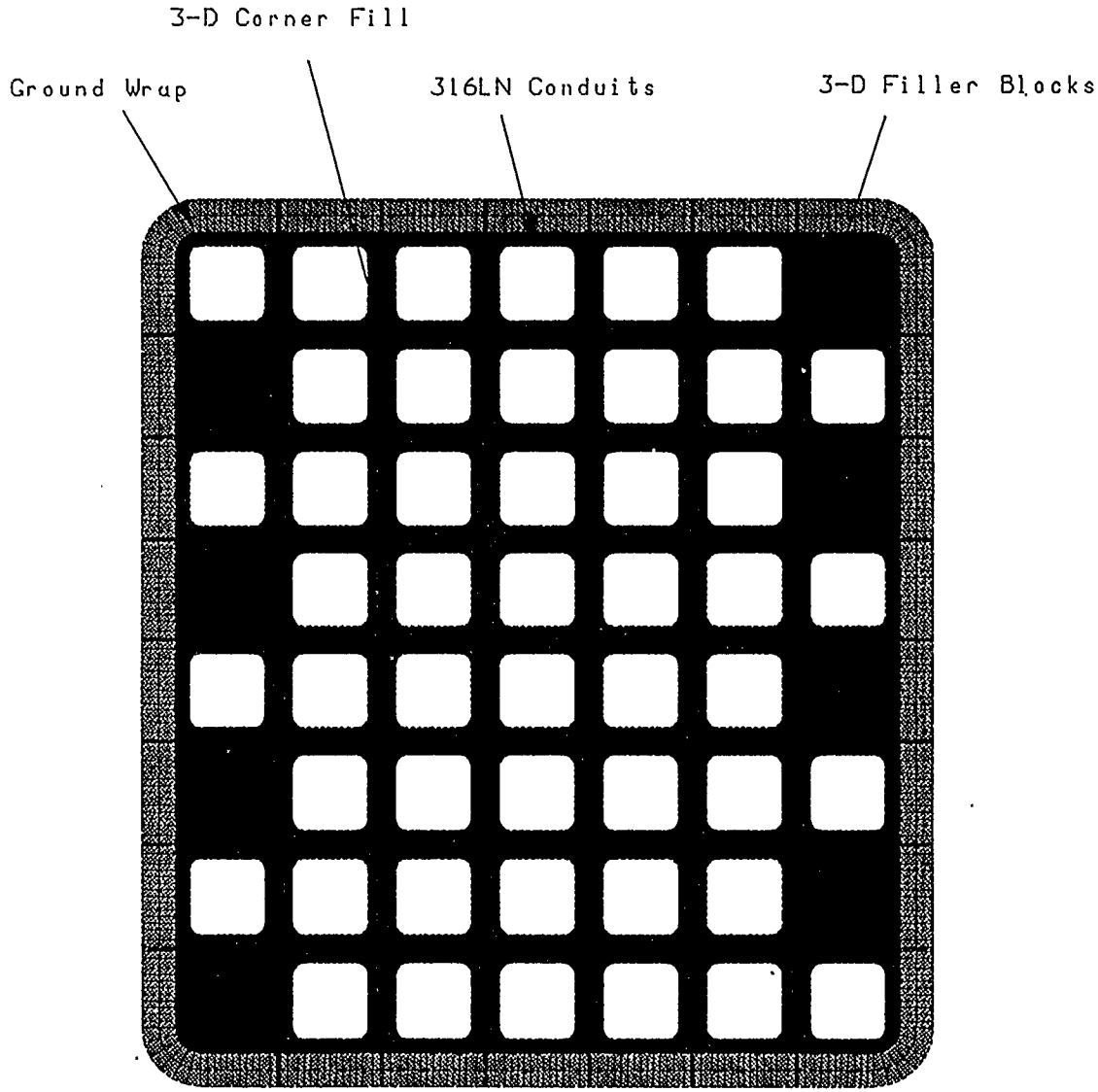

ANSYS 5.1
AUG 15 1995
06:58:06
PLOT NO. 1
ELEMENTS
MAT NUM

ZV =1
*DIST=6.126
*XF =148.408
*YF =3.411
CENTROID HIDDEN

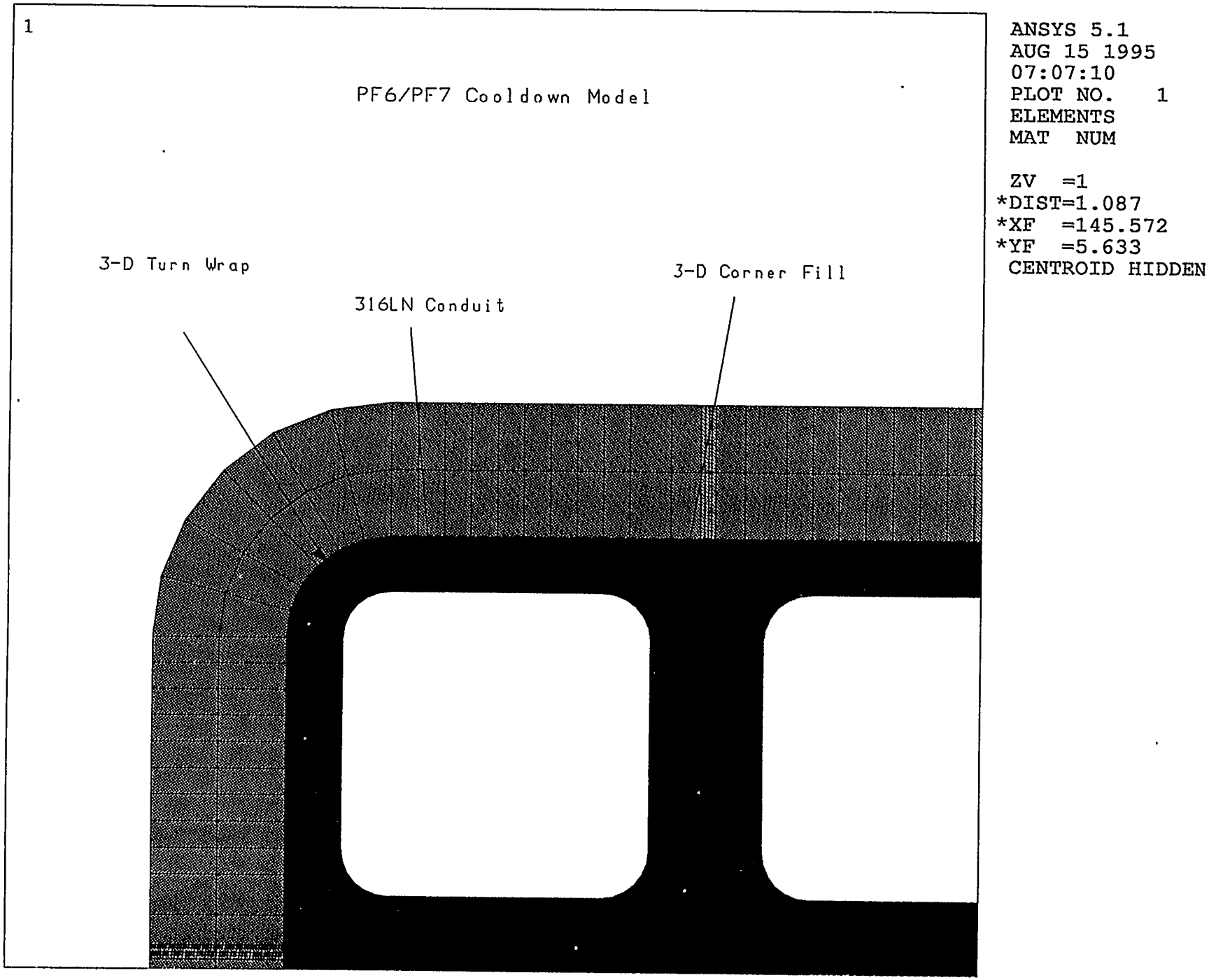
1
PF6/PF7 Cooldown Model
3-D Turn Wrap
316LN Conduit
3-D Corner Fill
ANSYS 5.1
AUG 15 1995
07:07:10
PLOT NO. 1
ELEMENTS
MAT NUM
ZV =1
*DIST=1.087
*XF =145.572
*YF =5.633
CENTROID HIDDEN

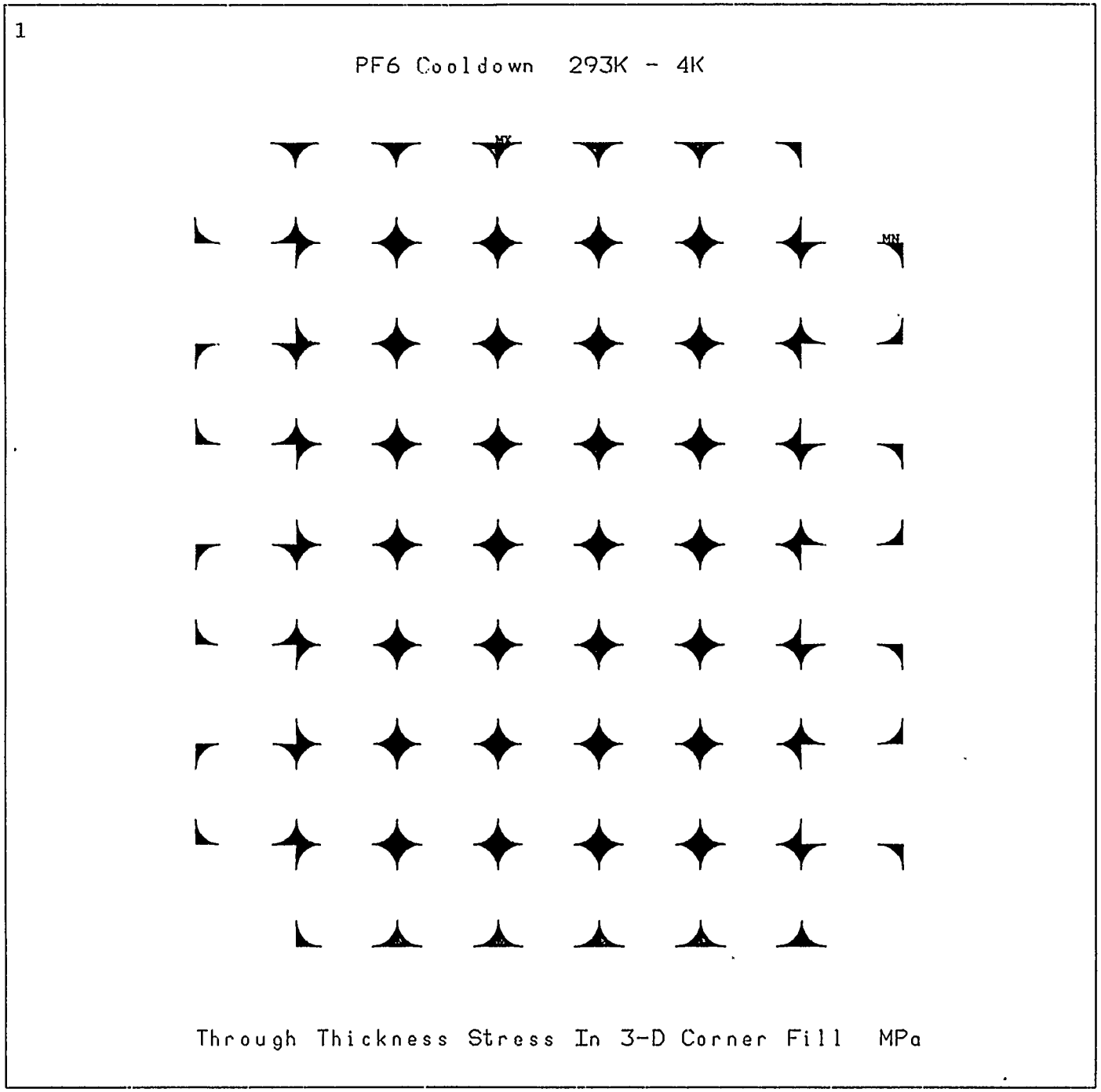

ANSYS 5.1
AUG 15 1995
07:43:51
PLOT NO. 1
NODAL SOLUTION
STEP=3
SUB =1
TIME=3
SX (AVG)
RSYS=SOLU
DMX =0.003049
SMN =-4.933
SMX =33.337

-4.933
-0.681179
3.571
7.823
12.076
16.328
20.58
24.833
29.085
33.337

1

PF6 Cooldown 293K - 4K

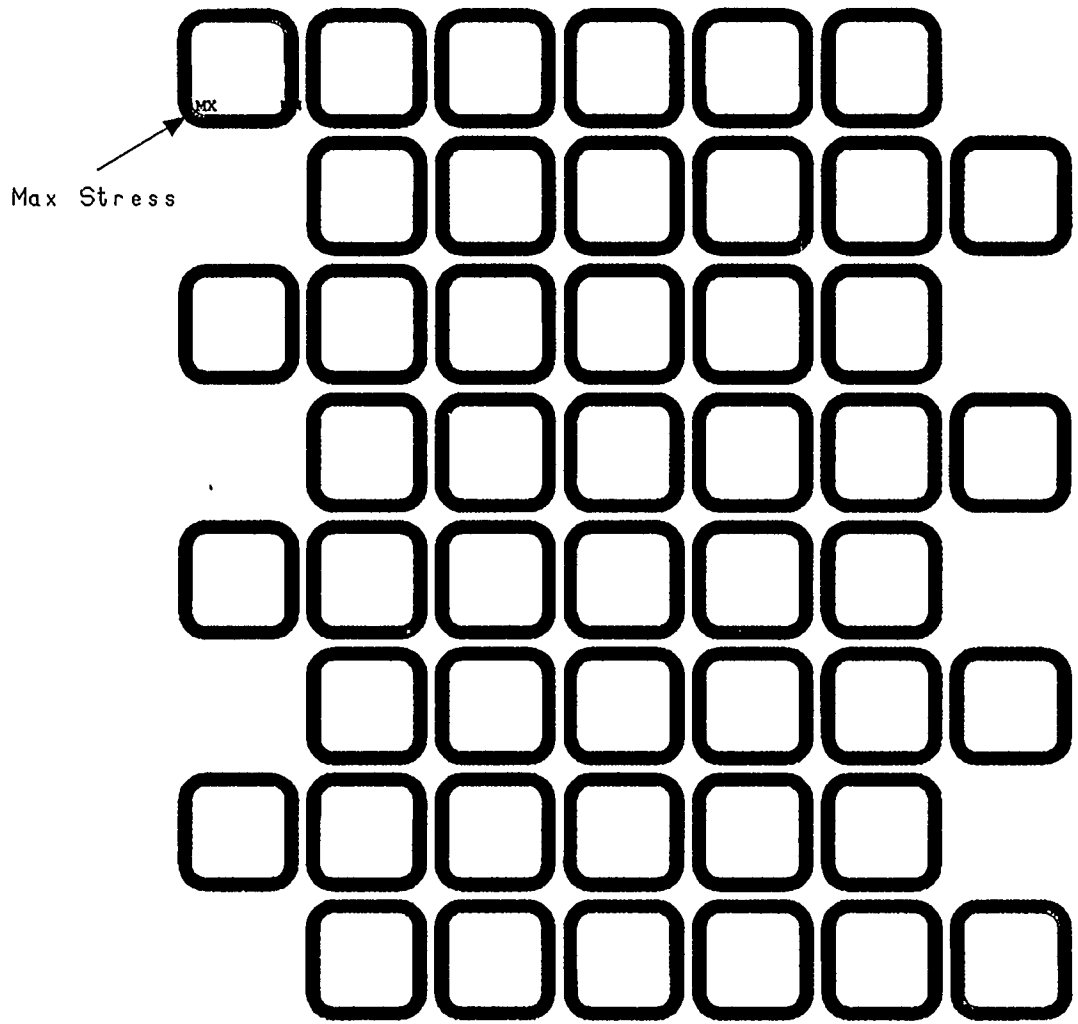

Maximum Principal Stress In Conduits MPa

ANSYS 5.1
AUG 15 1995
07:36:53
PLOT NO. 1
NODAL SOLUTION
STEP=3
SUB =1
TIME=3
S1 (AVG)
DMX =0.003048
SMN =-11.534
SMX =126.674

-11.534
3.822
19.179
34.535
49.892
65.248
80.605
95.961
111.318
126.674

Material Limits For Single Cycle.

Material	Fatigue Crack MPa 60000 cycles	Laminar Tension MPa single cycle	Interlaminar Tension MPa single cycle	Shear In The Interlaminar Direction MPa single cycle
316LN Conduit	420 MPa			205.
Turn Wrap		400.	10-20 MPa	73 MPa
Corner Fill		.	150 MPa	
3D Block Fill			10-20 MPa	
Ground Wrap			10-20 MPa	73 MPa

Thermal Stresses due to Cooldown.

Material	Max Tresca MPa	Max Principal MPa	Through Thickness MPa	Shear In Interlaminar Direction MPa	Max Stress Laminar Direction MPa	Hoop Stress MPa
316LN Conduit	118. MPa	127 MPa				
Kapton			2.6	4.3	31.8	19.7
Turn Wrap			11.8	17.5	128.1	34.0
Corner Fill			33.3	36.6	109.1	30.8
3D Block Fill			46.0	11.5	34.5	14.9
Ground Wrap			33.4	36.5	63.4	-11.1

Results Of Thermal Cooldown

- Magnetic loading cycles degrade material allowables and properties
  - 50% degradation of allowables is assumed for 60000 cycles
-
  - Through thickness stress of turn wrap, 3D Block fill, and ground wrap near or above degraded allowables
- Stresses do not include cycling effects on material properties, such as modulus and Coefficient of Thermal Expansion

Slip plane effects on shear transfer AND [illegible]

$M = E I \frac{\partial^2 y}{\partial x^2}$

M = [illegible] MOMENT, E = MODULUS

The following equation describes this effect. I = MOMENT OF INERTIA

$\frac{\partial^2 y}{\partial x^2}$ = CURVATURE

$I_C = I_L + A_L \times d^2$, where

I_C = Contribution of local component to the composite structure

I_L = Moment of Inertia of local component about its own neutral axis

A_L = Area of local component

d^2 = Square of distance from local neutral axis to composite neutral axis.

The A_L multiplied by d^2 term is not included if shear transfer does not exist.

Configuration 1 parameters for PF6. Baseline design which includes slip plane between the conduit and Kapton

Material	Effective Hoop Area m^2	Moment Of Inertia I_{rr} m^4	Moment Of Inertia I_{zz} m^4	Hoop Modulus GPa
316LN	.02039	.1211e-5	.1211e-5	205.
Glass Epoxy	.03323	.7436e-3	.1452e-3	32.

Configuration 2 parameters for PF6, assuming no slip plane between the conduit and Kapton.

Material	Effective Hoop Area m^2	Moment Of Inertia I_{rr} m^4	Moment Of Inertia I_{zz} m^4	Hoop Modulus GPa
316LN	.02039	.3893e-3	.3818e-4	205.
Glass Epoxy	.03323	.7436e-3	.1452e-3	32.

Magnetic Loads

- Magnetic Loads Cases Were Chosen From MIT Analysis Giving peak hoop and peak axial loads

- PF6 Magnetic Load case used equilibrium condition 9 during an upper plasma disruption with the plasma current turned off. This results in a radial load of 3.6 MN hoop tension and an axial load of 7.8 MN acting to pull PF6U toward PF6L. This axial load is within 5% of the axial load from disruption following equilibrium condition 18. The radial variation of load is higher than the axial variation.

- PF7 the largest axial load occurs after disruption of equilibrium condition 18, since the PF7 angular load variation is much large for axial loads than for radial loads this case was used for analysis.

PF 6Circumferential Variation Of Force Radial And Axial

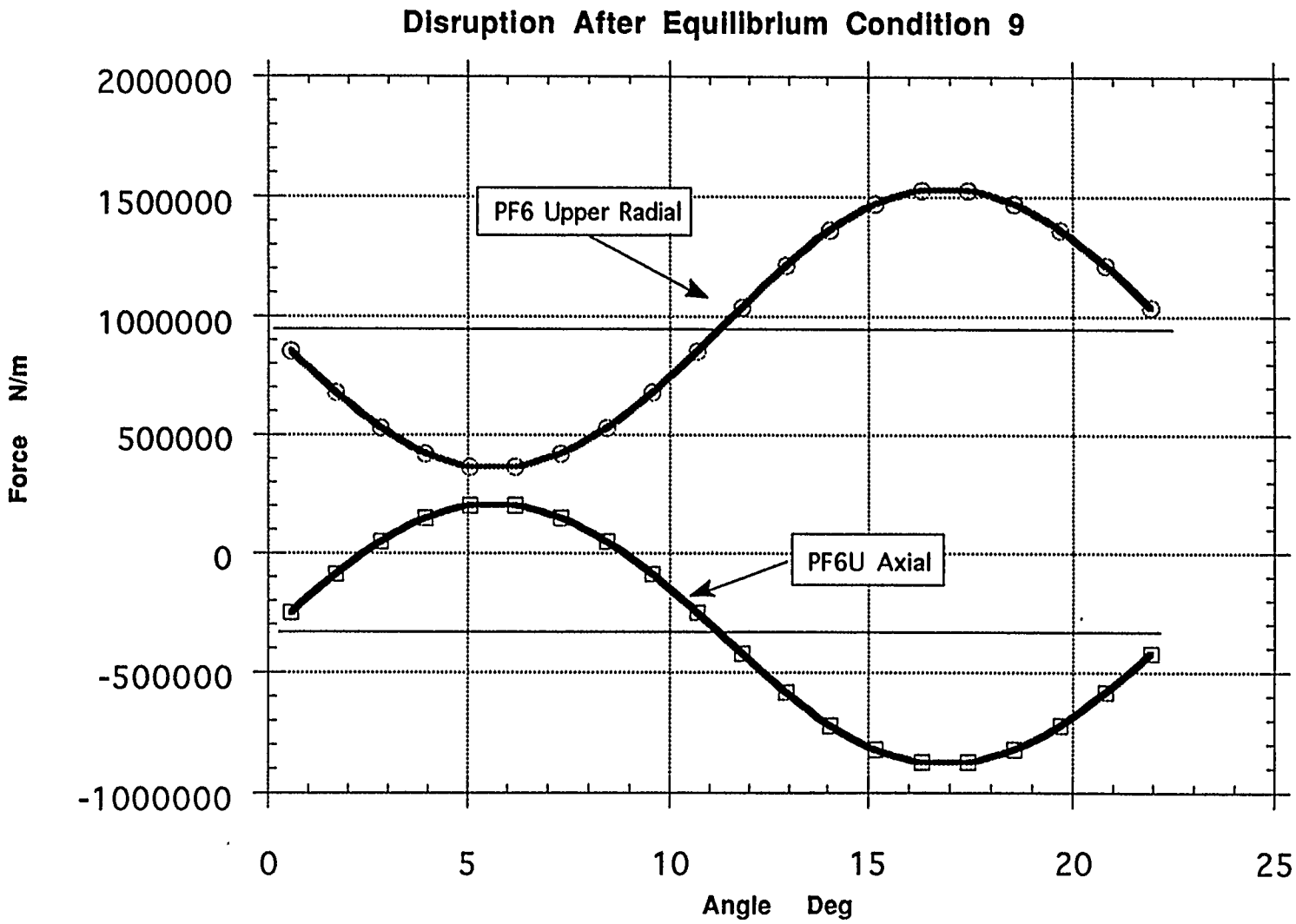

Circumferential Variation Of Force Radial And Axial

Disruption After Equilibrium Condition 18

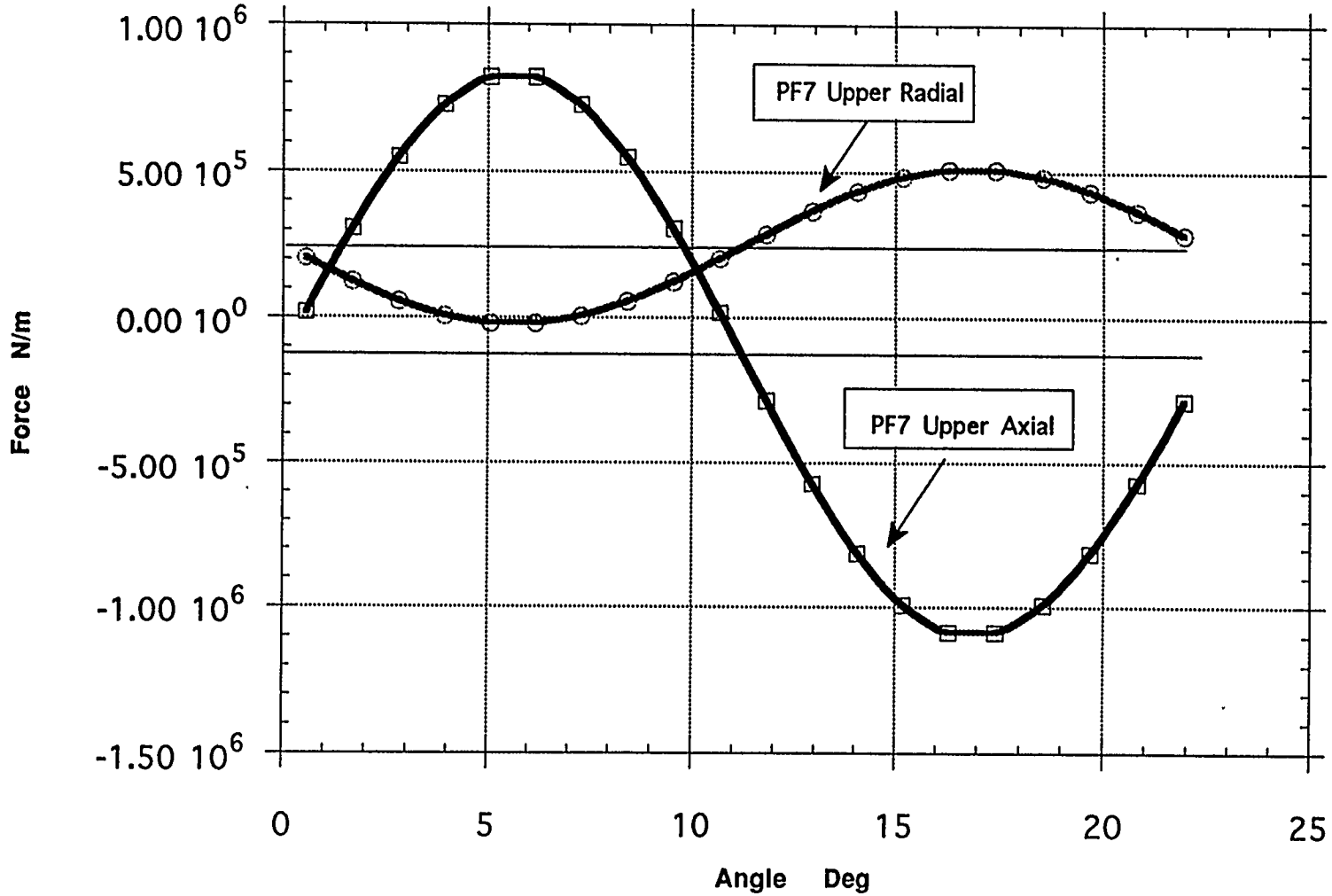

Model Configurations For Magnetic Loading

- Case 1 Baseline design which includes slip plane between the conduit and kapton
- Case 2 Assume no slip plane between the conduit and kapton
- Case 3 With slip plane assume failure of glass/epoxy
- Case 4 5/8 inch coil case with slip plane
- Case 5 1.725 inch thick radial band on outer radial surface with slip plane

Analysis Assumptions

- Assume all materials are continuous, no local epoxy rich or epoxy poor regions
- Assume no-friction slip plane between conduits and kapton. Conservative with respect to bending stresses, non conservative with respect to kapton and 3-D turn wrap stresses
- Assume glass epoxy composite material resists no load when a 5/8 coil case is included
- When band on outer radius is included assume bonding between ground wall and band

1

PF7 Loads And Vertical Support Locations

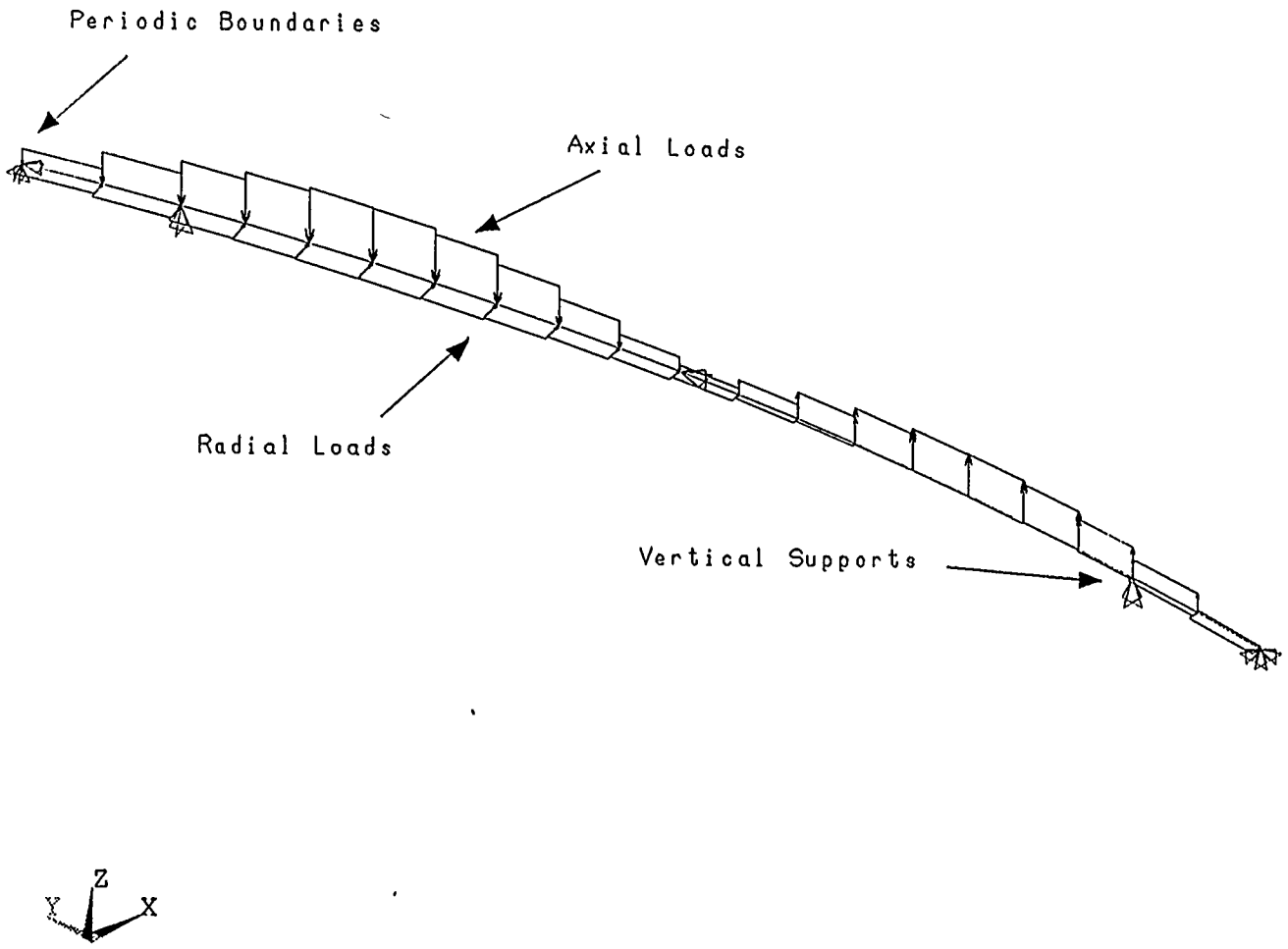

Bending Moment And Shear Load Model

ANSYS 5.1
AUG 14 1995
06:27:30
PLOT NO. 1
ELEMENTS
TYPE NUM
U
CP
PRES

XV =-1
YV =-1
ZV =1
DIST=0.766721
XF =4.133
YF =0.822195
VUP =Z
CENTROID HIDDEN

Hoop And Bending Stress
PF7 Configuration 1

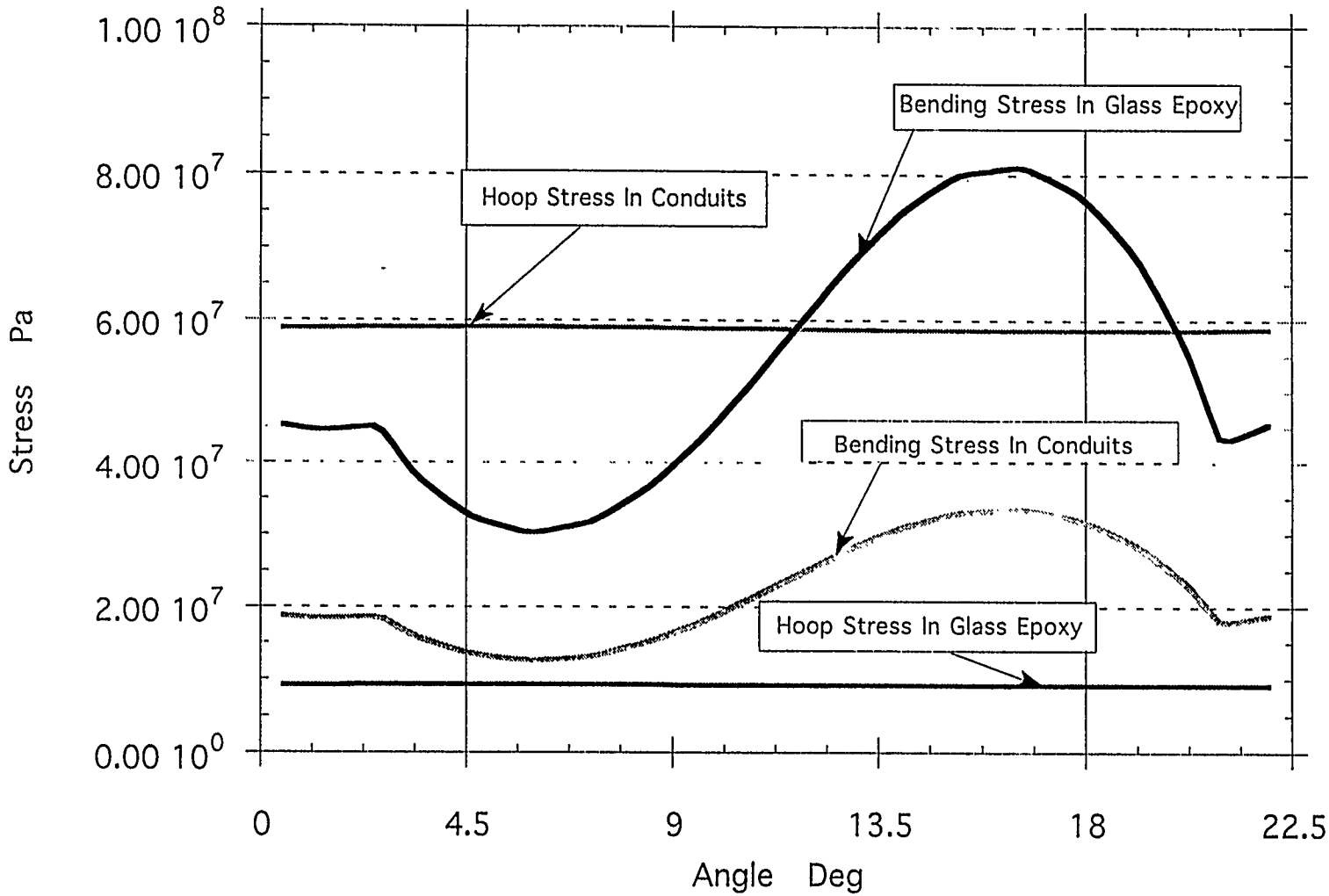

Hoop And Bending Stress
PF7 Configuration 2

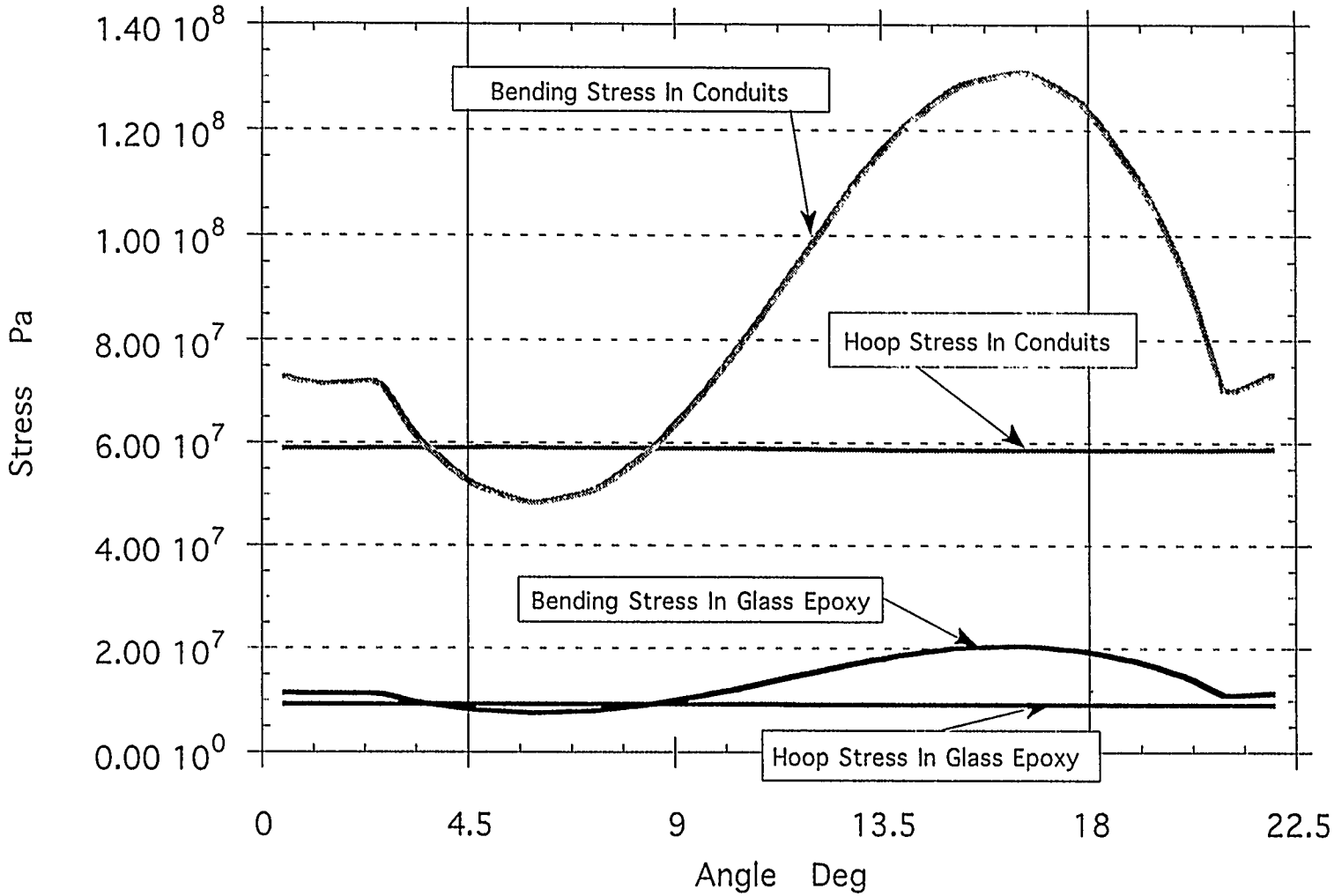

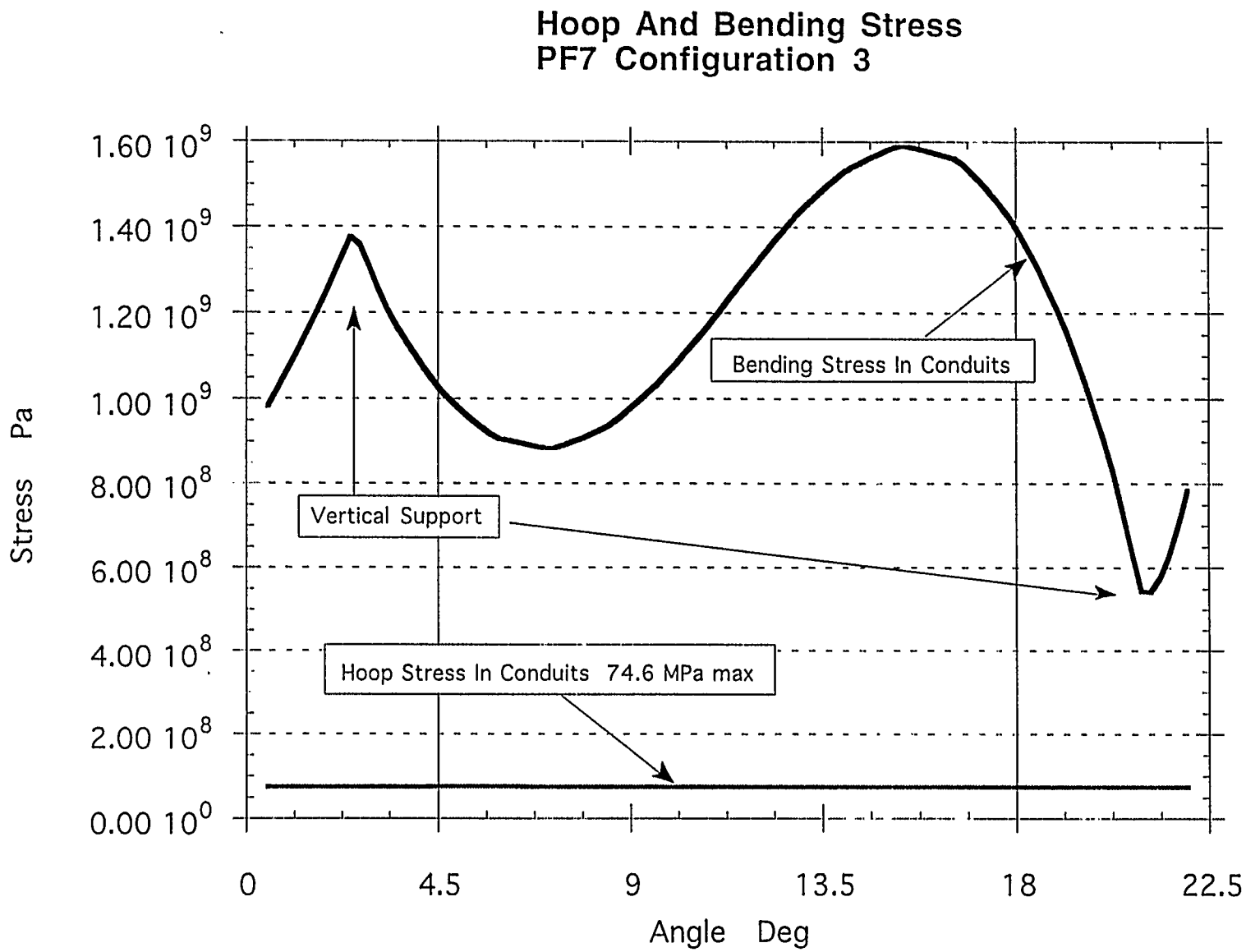
Hoop And Bending Stress
PF7 Configuration 3
1.60 10^9
1.40 10^9
1.20 10^9
1.00 10^9
8.00 10^8
6.00 10^8
4.00 10^8
2.00 10^8
0.00 10^0
Stress Pa
0
4.5
9
13.5
18
22.5
Angle Deg
Bending Stress In Conduits
Vertical Support
Hoop Stress In Conduits 74.6 MPa max

Hoop And Bending Stress
PF7 Configuration 4

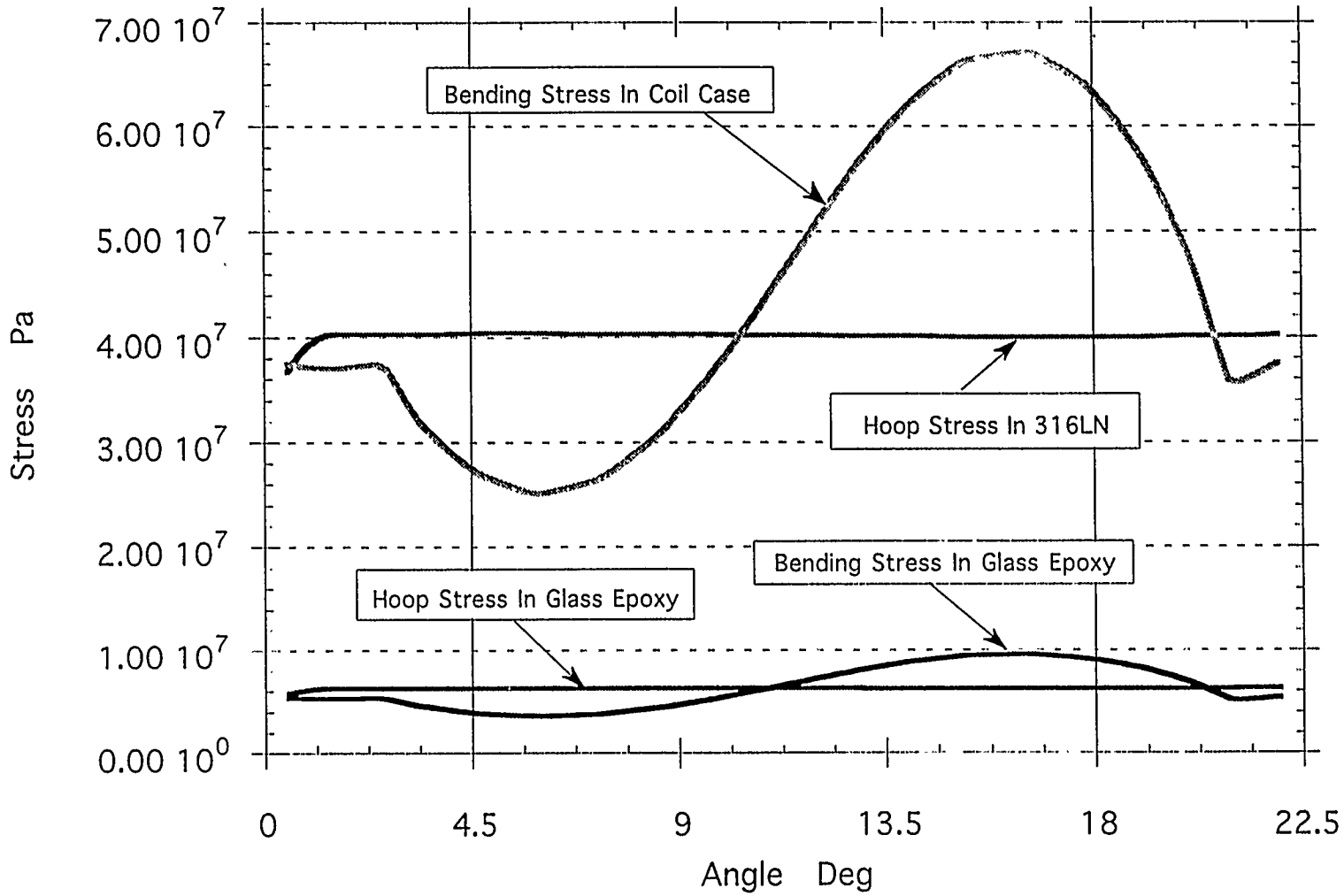

Hoop And Bending Stress
PF7 Configuration 5

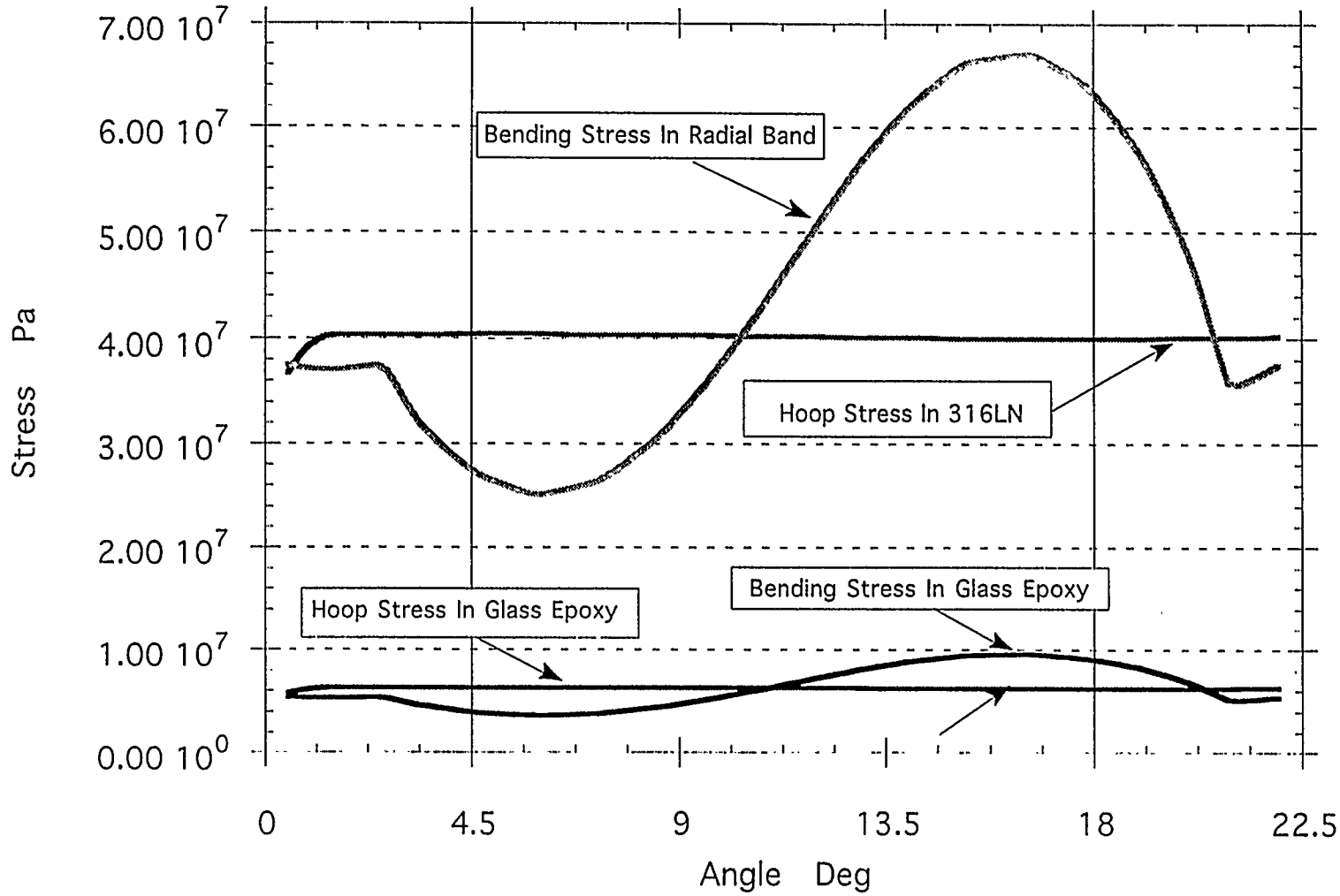

Summary of PF6 Max Hoop and Max Shear Stresses.

Configuration	Max Hoop 316LN Stress MPa SBR	Max Hoop Glass/Epoxy Stress MPa SBR	Max Shear Stress MPa 316LN SYZ	Max Bending Stress MPa Glass/Epoxy SYZ
PF6 Config 1	140.	21.8	.128	7.53
PF6 Config 2	140.	21.8	9.49	1.74
PF6 Config 3	175.	-	13.2	-
PF6 Config 4	74.2	11.6	5.15	1.01
PF6 Config 5	75.6	11.8	4.84	1.62

Summary of PF6 Max Bending Stresses.

Configuration	Max Bending Stress MPa 316LN SBR	Max Bending Stress MPa Glass/Epoxy SBR	Max Bending Stress MPa 316LN SBZ	Max Bending Stress MPa Glass/Epoxy SBZ
PF6 Config 1	15.4	19.7	22.0	75.9
PF6 Config 2	49.4	7.71	113.0	17.6
PF6 Config 3	304.	-	2110.	-
PF6 Config 4	17.3	2.30	64.9	10.1
PF6 Config 5	17.9	2.79	102.0	16.0

Summary of PF7 Max Hoop and Max Shear Stresses.

Configuration	Max Hoop 316LN Stress MPa SBR	Max Hoop Glass/Epoxy Stress MPa SBR	Max Shear Stress MPa 316LN SYZ	Max Shear Stress MPa Glass/Epoxy SYZ
PF7 Config 1	59.1	9.22	.261	7.96
PF7 Config 2	59.1	9.22	14.7	2.84
PF7 Config 3	74.6	-	31.5	-
PF7 Config 4	40.4	6.30	17.3	1.35
PF7 Config 5	42.3	6.61	1.53	2.63

Summary of PF7 Max Bending Stresses.

Configuration	Max Bending Stress MPa 316LN SBR	Max Bending Stress MPa Glass/Epoxy SBR	Max Bending Stress MPa 316LN SBZ	Max Bending Stress MPa Glass/Epoxy SBZ
PF7 Config 1	12.7	16.2	33.5	81.0
PF7 Config 2	41.3	6.40	131.	20.4
PF7 Config 3	254.	-	1590.	-
PF7 Config 4	13.8	1.83	67.1	9.58
PF7 Config 5	15.4	2.40	118.	18.4

Results Summary

- Case 1 — Stresses below limits for single load condition
- Case 2 — If conduits bonded to epoxy they would resist most of the bending loads due to the much higher modulus of 316LN
- Case 3 — If we assume glass epoxy losses its effectiveness after cycling 316LN conduits by themselves can not withstand bending loads
- Case 4 — 5/8 inch coil case will resist the bending loads and would be acceptable if glass epoxy was not effective. Since the nuetral axis of the coil case is the same as the neutral axis of Case 1 no bond is necessary between the coil case and ground wrap
- Case 5 — A radial band on the outside of the coil would be acceptable providing a bond to the ground wrap would exist throughout the load and cycling history

Issues

- Bending of PF6 and PF7 introduces risk in baseline design.
- Epoxy rich and epoxy poor regions can vary the properties
- Coil case eliminates uncertainties, all bending loads can be resisted by the case
- Coil case has same nuetral axis as coil without case therefore failure of bondline between coil case and groundwrap does <u>not</u> effect bending properties, a band scheme will be affected if bond is lost.

Recommendation

- Coil Case reduces risk by resisting most of the bending loads.
- Glass/epoxy no longer primary bending structure

Section VIII - E

PF6/7 Thermal Analysis

TPX

PF6/7 Steady-state Thermal Analysis

MARINE DIVISION

❑ Topics

- Requirements & Objectives
- Baseline Cooling Design & Modification Options
- Technical Approach
  - Overview
  - Assumptions (internal & interface heating, load line)
  - WETMAP Computer Model (description, implementation, & validation)
  - Margin Prediction
- Results
  - Temperature Margin & Headroom Predictions
  - Energy Margin
  - Helium Residence Times
  - Preliminary Flow Budget Estimate
  - Sample WETMAP Output (PF6 w/o case & PF7 w/ case)
- Conclusions & Recommendations

-- Goals for PF Coil Thermal Performance

Requirement	Parameter	Units	Value
Temperature Margin	ΔT_M	(K)	≥ 1
Temperature Headroom	ΔT_H	(K)	≥ 2
Energy Margin	ΔU_M	(mJ/cm^3)	≥ 300

1.3 OBJECTIVES

A steady-state thermal-hydraulic analysis was undertaken to address the following issues:

- Is it possible to cool the baseline PF6 and PF7 coil configuration so that both margin and headroom requirements are met during operation, given the non uniform neutron heating distributions associated with TPX?
- What coil modification options are available to improve cooling design feasibility?
- What coolant mass flow rate and inlet pressure are needed?

Table 2 -- Conductor Cooling Design Parameters and Values

Parameter	Units	Value
coolant flow area	mm^2	111.4
tot. no. of cable strands	-	360
strand diameter	mm	0.78
conduit external dimension	mm	22.3
conduit wall thickness	mm	2.41
conduit corner outside radius	mm	5.10
cable foil wrap thickness	mm	0.051
cable space wetted perimeter	mm	735.
conduit wetted perimeter	mm	65.
conduit cross-section area	mm^2	179.2

Hydraulic Circuit Design Parameters and Values

Parameter (units)	PF6 Value	PF7 Value
winding pack inside radius (m)	3.687	4.225
winding pack outside radius (m)	3.830	4.369
no. of turns per double-pancake	12	12
flow channel length (m)	283.4	324.
total no.of double-pancakes	10	7
no. of coolant inlet stubs	5	4
no. of coolant outlet stubs	6	4

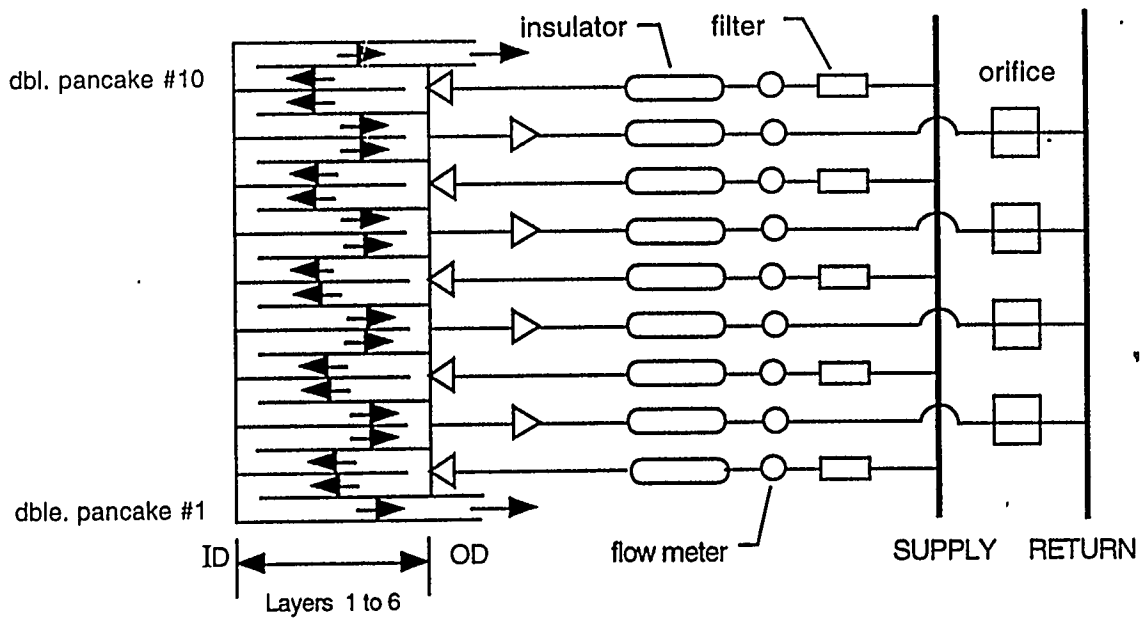

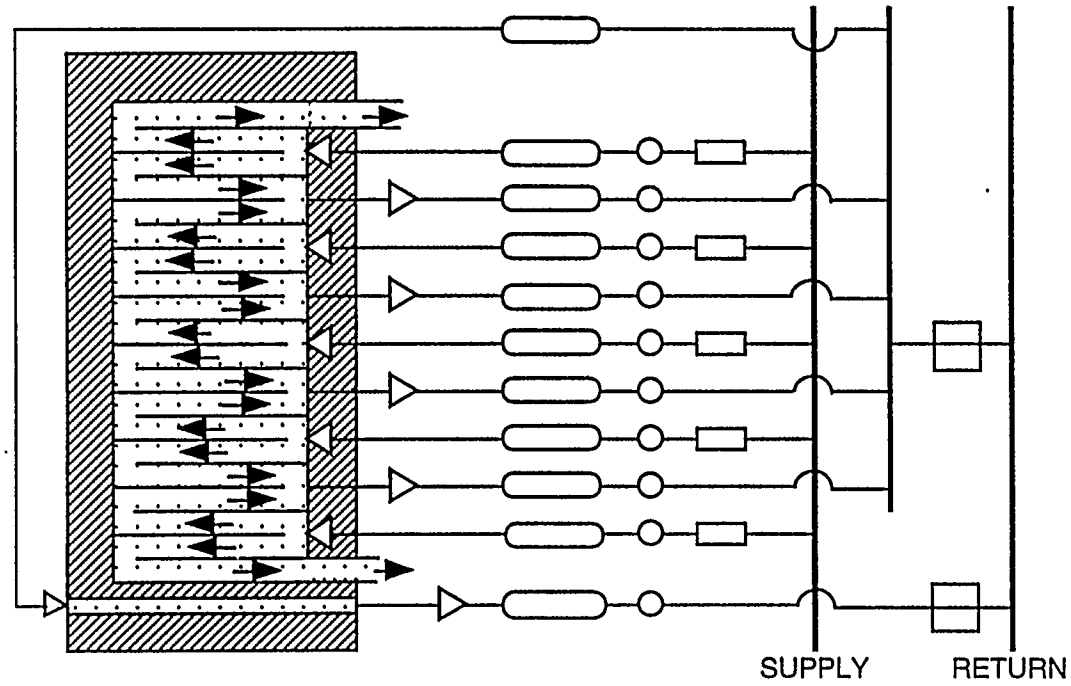

Figure 3 -- Modified baseline design using effluent-cooled external case to reduce coil heat.

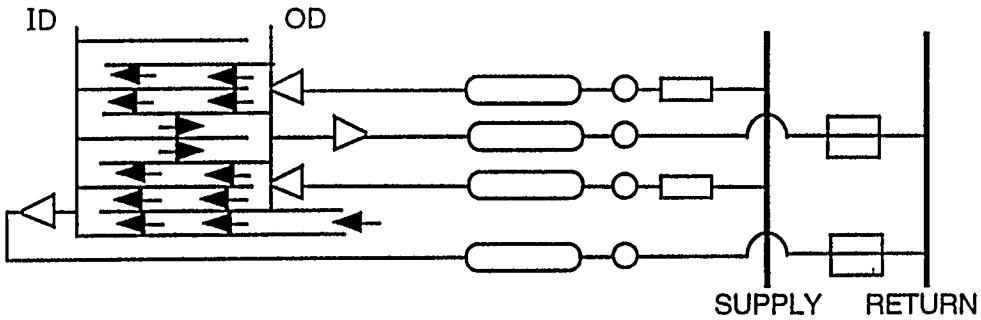

-- Modified baseline design using extra outlet stub at bore of worst case pancake.

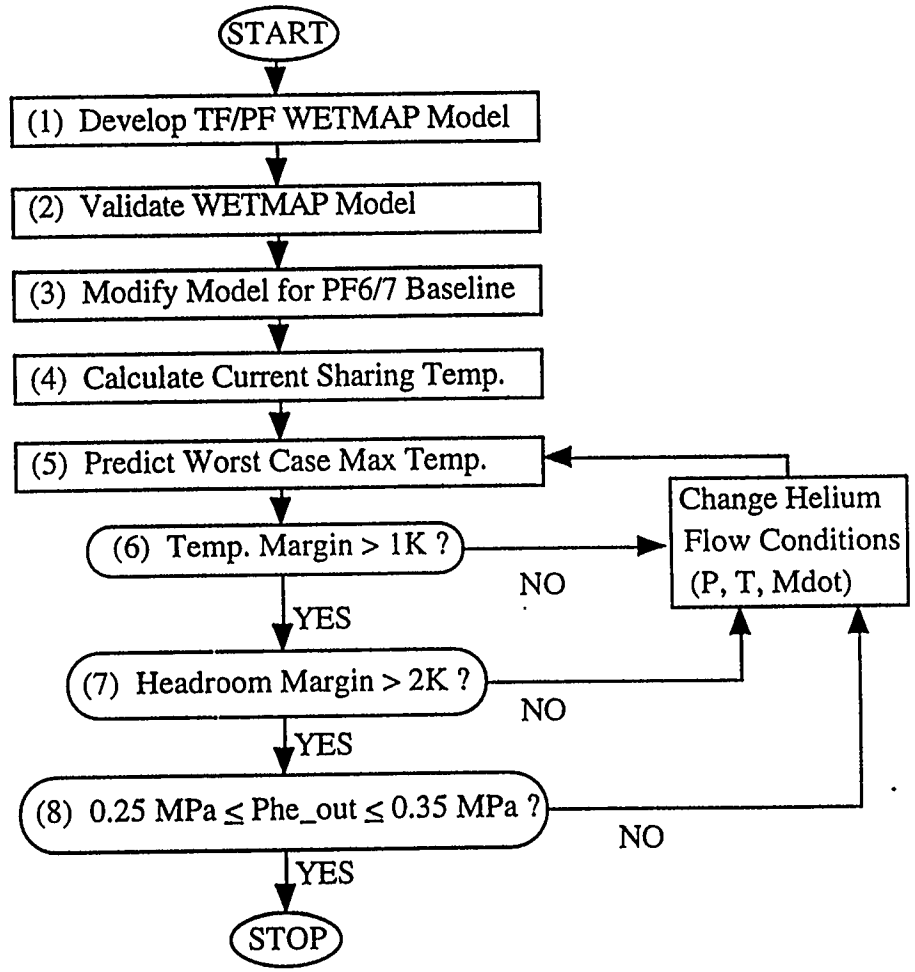

Figure 5 -- Methodology used to assess cooling design feasibility.

DOUBLE SPIRAL-WOUND PANCAKE COIL
Conduction Heat Flow Scenarios

Minimum
Interpancake Heat Conduction
Impedance
($\theta = 0$)

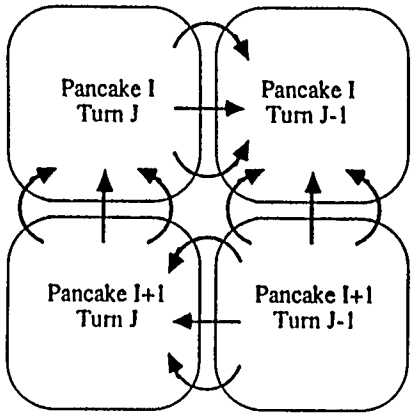

Increasing
Interpancake Heat Conduction
Impedance
($0 < \theta < \pi$)

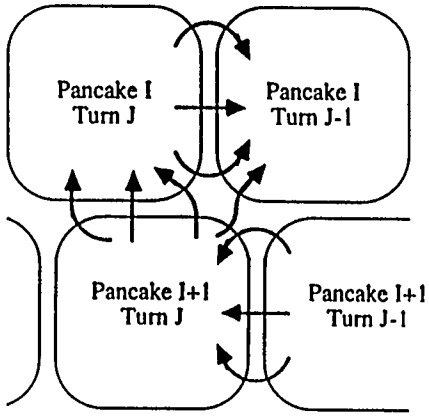

Maximum
Interpancake Heat Conduction
Impedance
($\theta = \pi$)

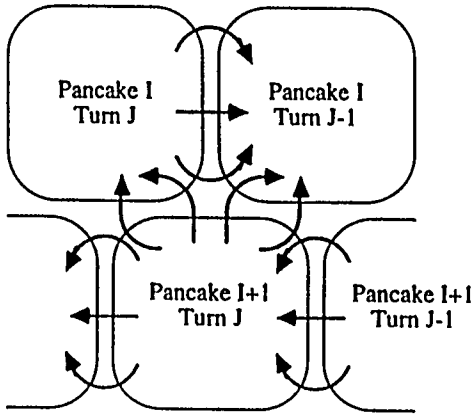

Conductor Temperatures: $T_{I+1,J-1,K} > T_{I+1,J,K} > T_{I,J,K} > T_{I,J-1,K}$

Coolant Pressures: $P_{I+1,J-1,K} < P_{I+1,J,K} < P_{I,J,K} < P_{I,J-1,K}$

Legend

→ Conduction Heat Flow

I = pancake index
J = turn index
K = circumferential location index

T. Kupiszewski
1/24/95

WINDING CELL
Corner Region Thermal Circuit Model Parameters

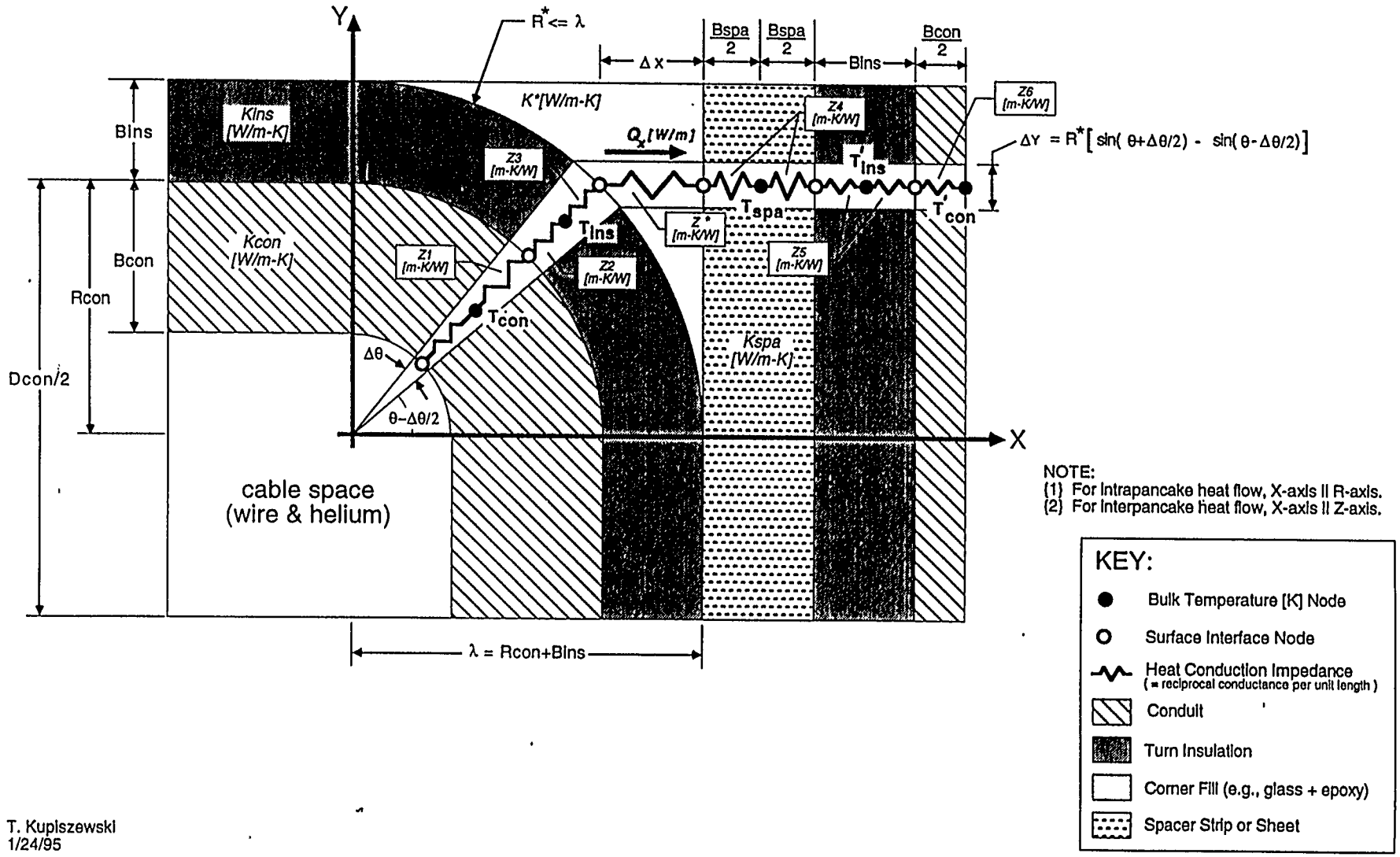

T. Kupiszewski
1/24/95

Comparison of Software Tools versus Experiments (cont'd)

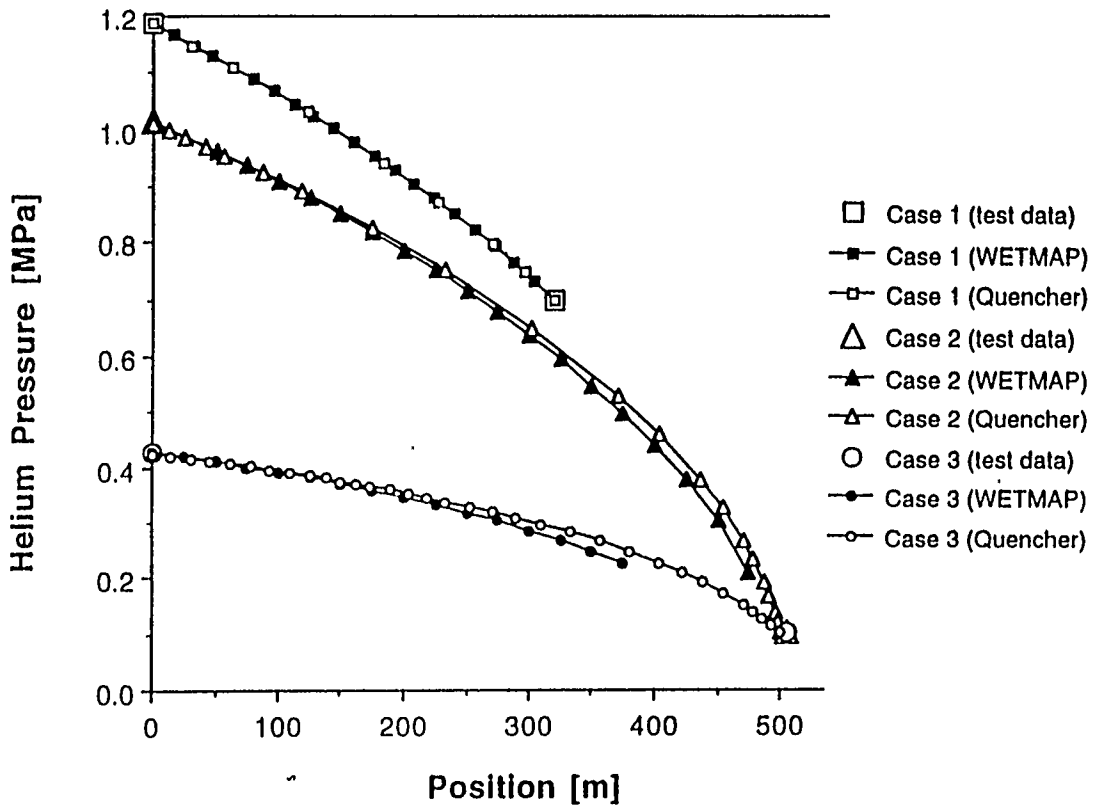

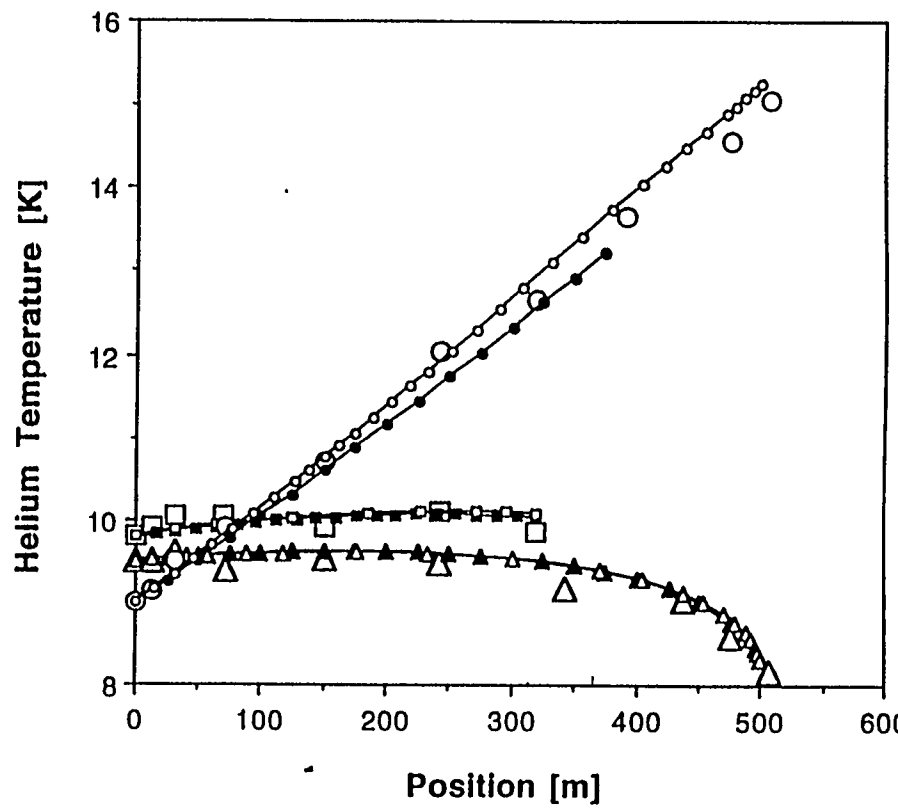

PARAMETER	WETMAP	HESS3D
Total Nuclear Heating	223 Watt	152 Watt
Max Channel Heat (Nuclear)	23.9 Watt	15.2 Watt
He Mass Flow	3 gm/sec	3 gm/sec
Helium Inlet Pressure	0.49 MPa	4.8 atm*
Helium Outlet Pressure	0.293 MPa	3. atm
Helium Outlet Temperature	5.58 K	5.5 K*
Max SC Cable Temperature	5.83 K	5.7 K*
Inlet He Enthalpy	14,630 J/kg	14,630 J/kg
Outlet He Enthalpy	24,450 J/kg	20,370 J/kg
Mass Flow x Enthalpy Rise	29.5 Watt	17.2 Watt

* HESS3D quantities estimated via visual inspection of plots in 14-940713-MIT/PWANG-01, "TPX PF ring coil steady-state heat removal"

Heating Distributions (nuclear)

TPX

MARINE DIVISION

PF7U/L
(total = 677 Watt)

	layer 1	layer 2	layer 3	layer 4	layer 5	layer 6
pancake 14	1 / F 1	2 / F 3	4 / F 5	6 / F 7	8 / F 9	10 / F 11
pancake 13	1 / F 1	2 / F 3	4 / F 5	6 / F 7	8 / F 9	10 / F 11
pancake 12	1 / F 1	2 / F 3	4 / F 5	6 / F 7	8 / F 9	10 / F 11
pancake 11	1 / F 1	2 / F 3	4 / F 5	6 / F 7	8 / F 9	10 / F 11
pancake 10	1 / F 1	2 / F 3	4 / F 5	6 / F 7	8 / F 9	10 / F 11
pancake 9	1 / F 1	2 / F 3	4 / F 5	6 / F 7	8 / F 9	10 / F 11
pancake 8	1 / F 1	2 / F 3	4 / F 5	6 / F 7	8 / F 9	10 / F 11
pancake 7	1 / F 1	2 / F 3	4 / F 5	6 / F 7	8 / F 9	10 / F 11
pancake 6	1 / F 1	2 / F 3	4 / F 5	6 / F 7	8 / F 9	10 / F 10
pancake 5	1 / F 1	2 / F 3	4 / F 5	6 / F 7	8 / F 8	9 / F 8
pancake 4	1 / F 1	2 / F 3	4 / F 5	6 / F 6	7 / F 6	7 / F 6
pancake 3	1 / F 1	2 / F 3	4 / F 4	5 / F 4	5 / F 4	5 / F 4
pancake 2	1 / F 1	2 / F 2	3 / F 2	3 / F 2	3 / F 2	3 / F 2
pancake 1	1 / 1	1 / F 1	1 / F 1	1 / F 1	1 / F 1	1 / F 1

layers 1 2 3 4 5 6

Neutron Radiation

F = 0.7

. - Winding Pack Nuclear Heating w/ and w/o External Case.

Pancake Number	Double-Pancake Number	Nuclear Heat (Watt)			
		PF6 Winding Pack		PF7 Winding Pack	
		No Case	With Case	No Case	With Case
1 & 2	1	23.91	11.73	97.58	47.78
3 & 4	2	11.32	5.55	46.18	22.61
5 & 6	3	9.63	4.72	39.3	19.24
7 & 8	4	9.52	4.66	38.85	19.02
9 & 10	5	9.52	4.66	38.85	19.02
11 & 12	6	9.52	4.66	38.85	19.02
13 & 14	7	9.52	4.66	38.85	19.02
15 & 16	8	9.52	4.66		
17 & 18	9	9.52	4.66		
19 & 20	10	9.52	4.66		
	Total (Watts)	111.5	54.6	338.5	165.7

Table 5 -- Thermal-hydraulic simulation parameters and WETMAP-predicted results.

Run No.	Coil	Pancake No.'s	Channel Length(m)	Case	Heating Distribution	Heating Input(W)	Flow (g/s)	Inlet T(K)	Inlet P(atm)	Outlet P(MPa)	Outlet T(K)	Hot Spot Ths(K)	Tcs (K)	Temp. Margin(K)	Headroom Margin(K)	Residence Time(s)
1	PF7	1 & 2	324	no	uniform	54.6	3	5	5.8	0.31	5.99	6.43	7.69	1.26	2.69	916
2	PF7	1 & 2	324	no	nonuniform	100.2	3.75	5	7.5	0.26	6.55	7.33	7.69	0.36	2.69	
3	PF7	1 & 2	324	no	nonuniform	100.2	4	5	8	0.29	6.54	7.33	7.69	0.36	2.69	
4	PF7	1 & 2	324	no	nonuniform	100.2	4.5	5	8.5	< 0.23	5.82	6.88	7.69	0.81	2.69	
5	PF7	1 & 2	324	no	nonuniform	100.2	4.5	5	9	0.34	6.56	7.37	7.69	0.32	2.69	
6	PF7	1 & 2	324	no	nonuniform	100.2	4.5	5	9.4	0.39	6.81	7.58	7.69	0.11	2.69	
7	PF7	1 & 2	324	no	nonuniform	100.2	5	5	9.4	0.26	5.98	6.97	7.69	0.72	2.69	
8	PF7	1 & 2	324	no	nonuniform	100.2	5	5	10	0.37	6.59	7.4	7.69	0.29	2.69	
9	PF7	1 & 2	324	no	nonuniform	100.2	5.5	5	10	< 0.23	5.27	6.73	7.69	0.96	2.69	
10	PF7	1 & 2	324	no	nonuniform	100.2	5	4.7	9.4	0.3	6.1	7	7.69	0.69	2.99	
11	PF7	1 & 2	324	no	nonuniform	100.2	3.5	4.7	7	0.25	6.52	7.33	7.69	0.36	2.99	
12	PF7	1 & 2	324	no	nonuniform	100.2	3	3.8	4.4	< 0.23	-	6.1	7.69	1.59	3.89	
13	PF7	1 & 2	324	no	nonuniform	100.2	3	3.8	4.5	< 0.23	-	6.18	7.69	1.51	3.89	
14	PF7	1 & 2	324	no	nonuniform	100.2	3	3.8	4.8	< 0.23	-	6.37	7.69	1.32	3.89	
15	PF7	1 & 2	324	no	nonuniform	100.2	3	3.8	5.2	< 0.23	-	6.53	7.69	1.16	3.89	
16	PF7	1 & 2	324	no	nonuniform	100.2	3	3.8	5.4	< 0.23	-	6.63	7.69	1.06	3.89	
17	PF7	1 & 2	324	no	nonuniform	100.2	3	3.8	5.6	< 0.23	-	6.79	7.69	0.9	3.89	
18	PF7	1 & 2	324	yes	nonuniform	47.8	3.17	5	5.8	0.31	5.84	6.22	7.69	1.47	2.69	
19	PF6	1 & 2	283.4	no	nonuniform	26.6	3.8	5	5.8	0.32	5.57	5.81	7.08	1.27	2.08	
20	PF6	1 & 2	283.4	no	nonuniform	26.6	4.8	5	7	0.32	5.53	5.81	7.08	1.27	2.08	711
21	PF6	9 & 10	283.4	no	nonuniform	10.2	4.8	5	7	0.34	5.36	5.64	7.08	1.44	2.08	
22	PF7	1 & 2	324	yes	nonuniform	47.8	4	5	7	0.33	5.84	6.29	7.69	1.4	2.69	850.7
23	PF7	7 & 8	324	yes	nonuniform	19	4.4	5	7	0.32	5.49	5.95	7.69	1.74	2.69	879.3

NOTE: Flow rates are per double pancake coil.

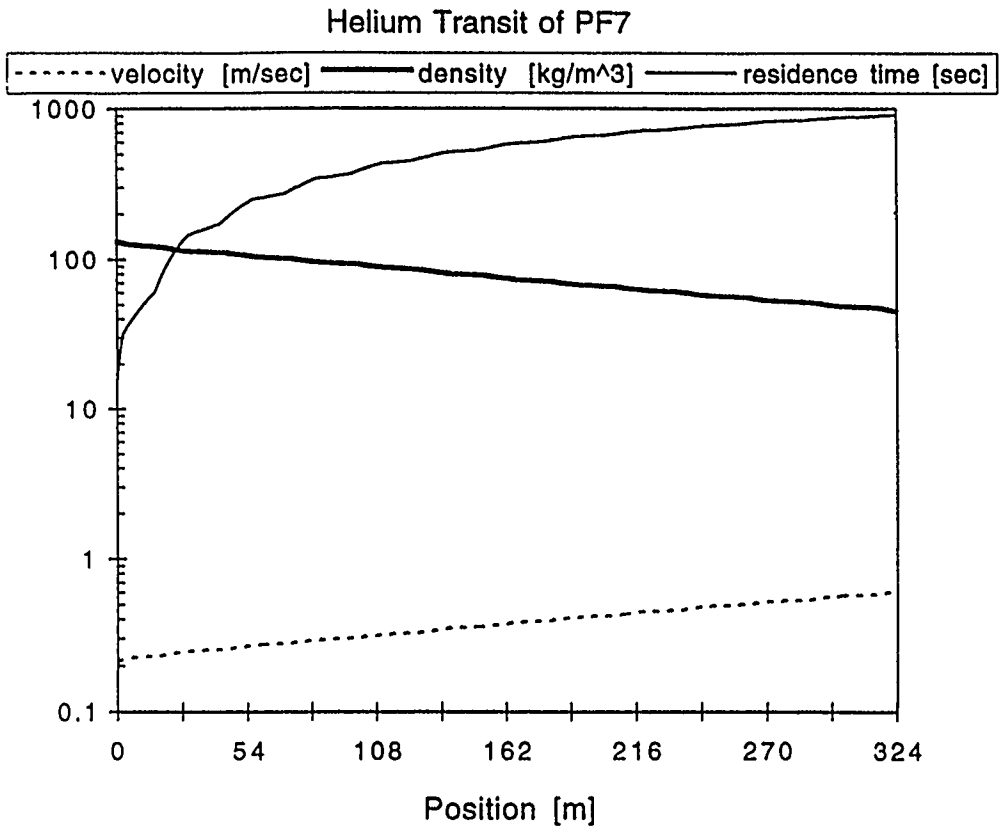
Helium Transit of PF7
velocity [m/sec]
density [kg/m^3]
residence time [sec]
1000
100
10
1
0.1
0
54
108
162
216
270
324
Position [m]

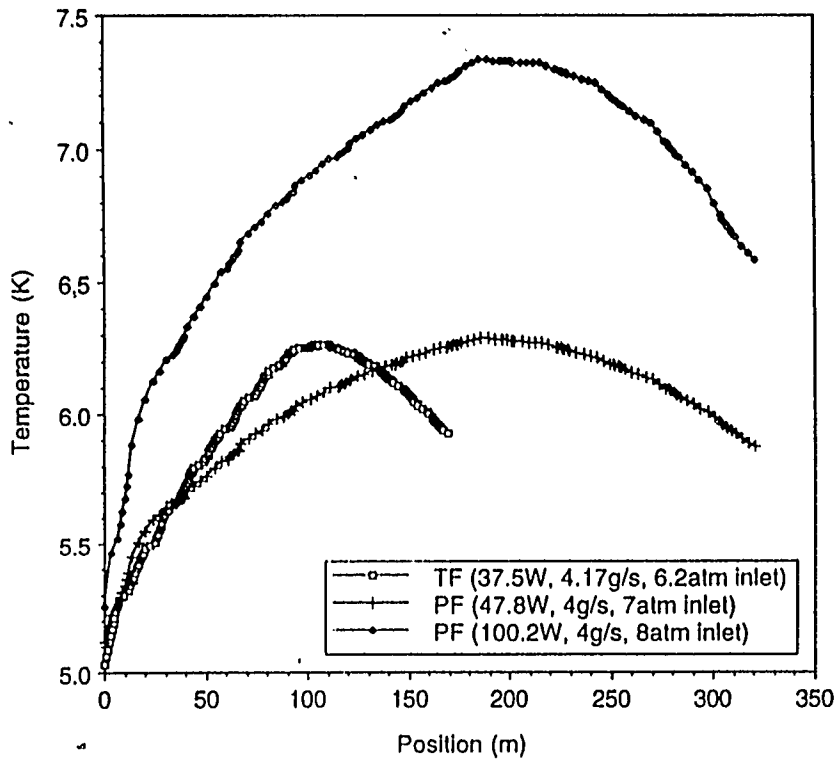

Figure 5. Predicted wire temperature profiles showing design scaling effects for the largest PF coil in TPX.

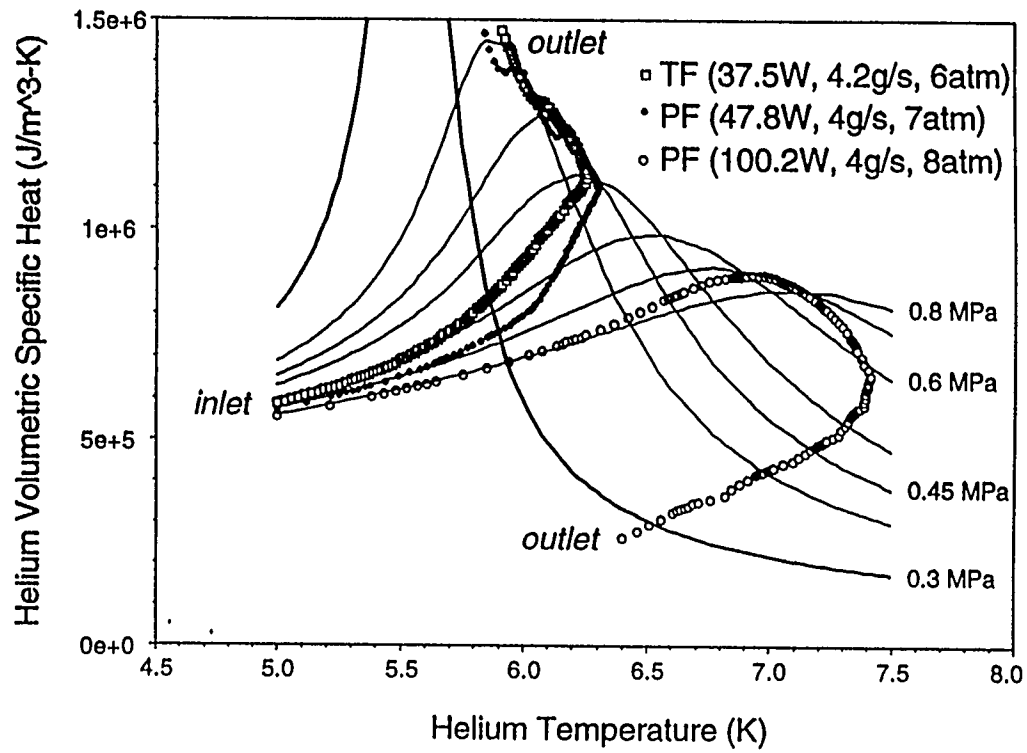

Figure 6. Plots of coolant state showing how different coil designs "surf" the helium heat capacity "wave".

ENERGY MARGIN

For PF6, at the worst case 5.81K hot spot location, the predicted helium pressure is roughly 0.44 MPa for 3.8 g/s flow. The associated density and helium internal energy for these pressure and temperature conditions is 101.8 kg/m^3 and 16047 J/kg, respectively. Substituting these values into equation (5) yields a minimum energy margin of 349 mJ/cm^3, based on a helium internal energy of 19477 J/kg at the 7.08K current sharing temperature. This value exceeds the 300 mJ/cm^3 minimum set by the design criteria.

For PF7, at the worst case 6.29K hot spot location, the predicted helium pressure is roughly 0.52 MPa for 4g/s flow. The associated density and helium internal energy for these pressure and temperature conditions is 92.27 kg/m^3 and 18614 J/kg, respectively. Substituting these values into equation (5) yields an energy margin of 358 mJ/cm^3, based on a helium internal energy value of 22492 J/kg at the 7.69K current sharing temperature. This value also exceeds the 300 mJ/cm^3 minimum set by the design criteria.

Summary of Preliminary Flow Budget Estimate for PF6 & PF7

	Coil				Case					Coil+Case
	Inlet	Outlet		Flow	Inlet		Outlet		Flow	Flow
	P(MPa)	T(K)	P(MPa)	(g/s)	T(K)	P(MPa)	T(K)	P(MPa)	(g/s)	(g/s)
PF6 (no case)	0.709	5.36	0.34	96					0	96
PF7 (w/ case)	0.709	5.49	0.32	60.8	5	0.709	5.4	0.32	197	257.8
	0.709	5.49	0.32	60.8	5	0.709	5.49	0.32	126	186.8
	0.709	5.49	0.32	60.8	5	0.709	5.6	0.32	83	143.8
PF7 (w/case & coil effluent)	0.709	5.49	0.32	60.8	5.49	0.32	5.43	0.25	60.8	60.8
	0.709	5.49	0.32	60.8	5.49	0.32	5.68	0.29	60.8	60.8

Conclusions

- PF6 baseline cooling design is adequate for dissipating heat loads.
  - predicted temp. margins > 1.25K > 1K(req.)
  - predicted temp. headroom = 2.08K > 2K(req.)
  - predicted energy margin = 349 mJ/cm^3 > 300 mJ/cm^3(req.)

- PF7 baseline cooling design is not adequate for dissipating heat loads.
  - temp. margin prediction = 0.11K to 0.72K versus 1K required
  - from thermal-hydraulics perspective, modifications are needed

- Shielding PF7 winding pack with ventilated external case is effective solution.
  - predicted temp. margins > 1.4K > 1K(req.)
  - predicted temp. headroom = 2.69K > 2K(req.)
  - predicted energy margin = 358 mJ/cm^3 > 300 mJ/cm^3(req.)
  - refrigeration burden increases by 160 Watt

- Coolant flow budget estimate (prelim.) is 160 g/s minimum for PF6 & PF7.
  - exceeds previous estimate of 106 g/s for PF5,6,&7 combined
  - design caveats are:
    - PF6/7 have cases ventilated with coil effluent
    - inlet @ 7 atm & 5K, outlet pressure of 0.3 MPa to 0.35 MPa

Recommendations

- Neutron transport analysis needed to predict detailed heating distribution in PF6 & PF7 with cases & ground wall included. Present WETMAP models should be modified for self-consistent calculation of case-to-coil conduction coupling.

- Further design optimization to reduce/refine required flow capacity estimate. Leverage with WETMAP simulations of case cooling options and hydraulic circuit changes for optimal flow redistribution.

- Sensitivity studies to assess effects of CICC friction factor variability and Cu:SC ratio variability.

Topics

- B-Spec Verification Matrix
  - Ref. PF Magnet System Spec, TPX-SPEC-14-0001, Rev. 0
- FMECA
  - Ref. TPX-14-950705-WEC-HCalvin-01
- Reliability Allocation
- Materials & Processes Selection
  - Ref. TPX-14-950811-WEC-HCalvin-01
- Integrated Test Plan
  - Ref. TPX-PLAN-14-001, Rev. 0 Draft

Verification Terminology

Quality conformance inspections

Table 25 summarizes the requirements that shall be verified and the method of verification. The methods of verification include:

Inspection: Refers to "inspection by attributes" whereby either the unit of product or characteristics thereof, is classified simply as defective or nondefective, or the number of defects in the unit of product is counted, with respect to a given requirement. [MIL-STD-109B]

Analysis: Verification by calculation or simulation, including computer modeling based on established material or component characteristics. [B&W suggestion][B&W suggestion] Processing accumulated results and conclusions, intended to provide proof of compliance with requirements.

Demonstration: Verification limited to readily observable functional operation to determine compliance with requirements. [Westinghouse suggested]

Test: Determination, by technical means, of the properties or elements of supplies, or components thereof, including functional operation, and involves the application of established scientific principles and procedures. [MIL-STD-109B]

B-Spec Verification Matrix

Verification Matrix

Table 1 - Requirements Verification Summary.

Specification Paragraph	Specification Title	N/A	Insp	Anal	Dem	Test p	Test s	Test a
3.2	Characteristics	X						
3.2.1	Performance	X						
3.2.1.1	General capabilities	X						
3.2.1.1.1	Four quadrant operation				X			
3.2.1.1.1.1	Quadrant definition	X						
3.2.1.1.1.2	First quadrant	X						
3.2.1.1.1.3	Second quadrant	X						
3.2.1.1.1.4	Third quadrant	X						
3.2.1.1.1.5	Fourth quadrant	X						
3.2.1.1.1.6	Initial configuration	X						
3.2.1.1.2	TF interconnect compensation			X				
3.2.1.1.3	Plasma chamber conditioning operations				X			
3.2.1.2	Vacuum environment operation	X						
3.2.1.2.1	Compatibility					X		

FMECA - Terminology (1)

- A SEVERITY CLASSIFICATION is assigned to each failure mode according to its effect on the system or major components. The failure mode SEVERITY CLASSIFICATIONS are defined as follows:

Category	Classification	Description
I	Catastrophic	A failure that may cause death, fatal cryogenic exposure or loss of TPX., i.e. damaged beyond repair.
II	Critical	A failure that may cause severe injury, major TPX or site damage that will result in TPX downtime of approximately one year or greater.
III	Marginal	A failure that may cause minor injury, minor TPX or site damage that will/may result in system downtime of approximately a month or more and/or limit TPX functions.
IV	Minor	A failure that is not serious enough to cause injury, or TPX or site damage, but will result in system downtime (at convenience) or have a minor impact on TPX functions.
V	No Effect	A failure that has no impact on TPX operation and does not result in downtime.

FMECA - Terminology (2)

- The PROBABILITY OF OCCURRENCE of the failure mode during the operating time interval of ten years is qualitatively estimated as follows:

  Level A - Frequent. A high probability of occurrence during the item operating time interval; equivalent to a single failure mode probability greater than 0.01.

  Level B - Reasonably Probable. A moderate probability of occurrence during the item operating time interval; equivalent to a single failure mode probability greater than 0.001 but less than 0.01 during the item operating time interval.

  Level C - Occasional. An occasional probability of occurrence during the item operating time interval; equivalent to a single failure mode probability greater than 0.0001 but less than 0.001 during the item operating time interval.

  Level D - Remote. A remote probability of occurrence during the item operating time interval; equivalent to a single failure mode probability greater than 0.00001 but less than 0.0001 during the item operating time interval.

  Level E - Extremely Unlikely. An extremely unlikely probability of occurrence during the item operating time interval (essentially zero); equivalent to a single failure mode probability less than 0.00001 during the item operating time interval.

FMECA - Results

Table 1. Item Failure Modes with Severity Category II Effects.

Indenture Level	Description	Probability of Occurrence
A.1.(1-4).1.2, A.(2-4).1.2 Insulation (Winding Pack)	Decrease in coil inductance resulting from layer-layer short	D
A.3.1.1.1.1 Plated SC Strand	RRR too low	D
A.3.1.1.3 Sheath	Leaks helium into cryostat	D
B.1.1-2 Quench detection voltage taps	Short-circuit across voltage tap pair	D
B.1.1-2 Quench detection voltage taps	Short-circuit of magnet double pancake by conventional voltage tap	D
B.1.1-2 Quench detection voltage taps	Short-circuit to ground	D
B.4 DAS	REAL Quench not interpreted as such	D
B.4 DAS	REAL Quench indication is not propagated to the protection system	D
C.1 VCL	Loss or reduction of helium flow	D

Reliability Allocation Highlights

- PF Magnet System Reliability Allocation = 0.9951
- Risk Assessment Leads to Allocation among Major Components
- Historical Database does not support our requirement
- Bottom-up exercise due in Phase 2
- High risk elements identified in FMECA
- Risk Reduction Approaches identified

Reliability Allocation

tpx191r.sg

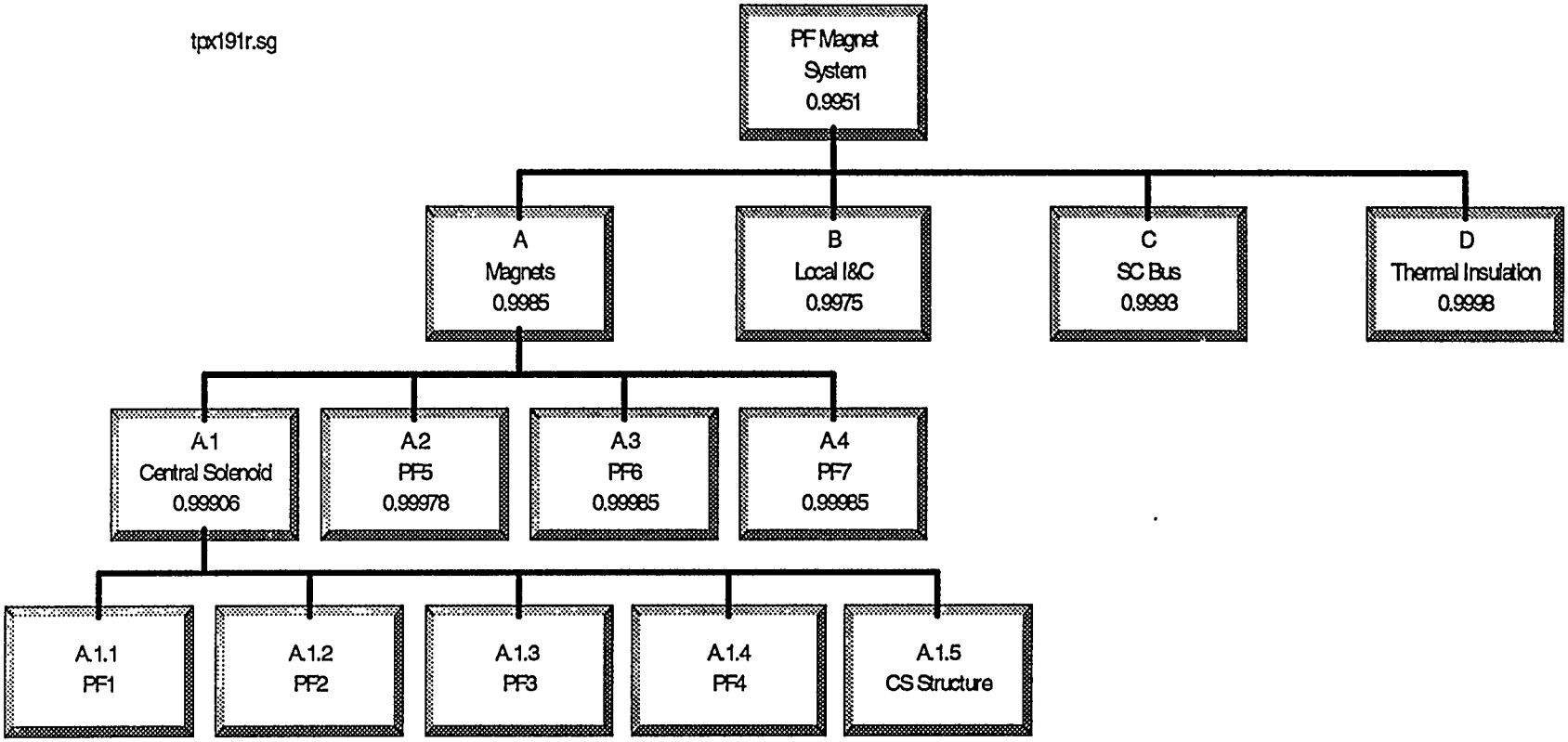

Mat'ls & Processes Selection Overview

- Purpose: Justify the selection of materials and mfg. processes used in PF Magnet System
- Developed Databases
  - PF1-7 Coil Materials
  - Helium Plumbing Materials
  - CS Structure Materials
  - PF Mounts Materials
  - PF6&7 Cases Materials
- Developed Mfg. Processes Database

PF1-7 Coil Materials Database

Component	Candidate Materials	Criteria or Notes	Selected Materials	Use
Winding Pack Conductor	Nb_3Sn CICC	Nb_3Sn: Cost, higher (Jc, Tc, Bc) and strain sensitivity than NbTi; CICC: Improved thermal performance, quench stability	Nb_3Sn CICC	PF1-5 coils
	NbTi CICC	NbTi: Lower (Jc, Tc, Bc) and strain sensitivity than Nb_3Sn; CICC: same as above	NbTi CICC	PF6-7 coils
Winding Pack Insulation				
Primary Insulation	Kapton	Excellent dielectric strength; Subject to pinholes, tearing, and abrasion damage.	Kapton	PF1-7 coils half-lapped layers arou CICC
S2 Glass tape	2D weave	Good thermal and mechanical properties in plane of tape. Best for use in regions of low stress perpindicular to tape.	2D weave	PF1-7 coils abrasion protection I
	3D weave	Through-thickness glass fibers improve orthotropic (3D) thermal and mechanical properties. Best for use in otherwise epoxy rich regions of high stress.	3D weave	PF1-7 coils basic cond glass wrap
	3D Corner preform	Molded to fill complex shape with glass. Tackified to retain shape.	3D Corner preform	PF1-7 coils to fill in cor voids

Helium Plumbing Mat'ls. Database

Table 1. Helium Plumbing Materials Database.

Component	Candidate Materials	Criteria or Notes	Selected Materials	Use
Helium Stub	316LN	Compatable with PF6&7 CICC	316LN	PF6-7 coils
	Incoloy 908 & 316LN	Compatable with PF1-5 CICC	Incoloy 908 & 316LN	PF1-5 coils
Tubing	316LN	Good cryogenic properties, clean, easy to work, etc.	TBD	PF1-7
Isolator	TBD			PF1-7
Flow meter	TBD			PF1-7
Filter	TBD			PF1-7
Manifold	316LN	Tubing attachment compatability	TBD	CS and PF
Electrical Insulation				
Primary insulation	Polyimid	Easily abraded (negative indication); excellent dielectric strength	Polyimid	PF1-7 tubi flowmeters isolators, fi
Insulation Overwrap	3D S2-glass/epoxy	See CPDR Volume 5 notes	3D S2-glass/epoxy	PF1-7 tubi flowmeters isolators, fi

CS Structure Materials Database

Table 1. CS Structure Materials Database.

Component	Candidate Materials	Criteria or Notes	Selected Materials	Use
Tie Rods	316LN, other 300 series ss	React preload; strength important; want to take advantage of different CTEs between coils and structure to reduce room temperature preload required (reduces creep at room T); should match Outer preload structure CTE.	316LN,	CS inner pl structure
Outer Preload Structure: shell, bottom plate, & slotted bracket	316LN,	Weldability; react preload; strength important; want to take advantage of different CTEs between coils and structure to reduce room temperature preload required (reduces creep at room T).	316LN,	CS outer p structure
Top Plates	316LN, other 300 series ss	(CTE mismatch is a disadvantage here.)	316LN	Ties inner a outer prelo structures t

PF Mounts Materials Database

Table 1. Materials Database for PF Mounts.

Component	Candidate Materials	Criteria or Notes	Selected Materials	Use
Installation Shims	316LN	Good cryo and radiation properties; lots of history; good dielectric properties	316LN	Coil alignm shims
TF Mount Brackets	316LN	strength	316LN	Primary Su
Slide Mount Leaf Spring	316LN	stiffness is an advantage	316LN	Coil center
Leaf Spring Slide Pad	Dicronite Dry Lube (WS_2), HPS 2832 (MoS_2, Sb_2O_3, and Au)	radiation resistant, abrasion resistant, distributes applied force, low material transfer	TBD	Lower fricti
Low Friction Surface Coating	Dicronite Dry Lube (WS_2), HPS 2832 (MoS_2, Sb_2O_3, and Au)	Radiation resistant, Low friction coefficient, hardness, abrasion resistant, low material transfer	TBD	Reduce lea spring forc requiremer

PF6&7 Cases Materials Database

Table 1. Materials Database for PF6&7 Coil Cases.

Component	Candidate Materials	Criteria or Notes	Selected Materials	Use
Case Walls	316LN	Compatable with CICC CTE	316LN	Stiffen win pack again bending
Wall Fasteners	Nitronic 60, 316LN, or other 300 series ss	Strength, availability	TBD	joining cas component
Wall Cooling Tubing	316LN, copper	Thermal conductivity, weld compatibility with case bottom, electrical resistivity	316LN	Removing caused by nuclear rac
Wall Tubing Fins	Copper	High thermal conductivity	copper	Collecting transportin to cooling t
Insulation Break	G-11CR	Good cryo and radiation properties; lots of history; good dielectric properties	G-11CR	Break up p eddy curre loops

Mfg. Processes Database

Table 1. Manufacturing Process Selection.

Critical Processes	Manufacturing Processes or Tooling	Selection Criteria	Selection Ration
Lead Bending	Closed Form Bending Die	Minimize conduit deformation and allow access to leads.	Closed form die minin conduit bulge and can used before and after winding.
Transition Bending	Closed Form Bending Die	Minimize conduit deformation, allow access to transitions in the preform condition. High reliability & repeatability	Closed form die is the repeatable method. I tool design enhances accuracy and reduces conduit deformation.
Coil Winding	Multiple bending roll former using servo motor positioning and pinch roller action. Bidirectional, quick action, labor saving clamps on the take up fixture.	Tool geometry must accommodate forward and back bending to maintain TF CICC straightness and curvature. Constant CICC input angle desired. Economical coil take -up fixture clamping (bidirectional)	Pyramid roller geomet rejected due to large variations in CICC inp angle. Multiple roller geometry eliminates i angle variations. Bac bending allows for straightness control ar supports TF coil manufacture.
Helium Stub Piercing	Roto-Bore Hole Drilling Steel foil extraction with tweesers	No damage to SC strands. No debris in CICC. No sharp edges.	Roto-Bore allows for c stop limits, preventing damage. Manual foil extraction prevents de entry.

Integrated Test Plan

- Final Design Phase Development Testing (Mfg. R&D)
- Source/Receiving Inspections (Mat'l. & Comp. Tests)
- In-Process Testing (Verification Tests)
- Acceptance Testing
  - Fabrication Site Testing
  - Integration Site Testing
- Prototype Testing
- System Testing

Test Plan is Coordinated with Other Docs

- FMECA
  - FMECA identified high risk areas and risk mitigation approaches
  - Test Plan identifies tests focused on high risk areas
- B- and C-Specs
  - Spec identifies verification test requirements
  - Test Plan identifies and describes tests

Test Plan Anticipates Resources

- ❑ Test Sequence developed
- ❑ Test Equipment and Facilities developed
- ❑ Test Data Requirements identified

Final Design Development Testing

- Helium stub leaktightness and process control
- VPI factorial parametric evaluation
- Winding Pack Spur Welding
- Tight Radius Bend / Instrumentation Integrity
- Insulating at Discontinuities
- Joint Preparation, Installation, Sensor extraction
- Helium Stub - Cooling and Stagnation Points
- Insulation - Glass-epoxy characterization with radiation
- Insulation Filler Development

Manufacturing Plan

Pat McAuliffe

Outline

- Tier 1 Process Flow Charts
- Production Schedule
- Long-Lead Procurement
- CS/PF5 Tooling (Doug Hartman
- PF 6-7 Tooling (Al Burger)
- TF Manufacturing Study (Pat McAuliffe

CS/PF5 Flow Chart

CS 6/7 Flow Chart

TF Flow Chart

Integrated Production Schedule

Long Lead Material Items

TPX Magnet System

Contractors Preliminary Design Review

CS/PF 5 Magnet Tooling

22 September 1995

CS/PF 5 Final Assy and Test

❑Winding System

Tier 2 Winding PF1-5, TF Coil Process Flowchart

Winding System Critical Components

- Control System
- Conductor Payout Fixture
- Cleaning Station
- Straightener
- Straighteness Measurement
- Roll Former
- Length Measuring System
  - Length Encoder
  - Position Index Marker
- Formed Radius Measurement Device
- Transition and Lead Bending Equipment
- Alchohol Wipe Position
- Helium Leak Check Station
- Winding Turntable & Clamping

PEDR Driven Changes

- Winding System Now Measures Arc Height after forming
- He Leak Test Chamber Supply and Vent Tubes are Repositioned
- Added Alchohol Wipe Cleaning Step to Process

PF Tooling

- Reaction System

Tier 2 Reaction PF1-5, TF Coil Process Flowchart

Flow Diagram Here

Reaction Process Features

- Zone Controlled, Radiant Heat
- Cable Space He Atmosphere Control and Monitoring
- Programmable Reaction Cycle
- 2-Stage Back-up Power Supply
- Gas Purification Systems
- Gettering Spacers/Hangers
- Argon Atmosphere for Initiation and Fail-Safe
- Treated Cu Conduction/Spacer Panels
- Data Recording
  - Gas Flowrates
  - He In-conduit purity monitoring
  - Zone Temperatures
  - Thermocouple Readings
  - Vacuum Integrity
  - Oxygen and H_2O Levels

CS/PF5 Reaction Make/Buy Trade Study

Trade Study Results

- Baseline
  - Vacuum Oven Selected
  - Retort Concept Determined To Be Not Desireable for Meeting Rapid Heat Rate
- Selection Criteria
  - Cost
  - Schedule
  - Technical Risk
- Process
  - RFQ Was Issued to Solicit PF Oven Procurement
  - Quote For Reaction Service Was Based on Previous (Lower Fidelity) RFQ
- Results/Responses
  - Two Reaction Service Providers Responded
  - Two Reaction Oven Designers Responded
- Decision
  - Service was selected
  - Cost of Upgrading Service's Equipment in Order to Meet Reaction Requirements was Reasonable Compared to Procurement of New Oven

PF Tooling

- Insulation Application System

Tier 2 Insulation PF1-5, TF Coil Process Flowchart

Insulation Application System Major Components

- Coil Support System
- Coil Separation System
- Taping Machine
- Coil Collection Fixture and Clamps
- Ground Wrap Tooling

PEDR Driven Changes

- In-Line Cleaning Process
- Continuous HV Probe Test of Kapton
- Separate Glass Application Head Follows HV Tester

Vacuum Pressure Impregnation System

- Preheat and Cure Oven
- V P I Fixture
- Multiple Resin Supply Feeds from Common Manifold
- Vacuum/Pressure Manifold
  - Individual Sight-Glass Risers
  - Individual Shut-off Valves
- Resin Mixing Tank
- Vacuum Pump
- Data Recorder
  - Oven Temperature
  - Mold Vacuum/Pressure
  - Mixing Tank Vacuum/Pressure
  - Resin Temperature
  - Mold Temperature
- N2 Available
  - Dry Gas Purge Prior to Preheat
  - Back-Pressurization during V P I cycle
  - Back-Pressurization during cure cycle thru glass transition

Coil/Structure Assembly

- ❑ Field Map Coil Using Fiducial/Probe Jig and Hall Probe Array
- ❑ Position Fiducials usig Jig for Registration
- ❑ Position Structure Base on Assembly Stand
- ❑ Position Coil on Structure Base
- ❑ Align Coil Fiducials to Structure Fiducials Optically
- ❑ Repeat for Successive Coils
- ❑ Attach Structure Upper Components and Tie Rods
- ❑ Preload Structure with Hydraulics
- ❑ Torque Set Screws
- ❑ Roll Cryogenic SubAssembly under Stand, Lift and attach with Struts
- ❑ Orbital Weld Cryo-Lines from Stubs to Manifolds
- ❑ Insulate Cryo-Lines using PrePreg

Everson Electric Facility Layout

TPX Magnet System

Contractors Preliminary Design Review

CS 6-7 Magnet Tooling

22 September 1995

PF 6 & 7 Integrated Manufacturing Fixture

Tier 1 PF 6-7 Coil Process Flowchart

Integrated Coil Station-Major Components

- Control System
- Conductor Payout Fixture
- Cleaning Station
- Straightener
- Straightness Measurement
- Roll Former
- Length Measuring System
  - Length Encoder
  - Position Index Marker

Integrated Coil Station-Major Components (con't)

- Formed Radius Measurement Device
- Transition and Lead Bending Equipment
- Alchohol Cleaning Position
- Helium Leak Check Station
- Helium Stub Installation
- Kapton Application Taping Head
- HV Kapton Integrity Check
- Glass Tape Application Head
- Winding Turntable & Clamping
- Ground Wrap Application Capability

Collection Table--Unique Features

- Utilizes Coil Case as Conductor Reciever
- Lift/Lower Capability
- Unique Clamping System
- Fixed Position Taping Heads (move Radially)

PEDR Driven Changes

- Revised Clamping Provides more Posative Securing of Coil in Position Within Case
- VPI Covers External Cases
- Analysis of Mechanical Vs Hydraulic Systems

Facility Overview

- Northrup-Grumman Aerospace Facilities

Facilities for TPX Program

- Engineering
  - Office Space 1600 m^2
    Building 25, Bethpage NY
- Manufacturing
  - Superconducting Dedicated
    Production - Air Conditiioned, Clean
    Building 1, Bethpage NY
    High Bay 7400 m^2
    Low Bay 4600 m^2
    High Bay 743 m^2
- TPX Program
  - Low Bay 465 m^2

Northrup Grumman Facility Layout

Northrup Grumman Facility Photograph

TF Winding Process Flow Chart

Insulation and VPI Process Flow Chart

Case/ICS Assembly Flow Chart

Final Assy & Test Flow Chart

Site General Arrangement

TF Tooling

- Critical Tools Only
  - Winding System
  - Reaction System
  - Insulation and Impregnation Systems
- Feature/Activity Summary
- TF Tooling Features which are both Unique and Critical

❑TF Winding System

Tier 2 Winding PF1-5, TF Coil Process Flowchart

Winding System Critical Components

- Control System
- Conductor Payout Fixture
- Cleaning Station
- Straightener
- Roll Former
- Length Measuring System
  - Length Encoder
  - Position Index Marker
- Transition and Lead Bending Equipment
- Bend Radius Adjustment Tooling Kit
- Helium Leak Check Station
- Winding Turntable & Clamping
  - Clamping Similar to CS & PF5. . . Turntable unique to TF
- Helium Stub Installation

TF Take-Up Turntable Concept Key Features

- Table is Driven Using Woods Belt
- Table is Guided by Grooves to Continuously Control Position
- Pivot Plate Rotates to Accomodate Changes in Conductor Orientation due to Changes in Bend Radius
- Pivot Plate Supports Table and Accomodates Grooves
- Table to Pivot Plate and Pivot Plate to Floor I'faces use Transfer Balls

TF Reaction System

Tier 2 Reaction PF1-5, TF Coil Process Flowchart

Flow Diagram Here

TF Reaction Furnace

Trade Study Results

- Baseline
  - Vacuum Oven Selected
  - Retort Concept Determined To Be Not Desireable for Meeting Rapid Heat Rate
- Selection Criteria
  - Cost
  - Schedule
  - Technical Risk
- Process
  - RFQ Was Issued to Solicit TF Oven Procurement
  - No Services Were Available Which Could Accommodate TF Size Coil
- Results/Responses
  - Two Reaction Oven Designers Responded
- Decision
  - Cost of TF Oven Designs Were Within 5% of Each Other
  - Decision Based on Vendor's Ability to Demonstrate Understanding of Customer's Concerns

TF Oven Concept

TF Oven Concept Drawing Here

TF Tooling

- Insulation Application System

Insulation Application System Major Components

- ❑ Coil Support System
- ❑ Coil Separation System
- ❑ Coil Collection Fixture and Clamps
- ❑ Taping Machines
- ❑ Ground Wrap Tooling

Arrangement, Orientation, and Quantities Revised from CS

TF Insulation Application System Features

- Stationary Stands Supporting Coil are on Outside of Coil
- Moving "Coil Separators" are Inside Coil Geometry
- Moving Components are Powered from Equipment Tree near Center (not shown)
- Arrangement puts Moving Hardware away from Coil Leads

TF Tooling

- Vacuum Pressure Impregnation System

V P I System Major Components

- Preheat and Cure Oven--Will use Localized Heat Source Similar to PF6-7
- V P I Fixture--Similar Design with Modification to Shape
- Multiple Resin Supply Feeds from Common Manifold
- Vacuum/Pressure Manifold
  - Individual Sight-Glass Risers
  - Individual Shut-off Valves
- Resin Mixing Tank
- Vacuum Pump
- Data Recorder
  - Oven Temperature
  - Mold Vacuum/Pressure
  - Mixing Tank Vacuum/Pressure
  - Resin Temperature
  - Mold Temperature
- N2 Available
  - Dry Gas Purge Prior to Preheat
  - Back-Pressurization during V P I cycle
  - Back-Pressurization during cure cycle thru glass transition

V P I Mold Key Features (similar to CS)

- O-Ring Seals to Bottom and Top Plates
- O-Ring Seals Between Segments of both Inner and Outer Walls
- Multiple Resin Supply Lines
- Multiple Riser and Pressurization Connections
- Supply Lines and Risers are Clocked to Promote Resin Crossflow
- Keys and Dowels to Fix Wall Positions to Bottom and Top
- Through Fasteners Preclude Leaking Resin Entry to Tapped Holes
- Jack Screws Provided to Assist in Separation
- Lead Exit and Insulation Design Remains TBD

VPI Fixture Penetration Concept, HE Stub

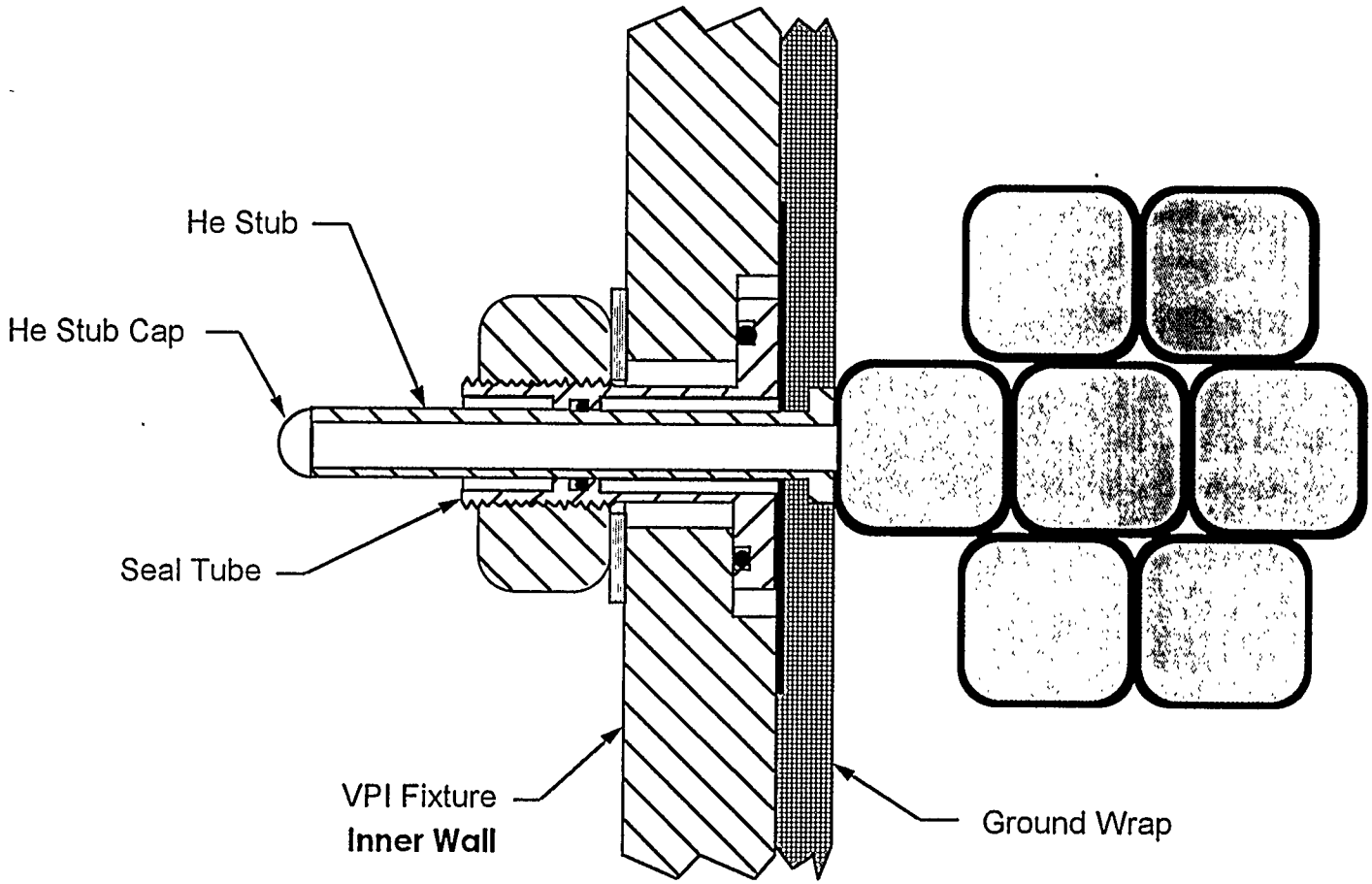

Note:Requires near-Parallel Stubs to permit Inner Wall Section Extraction

TF VPI Mold

- Mold Illustration Here

Westinghouse Facility Layout

- Facility Illus. Here

TPX-SDD-14 Rev. 0		Page: 1 of 102
Title Poloidal Field System System Design Description	Initiated by:	Effective Date: x/x/95
	Approved by: TPX Project Director	Supersedes: New

TPX Poloidal Field System Design Description (SDD)

TPX-SDD-14, Rev. 0

August 18, 1995

Edited and Updated by:

Hugh A. Calvin, WEC

Contributors

H. Calvin, D. Potter, P. Sanger, W. Hannan, WEC

P. Walstrom, NGC

Approvals

Prepared By:

Hugh A Calvin 8/17/95
Hugh A Calvin — Date
WEC Systems Engineering

Approved By:

David R. Potter 8-17-95
David R. Potter — Date
Manager, WEC TPX Engineering

Approved By:

Gary Deis — Date
TPX Deputy Project Manager
Lawrence Livermore National Laboratory

REVISION AND CHANGE RECORD

Revision No.	Description of Revision	Date Revised	Revision Written By	Revision Approved by

DRAFT

TABLE OF CONTENTS

1. FUNCTION & DESIGN REQUIREMENTS **10**

1.1 Functions **10**

1.2 Configuration Requirements & Essential Features **10**
1.2.1 PF Configuration Requirements 10
1.2.1.1 Configuration 10
1.2.1.2 Physical Characteristics 11
1.2.2 Electrical Isolation and Grounding 15
1.2.2.1 Modified Star Ground Topology. 15
1.2.2.2 Ground Plane. 15
1.2.2.3 CS structure grounding. 15
1.2.2.4 CS structure segment isolation. 15
1.2.2.5 Local I&C grounding. 15
1.2.2.6 Isolation. 16
1.2.2.7 Standoff. 16
1.2.2.8 Ground currents. 16
1.2.3 Material Selection Criteria 16
1.2.3.1 Materials Selection 16
1.2.4 Essential Features 16

1.3 Performance & Operational Requirements **17**
1.3.1 Plasma Shaping Requirements 17
1.3.2 Plasma Positioning Requirements 17
1.3.2.1 Control Interfaces. 17
1.3.2.2 Slow feedback functions. 17
1.3.2.3 Slow feedback currents. 18
1.3.3 Plasma Discharge Evolution Requirements 19
1.3.3.1 HC Scenario operating currents. 19
1.3.3.2 LC Scenario operating currents. 19
1.3.3.3 Steady state operation. 20
1.3.3.4 Flexibility scenarios. 20
1.3.3.5 Transient currents. 23
1.3.3.6 Discharge cleaning 23
1.3.3.7 Endure worst case forces 24
1.3.4 Toroidal Field/Plasma Directionality 27
1.3.4.1 Four quadrant operation. 27
1.3.5 Field Compensation 28
1.3.5.1 TF interconnect compensation. 28
1.3.6 PF Disruption Handling 28
1.3.6.1 Frequency of disruptions. 28
1.3.6.2 Disruption scenarios. 28
1.3.6.3 Currents induced by disruption. 29
1.3.7 PF Magnet Quenches 29

1.3.7.1 Quench frequency. 29
1.3.7.2 Endurance criteria. 29
1.3.8 Operational Requirements 30
1.3.8.1 Operate in a vacuum environment 30
1.3.8.2 Cool to operating temperature 30
1.3.8.3 Warm to room temperature 31
1.3.8.4 Lifetime Operating Limits 32

1.4 RAM Requirements 32
1.4.1 Reliability and Availability 32
1.4.1.1 PF Magnet System reliability 32
1.4.1.2 Availability 33
1.4.2 Maintainability 34
1.4.2.1 Maintainability features. 34
1.4.2.2 Remote maintenance. 34
1.4.2.3 Accessibility. 34
1.4.2.4 Limits to maintainability. 34

2. PF COIL DESIGN DESCRIPTION **34**

2.1 System Design Description Overview 34
2.1.1 Central Solenoid (PF1 to 4) 37
2.1.1.1 Central Solenoid (PF1 to 4) - Coil 37
2.1.1.2 Central Solenoid (PF 1 to 4) - Structure 54
2.1.1.3 Central Solenoid Interface to TF Structure 61
2.1.1.4 Central Solenoid Assembly 63
2.1.1.5 Superconducting Bus and Leads 64
2.1.2 Poloidal Field Coil 5 64
2.1.2.1 Coil description 64
2.1.2.2 Interface to TF Structure (PF 5) 66
2.1.3 Poloidal Field Coils 6 and 7 70
2.1.3.1 Coil description 70
2.1.3.2 Interface to TF Structure (PF 6 and 7) 72

2.2 System Performance 75
2.2.1 Nominal 2.0 MA, Double-Null (HC) Scenario 75
2.2.2 Nominal low-current, double-null divertor operation (LC) 77
2.2.3 Discharge Cleaning 77
2.2.4 β-l_i Flexibility 77

2.3 Interfacing Systems 82
2.3.1 Nomenclature. 82
2.3.2 External Functional Interfaces 83
2.3.3 External Physical Interfaces 83
2.3.4 Internal Interfaces 84

2.4 Instrumentation & Control (I&C) 84

2.4.1 Quench & Fault Detection (Protection System) 84

3. DESIGN BASIS 85

3.1 Codes and Standards 85

3.2 Analysis 88
3.2.1 Overview 88
3.2.2 Structural Analysis 88
3.2.2.1 Structural Analysis of the Central Solenoid 88
3.2.2.2 Structural Analysis of the Outer Poloidal Field Coils 89
3.2.3 Thermal Analysis 91
3.2.3.1 Nb_3Sn Temperature Margin Calculations. 91
3.2.3.2 PF6&7 Cooldown Stress 92

3.3 R&D Summary and Plans 93

4. DESIGN IMPLEMENTATION 94

4.1 Prototype Coil 94

4.2 Mockup 94

4.3 Component Procurement and Fabrication 94

4.4 PF Assembly, Installation, and Testing 94
4.4.1 Central Solenoid Installation and Removal 94
4.4.2 PF 5 Installation and Removal 94
4.4.3 PF 6 and 7 Installation and Removal 98
4.4.4 Leak Detection 98

5. MAINTENANCE 98

5.1 Failure Modes, Effects, and Criticality Analysis (FMECA) 98

5.2 Scheduled Maintenance Activities 101

5.3 Maintenance Equipment Lists 101

5.4 Remote Maintenance Category I and II Equipment Lists 101

6. REFERENCES 101

6.1 Drawing Tree 101

6.2 Reference Documents **102**

DRAFT

LIST OF FIGURES AND TABLES

FIGURE 1. US DPC AND PF1-7 CONDUCTOR DIMENSIONS (MM). 39
FIGURE 2. CENTRAL SOLENOID COIL LEADS (TYPICAL). 42
FIGURE 3. HELIUM STUB LOCATIONS AND DETAIL. 43
FIGURE 4. COOLANT FLOW SCHEMATIC. 44
FIGURE 5. PF WINDING PACK INSULATION SCHEME. 46
FIGURE 6. WINDING SYSTEM FOR PF COILS. 47
FIGURE 7. APPLICATION OF TURN TO TURN INSULATION AFTER REACTION. 49
FIGURE 8. CLEANING AND TAPING STATION. 50
FIGURE 9. CLEANING AND TAPING STATION WITH PARTIALLY UNCOILED WINDING PACK. 51
FIGURE 10. PF3&4 PRODUCTION VPI MOLD. 52
FIGURE 11. THE LEAD MOLD. 53
FIGURE 12. EXPLODED VIEW OF PART OF THE CS STRUCTURE. 55
FIGURE 13. CENTRAL SOLENOID ASSEMBLY. 56
FIGURE 14. CS ATTACHMENT STRUCTURE. 57
FIGURE 15. ADJUSTIBLE SNUBBER PLATES. 58
FIGURE 16. CS ASSEMBLY, CONDUCTOR, AND HELIUM LEAD DETAIL. 62
FIGURE 17. PF COIL SUPPORT STRUCTURES. 67
FIGURE 18. PF TO TF INTERFACE DETAIL. 68
FIGURE 19. PF5 MOUNTS, PLUMBING, AND LEADS. 69
FIGURE 20. DETAIL OF THE OUTER PF SUPPORT STRUCTURE. 74
FIGURE 21. COIL CURRENTS VS. TIME. 76
FIGURE 22. PF COIL VOLTAGES AND CURRENTS AT CRITICAL TIME POINTS DURING A 12-V PLASMA INITIATION SCENARIO. 81
FIGURE 23. THE PF MAGNET SYSTEM AND ITS ENVIRONMENT. 83
FIGURE 24. CENTRAL SOLENOID INSTALLATION AND REMOVAL.. 96

TABLE 1. PF MAGNET SYSTEM OPERATING TEMPERATURE CURRENT CENTER LOCATIONS. 13
TABLE 2. PF MAGNET SYSTEM DIMENSIONS. 17
TABLE 3. PEAK CONTROL CURRENTS, IN KA. 18
TABLE 4. PF COIL CURRENTS, IN KA, AT CRITICAL POINTS IN THE HC SCENARIO. 19
TABLE 5. PF COIL CURRENTS, IN KA, AT CRITICAL POINTS IN THE LC SCENARIO. 19
TABLE 6. PF COIL CURRENTS, IN KA, AT Q=3 DOUBLE NULL CORNER POINTS. 20
TABLE 7. PF COIL CURRENTS, IN KA, AT Q=3 SINGLE NULL CORNER POINTS. 22
TABLE 8. PF COIL CURRENTS, IN KA, AT Q=5 DOUBLE NULL CORNER POINTS. 23
TABLE 9. PF COIL CURRENTS, IN KA, FOR 1 MA DISCHARGE CLEANING. 24
TABLE 10. WORST CASE FORCES ON CENTRAL SOLENOID WINDING PACKS. 25
TABLE 11. WORST CASE FORCES ON PF5 WINDING PACKS. 26
TABLE 12. WORST CASE FORCES ON PF6&7 WINDING PACKS. 27
TABLE 13. CHANGE IN PF COIL CURRENTS, IN KA, DURING A VERTICAL DISRUPTION. 29
TABLE 14. PF SYSTEM COIL DIMENSIONS AT ROOM TEMPERATURE. 35
TABLE 15. PF COIL HYDRAULIC CIRCUIT DESCRIPTION. 36
TABLE 16. CS CONDUCTOR DATA. 37
TABLE 17. CS CONDUCTOR PERFORMANCE. 39
TABLE 18. HEAT TREAT REACTION SCHEDULE. 45
TABLE 19. PHYSICAL AND MECHANICAL PROPERTIES OF INCOLOY 908 AND 316 LN. 59

TABLE 20. MECHANICAL PROPERTIES OF POLYIMIDE. 59
TABLE 21. PF5 CONDUCTOR PERFORMANCE. 64
TABLE 22. PF6&7 CONDUCTOR DIMENSIONS 70
TABLE 23. PF6&7 CONDUCTOR PERFORMANCE SPECIFICATIONS. 70
TABLE 24. HC SCENARIO EVOLUTION. 75
TABLE 25. PEAK CURRENTS IN THE PF COILS DURING THE HC SCENARIO. 75
TABLE 26. LC SCENARIO EVOLUTION. 77
TABLE 27. FLEXIBILITY SPACE PARAMETERS. 77
TABLE 28. START-UP SPECIFICATIONS. 78
TABLE 29. PF COIL VOLTAGES AND CURRENTS AT CRITICAL POINTS DURING A 12-V PLASMA INITIATION. 79
TABLE 30. STANDARDS ASSOCIATED WITH THE CONSTRUCTION OF THE PF MAGNET SYSTEM HARDWARE. 85
TABLE 31. STRUCTURAL ANALYSES. 88
TABLE 32. SUMMARY OF PF6 MAX HOOP AND MAX SHEAR STRESSES. 90
TABLE 33. SUMMARY OF PF6 MAX BENDING STRESSES. 90
TABLE 34. SUMMARY OF PF7 MAX HOOP AND MAX SHEAR STRESSES. 91
TABLE 35. SUMMARY OF PF7 MAX BENDING STRESSES. 91
TABLE 36. MANUFACTURING R&D REPORTS. 93
TABLE 37. ITEM FAILURE MODES WITH SEVERITY CATEGORY II EFFECTS. 99

This document is an update of the CDR SDD for the PF Magnet System. It retains the structure of the CDR SDD, and incorporates elements of the PF Magnet System Specification. It is meant, not to be a definitive description of the PF Magnet System, but rather, to be a roadmap describing the Preliminary Design. The documents that provide a definitive description of the PF Magnet System Preliminary Design are referenced.

1. FUNCTION & DESIGN REQUIREMENTS

The PF Magnet System Specification, TPX-SPEC-14-0001, Rev. 0[1], defines the PF Magnet System, including the TPX environment in which the magnet system operates and the interfaces between the magnet system and its environment, the functional and physical characteristics of the PF Magnet System, its design and construction, required documentation, logistics, personnel and training, major component characteristics, and quality assurance provisions. The paragraphs in sections 1.2-1.4 are excerpts from the PF Magnet System Specification.

1.1 Functions

The Poloidal Field (PF) Magnet System provides the following essential functions:

- Poloidal fields and flux changes necessary for plasma shaping and positioning, and discharge evolution.
- Compensation for radial and vertical fields from the turn interconnecting the 16 TF Magnet System coils.

1.2 Configuration Requirements & Essential Features

1.2.1 PF Configuration Requirements

1.2.1.1 Configuration

1.2.1.1.1 TPX reference coordinate system.

1.2.1.1.1.1 Right-handed system.

The coordinate system shall be a right-handed coordinate system. z-axis location

The z-axis is vertical, passing through the center of the pedestal at the 102' elevation in the TFTR test cell. The direction of increasing z-values is up.

1.2.1.1.1.3 Origin.

The origin shall be a monument, permanently located on the floor of the TFTR test cell at the 100' elevation.

1.2.1.1.1.4 y-axis orientation.

The y-axis shall be perpendicular to the north wall of the TFTR test cell..

1.2.1.1.1.5 Toroidal angle origin.

The toroidal angle, ϕ, shall have its origin (i.e, $\phi = 0°$) 13.5° counterclockwise from the y-axis..

1.2.1.1.2 Reference data.

1.2.1.1.2.1 TPX Centerline.

The coil radial locations shall be referenced from the TPX centerline.

1.2.1.1.2.2 TPX Midplane location.

The TPX midplane shall be a horizontal plane a vertical distance, z = (TBD)-m, from the 100' elevation at operating temperature.TPX Midplane.

The coil vertical locations shall be referenced from the TPX midplane.

1.2.1.1.3 Number of coils.

There shall be 14 solenoidal-wound coils, arranged symmetrically about the TPX midplane at operating temperature, in 7 coil pairs known as PF1 through PF7.

1.2.1.1.4 Central solenoid.

There shall be four coil pairs, PF1-4, together with a constraining structure in an assembly referred to as the central solenoid.

1.2.1.1.5 Ring coils.

There shall be three additional coil pairs, PF5-7, and referred to as the ring coils.

1.2.1.1.6 PF6&7 Coil Cases.

The PF6 and PF7 coils shall be placed in 0.016-m (5/8") thick cases.

1.2.1.2 Physical Characteristics

1.2.1.2.1 Size and Location

1.2.1.2.1.1 Room temperature envelopes.

1.2.1.2.1.1.1 CS envelope.

Upon installation, the CS shall fit into the envelope shown in TPX-ICDP-1314.

1.2.1.2.1.1.2 Ring coil envelopes.

Upon installation, the ring coils (including cases, if applicable) shall fit into the envelope shown in TPX-ICDP-1314.

1.2.1.2.1.1.3 Location of coil leads.

The coil leads shall fit into the envelope shown in TPX Drawing TBD.

1.2.1.2.1.2 Current center locations and envelope at operating temperature.

1.2.1.2.1.2.1 Current center definition.

The *current center* of a coil is the location of a fictitious filament that would produce the same magnetic field in the far-field region as the coil if it carried the same equivalent current as the coil.

1.2.1.2.1.2.2 Equivalent current definition.

The equivalent current is the current conducted by each turn multiplied by the number of turns in the coil.

1.2.1.2.1.2.3 Current center locations.

The central solenoid coils and ring coils shall be designed such that the current centers of each coil at operating temperature are located as shown in Table 1.

Table 1. PF Magnet System Operating Temperature Current Center Locations.

Coil	R_c (meters)	Z_c (meters)	Tilt	Offset of Mean Center	Offset of Mean Elevation
PF1	0.810	±0.251	TBD	TBD	TBD
PF2	0.810	±0.706	TBD	TBD	TBD
PF3	0.810	±1.042	TBD	TBD	TBD
PF4	0.810	±1.306	TBD	TBD	TBD
PF5	1.213	±2.350	TBD	TBD	TBD
PF6	3.758	±2.144	TBD	TBD	TBD
PF7	4.297	±1.114	TBD	TBD	TBD

1.2.1.2.2 Support Interfaces

1.2.1.2.2.1 PF Magnet System vertical loads.

The PF Magnet System shall be supported at interfaces with the TF Magnet System for gravity and net vertical loads in accordance with the configuration and load limits of TPX-ICDP-1314.

1.2.1.2.2.2 PF Magnet System radial and bending loads.

The PF Magnet System interfaces with the TF Magnet System shall be designed to permit differential radial and bending motion of the two interfacing systems in accordance with the configuration and load limits of TPX-ICDP-1314.

1.2.1.2.3 Power supply connections.

All PF coil leads shall be connected to superconducting busses and brought out of the cryostat.

1.2.1.2.3.1 Interface to power supplies.

The interface to the power supplies shall be at the room temperature terminal of the vapor cooled leads in accordance with the configuration and load limits of TPX-ICDP-1443.

1.2.1.2.3.1.1 PF1 Coils in series.

Initially, PF1 shall have its upper and lower coils connected electrically so the same current flows through each coil at any time.

1.2.1.2.3.1.2 PF2, PF7 Coils in series.

The same connection topology used for PF1 shall apply to the PF2 and the PF7 upper and lower coils.

1.2.1.2.3.1.3 PF3 Coils independently powered.

Initially, PF3 shall have its upper and lower coils connected electrically to independent power supplies, so different currents can flow through each coil at any time.

1.2.1.2.3.1.4 PF4, PF5, PF6 Coils independently powered.

The same connection topology used for PF3 shall apply to the PF4, PF5, and PF6 upper and lower coils.

1.2.1.2.4 Cryogenic system connections

1.2.1.2.4.1 Interface to Cryogenic Systems.

The PF Magnet System shall interface with the Cryogenic Systems in accordance with the configuration and load limits of TPX-ICDP-1472.

1.2.1.2.4.2 Cooling power.

The Cryogenic System shall provide cooling power to the magnets and to the superconducting leads and busses in accordance with the configuration and load limits of TPX-ICDP-1472.

1.2.1.2.4.3 Heat load limitations.

The PF Magnet System shall be designed to operate within the heat load limitations of TPX-ICDP-1472.

1.2.1.2.5 Control Systems connections.

1.2.1.2.5.1 Interfaces.

The Local I&C shall interface with the following control systems:

1.2.1.2.5.1.1 Power Systems Control Systems.

The interface shall be developed in accordance with the configuration and load limits of TPX-ICDP-1446.

1.2.1.2.5.1.2 Plasma diagnostics.

The interface shall be developed in accordance with the configuration and load limits of TPX-ICDP-1462.

1.2.1.2.5.2 Plasma performance.

The plasma diagnostics shall provide plasma performance data to the local I&C in accordance with the configuration and load limits of TPX-ICDP-1462.

1.2.1.2.5.3 Machine protection.

The Local I&C shall provide a "fail-safe" magnet dump command to the power systems control system according to TPX-ICDP-1446.

1.2.2 Electrical Isolation and Grounding

1.2.2.1 Modified Star Ground Topology.

The "modified star" grounding topology shall be used in connecting the elements of the PF Magnet System.

1.2.2.1.1 Star ground definition.

In a "star" grounding topology, the ground connections radiate from a central ground point with no other connections between them.

1.2.2.1.2 Modified star grounding definition.

In a "modified star" grounding topology, the connections radiating from the single point ground may terminate in another "star."

1.2.2.2 Ground Plane.

1.2.2.2.1 Two element ground plane.

A two-element conducting ground plane shall surround each PF coil's insulated winding pack.

1.2.2.2.2 Single point ground connection.

One end of each element shall be connected to the cryostat single point ground extension in accordance with TPX-ICDP-1447..

1.2.2.2.3 Open end insulation.

The other end of each element shall be insulated from that of the second element to prevent current from flowing from one into the other.

1.2.2.2.4 Confinement of electric fields.

The elements shall arranged together to confine the electric field from the winding pack conductors to the volume between the conductors and the ground plane elements.

1.2.2.3 CS structure grounding.

Each segment of the CS structure shall be grounded to a different CS coil ground plane element.

1.2.2.4 CS structure segment isolation.

Each segment of the CS structure shall be capable of being electrically isolated from other segments.

1.2.2.5 Local I&C grounding.

The Local I&C ground shall be electrically isolated and independently connected to the *external* single point ground in accordance with TPX-ICDP-1447.

1.2.2.6 Isolation.

Each leg of the modified star grounding scheme shall be capable of isolation from the single point ground cryostat extension terminal to verify minimum stand-off voltage requirements.

1.2.2.7 Standoff.

Each leg of the modified star grounding scheme shall be able to withstand a 1 kV hipot test with the voltage applied between the isolated leg and the cryostat single point ground in accordance with the test procedure, TPX-PROC-14-TBD.

1.2.2.8 Ground currents.

All ground plane elements shall be capable of supporting currents induced by the changing PF magnetic fields and plasma without sustaining material or structural damage.

All ground plane elements shall be capable of supporting fault currents, TBD, without sustaining material or structural damage.

1.2.3 Material Selection Criteria

1.2.3.1 Materials Selection

1.2.3.1.1 Permeability.

All materials to be used in the PF Magnet System shall have a magnetic permeability of less than 1.02, unless otherwise authorized by the Project.

1.2.3.1.2 Project authorization of Incoloy-908.

The Project shall authorize the use of the CICC Incoloy 908 sheath material.

1.2.3.1.3 Activation.

Materials to be used in the PF Magnet System shall be such that none of the waste packages projected in the D&D plan to be generated during the end of the life disposal of TPX (including a small amount of mixed waste) shall exceed Class A low-level waste limits as defined in existing 10CFR61 regulations.

1.2.3.1.4 Materials database.

Only materials appearing in the Structural and Cryogenic Design Criteria Appendix I, TPX Materials Database shall be used in the construction of PF Magnet System components.

1.2.4 Essential Features

The topology of the TPX poloidal field system is the same as that of the ITER CDA[2]. The Central Solenoid (CS) is made of independently powered coils and independently powered *pairs* of coils and is supported by the TF coil structure. The Central Solenoid axial structure is on both the inside and outside of the coils and prevents axial tension anywhere in the interpancake insulation by the application of mechanical precompression to the stack. The CS to TF connection utilizes eight flex-mounts to permit differential radial motion of the two coil systems. PF5-7 are clamped to the TF cases through slip mounts with leaf springs to permit relative radial motion and coil centering. The major design features of the PF system are listed in Table 2.

Table 2. PF Magnet System Dimensions.

Parameter	Units	Value
Number of Coils		14
Maximum Current	(kA)	27.3
Stored Energy	(MJ)	123
Coil Mass	(tonnes)	52.6
Conductor Length	(km)	15.6
Peak Field	(T)	5.9
Volt-Second$_{swing}$	(Wb)	19.1

1.3 Performance & Operational Requirements

1.3.1 Plasma Shaping Requirements

Plasma shaping requirements over the full range of flexibility (per GRD Section 1.2) in steady state operation are covered in 1.3.3.3.

1.3.2 Plasma Positioning Requirements

1.3.2.1 Control Interfaces.

The Local I&C shall provide control information to the Control Systems in accordance with TPX-ICDP-1446.

The Local I&C shall receive information from Plasma Diagnostics in accordance with TPX-ICDP-1462.

1.3.2.2 Slow feedback functions.

The PF Magnet System will provide specified feedback control functions to relieve the internal control, IC, coils on slow time scales. There are three functions the PF coils shall perform:

1.3.2.2.1 Vertical positioning.

Vertically position the plasma within ±3 cm of the midplane and maintain it within ±1 cm of its nominal position with a 5 second response time using the PFcoils.

1.3.2.2.2 Strikepoint positioning.

Position the location of the outboard strikepoint within ±5 cm of the nominal location, and maintain it within ±1 cm with a 5 second response time using the PF coils.

1.3.2.2.3 Radial control.

Position the radial location of the separatrix at the outboard midplane within ±2 cm of the nominal location, and maintain it within ±1 cm with a 5 second response time using the PF coils.

1.3.2.3 Slow feedback currents.

The slow timescale plasma position control shall change the operating currents by no more than shown in Table 3, TBD.

Table 3. Peak Control Currents, in kA.

PF Coils	Vertical +3cm	Strikept +5cm	Radial +2cm	TF Comp
PF5U	1.17	TBD		
PF5L	-1.85	TBD		
PF6U	0.41	TBD		-0.23
PF6L	-0.75	TBD		0.02
PF7U			0.21	
PF7L			0.21	

1.3.3 Plasma Discharge Evolution Requirements

1.3.3.1 HC Scenario operating currents.

The PF Magnet System shall be capable of supporting the combinations of currents shown in

Table 4for the HC reference scenario. The time it takes to achieve the stage shown at the top of each column is given in the bottom row.

Table 4. PF Coil Currents, in kA, at Critical Points in the HC Scenario.

	12-v Startup		HC Scenario		RampDn	
PF coils	Pre-Blip	Blip	SOF	SOB	EOB	EOF
PF1	7.79	3.67	-24.61	-19.54	-21.64	-21.08
PF2	24.14	17.84	-7.07	-6.61	-11.24	-13.36
PF3	24.13	23.88	1.92	0.67	-3.10	-5.58
PF4	23.43	24.40	5.32	3.57	-0.13	-0.53
PF5	21.64	16.57	26.16	24.10	19.26	9.45
PF6	1.20	1.03	-14.16	-8.68	-9.05	-10.58
PF7	1.43	0.56	-2.40	-10.77	-10.88	-1.90
Δt	4s	185ms	4s	1s	9s	4s

1.3.3.2 LC Scenario operating currents.

The PF Magnet System shall be capable of supporting the combinations of currents shown in Table 5 for the LC reference scenario.

Table 5. PF Coil Currents, in kA, at Critical Points in the LC Scenario.

	12-v Startup		LC Scenario		RampDn	
PF coils	Pre-Blip	Blip	SOF	SOB	EOB	EOF
PF1	7.79	3.67	-0.50	3.14	-21.64	-21.08
PF2	24.14	17.84	8.11	3.88	-11.24	-13.36
PF3	24.13	23.88	13.60	11.65	-3.10	-5.58
PF4	23.43	24.40	17.15	16.90	-0.13	-0.53
PF5	21.64	16.57	12.87	13.64	19.26	9.45
PF6	1.20	1.03	2.18	1.58	-9.05	-10.58
PF7	1.43	0.56	-4.11	-4.43	-10.88	-1.90
Δt	4s	185ms	2s	1s	30s	4s

1.3.3.3 Steady state operation.

The PF coils shall be designed such that any combination of PF coil currents appearing between SOF and EOB for the HC and LC reference scenarios can be run steady state.

1.3.3.4 Flexibility scenarios.

1.3.3.4.1 q=3, Double Null operating currents.

The PF Magnet System shall be capable of supporting the combinations of currents shown in Table 6 for steady state operation at the corners of the q=3 Double Null flexibility space.

Table 6. PF Coil Currents, in kA, at q=3 Double Null Corner Points.

PF coils	(l, β) (0.4, 5.0)	(0.5, 2.2)	(0.7, 0.0)	(1.2, 0.0)	(1.2, 5.0)
PF1	-12.00	-19.32	-25.23	-25.13	-19.15
PF2	-24.22	-20.68	-6.89	4.88	-2.97
PF3	-16.80	-11.78	2.27	12.03	5.50
PF4	-12.97	-7.98	5.70	14.28	5.73
PF5	26.54	23.77	26.31	24.13	22.77
PF6	-19.57	-19.08	-14.65	-4.32	-5.76
PF7	-3.21	-0.68	-1.75	-11.01	-15.10
Plasma	2000	2000	2000	2000	1932

1.3.3.4.2 Single null operation.

PF coils shall be capable of single null operation where the active null may be above or below the midplane. [GRD 1.2.2]

1.3.3.4.2.1 q=3, Single Null Below the Midplane operating currents.

The PF Magnet System shall be capable of supporting the combinations of currents shown in Table 7 for steady state operation at the corners of the q=3 Single Null flexibility space.

Table 7. PF Coil Currents, in kA, at q=3 Single Null Corner Points.

PF coils	(l_i, β) (0.4, 5.0)	(0.5, 2.2)	(0.7, 0.0)	(1.2, 0.0)	(1.2, 5.0)
PF1U	-12.44	-20.76	-24.98	-21.04	-15.05
PF1L	-12.44	-20.76	-24.98	-21.04	-15.05
PF2U	-24.88	-19.27	-7.82	-2.52	-2.29
PF2L	-24.88	-19.27	-7.82	-2.52	-2.29
PF3U	-10.90	-4.62	5.17	2.37	3.27
PF3L	-16.48	-12.10	-2.97	6.25	2.03
PF4U	-2.95	-.57	7.28	4.83	4.52
PF4L	-13.75	-8.43	1.15	8.37	4.30
PF5U	14.37	11.78	14.78	16.82	10.89
PF5L	27.40	25.27	26.66	20.43	21.95
PF6U	-15.88	-15.74	-12.26	-0.75	-0.88
PF6L	-19.52	-19.50	-15.62	-4.98	-4.93
PF7U	-4.27	-1.48	-2.01	-11.14	-15.06
PF7L	-4.27	-1.48	-2.01	-11.14	-15.06
Plasma	2000	2000	2000	2000	1932

1.3.3.4.2.2 q=3, Single Null Above the Midplane operating currents.

Table 7 shows the currents when the active null is below the midplane. If the upper and lower coil currents are interchanged, the active null will be above the midplane.

The PF Magnet System shall be capable of supporting the combinations of currents with the active null above the midplane for steady state operation.

1.3.3.4.2.3 q=5, Double Null operating currents.

The PF Magnet System shall be capable of supporting the combinations of currents shown in Table 8 for steady state operation at the corners of the q=5 Double Null flexibility space:

Table 8. PF Coil Currents, in kA, at q=5 Double Null Corner Points.

PF coils	(l_i, β) (0.4, 7.0)	(0.4, 5.0)	(0.7, 0.0)	(1.5, 0.0)	(1.5, 7.0)
PF1	-7.47	-8.73	-16.89	-14.59	-3.56
PF2	-21.83	-20.61	-5.23	6.96	4.97
PF3	-15.97	-14.73	0.90	10.50	5.98
PF4	-12.63	-11.58	3.17	11.45	6.97
PF5	21.93	20.70	16.51	13.78	21.86
PF6	-14.93	-15.46	-9.68	0.84	0.13
PF7	-7.24	-4.00	-1.17	-9.26	-14.88
Plasma	1.707	1.588	1.266	1.096	1.137

1.3.3.5 Transient currents.

The PF Magnet System shall be capable of supporting other currents, transients caused by plasma disruptions, faults, and by the control functions, in addition to those included in the tables, Table 3 - Table 8, above. The peak currents for these conditions are listed in paragraphs 1.3.6.3 and 1.3.2.3.

1.3.3.6 Discharge cleaning

1.3.3.6.1 1-MA Inductive Discharge Startup.

The PF Magnet System shall be capable of initiating a 1-MA inductive discharge scenario, as shown in Table 9, initiated with the 20-volt startup.

Table 9. PF Coil Currents, in kA, for 1 MA Discharge Cleaning.

PF coils	20v Startup Pre-Blip	Blip	Heating	RampDn
PF1	7.57	3.34	TBD	TBD
PF2	22.80	12.84	(a)	(a)
PF3	24.50	20.77	(a)	(a)
PF4	24.11	23.74	(a)	(a)
PF5	20.85	12.84	(a)	(a)
PF6	1.02	.59	(a)	(a)
PF7	1.99	.40	(a)	(a)
Δt	(4)s	178ms	(a)	(a)

1.3.3.7 Endure worst case forces

The PF Magnet System components shall be designed to endure the worst case forces shown in Table 10-Table 12, respectively.

Table 10. Worst Case Forces on Central Solenoid Winding Packs.

Condition / location	*Force Component*	*Peak Force Component Magnitude*
Normal operating conditions; - force acting to increase hoop tension	Radial loading	45.6 kN/turn
Fault operating conditions; - force acting to increase hoop tension	Radial loading	97.0 kN/turn
Normal operating conditions - force acting to compress coil	Net Compressive loading	32.4 MN
Normal operating conditions - max radial differential loading between coils	Shear	TBD

Table 11. Worst Case Forces on PF5 Winding Packs.

Condition	Force Component	Peak Force Component Magnitude
Normal operating	Radial loading	3.51 MN
Fault operating condition	Radial loading	3.84 MN
Normal operating	Vertical centering (toward midplane) load	6.32 MN
Disruption	Vertical launching (away from midplane)load	7.23 MN
[Normal | disruption |fault] operation at mount locations	Bending stresses	TBD

Table 12. Worst Case Forces on PF6&7 Winding Packs.

Condition / location	Force Component	Peak Force Component Magnitude
Normal operating / PF6	Radial loading	TBD
Fault operating condition / PF6	Radial loading	3.54 MN
Disruption / PF6	Vertical centering (toward midplane) load	8.21 MN
Disruption + Fault / PF7	Radial loading	1.25 MN
Disruption + Fault / PF7	Vertical centering (toward midplane)load	3.58 MN
Disruption + Fault / PF7	Vertical launching(away from midplane)load	3.25 MN
[Normal | disruption |fault] operation at mount locations	Bending stresses	TBD

1.3.4 Toroidal Field/Plasma Directionality

1.3.4.1 Four quadrant operation.

PF coils shall be designed for four quadrant operation, [GRD 1.2.3]

1.3.4.1.1 Quadrant definition.

The axes that divide the operating space into four quadrants are the plasma current density direction and the toroidal field direction. A positive plasma current density is defined in the direction of a plasma current circulating counterclockwise, and a positive toroidal field is defined as a toroidal field pointing in the same direction as a positive plasma current density.

1.3.4.1.2 First quadrant.

In first quadrant operation, the plasma current density and the TF field are positive. The PF magnet system current direction is positive. The currents listed tables, Table 3 - Table 9, define the positive PF magnet system current direction.

1.3.4.1.3 Second quadrant.

In second quadrant operation, the plasma current density is negative and the TF field is positive. The PF magnet system current direction is negative, i.e., all the currents in the positive PF magnet system current direction are multiplied by -1.

1.3.4.1.4 Third quadrant.

In third quadrant operation, the plasma current density and the TF field are negative. The PF magnet system current direction is negative.

1.3.4.1.5 Fourth quadrant.

In fourth quadrant operation, the plasma current density is positive and the TF field is negative. The PF magnet system current direction is positive.

1.3.4.1.6 Initial configuration.

The initial configuration of the tokamak shall be the fourth quadrant.

1.3.5 Field Compensation

1.3.5.1 TF interconnect compensation.

PF5U and PF6U shall be operated such that the radial and vertical fields due to the TF interconnecting turn are zero when averaged over a loop at R=2.25m at the tokamak midplane.

1.3.6 PF Disruption Handling

The PF Magnet System shall be designed to endure a disruption without sustaining structural or material damage.

1.3.6.1 Frequency of disruptions.

Plasma disruptions are normal events, and they shall be expected to occur, in any phase or mode of operation, at a shot frequency of 50%.

1.3.6.2 Disruption scenarios.

The PF Magnet System shall be designed to operate during the disruption scenarios without quenching.

1.3.6.2.1 Common Disruption.

The PF Magnet System shall endure the Common Disruption scenario, expected at a frequency of 49% in any phase or mode of operation.

1.3.6.2.2 Rare Disruption

The PF Magnet System shall endure the Rare Disruption scenario, expected at a frequency of 1% in any phase or mode of operation

1.3.6.3 Currents induced by disruption.

The maximum change in coil currents due to disruption shall be no greater than those shown in Table 13

Table 13. Change in PF Coil Currents, in kA, during a Vertical Disruption.

PF Coils	$\Delta I_{(max)}$ kA	$-\Delta I_{(max)}$ kA
PF1U	2.94	0
PF1L	3.02	0
PF2U	2.18	-0.04
PF2L	2.31	0
PF3U	0.88	-0.79
PF3L	1.00	-0.11
PF4U	1.35	-0.93
PF4L	1.52	0
PF5U	0.26	-0.79
PF5L	0.44	-0.19
PF6U	0.55	-0.16
PF6L	0.68	0
PF7U	2.46	0
PF7L	2.52	0

1.3.7 PF Magnet Quenches

1.3.7.1 Quench frequency.

Each PF coil shall endure up to 50 quenches over the lifetime of the system.

Quenches shall be considered off-normal events

1.3.7.2 Endurance criteria.

In the event of a quench in the PF or TF Magnet systems, the PF coils shall meet the following requirements:

1.3.7.2.1 Maximum voltage.

The PF coils shall be designed to withstand a terminal to terminal voltage no greater than 15kV and a terminal to ground voltage no greater than ±7.5kV

1.3.7.2.2 Maximum temperature.

The maximum hot-spot temperature in any coil after it quenches shall be 150K.

1.3.7.2.3 Secondary quenches.

The PF Magnet system shall not quench as a result of dumping the energy stored in the PF magnet system into the Power Systems dump resistors [see TPX SRD for Power Systems, Rev. I].

1.3.7.2.4 Quench detection time.

The Local I&C system shall be capable of detecting a quench in any section of any coil in a time sufficient to initiate a quench dump as described in TPX-ICDP-1446.

1.3.7.2.5 Redundant quench detection.

Each coil in the PF Magnet System shall have at least two independent methods to detect a quench.

1.3.8 Operational Requirements

1.3.8.1 Operate in a vacuum environment

1.3.8.1.1 Compatibility.

The PF Magnet System shall be compatible with the vacuum environment as defined in TPX-ICDP-1415.

1.3.8.1.2 Operating pressure.

The PF Magnet System will operate at a vacuum pressure no greater than 0.1 Pa.

1.3.8.2 Cool to operating temperature

1.3.8.2.1 Operating temperature.

The operating temperature of the PF Magnet System shall be no greater than 5K.

1.3.8.2.2 Endurance during cooldown.

The PF Magnet System shall withstand the cool down cycle without suffering structural or material damage. Endurance during re-cooling.

The PF Magnet System shall withstand a re-cooling cycle following a coil quench without suffering structural or material damage. Cooldown Time.

1.3.8.2.4.1 Cooldown from room temperature.

All elements of the PF Magnet System shall cool from room temperature to operating temperature within 120 hours.

1.3.8.2.4.2 Re-cooling after quench.

The time to re-cool the PF Magnet System following a quench shall not exceed 12 hours.

1.3.8.2.4.3 Re-cooling after conditioning plasma chamber.

The time to re-cool the PF Magnet System following plasma chamber conditioning shall not exceed (24) hours.

1.3.8.2.5 Initiating current flow.

The PF Magnet System shall reach operating temperature before initiating current flow in excess of 10 A.

1.3.8.3 Warm to room temperature

1.3.8.3.1 Endurance.

The PF Magnet System shall withstand a warm up cycle without sustaining structural or material damage.

1.3.8.3.2 Warm-up time.

The PF Magnet System shall warm from operating temperature to room temperature in no more than 5 days. [A-Spec 3.2.1.2.b

1.3.8.3.3 Current assisted warm-up.

Currents used to reduce the warm-up time of any PF coil shall be limited to those developing an IR drop of less than 100 volts across the coil.

1.3.8.3.4 Exposure to ambient.

Only air with a dew point temperature higher than the lowest temperature in the PF Magnet System will be introduced into the cryostat.

1.3.8.3.5 Cool-down and Warm-up Time

PF coils shall be capable of being cooled down from room temperature to operating temperature in 10 days.

PF coils shall be capable of being warmed up from operating temperature to room temperature in 5 days.

PF coils shall be capable of being cooled down to operating temperature following a coil quench in 12 hours.\

1.3.8.4 Lifetime Operating Limits

Operating limits are defined in 1.4.

1.4 RAM Requirements

1.4.1 Reliability and Availability

1.4.1.1 PF Magnet System reliability

1.4.1.1.1 Mission reliability.

Provisions shall be made to recover from *every* failure mode which:

- has a reasonable probability of occurrence (P ≥ 10-4) over the life of the system, or
- has a low probability of occurrence (10-4 > P ≥ 10-6) over the life of the device, is not exempt from the Project based on cost-risk-benefit considerations (as defined by whom?), and would directly or indirectly compromise the required operational capability of the device and facility.

1.4.1.1.2 Shot reliability.

The shot reliability shall be greater than 0.9951, where shot reliability is defined as the probability of not experiencing a failure that would prevent taking another shot.

1.4.1.1.3 Limits on reliability assessment.

The reliability requirements apply prior to injecting tritium into the Tokamak.

1.4.1.1.4 Service Life

The service life of the PF Magnet System shall be 10 years.

1.4.1.1.5 Cycle Life

1.4.1.1.5.1 Cool-down / warm-up.

The PF Magnet System shall support 300 cool-down / warm-up cycles between room temperature and operating temperature.

1.4.1.1.5.2 Lifetime number of shots.

The PF Magnet System shall support up to 30,000 pulses subject to the following conditions

1.4.1.1.5.2.1 Reference scenarios.

It shall be operated per the reference scenarios.

1.4.1.1.5.2.2 Flexibility.

It shall be operated within the full range of flexibility.

1.4.1.1.5.3 Annual number of shots.

The PF Magnet System shall support up to 3000 pulses in any year subject to the following conditions

1.4.1.1.5.3.1 Reference scenarios.

It shall be operated per the reference scenarios.

1.4.1.1.5.3.2 Flexibility.

It shall be operated within the full range of flexibility.

1.4.1.1.5.4 1000-s pulse duty cycle.

The PF Magnet System shall support the 1000-s pulse duty cycle: 10 consecutive 1000-s pulses at 75 minute intervals in any 24 hour period when operated per the HC, LC and steady state reference scenarios.

1.4.1.1.5.5 100-s pulse duty cycle.

The PF Magnet System shall support the 100-s pulse duty cycle: 30 consecutive 100-s pulses at 20 minute intervals in any 24 hour period when operated per the HC, LC and steady state reference scenarios.

1.4.1.1.5.6 1-s pulse duty cycle.

After upgrading the TPX facility for DT operation, the PF Magnet System shall support TBD consecutive 1-s DT pulses at TBD intervals in a TBD period.

1.4.1.1.6 Operating Life

1.4.1.1.6.1 Lifetime operations.

The PF Magnet System shall support 5×10^6 seconds of operation of which 2×10^6 seconds will be D operation.

1.4.1.1.6.2 Annual operations.

The PF Magnet System shall support 5×10^5 seconds of operation in any year of which 2×10^5 seconds will be D operation.

1.4.1.2 Availability

1.4.1.2.1 Definition of PF Magnet System Availability.

PF Magnet System Availability is defined as the ratio of the number of shots in an operational run period in which the PF Magnet System is operational at its rated performance level to the number of shots which could be achieved during that run period in the absence of PF Magnet System component failures and software errors

1.4.1.2.2 PF Magnet System Availability.

The PF Magnet System shall achieve an operational availability of at least 0.965 when operated per the reference scenarios.

1.4.1.2.3 Limits on availability assessment.

The availability requirements apply prior to injecting tritium into the Tokamak.

1.4.2 Maintainability

1.4.2.1 Maintainability features.

The PF Magnet System shall incorporate maintainability features which are consistent with achieving the mission reliability, operational availability, and scheduled maintenance requirements.

1.4.2.2 Remote maintenance.

There shall be no remote maintenance performed on elements of the PF Magnet System.

1.4.2.3 Accessibility.

1.4.2.3.1 Hands on maintenance during first two years of operation.

The PF Magnet System design shall accommodate hands-on maintenance within two weeks of shutdown during the first two years of operation.

1.4.2.3.2 Coil Removal.

The central solenoid assembly, PF5U, PF6U, PF7U, and PF7L shall be capable of being removed and replaced from overhead without requiring the disassembly of TF Magnet System components.

1.4.2.3.3 CS Disassembly.

The central solenoid assembly, PF5U, PF6U, PF7U, and PF7L shall be capable of being disassembled and reassembled following a one year shutdown during which activated in-vessel components which would otherwise preclude access inside the vacuum vessel, would be remotely removed.

1.4.2.4 Limits to maintainability.

Maintainability requirements only apply prior to tritium being injected into the tokamak.

2. PF COIL DESIGN DESCRIPTION

2.1 System Design Description Overview

The TPX poloidal field system design resembles that of the ITER CDA. The PF Magnet System consists of the Central Solenoid and the Ring Coil magnets. The Central Solenoid (CS) is made of 4 pairs of Nb_3Sn coils and is supported from the TF coil structure. The CS mounts allow radial motion to account for the differential contraction (expansion) as the CS and TF structure cool (warm up). The mounts also center the CS assembly. The CS axial structure prevents axial tension anywhere in the interpancake insulation by the application of mechanical precompression to the stack. The ring coil, PF5, made of Nb_3Sn, is mounted to the TF structure in a manner to permit relative radial motion and coil centering. The PF6&7 coils, made of NbTi, are enclosed in cases are also mounted to the TF structure in a manner to permit relative radial motion and coil centering.

A jointless solenoid design is used for the Nb_3Sn coils, and hydraulic connections are avoided on the outer circumference of the CS coils to avoid a large gap between the CS and the TF structure. Joints between pancakes and helium connections on the outside of the CS would reduce the coil diameters, increase the likelihood of quenching, and would impose other design requirements. Each Nb_3Sn coil is continuously pancake wound without interpancake joints.

Specially designed tooling will be used to wind the pancakes radially inward and outward. The leads from the coils are extensions of the conductor, and they extend to terminations located in a service area below the CS. The vertical and radial size of the hydraulic lines and manifolds permit vertical removal of the central solenoid, while satisfying the crane height restrictions of the TFTR test cell. Hydraulic inlet and outlet connections follow the US-DPC concept at alternating pancakes on the inside radius of each module. Each hydraulic line is connected through an electric isolator, similar to those proposed for the NET CS Model Coil[3], to a manifold located below the CS assembly. The cooling flow rate is such that helium can move from the inlet to the outlet of a channel in less than one operating cycle.

All PF conductors use cable-in-conduit superconductors with cooling by forced-flow supercritical helium. The PF1-5 coils use a conductor similar to that of the US-DPC[4], including a thin 316LN tape wrapped around the cable, but with an improved Nb_3Sn strand. The PF1-5 coils use a the thick outer Incoloy 908 conduit of the US-DPC and a larger, 360 strand, cable of modified US-DPC Nb_3Sn conductor. Incoloy is chosen for the conduit material for two main reasons. First, the contraction properties of Incoloy 908 from the reaction temperature of 700 °C are very close to those of the Nb_3Sn, which minimizes J_c degradation. Second, Incoloy 908 has very good fatigue properties in thin sections[5].

The conductors for PF6-7 are topologically and dimensionally the same as the US-DPC, but use Nb-Ti composite strands. The Nb_3Sn composite strands in the central solenoid and in PF5 all have a 3.5:1 copper to non-copper ratio, while the Nb-Ti strands are 2.5:1. The PF cable designs are hybrid cables with one pure copper strand in each triplet.

While the pancakes are wound, steel shims will be inserted as place-holders for the magnet insulation. The Nb_3Sn coils are then heat treated without any insulation in the winding pack. After heat treatment, specially designed tooling is used to separate the turns in the pancakes. Each turn is wound with two half-lapped layers of Kapton followed by one half-lapped layer of 3D woven S2-glass. The turns are returned to the plane of the pancake and 3D corner filling is applied. Insulating filler tape is arranged to support the lead stems, and a 2D woven S2-glass ground wrap is wrapped around the winding pack; a ground plane (screen) is wrapped around the S2-glass ground wrap leaving two insulated gaps to prevent primary eddy currents; and an abrasion layer of S2-glass is applied around the ground plane. The coil is then placed in a mold and undergoes impregnation under vacuum and pressure.

The overall dimensions of the TPX PF coils are shown in Table 14.

Table 14. PF System Coil Dimensions at Room Temperature.

Coil	R	Z	dR	dZ	nturns	nstrands
	(m)	(m)	(m)	(m)		
PF1,U+L	0.811	±0.252	0.186	0.496	120	360
PF2,U+L	0.811	±0.708	0.186	0.400	96	360
PF3,U+L	0.811	±1.044	0.186	0.257	60	360
PF4,U+L	0.811	±1.309	0.186	0.257	60	360
PF5,U+L	1.215	±2.355	0.186	0.400	128	360
PF6,U+L	3.769	±2.150	0.186	0.496	120	360
PF7,U+L	4.309	±1.117	0.186	0.352	84	360

The hydraulic circuits of the PF winding packs are described in Table 15.

Table 15. PF Coil Hydraulic Circuit Description.

Coil	SC type	$n_{pancakes}$	$n_{turns/pancake}$	$n_{channels}$	$L_{channel}$	P_{in}	p_{in}
					(m)	(m)	(MPa)
PF1,U+L	Nb3Sn	20	6	10	61.1	TBD	TBD
PF2,U+L	Nb3Sn	16	6	8	61.1		
PF3,U+L	Nb3Sn	10	6	5	61.1		
PF4,U~L	Nb3Sn	10	6	5	61.1		
PF5,U+L	Nb3Sn	16	8	8	122.0		
PF6,U+L	Nb-Ti	20	6	10	283.0		
PF7,U+L	Nb-Ti	14	6	7	324.0		

This Central Solenoid structure consists of inner and outer axial preload elements running from top to bottom of the CS coil stack. It provides both support of the coils when they are not energized and the preload that maintains the coil insulation in compression under all operating conditions. The inner preload elements are pairs of vertical rods that are bolted at the top and at the bottom to a section of a segmented ring. There are eight segments. The outer preload elements are 8 sheets of 316 LN that are curved to conform with the solenoid stack to reduce the space between the CS and the TF coils.

2.1.1 Central Solenoid (PF1 to 4)

2.1.1.1 Central Solenoid (PF1 to 4) - Coil

2.1.1.1.1 Conductor and Conductor Properties

The conductor data for the central solenoid are listed in Table 16.

Table 16. CS Conductor Data.

Parameter	Units	Value
Conductor		Nb3Sn
Conduit		Incoloy 908
nstrands		360

Parameter	Units	Value
D_{strand}	(mm)	0.78
P_w	(mm)	735
RRR		75
$D_{f,eff}$	(μm)	TBD
Coupling time (B=0)	(ms)	TBD
$w_{conduit}$	(mm)	22.3
$h_{conduit}$	(mm)	22.3
A_{cu}	(cm^2)	1.465
A_{noncu}	(cm^2)	0.255
$A_{conduit}$	(cm^2)	1.792
A_{Hecond}	(cm^2)	1.114
$A_{cond\ env}$	(mm^2)	571.2

The dimensions of the US-DPC, CS and PF6&7 conductor are shown in Figure 1.

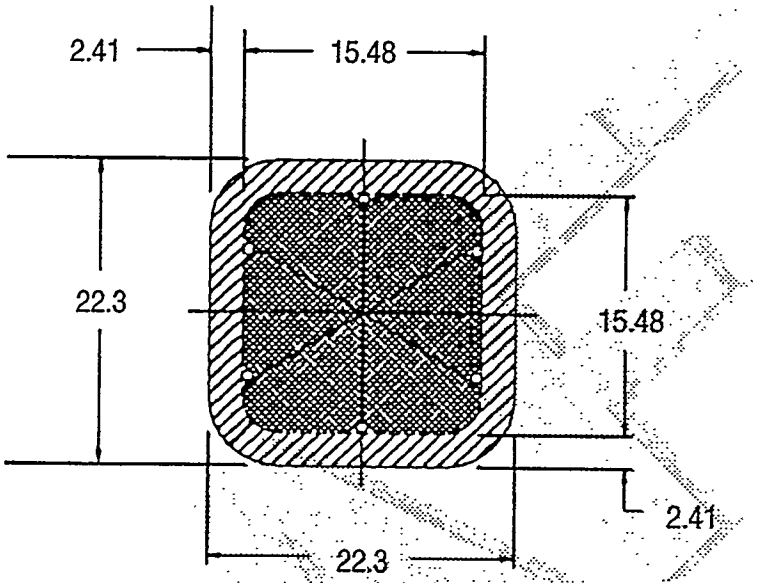

Figure 1. US DPC and PF1-7 Conductor Dimensions (mm).

The specified performance of the CS conductors is shown in Table 17.

Table 17. CS Conductor Performance.

Parameter	Units	Common Value	PF1	PF2	PF3	PF4
$B_{max,CS}$	(T)		5.07	3.66	2.11	1.32
$T_{b,nom}$	(K)	5				
ε_{sc}	(%)	-0.3				
$J_c(B,T,e)$	(A/mm^2)	1300 @7.6 T,4.2 K				
$\Delta T_{headroom}$	(K)		2.752	2.97	2.911	4.058

Parameter	Units	Common Value	PF1	PF2	PF3	PF4
T_{margin}	(K)			2.86		3.64
$f_{critical}$			0.594	0.591	0.583	0.570
h^2_{IR}	(W/cm^2-K)		185	169	166	168
Df,eff	*(μm)*	*20*				
LossNoncu (± 3 T)	*(mJ/cc)*	*460*				
Coupling time (B=0)	*(ms)*	*30*				
RRR		75				

2.1.1.1.2 Coil Transitions and Leads

The leads are on the inside diameter(seeFigure 2) of the CS coils. The coils are wound in a continuous spiral from the inside radius to the outside radius to facilitate using the roll bending technique as in the case of the TF coil. The pancake-to-pancake transitions are joggles on both the inside and outside diameters. The transitions and leads are centered along the same radial line to improve field quality at the plasma. The superconducting bus from the lead stems to the vapor cooled leads is Nb-Ti. There is a joint at the bottom of the central solenoid assembly from the Nb_3Sn lead stems to the Nb-Ti bus.

2.1.1.1.3 Coil Hydraulics

The cooling connections are located at the inside diameter, high field side, of the coils and are in the pancake-to-pancake transition regions as shown in Figure 3. The helium flows through a double pancake before exiting the coil. Each connection is a Tee with split flow at the conductor. Figure 4 is a coolant flow schematic showing helium flowing into and out of the PF1-4 (upper or lower) coils. The supply flow passes through a filter, flowmeter, and isolator (*insulator* in the figure) before flowing through the double pancake; the return flow passes through an isolator and flowmeter before flowing into the return manifold.

The cooling lines are connected to the manifolds located at the bottom of the central solenoid assembly. The filters, flowmeters, and isolators are located near the manifold. The inlet and outlet manifolds are split to prevent large induced currents.

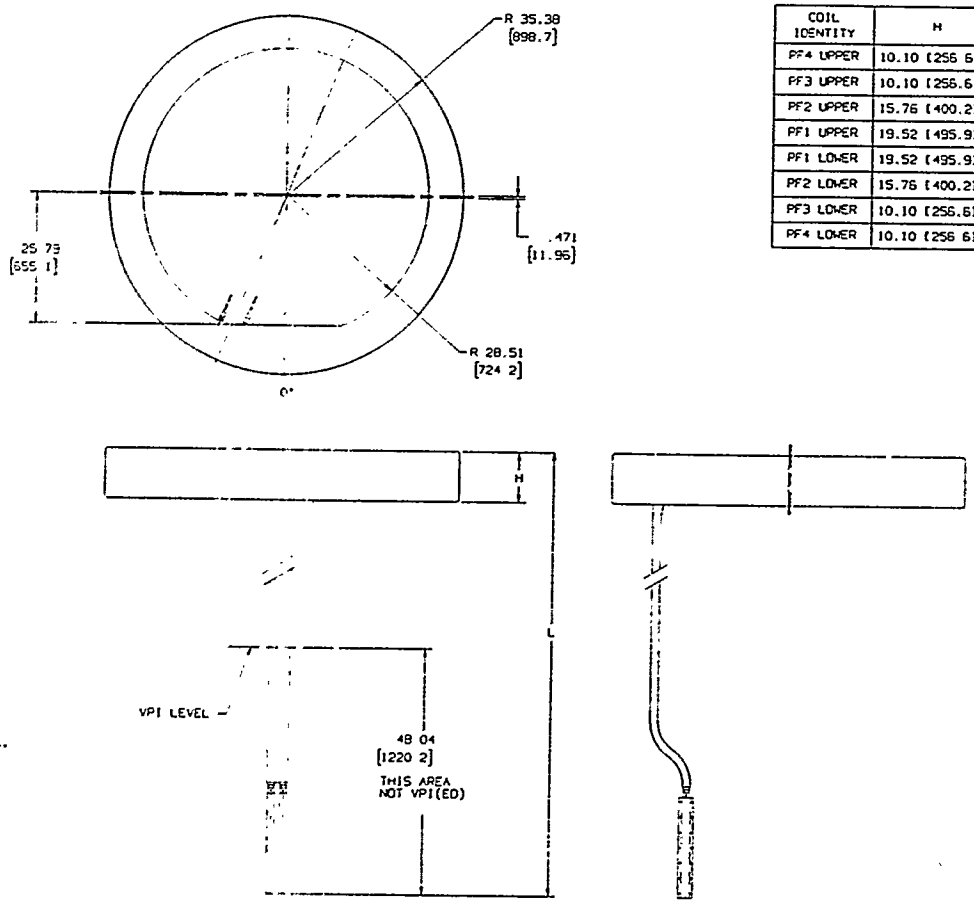

COIL IDENTITY	H	L
PF4 UPPER	10.10 [256 6]	155.00 [3937.0]
PF3 UPPER	10.10 [256.6]	144.58 [3672.3]
PF2 UPPER	15.76 [400.2]	134.15 [3407 4]
PF1 UPPER	19.52 [495.9]	118.09 [2999.5]
PF1 LOWER	19.52 [495.9]	98.28 [2495.3]
PF2 LOWER	15.76 [400.2]	78.45 [1992.6]
PF3 LOWER	10.10 [256.6]	62.36 [1583.9]
PF4 LOWER	10.10 [256 6]	51 95 [1319 5]

Figure 2. Central Solenoid Coil Leads (typical).

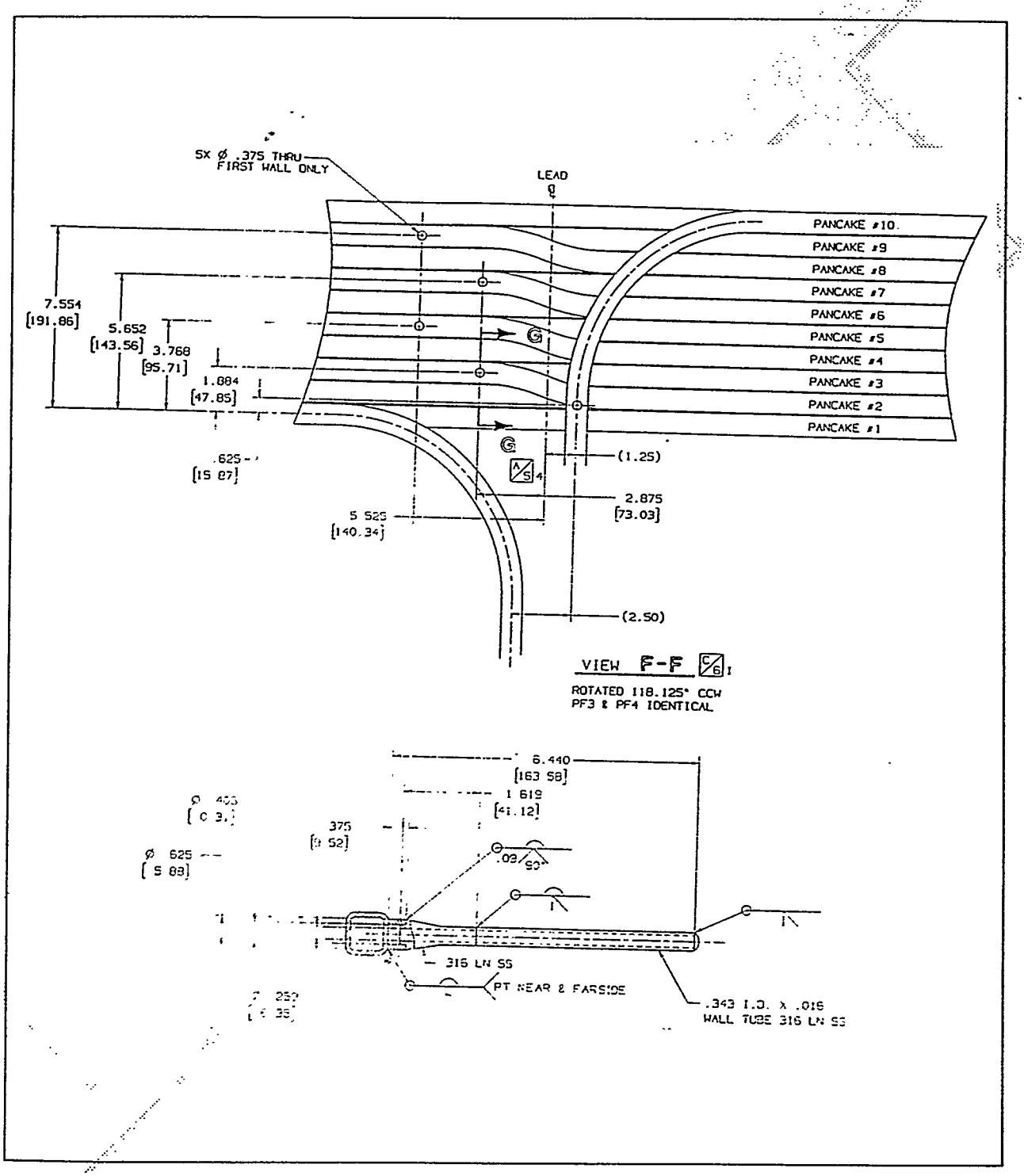

Figure 3. Helium Stub Locations and Detail.

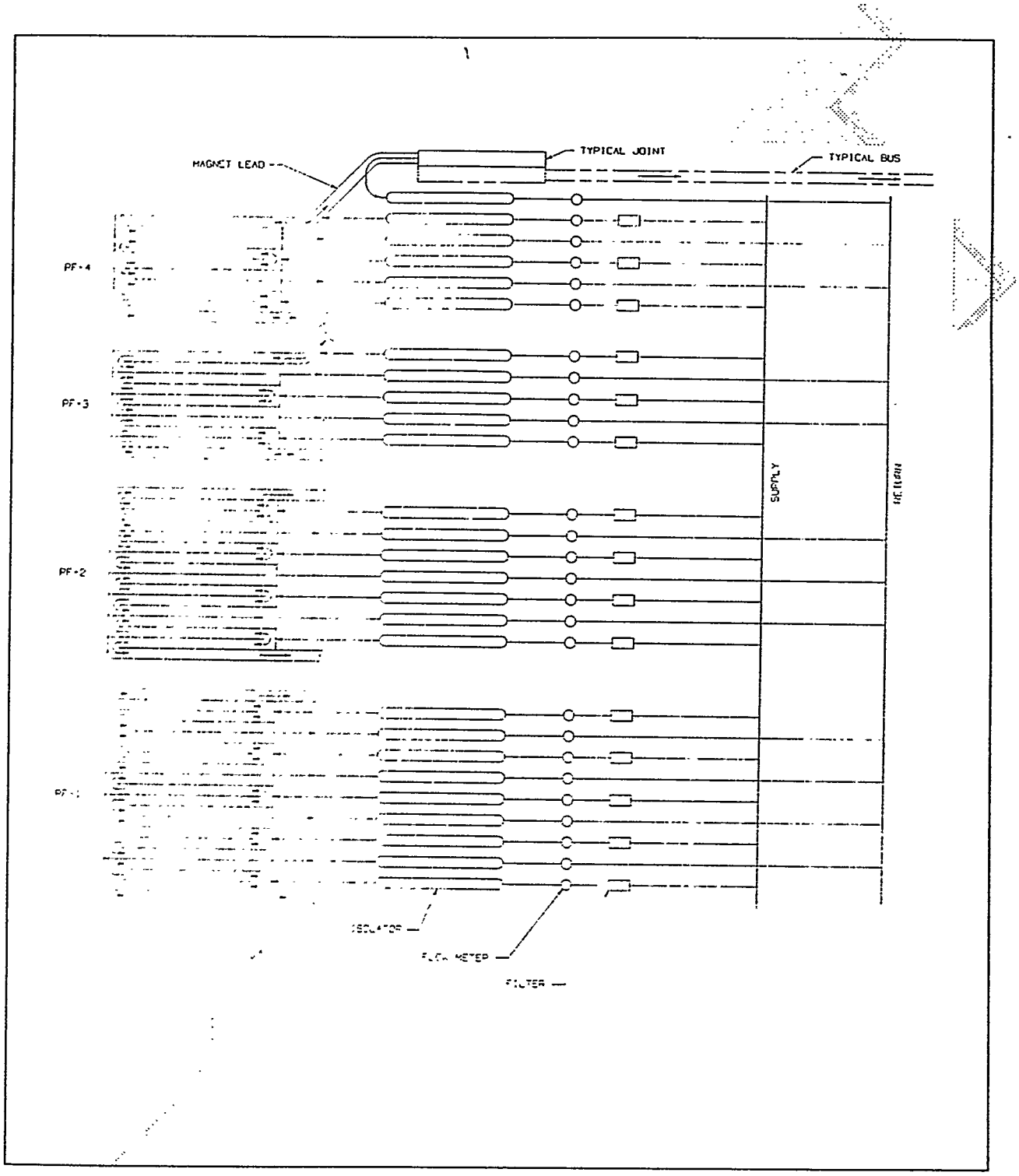

Figure 4. Coolant Flow Schematic.

2.1.1.1.4 Coil Insulation

Figure 5 illustrates the coil insulation scheme. The coil insulation system of the central solenoid coils is similar to that of the other PF and TF coils. After the coil is reacted, the conductor is wrapped with 0.0165" (0.42 mm) of 3D S2-glass tape 1" wide. (We expect the tape thickness to reduce the the dimensions shown in the figure under the influence of the winding tension, and we expect some "nesting" of the fibers to take place as well.) The 3D tape improves the thermal and mechanical properties of the insulation system, making the epoxy-glass CTE closer to that of the Incoloy-908 and improving epoxy-glass strength in the direction perpindicular to the tape plane. A 3D corner preform is inserted as taped coil is reasssembled. A 3D S2-glass tape 0.040" (1 mm) thick and 0.942" wide will be used to fill banana gaps and other large gaps. A ground wrap of half-lapped 2D S2-glass will be applied with a thickness of 0.176 inches (4.5 mm), then a ground plane screen will be wrapped around the ground wrap; finally, an abrasion layer will be added so the build height is 0.292 inches (7.4 mm). The coils are vacuum impregnated after wrapping.

2.1.1.1.5 Coil Manufacturing Process (PF 1-4)

- The conductor will be received from the manufacturer on spools with sufficient conductor per spool to completely wind a particular coil, thus eliminating any conductor joints within a coil. Receiving inspections will confirm the conductor is leaktight, free of surface damage, and of the proper length.
- The spools will be transferred to the winding station. Figure 6 illustrates the winding station layout. The system is automatic and has feedback controls, but it has provisions for manual override.
- The conductor will be fed from the spool and roll formed to its proper diameter into the coil take-up fixture. During the forming operation, a gas sniffer will check for helium leaks and Incoloy shims will be placed between turns and layers to account for, later to be installed, turn to turn insulation.
- After the coil has been wound, the helium feed throughs will be installed, by boring through the Incoloy wall and TIG welding the feed-through in place.
- The coil will then be helium leak tested to verify the integrity of the conductor jacket in the feed-through areas.
- The coil will be placed into a vacuum oven for a heat treatment process and baked according to the schecule in Table 18. All of the fixturing which securely holds the coil in place shall be fabricated from Incoloy 908 or shall provide for CTE variability.

Table 18. Heat Treat Reaction Schedule.

Period	Stage	Temperature (degC)	Tolerance (deg C)	Duration/Rate	Furnace Atmosphere
1	Preheat/Purge	RT	± 20	16 hrs max	Inert Gas
2	RT to Stage 1	RT - 185		25 degC/hr max	Inert Gas
3	Stage 1	185	± 5	120 hrs min	Inert Gas
4	Stage 1 to 2	185 - 340		45-55 degC/hr	10E-05 torr
5	Stage 2	340	± 5	72 hrs min	10E-05 torr
6	Stage 2 to 3	340 - 650		75 degC/hr min	10E-05 torr
7	Stage 3	650	± 5	200 hrs min	10E-05 torr
8	Cooldown	650 - RT		24 - 36 hrs	10E-05 torr
			Nominal Cycle	**452 hours**	

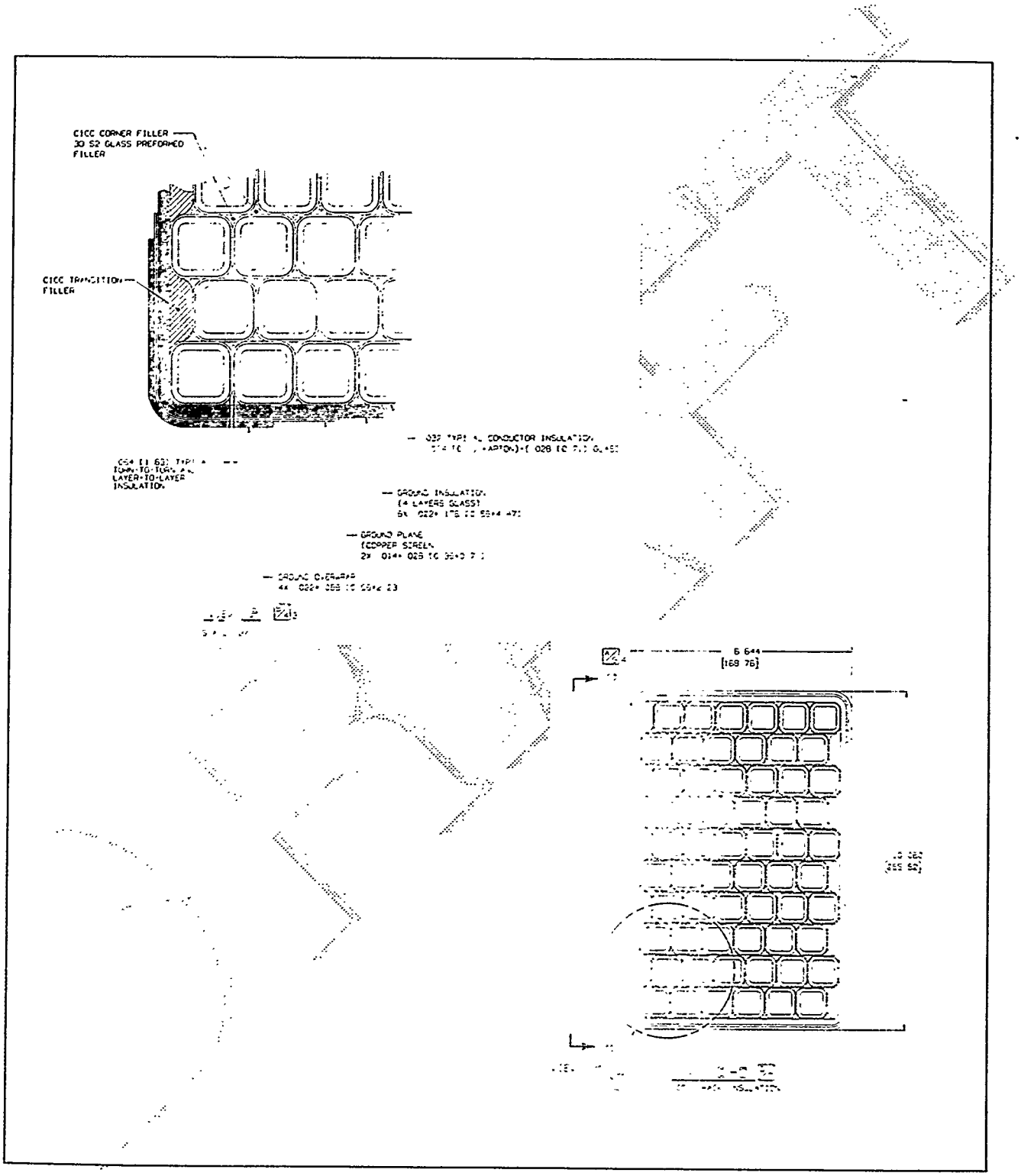

Figure 5. PF Winding Pack Insulation Scheme.

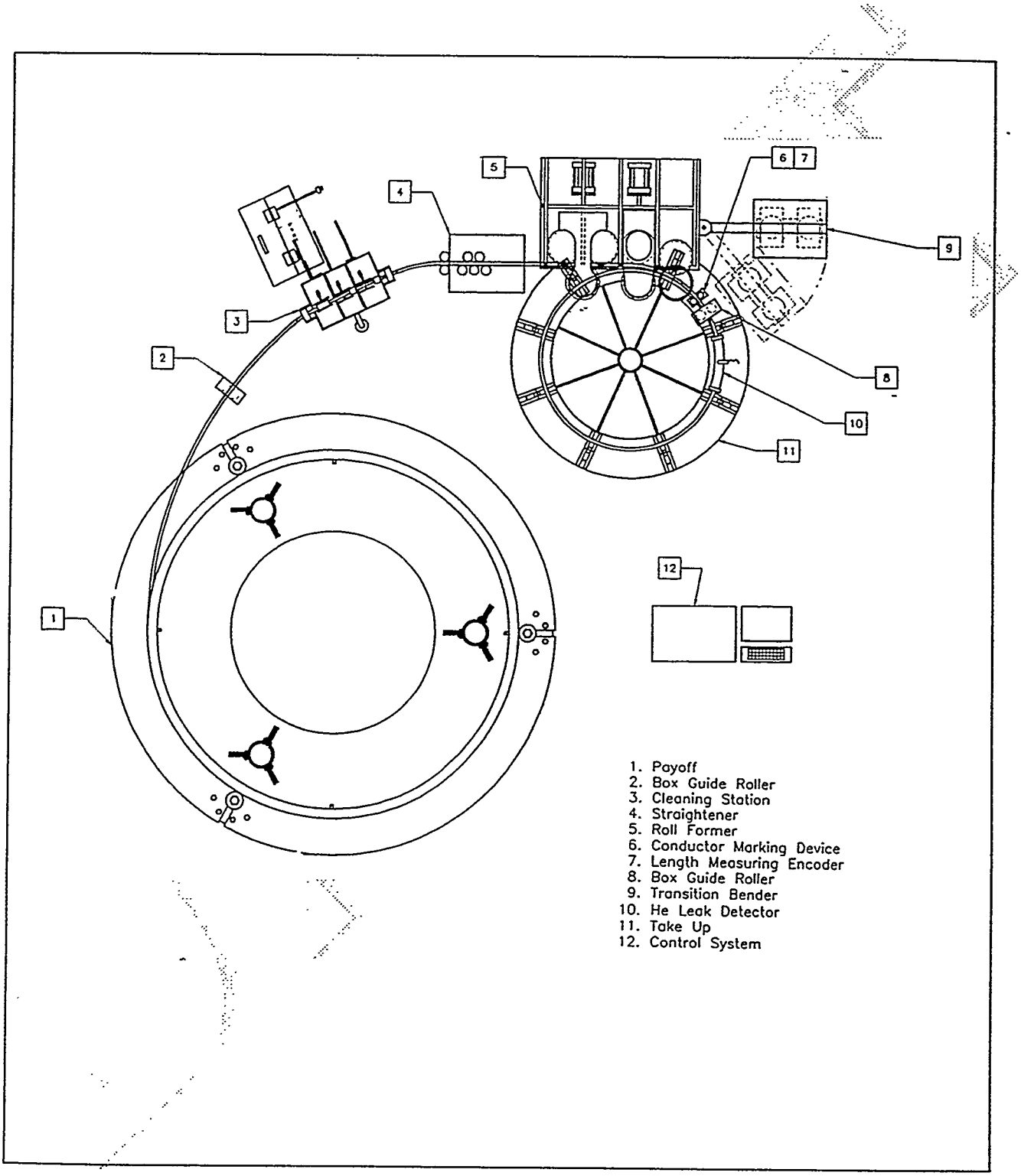

Figure 6. Winding System for PF Coils.

- After the coil has returned to room temperature, it will be transferred to the cleaning/taping station where it is uncoiled and taped as shown schematically in Figure 7. The tool used to facilitate this is illustrated in Figure 8 and. Figure 9. At this station, the coil shall be fixtured, so that the turns can be individually separated. Figure 8 shows the coil in its initial state, completely suspended above the catch plate. Figure 9 shows the coil at some intermediate state, with some of the turns in transition between their initial position and the catch plate. Each turn once separated shall be scotchbrite cleaned, and wiped with ethanol to remove any residue which may remain after bakeout. During the separating of turns, the Incoloy shims between turns and layers are removed. The conductor will then be insulated with (2) half-lapped layers of polyimid film and (1) half-lapped layer of dry glass insulation.
- The coil bundle is then ground wrapped using 4 layers of half-lapped layers of glass insulation. Prior to the first layer of ground wrap, glass fill material will be applied between turns on the outside of the bundle to fill any potentially resin rich areas. A ground plane, a layer of conductive mesh (screen), will be overlayed, and an abrasion layer of glass insulation will be wrapped around the ground plane. Glass fill material will be applied between turns on the outside of the bundle to fill any potentially resin rich areas.
- The PF coil is then vacuum-pressure impregnated (VPI) in a fully formed mold with a heat cured resin system. The mold for PF3 and PF4, illustrated in Figure 10, incorporates a number of features: The baseplate supports the coil and has resin inlets spaced about a foot apart. The 3 segment inner and outer walls are bolted to the baseplate after the coil is in position. The inner and outer walls are eccentric to accomodate the spiral wound coil eccentricity. The top plate slips over the leads and incorporates vacuum pumping outlets spaced a foot apart and offset with respect to the epoxy inlets on the baseplate. O-rings seal the wall segments, baseplate, and top. The coil is placed in the mold and a vacuum is applied. The epoxy resin is then allowed to flow into the mold to wet the dry glass insulation. Pressure is added as required to assure full saturation has occurred The coil is then heat cured for a predetermined period of time.
- After being impregnated and cured, the coil will be removed from the mold by removing the lead mold, shown in Figure 11, from the top plate, disassembling the outer wall segments, disassembling the inner wall segments, and finally jacking the baseplate off the potted coil using the jacking plates built-into the baseplate. The coil will be cleaned up.
- Final electrical testing will be performed. A DC Hipot Test will establish the voltage holdoff capability between the conductor and the ground plane. This test will confirm that 7.5 kV can be withstood with a leakage current of less than TBD. This test will not stress the insulation between the coil turns or layers, however, so either an impressed or an induced voltage test will be performed. In an impressed voltage test, a capacitor bank discharges into the inductive coil (room temperature), and the voltage across the coil divides according to its impedance. Alternatively, the coil could form the secondary of a transformer, and a rapid change in the primary current could induce voltage in the coil. Care must be taken not to damage the internal voltage taps when these tests are conducted. Detailed models and calculations will be developed to establish the test requirements.
- PF coils 1 thru 4 (upper and lower) will then be stacked together in the CS support structure to form the Central Solenoid (CS).

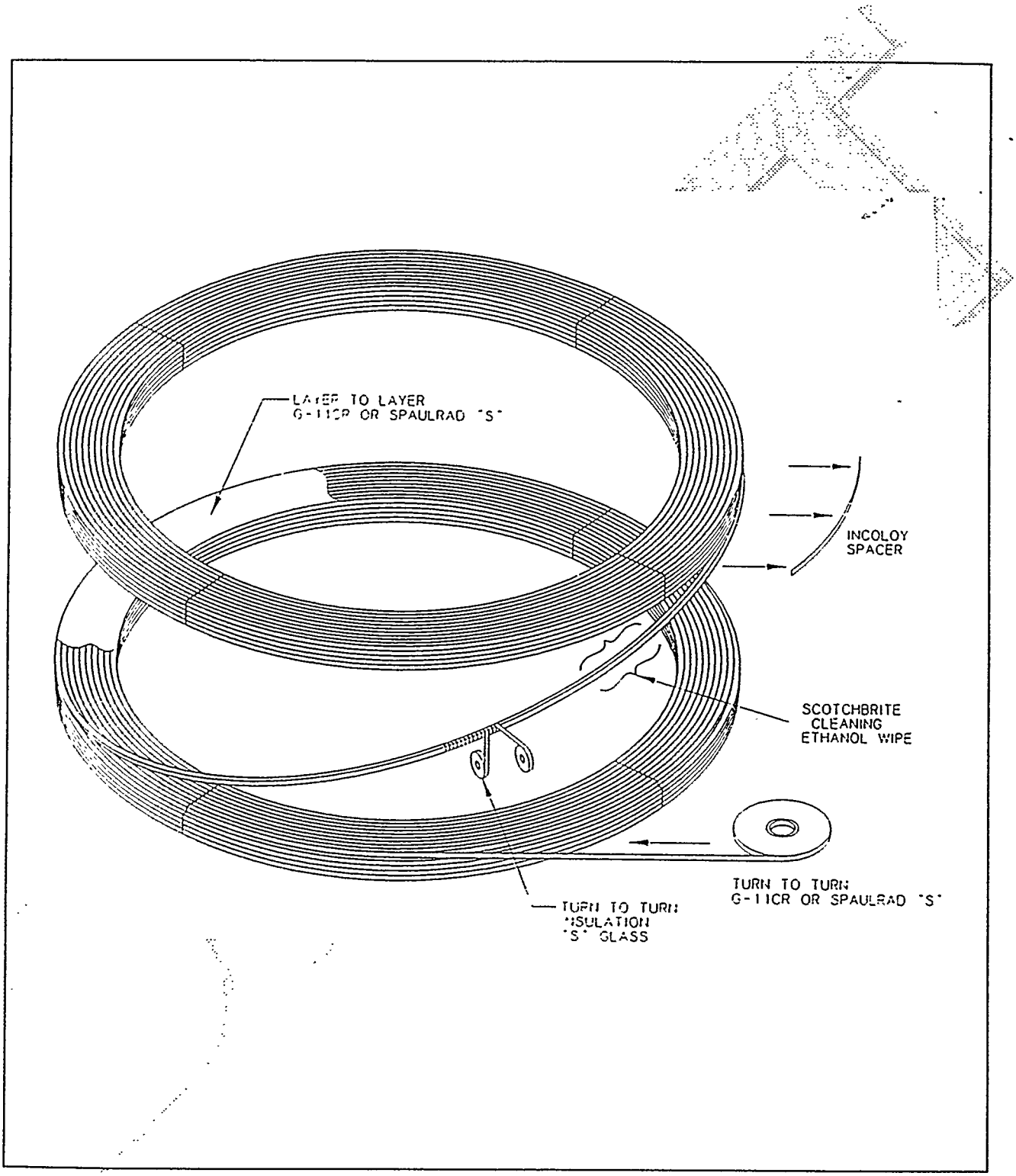

Figure 7. Application of Turn to Turn Insulation after Reaction.

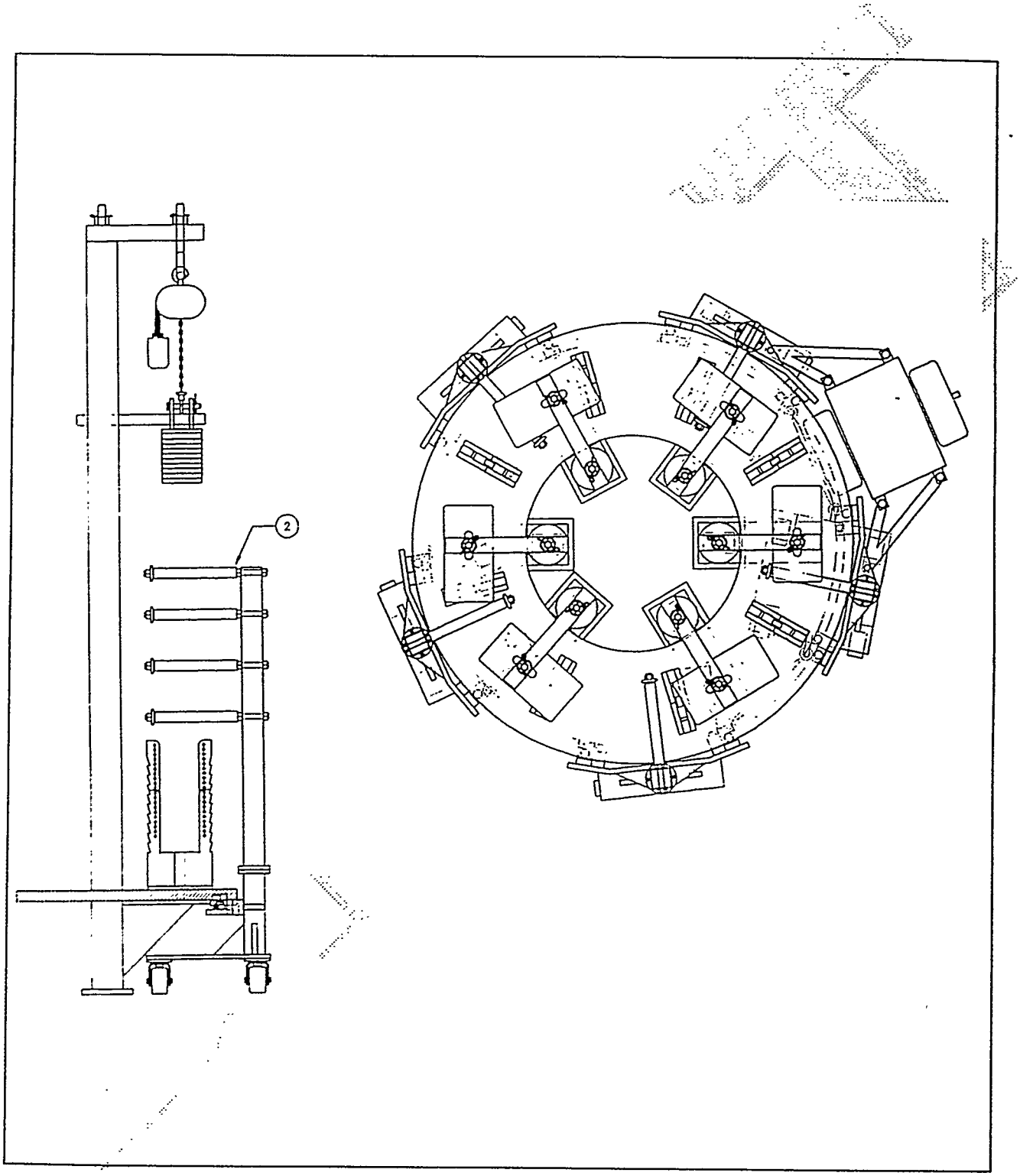

Figure 8. Cleaning and Taping Station.

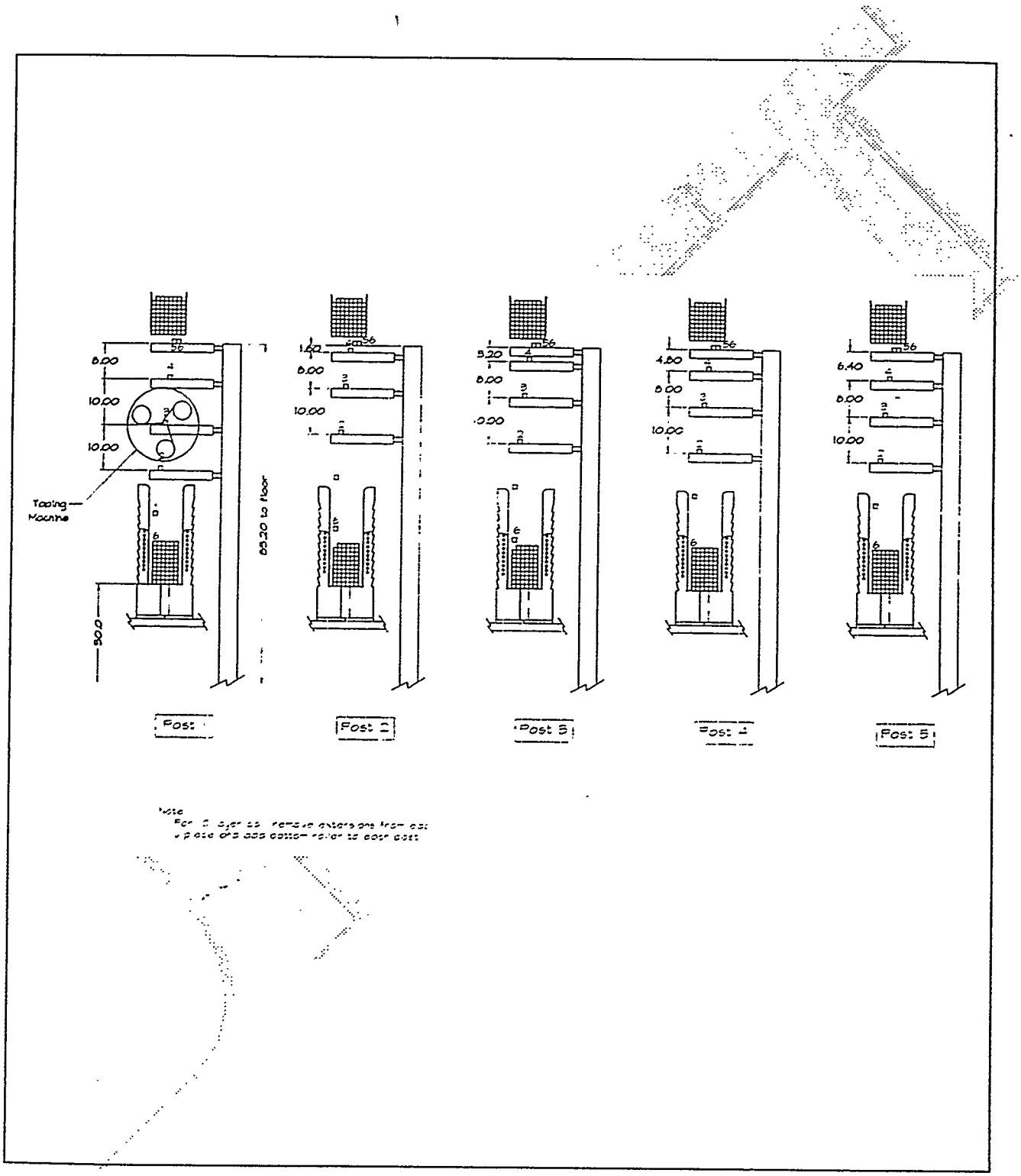

Figure 9. Cleaning and Taping Station with Partially Uncoiled Winding Pack.

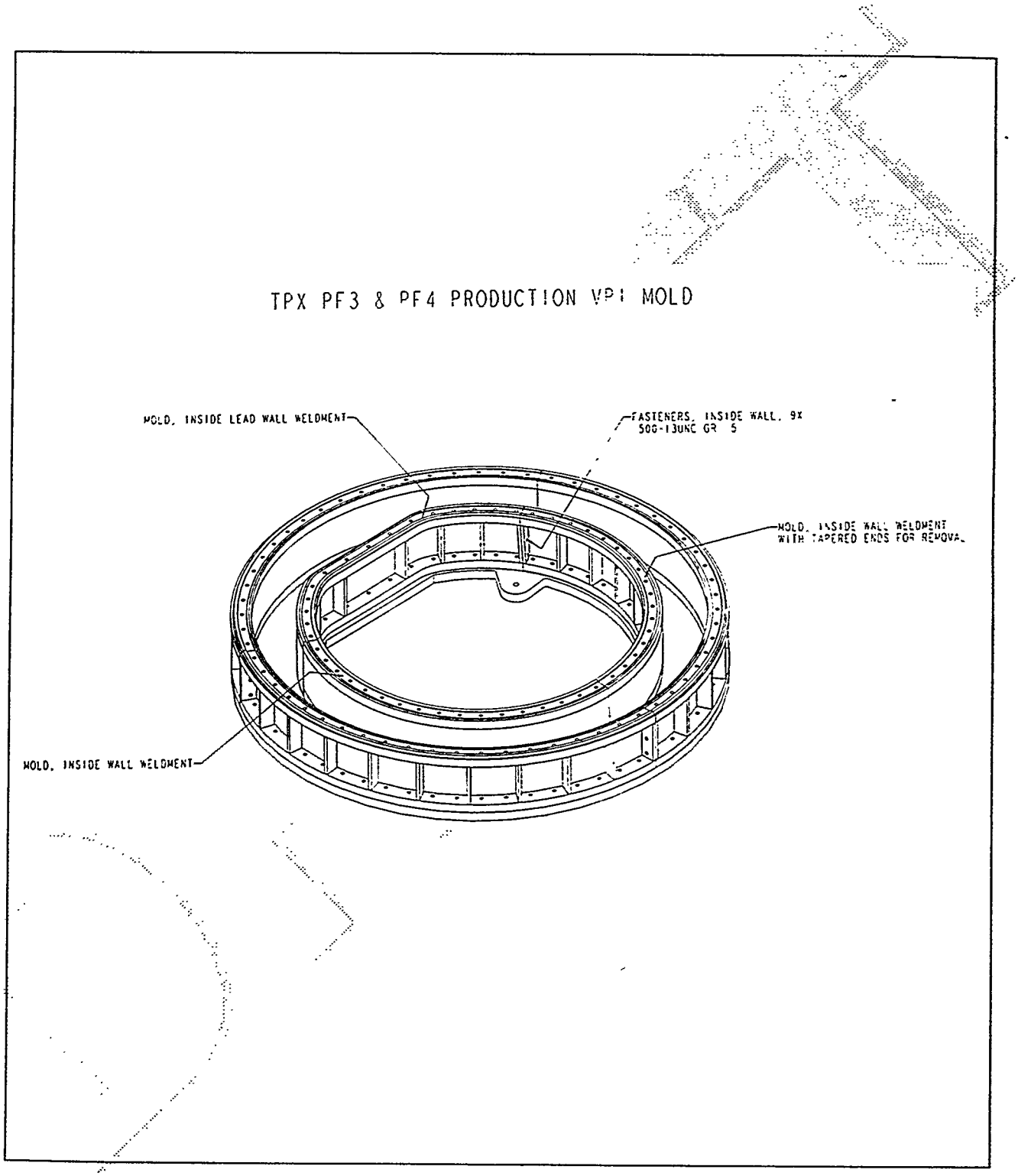

Figure 10. PF3&4 Production VPI Mold.

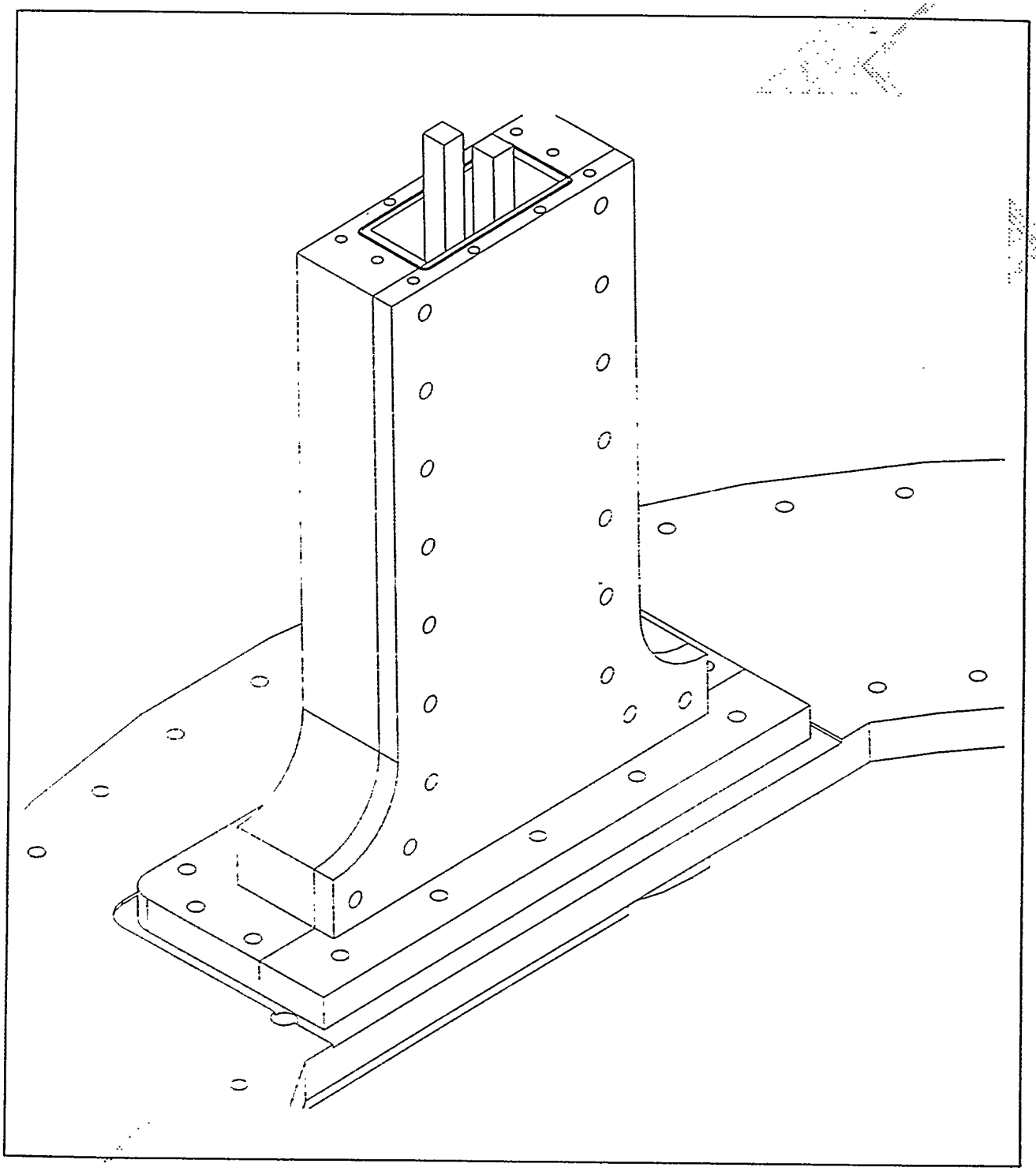

Figure 11. The Lead Mold.

2.1.1.2 Central Solenoid (PF 1 to 4) - Structure

The central solenoid is composed of 8 solenoid coils, PF 1U through 4U (upper) and PF 1L through 4L (lower). The Incoloy 908 conduit used to construct the coils is an adequate Lorentz-force-reaction structure; therefore, the coils are individually self-supporting against radial movement, but some combinations of magnetic fields may destabilize the stack. The CS structure holds the coils in position and restrains their movement during operation.

The central solenoid structure is made entirely of 316 LN stainless steel. The individual winding packs are separated by 3/8" bearing plates. The 8 plates form a segmented ring that reduces the magnitude of eddy currents associated with the changing magnetic fields. The entire stack of 8 CS coils is held together by 16, 2" diameter tie-rods on the inside diameter and 8, 1/2" thick plates on the outside diameter. Figure 12 is an exploded view of part of the CS structure showing the typical component arrangement. The plates were used instead of bolts on the outside diameter to reduce the gap between the TF structure and the central solenoid. The tie-rods and plates are bolted to thick covers at the top and bottom. The covers are segmented into 8 wedge shaped pieces to reduce eddy currents. Each cover segment is connected top and bottom by 2 tie-rods on the inside diameter and 1 plate on the outside diameter. The tie-rods, support plates and end covers are pre-loaded to provide axial compression to the entire solenoid coil stack. The tie-rod pre-load ensures coil stack compression throughout the pulse even when the coils experience axially separating loads. The axial compression also enhances the shear capacity of the pancake-to-pancake insulation. Figure 13 shows an assembled CS.

The entire coil stack and pre-load structure are attached to the TF support structure with flex-support hangers. These hangers have three functions: 1) to allow radial displacement of the top end of the coil, 2) to prevent rotation of the top end of the coil, and 3) to support the entire coil stack dead weight. The main purpose of these hangers is to allow the coil to displace without generating bending stress in the coil stack up, i.e. to approach a free end condition. The attachment to the TF structure is shown in Figure 14.

The nominal radial clearance between the CS pre-load structure and the TF coils is 1/2 inch, (see Section 2.1.1.3 for more discussion on the interface). The radial gap thickness at the bottom end of the CS is reduced to minimize motion during a disruption or seismic event. The tighter gap tolerance is accomplished with 8 thick adjustable snubber plates located at the bottom of the pre-load structure, see Figure 15. These adjustable plates can also be used to facilitate CS assembly installation.

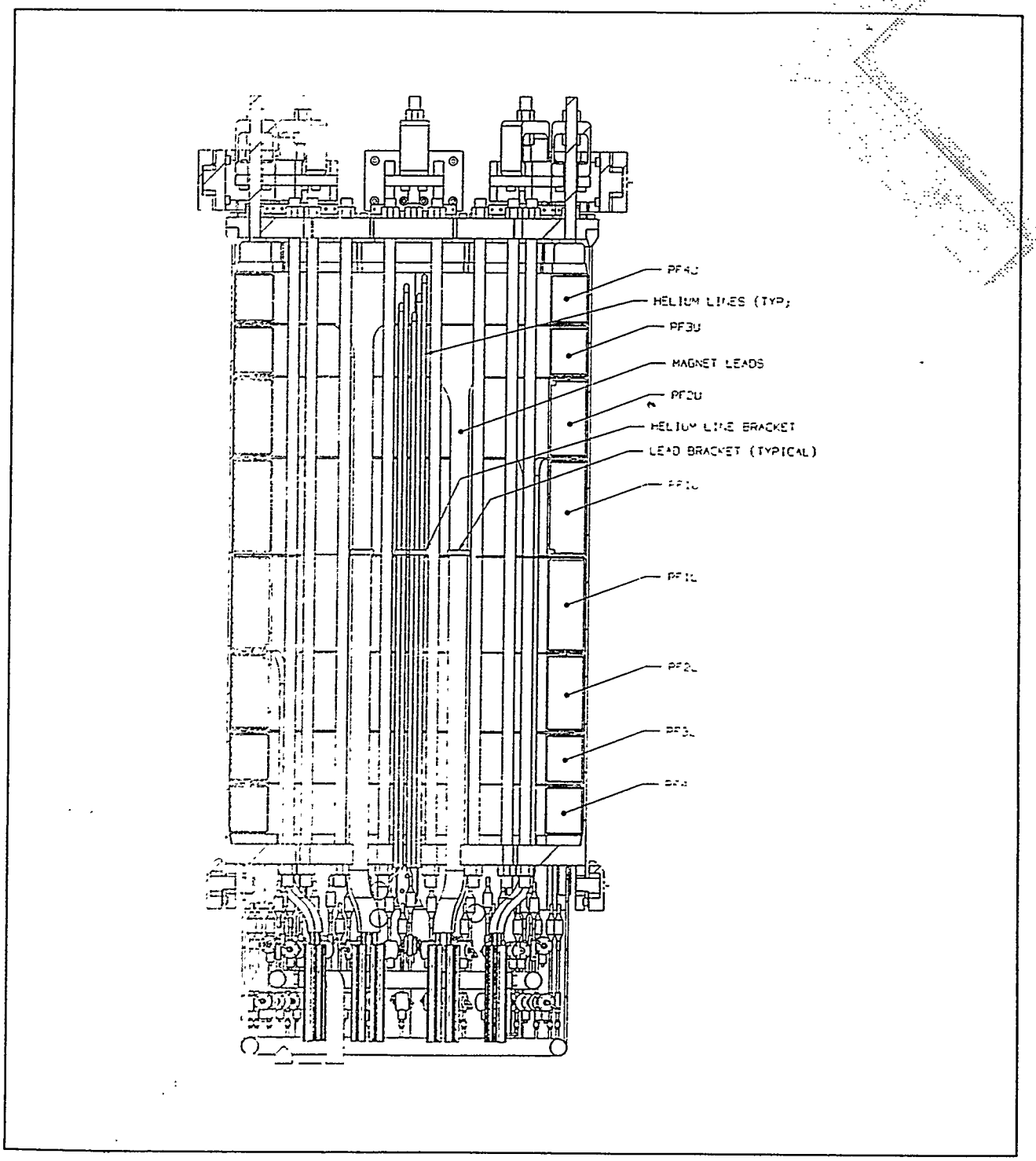

Figure 12. Exploded View of part of the CS Structure.

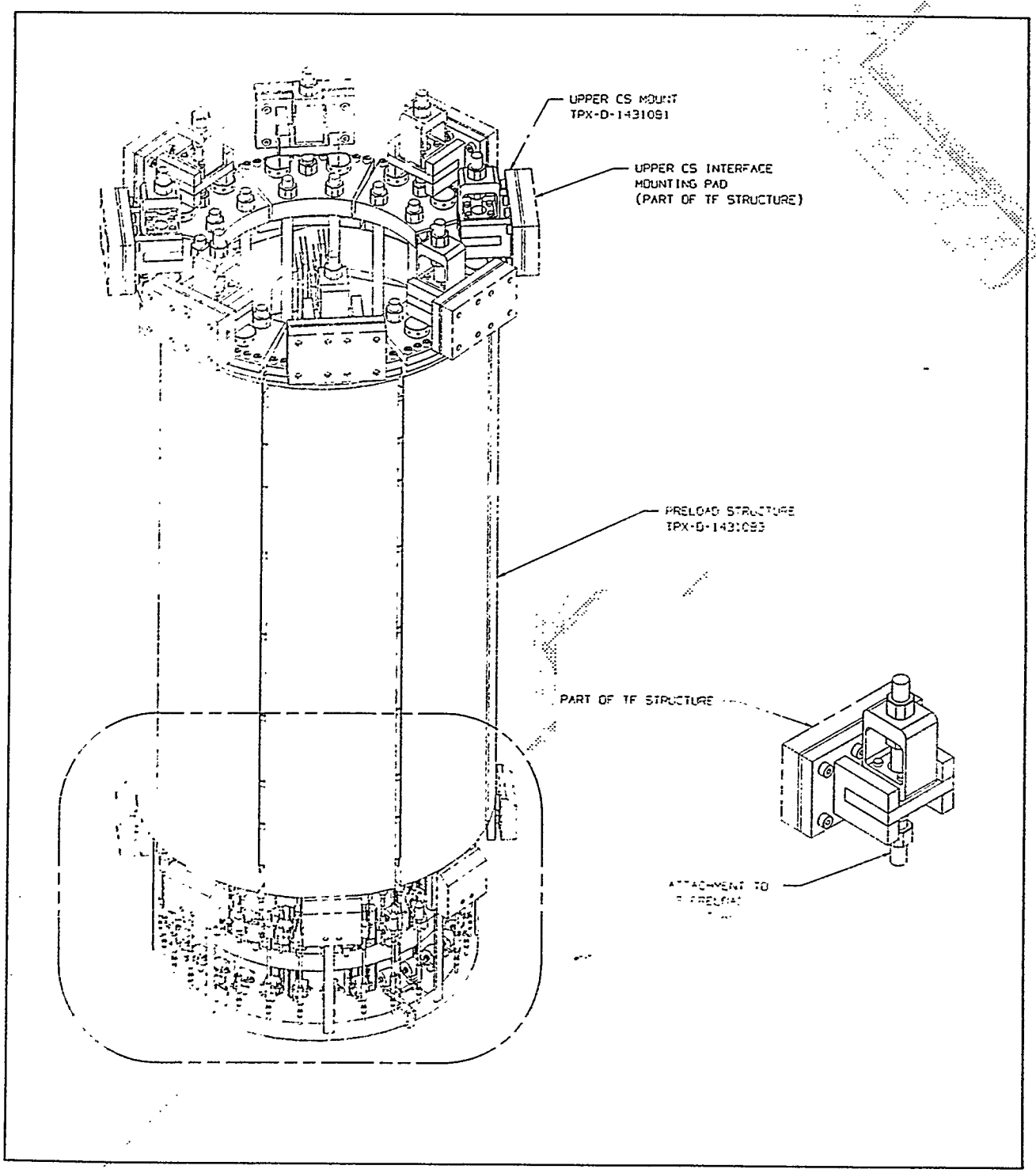

Figure 13. Central Solenoid Assembly.

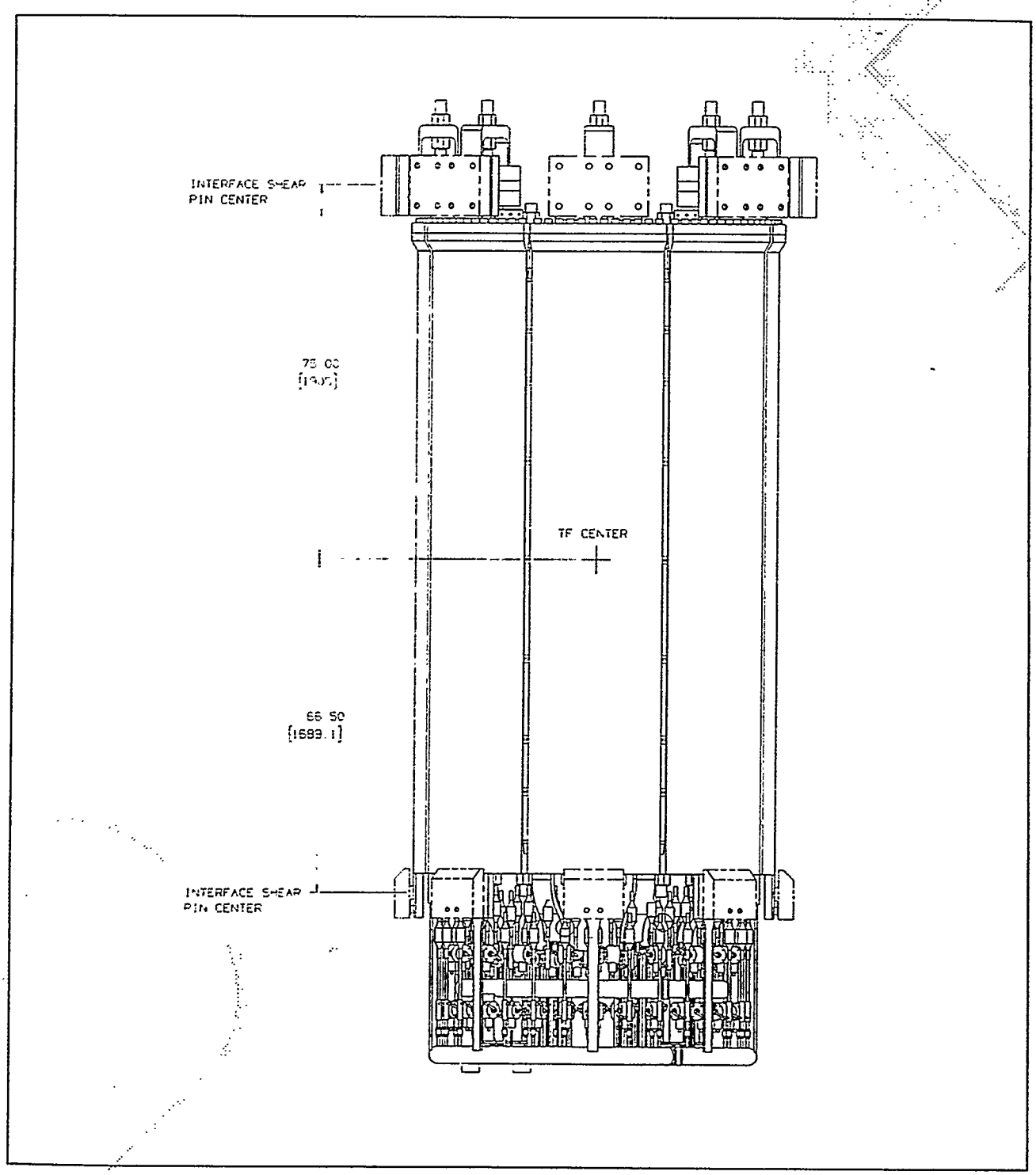

Figure 14. CS Attachment Structure.

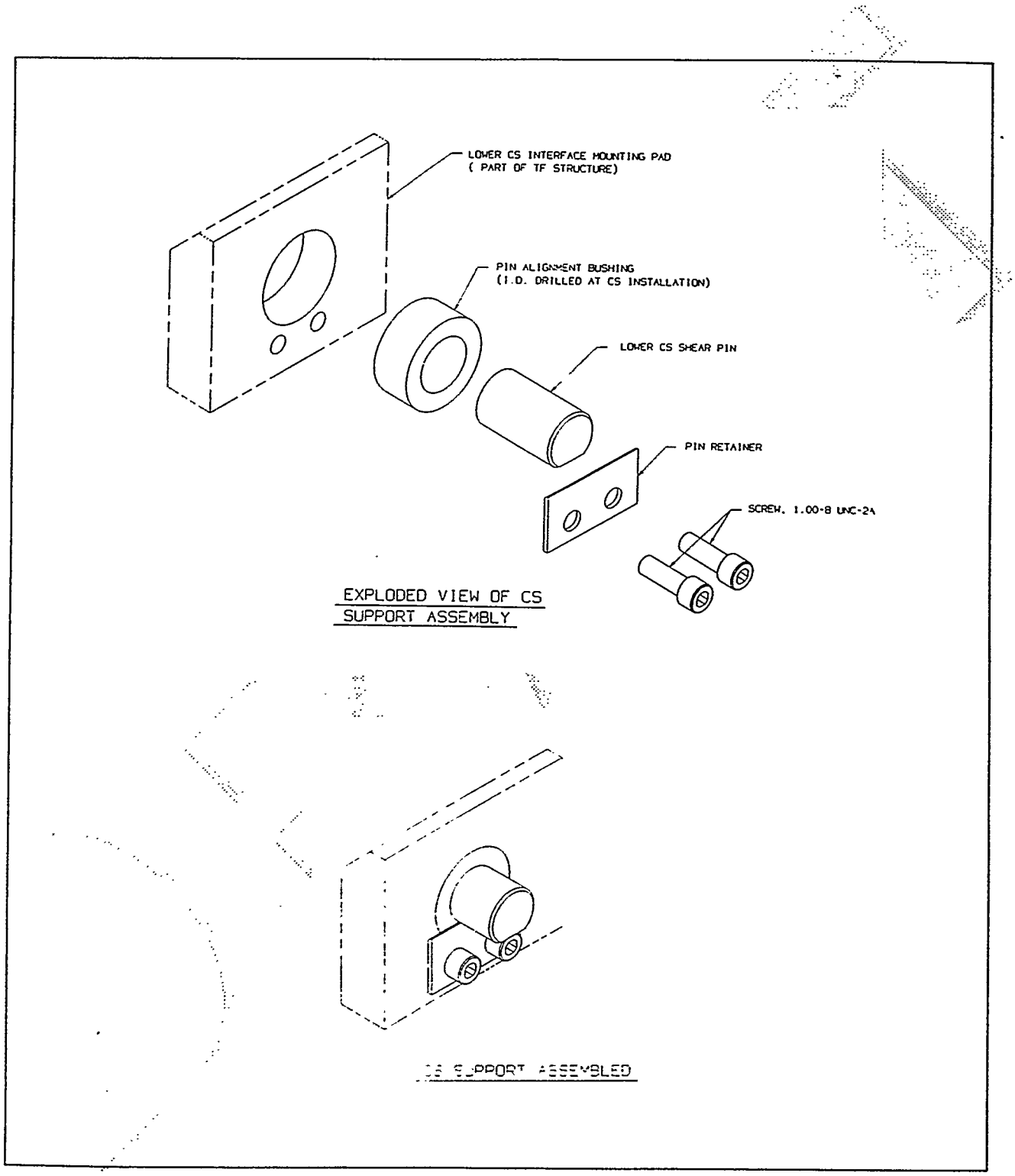

Figure 15. CS Lower Support.

2.1.1.2.1 Structure Material and Material Properties

The bearing plates, pre-load and support structure are made out of 316 LN stainless steel in the annealed condition. In the winding pack the conduit is Incoloy 908 and the insulation is a polyimide and glass epoxy. These materials will be supplied with certification per the ASME code documentation requirements[6]. The material properties for Incoloy 908, 316 LN stainless steel, and polyimide are shown in Table 19 and Table 20.

Table 19. Physical and Mechanical Properties of Incoloy 908 and 316 LN.

Property	Temp (K)	Units	Incoloy 908[7,8]		316 LN[9,10]
Thermal contraction from 700 C	4	(%)	-1.1		-1.62
	77	(%)	-1.08		-1.61
	298	(%)	-0.94		-1.4
Elastic modulus	4	(GPa)	182.3		199
	77	(GPa)	182.0		205
	298	(GPa)	179.0		188
Poisson's ratio	4		0.303		0.282
	77		0.303		0.282
	298		0.297		0.294
			Base	Weld	
Yield strength	4	(MPa)	1227	1279	1000
	77	(MPa)	1189	1137	775
	298	(MPa)	1075	1062	375
Tensile strength	4	(MPa)	1892	1648	1500
	77	(MPa)	1664	1413	1200
	298	(MPa)	1443	1316	700
Elongation	4	(%)	28.5	8.0	38
	77	(%)	21.7	10.0	30
	298	(%)	16.5	78	36

Table 20. Mechanical Properties of Polyimide.

Material	E_x	E_y	E_z	G_{xy}	ν

Material	E_x	E_y	E_z	G_{xy}	υ
Polyimide	15 GPa	30 GPa	30 GPa	8.6 GPa	0.3

Note: The insulation X-direction is through the thickness, Y and Z are in the plane of the sheet. E = modulus of elasticity, G = shear modulus, υ = Poisson's ratio.

DRAFT

2.1.1.2.2 Structure Welds

The most important structure weld in the central solenoid assembly is the weld between the pre-load plates and the bottom segmented cover, see Figure 15. The cross-sectional weld area is increased by a factor of two so that a weld efficiency of 50% would still produce a good structure. A back-to-back V grove weld was chosen to limit weld distortion. See the Design Criteria Document for weld type and inspection requirements.

2.1.1.2.3 Structure Hydraulics

Structure cooling is used in the PF6&7 cases.

2.1.1.2.4 Structure Manufacturing Sequence

The pre-load structure is assembled in conjunction with the coil stacking during the assembly of the central solenoid.

2.1.1.2.5 Coil/Structure Interface

The central solenoid coils are separated from each other by a 3/8 thick 316 LN stainless bearing plate. The bearing plates are made up of 8 wedge shaped segments to reduce eddy currents, see Figure 16. These bearing plates extend radially into the inside diameter of the central solenoid and are used to support the conductor leads and Helium lines, as shown in the figure. G11 support flanges are used to attach the conductor leads to the bearing plates. These G11 flanges act as structural support and as an insulator between the conductor leads and the bearing plates.

The bearing plates are bonded to the adjacent coils with epoxy to eliminate any relative motion between the coils. The 8 coil stack up will then act as a monolithic structure. Load blocks located at the top and bottom of the coil stack are adjustable, see Figure 14 and Figure 15. These adjustments account for vertical winding pack assembly tolerance build-up, creep, and pre-load margin adjustment.

2.1.1.3 Central Solenoid Interface to TF Structure

The central solenoid support structure is bolted just above the straight leg of the TF structure, see Figure 14. To account for radial motion during cool down, operation, and warmup, the CS is allowed to move in the radial direction with respect to the TF structure via slotted clearance holes in CS flex-support structure, see the inset in Figure 13. During cool down the outside diameter of the CS is reduced 2.3 mm and the TF structure moves in towards the CS 3.8 mm for a loss of gap clearance of 1.5 mm between them. The overall gap clearance will be reduced from 12.7 mm (1/2 inch) down to 11.2 mm which will not cause an interface problem; see Figure 14. At this time, the CS is electrically isolated from the TF structure via an insulating break at the interface. (There are, however, significant benefits to having the CS structure grounded to the TF structure. The usual requirements to maintain the modified star ground topology could be retained, and the CS coils would be isolated from the TF structure, but it eliminates the need to use an insulating break that may creep, causing the CS to relax into the wrong axial position.)

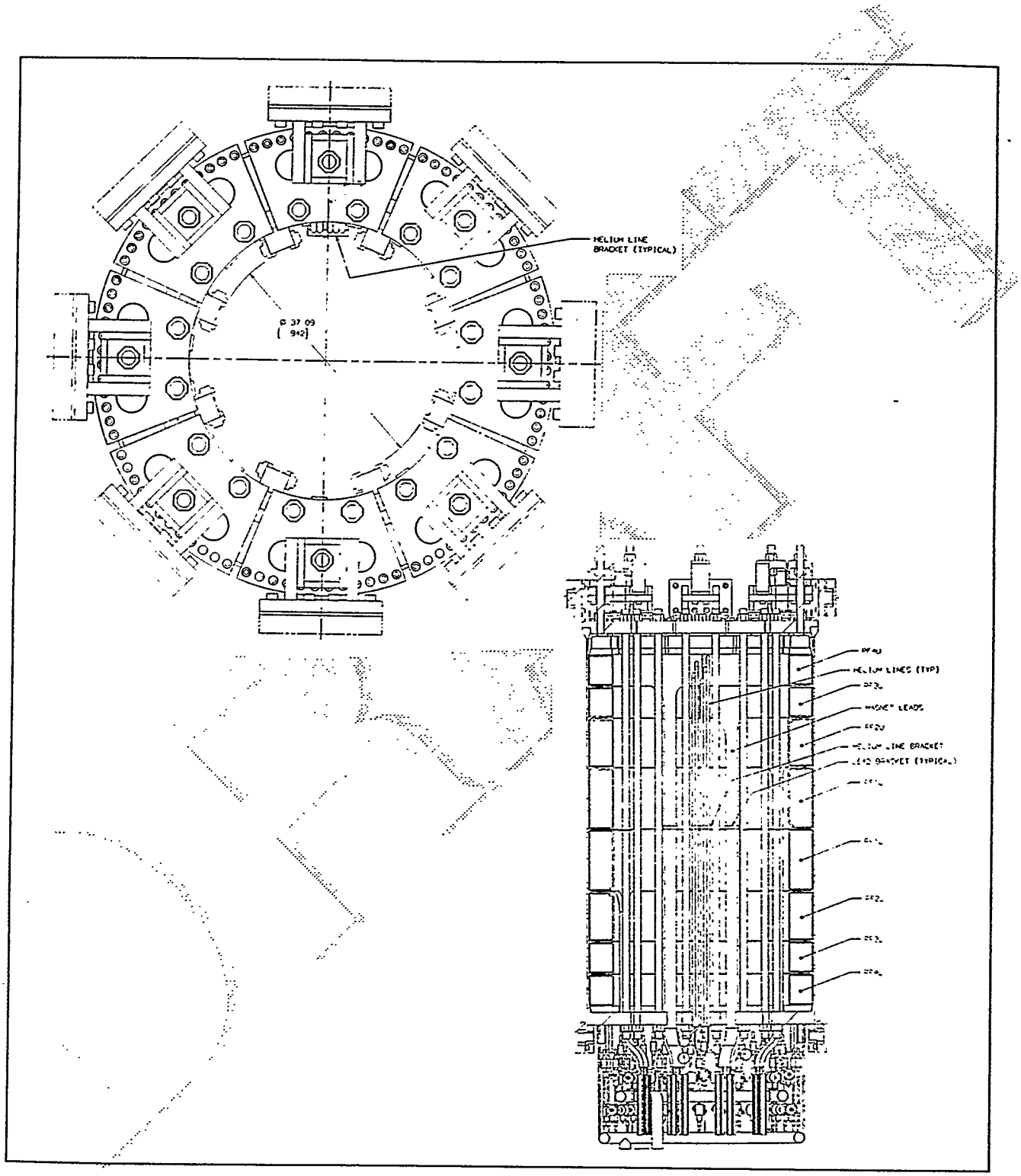

Figure 16. CS Assembly, Conductor, and Helium Lead detail.

2.1.1.4 Central Solenoid Assembly

The central solenoid is assembled from the bottom up. The 8 coils and the pre-load structure are assembled at the factory. The top support structure is later bolted to the top of the pre-load structure during installation. Each coil has a conductor lead long enough to reach to the bottom of the cryogenic cooling assembly; therefore eliminating the need for a conductor splice inside the central solenoid bore. The detail of the assembly is as follows:

1. Start with the lower plates and outer preload structure located on the assembly which defines the CS structure centerline.
2. Take actual measurements of all items to be stacked to determine actual vertical stack-up.
3. Determine the size of the adjustable shims to ensure that coil will be centered properly.
4. Install the adjustable shims onto the bottom plate segments.
5. Install PF4L onto the adjustable shims, aligning the coil centers with the CS structure centerline.
6. Install the 8 wedge shaped bearing plates
7. Repeat steps 4 through 6 until all 8 of the coils are installed.
8. Install the adjustable shims onto PF 4U.
9. Install the upper pre-load subassemblies onto the outside diameter of the coil assembly.
10. Move the cryogenic cooling assembly beneath the coils and attach the Helium extension lines.
11. Install tie rods and preload the sturcture. Pre-load to be determined with strain gages backed up by measuring the vertical elongation of the pre-load structure and pre-load tool hydraulic pressure.

2.1.1.5 Superconducting Bus and Leads

This section will be provided under separate cover.

2.1.2 Poloidal Field Coil 5

2.1.2.1 Coil description

PF5, upper and lower, are superconducting cable-in-conduit conductors, using Nb_3Sn composite strands and Incoloy 908 single conduits. The winding packs are continuously wound without joints. The winding packs have no cases and are self-supporting against radial hoop forces. After vacuum pressure impregnation, each winding pack is mounted to the TF coil structure in 8 places. Brackets to support and center the winding packs are bolted and keyed to the TF structure. PF5 upper can be removed vertically without tokamak disassembly.

2.1.2.1.1 Conductor and Conductor Properties

The conductor dimensions of PF5, upper and lower, are identical to those of PF1-4, shown in Figure 1.

The specified performance of the PF5 conductors is shown in Table 21.

Table 21. PF5 Conductor Performance.

Parameter	Units	PF5
$B_{max,PF5}$	(T)	4.74
$T_{b,nom}$	(K)	5
ε_{sc}	(%)	-0.3
$J_c(B,T,e)$	(A/mm^2)	1850 @ 5.3 T, 4.5 K, ε=-0.3
$\Delta T_{headroom}$	(K)	3.77
ΔT_{margin}	(K)	3.64
$f_{critical}$		0.597
h^2_{1R}	(W/cm^2-K)	658
$D_{f,eff}$ $Loss_{Noncu}$ (± 3 T)	(μm) (mJ/cc)	20 460
τ_{coup} (B=0)	(ms)	30
RRR		75

2.1.2.1.2 Coil Transitions and Leads

The winding of PF5 is very similar to the central solenoid coils except that the coil is constructed with 16 pancakes of 8 turns each. There are no joints in the coil and it is made from a single conductor 976 meters long. The coil leads are on the inside.

2.1.2.1.3 Coil Hydraulics

The cooling paths of PF5 have the same topology as the paths of the central solenoid coils. The cooling connections are located on the inside diameter of the coil and are located in the pancake-to-pancake transitions. The helium coolant flows through one double pancake before exiting the coil.

2.1.2.1.4 Coil Insulation

The insulation system on PF5 is identical to the insulation of the central solenoid.

2.1.2.1.5 Coil Manufacturing Process (PF-5)

The manufacturing process for the PF5 coils is identical to that for the CS coils described in 2.1.1.1.5.

2.1.2.2 Interface to TF Structure (PF 5)

PF5U and PF5L are mounted to the TF structure at 8 locations, on every other TF magnet case: see Figure 17 and Figure 18. A toroidally segmented steel case surrounds the coil at each support location to better distribute the in-plane and out-of-plane bending stress. This is shown, along with other details, in Figure 19. Shims are used as necessary to adjust the coil current center location inside the support structure. Keys are used to transfer shear from the PF coils to the TF structure.

The PF 5 superconductor is Nb_3Sn, and the Incoloy 908 conduit have similar coefficients of thermal expansion, but they are different than that of the 316LN TF structure. The resulting thermal mismatch drives the requirement for a mount that allows differential radial motion between the high contraction stainless steel TF structure and the low contraction Incoloy steel conduit. The mounts connecting PF5U and PF5L to the TF structure have a radial gap between the outside diameter of the coil and the TF coil case which allows the coils to move in the radial direction relative to the TF structure during cool down. A leaf spring on each mount exerts a radial centering force on the coil. The structural support only allows radial motion during cool down (bending may occur during operation), and once PF5U and PF5L are at an operating temperature of 5 K, the gap will disappear and the coil will be anchored radially at each of the mount locations.

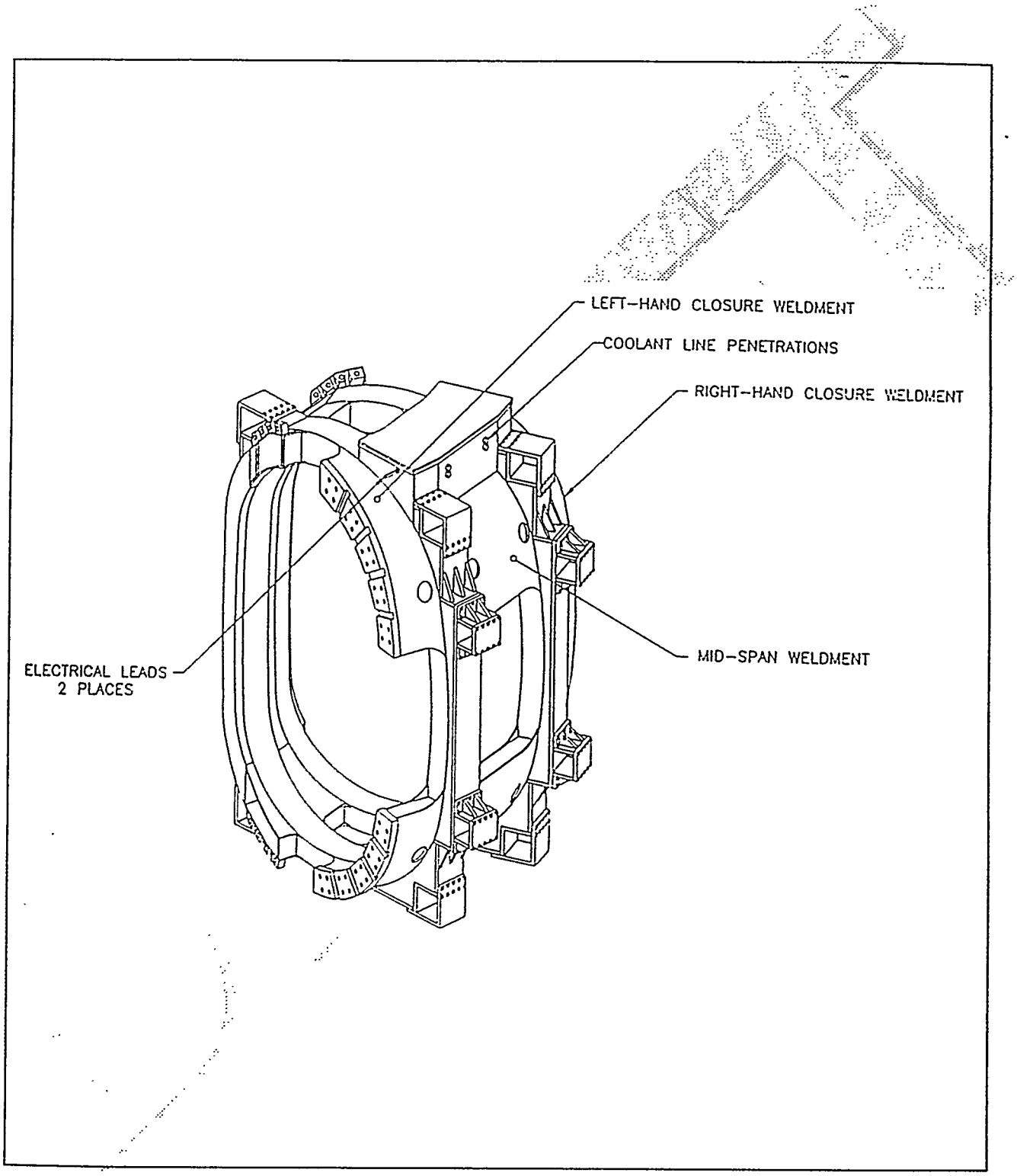

Figure 17. PF Coil Support Structures.

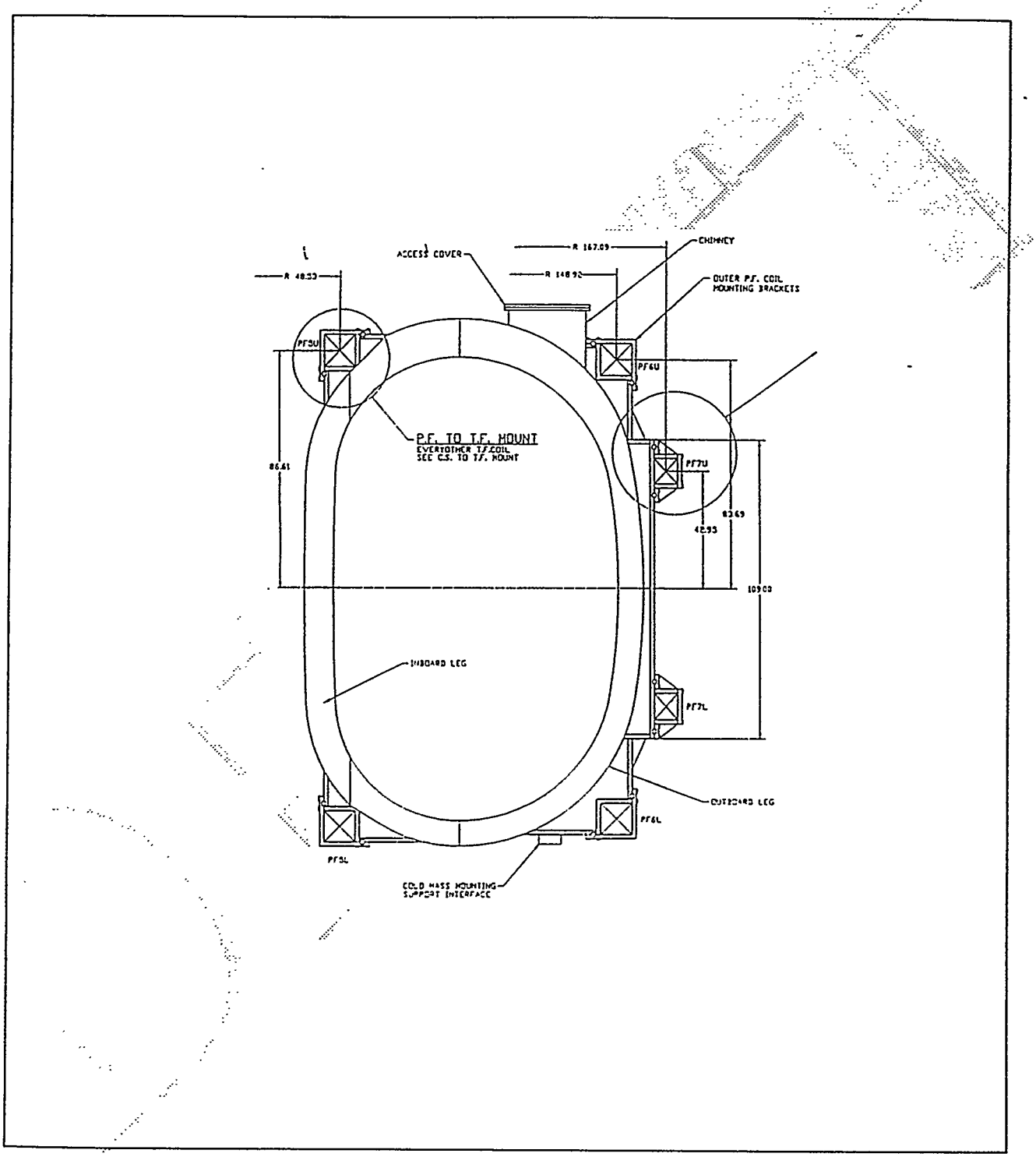

Figure 18. PF to TF Interface Detail.

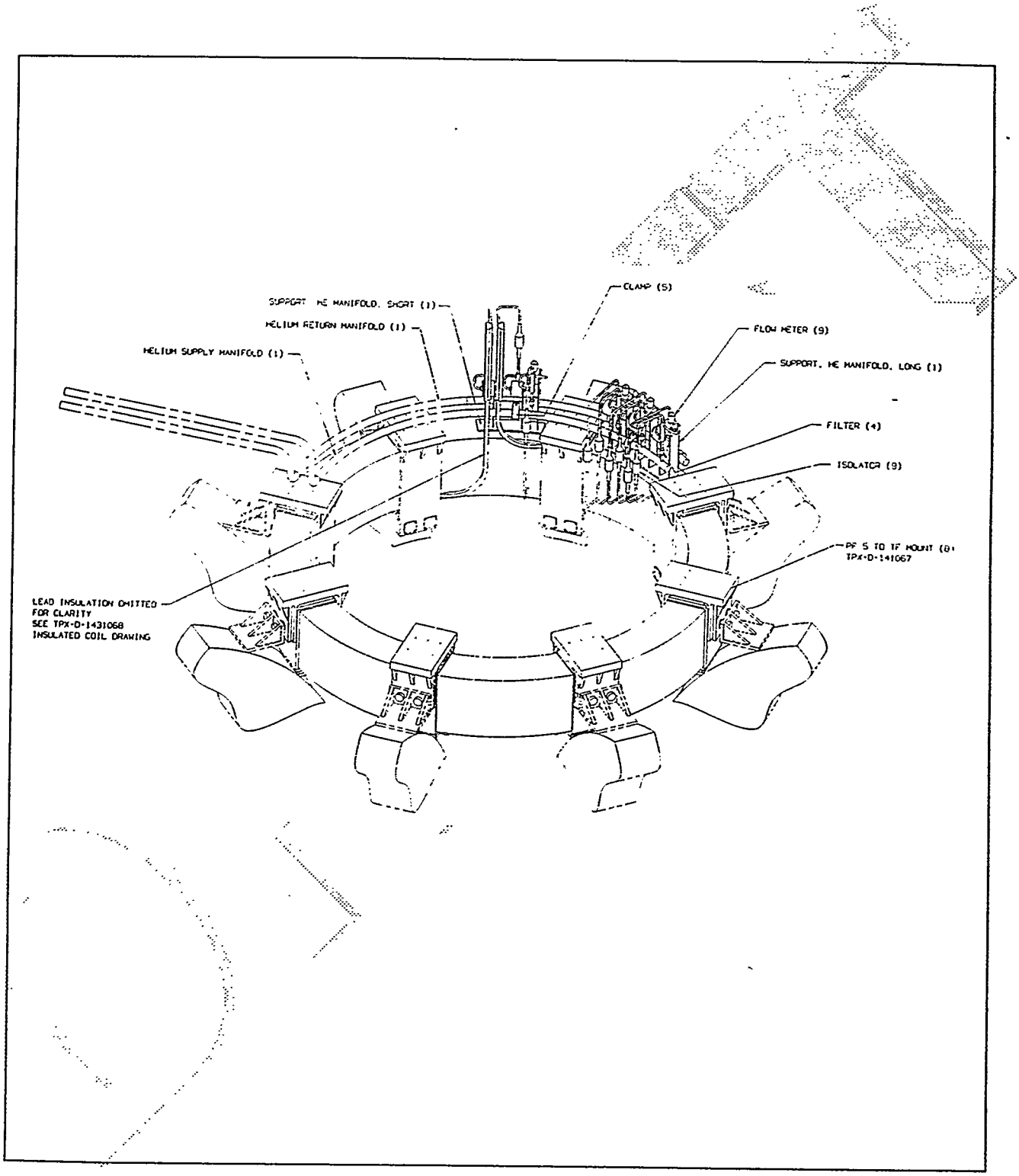

Figure 19. PF5 Mounts, Plumbing, and Leads.

2.1.3 Poloidal Field Coils 6 and 7

2.1.3.1 Coil description

PF6 and PF7, upper and lower, are superconducting cable-in-conduit conductors, using Nb-Ti composite strands and 316LN conduits. The required conductor length dictates that the winding pack construction for PF6 includes one mid-coil joint, and PF7 includes two. The coils have complete cases, each with two eddy current breaks, to support the winding packs against forces that tend to overstress the insulation and CICC. Each cased coil is clamped to the TF coil structure at 16 locations. The mounting brackets, similar in design to those for the PF5 coils, are bolted and keyed to the TF structure. After the mounts are disassembled, PF6U, PF7U, and PF7L can be removed vertically without tokamak disassembly.

2.1.3.1.1 Conductor and Conductor Properties

The conductor dimensions of PF6 and 7, upper and lower, are listed in Table 22 and the specified performance of the PF6 and PF7 conductors is shown in Table 23.

Table 22. PF6&7 Conductor Dimensions

Parameter	Units	Value
Conductor		Nb-Ti
Conduit		316LN
$n_{strands}$		360
D_{strand}	(mm)	0.78
P_w	(mm)	TBD
RRR		150
$w_{conduit}$	(mm)	22.3
$h_{conduit}$	(mm)	22.3
A_{cu}	(cm^2)	1.393
A_{noncu}	(cm^2)	0.328
$A_{conduit}$	(cm^2)	1.792
A_{Hecond}	(cm^2)	1.114
$A_{cond\ env}$	(mm^2)	571.2

Table 23. PF6&7 Conductor Performance Specifications.

Parameter	Units	PF6	PF7
B_{max}	(T)	3.28	2.31
$T_{b,nom}$	*(K)*	*4.2*	*4.2*
$J_c(B,T,e)$	(A/mm^2)	2075 @ 5 T, 4.2 K	2075
$\Delta T_{headroom}$	(K)	*<2.00**	2.605
$f_{critical}$		0.317	0.181
h^2_{IR}	(W/m^2-K)	567	249
$D_{f,eff}$	*(μm)*	*7*	*7*
$Loss_{Noncu}$ (± 3 T)	*(mJ/cc)*	*150*	*150*
Coupling time (B=0)	*(ms)*	*30*	*30*
RRR		*75*	*75*

*Does not meet S&CDC requirement

2.1.3.1.2 Coil Transition and Leads

PF6 is comprised of 20 pancakes with 6 turns in each pancake for a total of 120 turns. PF7 has 14 pancakes with 6 turns per pancake for a total of 84 turns.

Both PF coils are manufactured using the same roll forming process as that used in the construction of the PF1-5 coils. The process will pause part way through the roll forming to join the separate lengths of coil conductors together. The joints will occur at the outside diameter of the winding pack. Since, these NbTi coils will not be reacted, the coils will be cleaned and taped as they leave the roll-formers, and the turns will be deposited and located directly in the coil case. The coils will be vacuum pressure impregnated in their cases.

The leads for both coils are located on the outside diameter of the coil bundle and will incorporate lead spurs which will secure them structurally to the coil package.

2.1.3.1.3 Coil Hydraulics

The helium stubs are located on the outside diameter of the PF6&7 coils near the lead transition area. The cooling path schematic for PF6 and PF7 is similar to that illustrated for the CS coils shown in Figure 4. Each helium flow-path is comprised of a double coil pancake. The helium feed-throughs are located on the outer transition turns between pancakes. Each feed-through divides the supply or return flow between the two adjacent pancakes. The end of each lead will be capped to allow for an additional helium feed-through.

2.1.3.1.4 Coil Insulation and Insulation Properties

The PF6 and PF7 coil insulation scheme is identical to that of PF1-5.

2.1.3.1.5 Coil Manufacturing Process (PF 6 & 7)

- The Nb-Ti conductor will be received from the manufacturer on spools with sufficient conductor per spool to wind part of the coil continuously. A PF6 coil will contain 2 joints, so each spool will have approximately a third of the conductor length required. A PF7 coil will contain one joint, so each spool will contain approximately half of the conductor length required.
- The spools will be transferred to the winding station. The PF6 and PF7 winding station is similar to the CS winding station shown in Figure 6.
- The conductor will be fed from a spool, roll formed to the proper dimensions, and deposited directly into the coil case as it comes out of the roll forming tool. After the conductor passes the roll forming station, it will be wiped clean using a solvent (like ethanol) and insulated with (2) layers of polyimide film and one layer of dry glass tape. When a helium feed-through is reached, the conductor will be bored and the feed-through will be welded into position prior to insulating that portion of conductor (Figure 3).
- The coil bundle is then ground wrapped using 4 layers of half-lapped layers of glass insulation. Prior to the first layer of ground wrap, glass fill material will be applied between turns on the outside of the bundle to fill any potentially resin rich areas. A ground plane, a layer of conductive mesh (screen), will be overlayed, and an abrasion layer of glass insulation will be wrapped around the ground plane. Glass fill material will be applied between turns on the outside of the bundle to fill any potentially resin rich areas.
- The PF coil is then vacuum-pressure impregnated (VPI) using the case as a vacuum chamber, within a specially fabricated heat chamber,using a heat cured resin system. The case is evacuated and the epoxy resin is allowed to flow into the mold to wet the dry glass insulation. After a period of time the pressure is increased squeezing in the full compliment of epoxy resin. The coil is then heat cured for a pre-determined period of time.
- Final electrical testing will be performed. A DC Hipot Test will establish the voltage holdoff capability between the conductor and the ground plane. This test will confirm that 7.5 kV can be withstood with a leakage current of less than TBD. This test will not stress the insulation between the coil turns or layers, however, so either an impressed or an induced voltage test will be performed. In an impressed voltage test, a capacitor bank discharges into the inductive coil (room temperature), and the voltage across the coil divides according to its impedance. Alternatively, the coil could form the secondary of a transformer, and a rapid change in the primary current could induce voltage in the coil. Care must be taken not to damage the internal voltage taps when these tests are conducted. Detailed models and calculations will be developed to establish the test requirements.

2.1.3.2 Interface to TF Structure (PF 6 and 7)

PF 6U, 6L, 7U, and 7L are connected to the TF structure at 16 locations, every TF magnet case, see Figure 17 and Figure 18. A split steel collar surrounds the coil at the support locations to better distribute the in-plane and out-of-plane bending stress, see Figure 19. Shims are used as necessary to locate the coil current centers. Square keys are used to transfer shear from the PF coils to the TF structure. The mounts connecting PF 6 and 7 to the TF structure are similar to those for PF5 to allow for and differential radial motion between the coil and the structure; furthermore, the leaf spring in each mount centers the coil.

The PF 6 and 7 superconductors are Nb-Ti in a stainless steel conduit. Therefore, after cooldown or warmup, there is little thermal contraction difference between the TF structure and the PF 6 and 7 coils because all are constructed with stainless steel. See section 3.2.2.2 for discussion of analysis on PF 6 and 7 support structure.

DRAFT

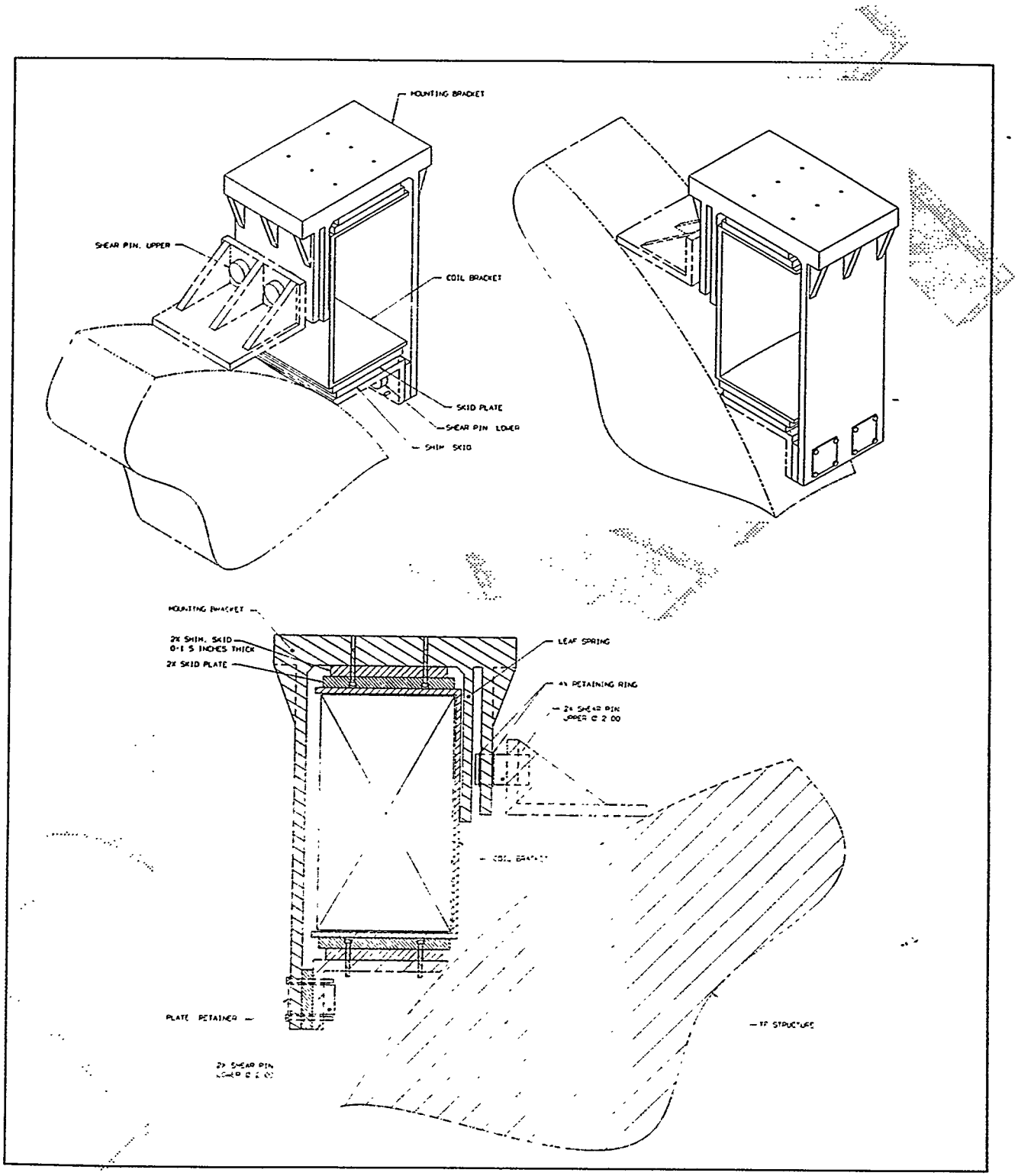

Figure 20. Detail of the Outer PF Support Structure.

2.2 System Performance

2.2.1 Nominal 2.0 MA, Double-Null (HC) Scenario

As described in the General Requirements Document[11] and the PF Magnet System Specification[1], the HC scenario is characterized by inductively ramping the plasma current to a full current of 2MA, applying auxiliary heating to raise the beta from its ohmic value to the Troyon limit, maintaining the plasma at full current and full beta, and then ramping the plasma current and beta down simultaneously.

Timing, volt-second, current requirements for the HC scenario are given in Table 24

Table 24. HC Scenario Evolution.

	Δt (s)	ΔΦ (total)	ΔΦ (cumulative)
Ramp Ip from 0 to full current (SOF state)	4	14.83	14.83
Heat plasma to full beta (SOB state)	1	0.54	15.37
Hold plasma at constant Ip, β_N (EOB state)	9	1.80	17.17
Simultaneously ramp Ip, β_N to 0	4	-4.19	12.98

The absolute value of the peak current requirements for the PF coils for the nominal HC scenario (excluding startup) are shown in Table 25 and the time dependent currents are shown in Figure 21. Individual coil terminal voltage differences are always less than 4.5 kV.

Table 25. Peak Currents in the PF Coils During the HC Scenario.

Coil	I cond_max (kA)	I cond_min (kA)	V term_max (kV)	V term_min (kV)
PF1,U+L	7.79	-24.61	0.25	-2.98
PF2,U+L	24.15	-13.36	0.19	-2.65
PF3,U+L	24.13	-5.58	0.12	-1.49
PF4,U+L	24.40	-0.54	0.22	-1.36
PF5,U+L	27.33	0.00	0.31	-4.46
PF6,U+L	1.23	-14.40	0.68	-2.88
PF7,U+L	1.43	-10.88	1.21	-4.08

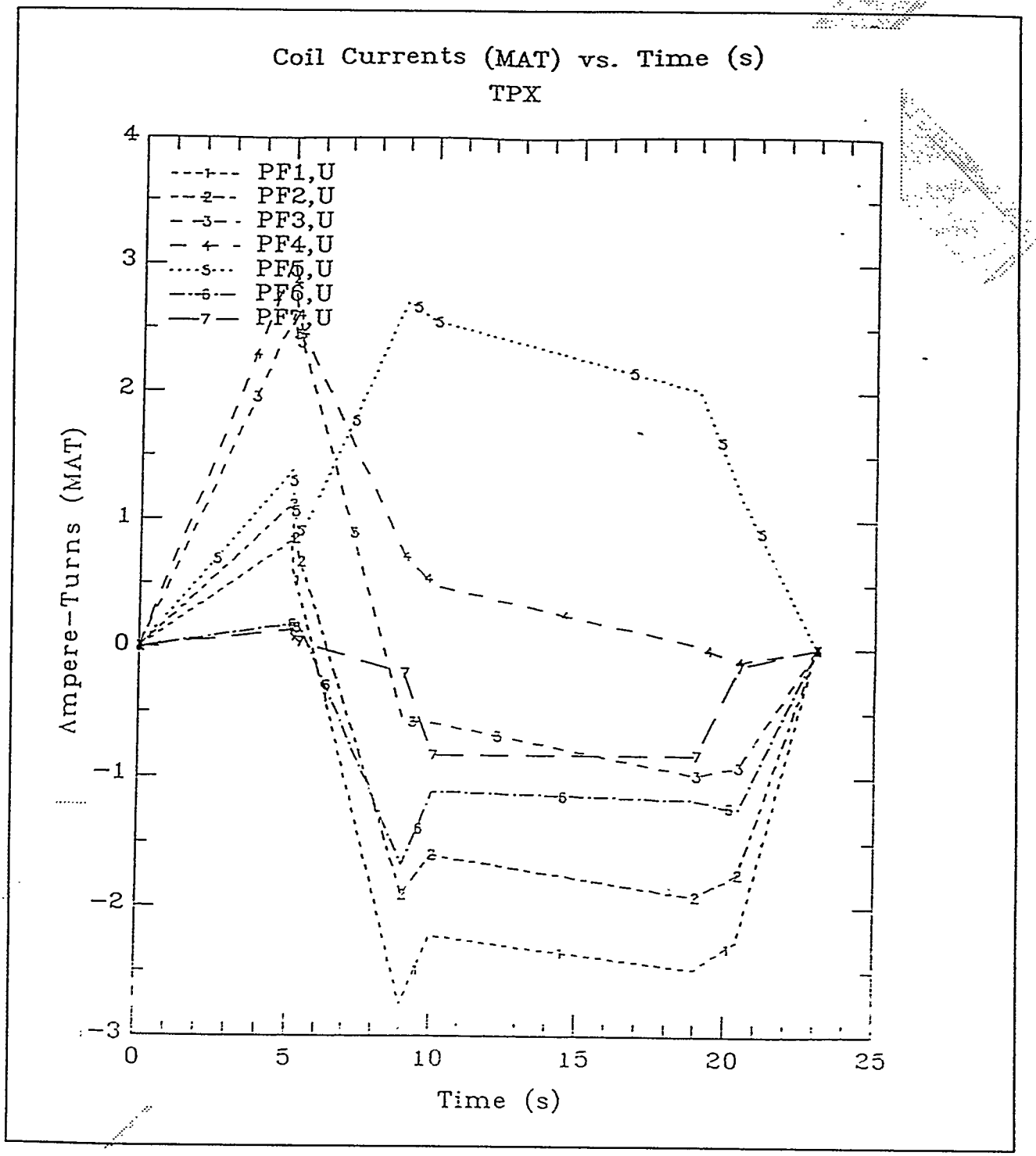

Figure 21. Coil Currents vs. time.

2.2.2 *Nominal low-current, double-null divertor operation (LC)*

The LC scenario is characterized by inductively ramping the plasma current to a full current of 0.4MA, applying auxiliary heating to raise the beta from its ohmic value to full beta at 0.4MA, linearly ramping the plasma current and beta to the EOB condition prescribed in the HC scenario, and then ramping the plasma current and beta down simultaneously. The timing and volt-second requirements for the LC scenario are given in Table 26:

Table 26. LC Scenario Evolution.

	t (s)	ΔΦ (total)	ΔΦ (cumulative)
Ramp I_P from 0 to 0.4MA (SOF state)	2	4.52	4.52
Heat plasma to full beta at 0.4MA (SOB state)	1	0.30	4.82
Ramp I_P and β_N to HC/EOB values (EOB state equivalent to HC/EOB state)	30	12.35	17.17
Simultaneously ramp I_P, β_N to 0	4	-4.19	12.98

2.2.3 *Discharge Cleaning*

The PF system is used for pulsed discharge cleaning. Discharge cleaning requires a 20 volt startup, and the capability to increase the plasma current to 1 MA, then drop the current to zero. The discharge cleaning scenario is TBD.

2.2.4 *β-l_i Flexibility*

The PF system is designed to provide a range of operation in β and l_i over which plasma equilibria may be controlled. This range is defined by the following plasma flexibility table, Table 27, described in the General Requirements Document (Section 1.2).

Table 27. Flexibility Space Parameters.

Double null, full current (Ip=2.0 MA or q=3, whichever is smaller)		Double null, q=5		Single null (Ip=2.0 MA or q=3, whichever is smaller)	
$l_i(3)$	β_N	$l_i(3)$	β_N	$l_i(3)$	β_N
0.5	2.2	0.4	5.0	0.5	2.2
0.4	5	0.4	7	0.5	5
0.7	0	0.7	0	0.7	0
1.2	0	1.5	0	1.2	0
1.2	5	1.5	7	1.2	5

2.2.5 Start-Up Simulations

The Poloidal Field Coil system for TPX must be capable of inductively initiating the HC and LC discharge scenarios with a preprogrammed startup sequence of coil current/voltage waveforms. The rapid current changes in the PF coil system required for this function will induce eddy currents in the nearby conducting structure which will perturb the magnetic field environment.

Simulations have been performed to show that the PF set is capable of producing the requested field environment in the presence of the passive stabilizing plates and the vacuum vessel[12]. The results of these simulations are presented in Table 28 which lists the requirements from Section 1.3.3.1 and along with the computed values for the 12 V start-up case.

Table 28. Start-Up Specifications.

	REQUIREMENT	REQUIRED VALUE	COMPUTED VALUE
CHARGE			
	FLUX LINKAGE	9 V-s	9 V-s
BLIP			
	VERTICAL FIELD	NULL for 5 ms; $\lvert B_z \rvert < 1$ mT over 0.3m	Null for 20 ms; $\lvert B_z \rvert < 1$ mT over 2.1 m < R < outer limiter at Z=0 m and -0.3 m < Z < 0.3 m at R=2.47 m
	FIELD GRADIENT	$\lvert \nabla B \rvert$ <10 mT/m over <0.25m	-6.2 mT/m <$\lvert \nabla B \rvert$ <1.1 mT/m at Z=0 m
	LOOP VOLTAGE	12 V	12 V
PLASMA CURRENT RISE			
	VERTICAL FIELD	SHAFRANOV	Good
	FIELD GRADIENT	$0.2 < n_f < 1.0$	Good
	DURATION	I_p>100 kA in 0.1 sec	I_p=101 kA in 0.1 sec

Table 29 summarizes the power supply voltages and currents, the blip resistors, and the PF coil terminal voltages at the major time points at which power supply voltages or resistors are changed. Similar information is presented in Figure 22, which shows a simplified circuit diagram for each coil for each of the time points. The time points detailed are: $t = 0^-$, 0^+, 0.085^-, 0.085^+ seconds. These time points correspond to the end of charge, start of blip, 12 V end of blip, and 12 V start of plasma current ramp, respectively.

Table 29. PF Coil Voltages and Currents at Critical Points during a 12-V Plasma Initiation.

TIME (s)	COIL	R (Ω)	V_{PS} (kV)	I (kA)	V_{term} (kV)
0.0^-	PF1		0.364	7.875	0.182
	PF2		0.383	2.468	0.192
	PF3		0.240	2.372	0.120
	PF4		0.210	2.363	0.105
	PF3		0.607	2.099	0.304
	PF6		0.432	1.064	0.216
	PF7		0.344	1.514	0.172
0.0^+	PF1	0.330	-1.2	7.875	-1.899
	PF2	0.070	-1.2	2.468	-1.464
	PF3	0.025	-1.2	2.372	-0.896
	PF4	0.015	-1.2	2.363	-0.777
	PF5	0.190	-1.2	2.099	-2.594
	PF6	1.5	-1.2	1.064	-1.398
	PF7	1.0	-1.2	1.514	-1.357
0.085^-	PF1	0.330	-1.2	5.519	-1.511
	PF2	0.070	-1.2	21.88	-1.366
	PF3	0.025	-1.2	20.47	-0.856
	PF4	0.015	-1.2	20.51	-0.754
	PF5	0.190	-1.2	17.85	-2.296
	PF6	1.5	-1.2	0.951	-1.313
	PF7	1.0	-1.2	1.168	-1.184

TIME (s)	COIL	R (Ω)	V_{PS} (kV)	I (kA)	V_{term} (kV)
0.085+	PF1	0.330	-0.525	5.519	-1.173
	PF2	0.070	-0.113	21.88	-0.822
	PF3	0.025	0.469	20.47	-0.022
	PF4	0.015	0.857	20.51	0.275
	PF5	0.190	0.826	17.85	-1.283
	PF6	1.5	0.309	0.951	-0.559
	PF7	1.0	-1.042	1.168	-1.105

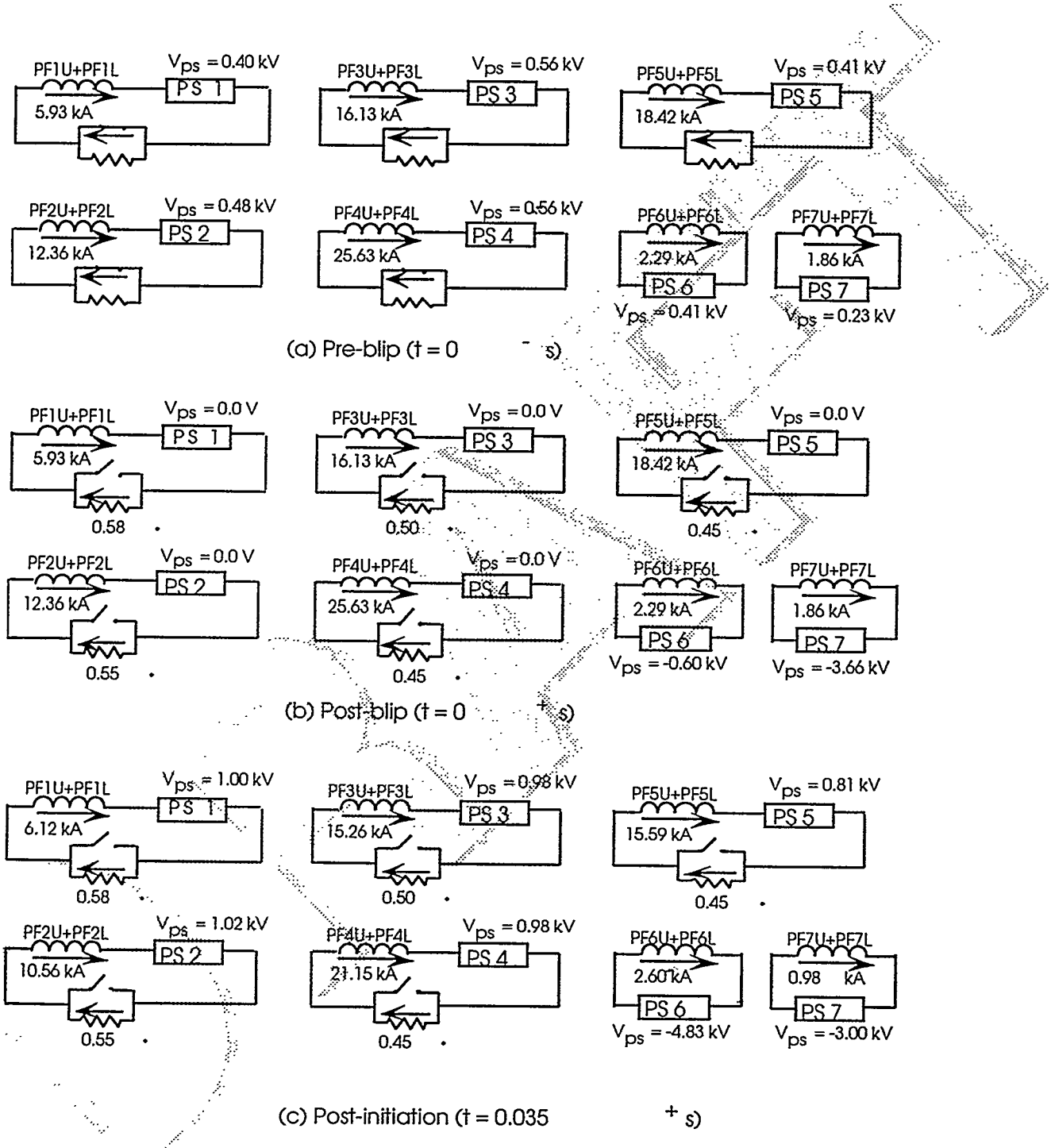

Figure 22. PF coil voltages and currents at critical time points during a 12-v plasma initiation scenario.

2.3 Interfacing Systems

2.3.1 Nomenclature.

The PF Magnet System interactions are shown as arrows from one element to another in Figure 23. The external interfaces are interactions between WBS 14 elements and elements outside the WBS 14 boundary, and the internal interfaces are those within the WBS 14 boundary. Functional interfaces are those that, with the transfer of information across the interface, may change the state of one or both of the interfacing elements. Physical interfaces are those that provide mechanical connections from one element to another.

The primary type of interaction is described by the arrow label in the figure. Interface Control Documents (ICDs) have been (or will be) developed to describe each interface. The ICD is the definitive description of the interface. The following paragraphs summarize the most important interfaces.

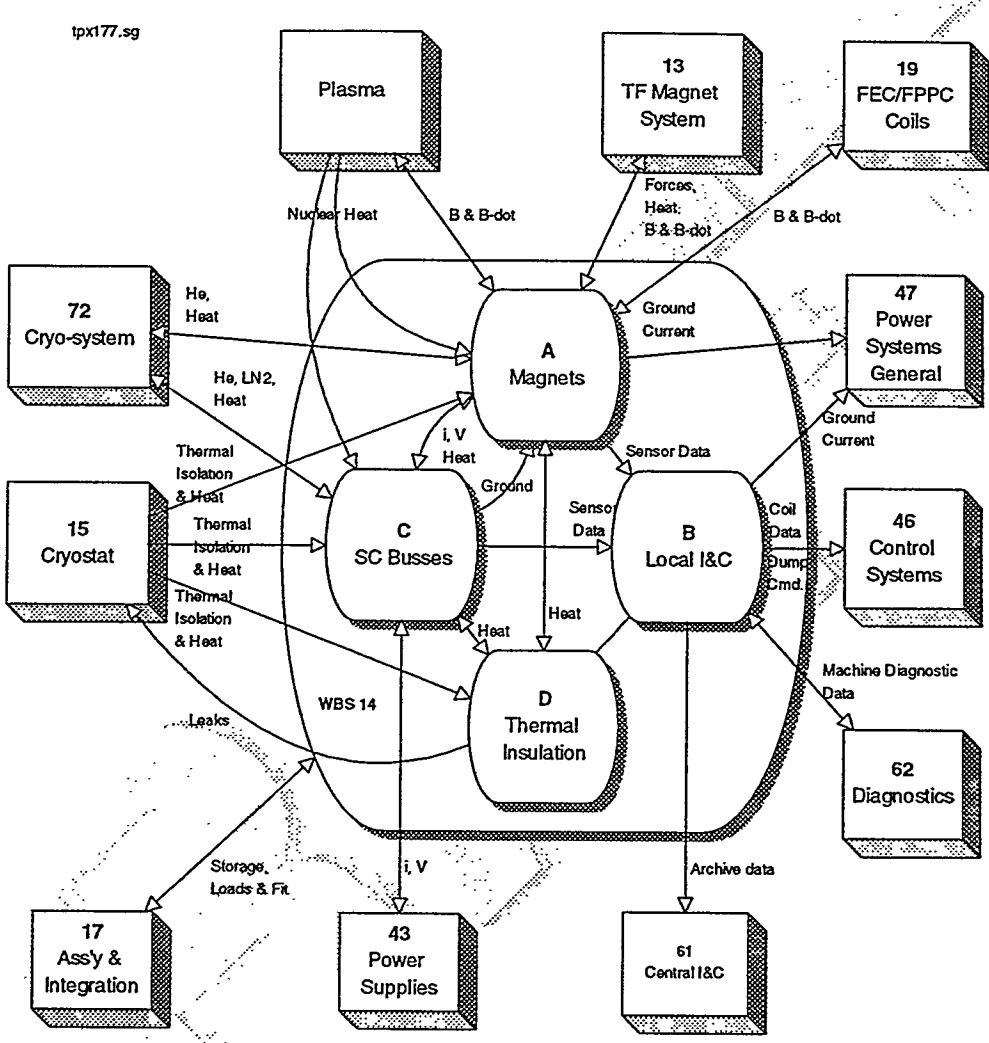

Figure 23. The PF Magnet System and its Environment.

2.3.2 *External Functional Interfaces*

WBS 13: The PF Magnet System provides gravitational, thermal, and magnetic loads on TF magnet coils. The details of this interaction are specified in TPX-ICDP-1314.

WBS 15: The Cryostat provides thermal isolation to the PF magnets, busses, and thermal insulation. The Cryostat evacuates outgassed and leaking material from the PF Magnet System. The details of this interaction are specified in TPX-ICDP-1415.

WBS 17: The PF Magnet System components must be stored at the TPX site, and they must be assembled and integrated into the tokamak. The details of this interaction are specified in TPX-ICDP-1417.

WBS 19: The PF Magnet System changing magnetic fields induce voltage in the FEC/FPPC coil circuits and vice versa.

WBS 43: The PF Power system provides current and voltage to the PF coils. The details of this interaction are specified in TPX-ICDP-1443.

WBS 46, The Power Systems Controls receive coil dump control commands specified in TXP-ICDP-1446.

WBS 61: The PF Magnet System provides archive data to the Central I&C system. The details of this interaction are specified in TPX-ICDP-1461.

WBS 62. The PF Magnet System provides machine diagnostic data to the Diagnostics subsystem.

WBS 72: The Cryogenic System provides helium and LN_2 the PF Magnet System and the PF Magnet System transfers heat to cryogenic system's coolants. The details of this interaction are specified in TPX-ICDP-1472.

Plasma. The PF Magnet System provides magnetic fields and changing magnetic fields that heat, control, and shape the plasma. The magnetic field or changing magnetic field of the plasma couples to the PF Magnet System circuits. The plasma also provides nuclear radiation which is absorbed by components of the PF Magnet System.

2.3.3 External Physical Interfaces

WBS 13, TF Magnet Interfaces: The central solenoid, and each ring coil are each supported at interfaces to the TF Magnet System. This interface is specified in TPX-ICDP-1314.

WBS 17, Assembly & Maintenance Interfaces: There are lifting provisions for assembling and maintaining the PF magnets. This interface is specified in TPX-ICDP-1417.

WBS 43, PF Power System Interfaces: Central solenoid coils and ring coils are electrically connected to PF Power System power leads at the warm end of the vapor cooled bus. This interface is specified in TPX-ICDP-1443.

WBS 47, Power Systems General: The leads of the ground planes are connected to the Power Systems single point ground. This interface is specified in TPX-ICDP-1447.

WBS 61, Central I & C Interfaces: Local I & C signals are electrically connected to the Central I & C. This interface is specified in TPX-ICDP-1461.

WBS 72, Cryogenic System Interfaces: Helium coolant supply and return manifolds are connected to Cryogenic System manifolds as specified in TPX-ICDP-1472.

2.3.4 Internal Interfaces

Superconducting Busses to Magnets: The superconducting leads from the PF1-PF5 coils will be Nb3Sn and the superconducting leads from the PF6 and PF 7 coils will be NbTi. The coil leads will be connected electrically and thermally to the NbTi superconducting bus. The Magnet and SC Busses grounds are joined together. This interface is specified in TPX-ICDS-143146.

Local I&C to Magnets: The PF Magnet System quench detection sensors, flow meters, and temperature sensors will connect to the Local I&C system. This interface is specified in TPX-ICDS-143145.

Thermal Insulation to SC Bus and to Magnets: Thermal insulation, such as Multi-Layer-Isulation (MLI), may be attached to the SC Bus and Magnets components. Heat is transferred between PF Magnet System elements via the Thermal Insulation. This interface is specified in TPX-ICDS-TBD.

2.4 Instrumentation & Control (I&C)

This section will be provided under separate cover.

2.4.1 Quench & Fault Detection (Protection System)

This section will be provided under separate cover.

2.5 RAM Requirements

These are described in other sections

2.6 Component Design Description

These are described in other sections

3. DESIGN BASIS

3.1 Codes and Standards

Many components of the TPX PF magnet system are not covered by specific codes or standards due to the unique nature of the designs, environment, and materials used. The TPX Structural and Cryogenic Design Criteria (Ref. 5), specifies the criteria that the PF magnet system will be designed to meet. The TPX Structural and Cryogenic Design Criteria (Ref. 5) follows the guidance of the ASME Boiler and Pressure Vessel Code to the extent practical. Where the TPX Structural and Cryogenic Design Criteria do not apply, the standards and codes shown in Table 30 shall apply to the design and construction of the PF Magnet System components:

Table 30. Standards Associated with the Construction of the PF Magnet System Hardware.

Item	*Standard / Code*	*Section(s)*
Central Solenoid Structure		
Weldments	ANSI/AWS Structural Welding Code	D1.1-90
	ANSI/AWS Recommended Practices for Welding Austenitic Chromium-Nickel Stainless Steel	D10.4-79
	Structural & Cryogenic Design	

Item	Standard / Code	Section(s)
	Criteria	
Fasteners	Structural & Cryogenic Design Criteria	
Hydraulic manifolds and piping	ASME Boiler and Pressure Vessel Code	Sec VIII
	ANSI/AWS Specification for Qualification of Welding Procedures and Welders for Piping and Tubing	D10.9-80
	DOE Pressure Safety Guidelines	
Coils		
Weldments	ANSI/AWS Structural Welding Code	D1.1-90
	ANSI/AWS Recommended Practices for Welding Austenitic Chromium-Nickel Stainless Steel	D10.4-79
	Structural & Cryogenic Design Criteria	
Nb_3Sn Reaction		
Conductor insulation	Structural & Cryogenic Design Criteria	
Hydraulic manifolds and piping	ASME Pressure Pipe Code	
	ANSI/AWS Specification for Qualification of Welding Procedures and Welders for Piping and Tubing	D10.9-80
	DOE Pressure Safety Guidelines	
Grounding	TPX Grounding	All
Radioactive Waste	Code of Federal Regulation	Title 10
Coil cases		
Weldments	ANSI/AWS Structural Welding Code	D1.1-90

Item	Standard / Code	Section(s)
	ANSI/AWS Recommended Practices for Welding Austenitic Chromium-Nickel Stainless Steel	D10.4-79
	Structural & Cryogenic Design Criteria	
PF Magnet System	TPX Seismic Design Criteria	All
	ANSI Y-14.5M, Geometrical Tolerancing and Dimensioning	

3.2 Analysis

3.2.1 Overview

Thermal and structural analysis has been completed for the PF winding pack and structure. Neutron and gamma heating, superconductor pulsed field losses have been calculated, along with the ability of the coil cooling system to remove them. Quench detection signals have been calculated along with the electrical and thermohydraulic behavior of a PF channel during a quench and dump. (These analyses are covered in MIT reports.) Only the 2 MA HC operation has been analyzed. Thermal and structural analyses at the corners of flexibility space specified in Section 1.3.1 have been performed.

3.2.2 Structural Analysis

We have performed the structural analyses shown in Table 31.

Table 31. Structural Analyses.

Description	Results	Reference
2D Axisymmetric Model of PF3 with staggered and aligned conduits	Winding pack analysis confirmed by the large scale test program	TPX-14-950801-WEC-WHannan-01
Smeared Properties for Regimented Winding Pack	Used to analyze PF6&7	TPX-14-950801-WEC-WHannan-01
Beam Model for PF6&7	Confirmed that, without a coil case on PF6&7, there is a heavy reliance on the epoxy matrix to limit conduit stresses.	TPX-14-950810-WEC-TSchultheiss-03
Detailed 3D Model of PF6&7 Winding Pack	Never converged	TPX-14-950810-WEC-TSchultheiss-03
Detailed 3D Model of PF5	Conduit plays a major role in limiting bending	TPX-14-950808-WEC-MKrefta-03

3.2.2.1 Structural Analysis of the Central Solenoid

The report, TPX-14-950801-WEC-WHannan-01, TPX PF1-4 Coil Pack Structural Analysis,. presents the results of the finite element analysis of the TPX CS winding pack for the CDR and CPDR designs. Models were constructed and analyzed using ANSYS and give the stress fields for the conduit, conduit wrap, corner fillers, transition pieces and the ground wall insulation. For the CDR design, unacceptable shear and through thickness tensile stresses were found. Only 61% of the area of insulation passed the shear stress design criteria with 56% of the area experiencing through thickness tension, two thirds of which exceeded 50 MPa. These stresses were driven by, in order of importance, the anisotropic properties, principally thermal contraction and modulus, of the insulating components, the thermal contraction mismatch between the Incoloy 908 conduit and the insulating system, and the concave deformation of the conduit under load. To improve the design, glass weaves providing more through thickness fibers were developed to better approach isotropic properties and reinforce the corner fillers against tension. The shear properties of the glass/epoxy components were measured both in compression and in tension. Finally a non-bonded insulation to conduit interface (also known as "slip plane") was adopted. The results are as follows:

1. 99.87% of the conduit wrap passes the design criteria
2. 100% of the ground wall insulation passes the design criteria.

3. The corner fillers are still under very high combined tensile and shear stress with only 36% passing the criteria.

4. 90% of the transion pieces/spacer blocks pass the criteria

Further work should be directed at stronger reinforcement of the corner fillers increasing the glass in the tips of the fillers from 1-2% to 10-12% and increase the through thickness glass of the spacer blocks particularly at the edges to reduce the stresses at the interface with the other insulating components.

3.2.2.2 Structural Analysis of the Outer Poloidal Field Coils

3.2.2.2.1 Stresses From Magnetic Loads in PF6&7.

The presence of a slip plane between the conduits and the glass/epoxy results in a unique type of structure. This structure will allow hoop loads to be shared between the conduits and the glass/epoxy, according to the usual ratio of membrane stiffness (E_1A_1/E_2A_2) for two constituents 1 and 2, where E_1 is the Young's modulus and A_1 the cross-sectional area of the first constituent, and similarly for the second constituent. If no coil case is used, the bending loads are shared between the 316LN conduits and the glass/epoxy by the bending stiffness ratio (E_1I_1/E_2I_2), where I_1 and I_2 are the moments of inertia of the glass-epoxy and stainless-steel conduits, respectively. In calculating the moment of inertia of the glass-epoxy, the moment is calculated for the multiply-connected glass-epoxy as one single piece, ignoring possible cracks and defects that may be present. The moment of inertia of the conduits taken together is, however, taken to be the sum of the individual moments of inertia of the conduits, since the conduits are allowed to slip with respect to the glass/epoxy. As a result, the moment of inertia of the conduits as a unit is low and they resist less than 5% of the bending load. Without a coil case, 95% of the bending load would be resisted by the glass/epoxy structure. When a case is added, it carries almost all of the bending loads since its stiffness dominates the overall coil stiffness, and bending stresses in the interior drop dramatically from their no-case values. This structural report presents the sharing of magnetic loads between the 316LN stainless steel structure (with and without a coil case, or a radial band on the outer radius of the ground wrap which has been suggested as an alternative to the coil case) and the glass/epoxy and resulting stresses. For purposes of understanding the effects of the slip plane a design assuming a bond between the conduits and Kapton was also examined.

Analyses to determine the effects of magnetic loads were performed to achieve the following:

- Separate bending loads from hoop loads.
- Determine the level of stress in the glass/epoxy and 316LN for different configurations.
- Determine the effects of a coil case.
- Determine the effects of a radial band.

Determine the performance of a winding pack which has structurally failed in the glass epoxy and in which all bending loads are resisted in the conduits, assuming no coil case or radial band.

Solid finite element models were not used to determine the results of these configurations. Instead, beam models were used to input the azimuthal variation in radial and axial load and to obtain the bending moments, hoop loads, and shear loads separately. From the ratios of membrane stiffness and bending stiffness, the loads and stresses in the 316LN structure and the glass/epoxy were determined. Five different configurations were analyzed as follows:

- Configuration 1. Baseline design which includes slip plane between the conduit and kapton

- Configuration 2. Assume no slip plane between the conduit and kapton
- Configuration 3. With slip plane assume failure of glass/epoxy
- Configuration 4. 5/8 Coil Case with slip plane
- Configuration 5. 1.725 inch thick radial band on outer radial surface with slip plane

A summary of the maximum stresses resulting from the magnetic load analyses are given in **Table 33** through **Table 35.** The load share between the 316LN stainless steel and the glass/epoxy was determined from the ratio of the appropriate stiffness. The stresses were then determined base on this load share. **Table 32** and **Table 34** show PF6 hoop stress and PF7 hoop stress respectively. For all configurations and for both coils the 316LN carries most of the hoop load. Bending loads result in a much different load share. The slip planes between the conduits and glass epoxy reduce the moment of inertia of the conduits to such a small level that 95% of the bending loads are carried in the glass/epoxy for the baseline configuration (configuration 1).

Table 32. Summary of PF6 Max Hoop and Max Shear Stresses.

Configuration	Max Hoop 316LN Stress MPa SBR	Max Hoop Glass/Epoxy Stress MPa SBR	Max Shear Stress MPa 316LN SYZ	Max Shear Stress MPa Glass/Epoxy SYZ
PF6 Config 1	140.	21.8	.128	7.53
PF6 Config 2	140.	21.8	9.49	1.74
PF6 Config 3	175.	-	13.2	-
PF6 Config 4	74.2	11.6	5.15	1.01
PF6 Config 5	75.6	11.8	4.84	1.62

Table 33. Summary of PF6 Max Bending Stresses.

Configuration	Max Bending Stress MPa 316LN SBR	Max Bending Stress MPa Glass/Epoxy SBR	Max Bending Stress MPa 316LN SBZ	Max Bending Stress MPa Glass/Epoxy SBZ
PF6 Config 1	15.4	19.7	22.0	75.9
PF6 Config 2	49.4	7.71	113.0	17.6
PF6 Config 3	304.	-	2110.	-
PF6 Config 4	17.3	2.30	64.9	10.1

PF6 Config 5	17.9	2.79	102.0	16.0

Table 34. Summary of PF7 Max Hoop and Max Shear Stresses.

Configuration	Max Hoop 316LN Stress MPa SBR	Max Hoop Glass/Epoxy Stress MPa SBR	Max Shear Stress MPa 316LN SYZ	Max Shear Stress MPa Glass/Epoxy SYZ
PF7 Config 1	59.1	9.22	261	7.96
PF7 Config 2	59.1	9.22	14.7	2.84
PF7 Config 3	74.6	-	31.5	-
PF7 Config 4	40.4	6.30	17.3	1.35
PF7 Config 5	42.3	6.61	1.53	2.63

Table 35. Summary of PF7 Max Bending Stresses.

Configuration	Max Bending Stress MPa 316LN SBR	Max Bending Stress MPa Glass/Epoxy SBR	Max Bending Stress MPa 316LN SBZ	Max Bending Stress MPa Glass/Epoxy SBZ
PF7 Config 1	12.7	16.2	33.5	81.0
PF7 Config 2	41.3	6.40	131.	20.4
PF7 Config 3	254.		1590.	-
PF7 Config 4	13.8	1.83	67.1	9.58
PF7 Config 5	15.4	2.40	118.	18.4

Results of adding a coil case are shown in the results of configuration 4, which shows that most of the bending loads are resisted by the coil case, in fact all of the bending loads can be resisted by the coil case. Configuration 5 shows the results from a radial band which replaces the coil case. This band will resist the bending loads if the shear bond between it and the ground wrap holds.

Configuration 3 represents failure of the glass/epoxy. The stresses in the conduit go above their allowable and the conduits fail. The glass/epoxy therefore must be considered the primary structure for resisting bending loads.

3.2.3 Thermal Analysis

3.2.3.1 Nb_3Sn Temperature Margin Calculations.

The report, Verification of Margin in PF2 & 5, TPX-14-950731-WEC-OChristianson-02, describes the calculations used to verify the MIT temperature margin calculations during the HC scenario. Coils 2 and 5 are analyzed. The computer code, QUENCHER, is used to calculate the temperature rise due to AC losses and nuclear heating. The

temperatures are slightly less than in the MIT analysis because the AC heating is reduced. The temperature distributions agree well with the MIT calculations. Current sharing temperatures are found from the superconducting temperature, peak magnetic field, and the transport current. The values found in this analysis are slightly lower than the MIT values, probably because it is conservatively assumed that the peak temperature and magnetic field occue at the same location. Temperature margin and headroom system requirements are met. Results closely, but not exactly, match the MIT values, indicating this analysis confirms the MIT margin calculations. Flow reversal occurs during the initial and final heating parts of the HC scenario. Flow is re-established when the heating decreases at about 10 seconds into the HC scenario. A quick analysis suggests that dwell times of 20 and 40 minutes will prevent ratcheting in the coils..

3.2.3.2 PF6&7 Cooldown Stress

Thermal stresses were determined from an axisymmetric finite element model, which included all the conduit cell components, the filler block, and the ground wrap; the effects of the coil case are not yet included. The model is the full width of the PF6 and PF7 coils, 6 turns. Only a partial height model was used (8 pancakes) since this is large enough to capture all the important thermal stress effects. The model includes gap elements between the 316LN conduits and the Kapton. Material properties which were used were provided by Westinghouse STC. The model was run to determine stresses due to only thermal loads set up from a reference temperature of 293K and assuming all materials are at 4K. The model does not include a coil case. Thermal stresses including a coil case will be determined in the next phase.
Stress limits for the glass/epoxy are given as follows. The equation to predict the failure for the 3D weave components under shear and normal compression are as follows:

- Allowable shear/compression stress (MPa) = .7*compressive stress + 52 MPa
- Tension only Allowable (MPa) = 46.12
- Allowable shear/tension stress (MPa) = -1.13*tensile stress + 52 MPa

Stresses due to a difference in coefficient of thermal expansion between the 316LN conduits, the 3-D corner fill and the ground wrap are shown in Table D.1

Table D.1 Summary of Thermal Stresses Due to Cooldown.

Material	Max Tresca MPa	Max Principal MPa	Through Thickness MPa	Shear In Interlamina r Direction MPa	Max Stress Laminar Direction MPa	Hoop Stress MPa
316LN Conduit	118. MPa	127 MPa				
Kapton			2.6	4.3	31.8	19.7
Turn Wrap			11.8	17.5	128.1	34.0
Corner Fill			33.3	36.6	109.1	30.8
3D Block Fill			46.0	11.5	34.5	14.9

Ground Wrap			33.4	36.5	63.4	-11.1

The stresses shown in the shaded region indicate values which are near or over the limits assumed for 60000 cycles (50% degradation). This represents risk since the glass/epoxy structure must carry 95% of the magnetic bending loads. This is shown in the next section where bending stresses are compared for several different winding pack configurations.

3.3 R&D Summary and Plans

The Manufacturing R&D program conducted during Phase 1 by the PF Magnet System contractor is documented in a series of reports shown in Table 36. The R&D topics included Insulation R&D and Helium Stub R&D. The results of the R&D programs have been incorporated into both the PF and TF coil designs.

Table 36. Manufacturing R&D Reports.

Report Number	*Title*
14-950718-WEC-PSanger-01	TPX Shear / Compression Testing
14-950720-WEC-PSanger-01	TPX Through Thickness Tension Testing
14-950714-WEC-FRoach-01	1x2 Insulation Electrical Test Report
14-950719-WEC-FRoach-01	3x3 Insulation Electrical Test Report
14-950719-WEC-JHillenbrand-01	3x3 Insulation Mechanical Test Report
14-950605-WEC-FRoach-01	Mechanical Properties Matrix of Insulation Materials for Structural / Thermal Analysis
14-950615-WEC-FRoach-01	Acceptance Testing Criteria and Test Voltages to TPX 3X2 and 5x5 Insulation R&D Models
14-950621-WEC-PSanger-01	TPX Magnet Insulation Large Scale Verification Test Program - Part 1, Objective and Success Criteria
14-950621-WEC-JHillenbrand-02	TPX Magnet Insulation Large Scale Verification Test Program - Part 6, Description of Test and Test Sequence.
14-950818-WEC-PSanger-01	TPX Magnet Insulation Large Scale Verification Test Program
14-950818-WEC-JHillenbrand-02	TPX Magnet Helium Stub Manufacturing R&D

In Phase 2, we plan to continue the Manufacturing R&D programs. A description of the topics and scope of the programs is given in TBD.

DRAFT

4. DESIGN IMPLEMENTATION

4.1 Prototype Coil

This section will be provided under separate cover.

4.2 Mockup

The PF coils are shielded by the TF and other structures to prevent them from becoming radioactive. Thus, there is no need for a mockup of any of the PF coils.

4.3 Component Procurement and Fabrication

The Integrated PF Magnet Plan[13] describes the Phase 2 efforts. The TPX PF Magnet System preliminary design will continue until the PDR scheduled for May 1996. Other milestones include the Final Design Review in May 1997, the prototype coil fabrication in February 1998, the production readiness review in August 1998, and PF coil deliveries beginning in June 1999.

4.4 PF Assembly, Installation, and Testing

4.4.1 Central Solenoid Installation and Removal

The entire central solenoid assembly is installed with the 50 ton crane at the TPX site. During assembly the large cryostat top lid in not installed; so there is enough (height) clearance to install the CS assembly. The CS assembly is lifted via the crane pick point located on the centerline of the support structure, see Figure 24.. The CS assembly is lowered into place, shown in phantom in the figure, and bolted to the TF structure.

The removal of the CS assembly is through the smaller center lid on top of the cryostat larger lid . With the larger cryostat lid in place the height clearance is reduced by 50 inches. In this case the CS assembly is removed one of two ways. If there is enough height clearance, the CS assembly is removed the same way it was installed after the conductor and helium leads are disconnected. However, if there is not enough room the following alternative will prevail: First, the CS is temporally supported from below, next the top support structure is removed and replaced with a lifting fixture that fits into the bore of the CS. The conductor and helium leads are disconnected and the CS assembly is removed.

4.4.2 PF 5 Installation and Removal

A strongback installation/removal fixture is used for all of the PF ring coils. Each coil has a different location for its support straps depending upon its radius. The large cryostat lid must be removed during installation or removal of any of the PF ring coils. The PF5 coil is connected to the installation/removal fixture via straps and is lowered into place by the 50 ton crane. PF5U can be installed or removed independent of the other PF and TF coils. However, PF5L must be fixtured temporary at a lower location during the installation of the TF magnets and then raised into its final location. The removal of PF 5L requires that all of the other PF magnets and half of the TF magnet system be removed first, making this a difficult and costly process.

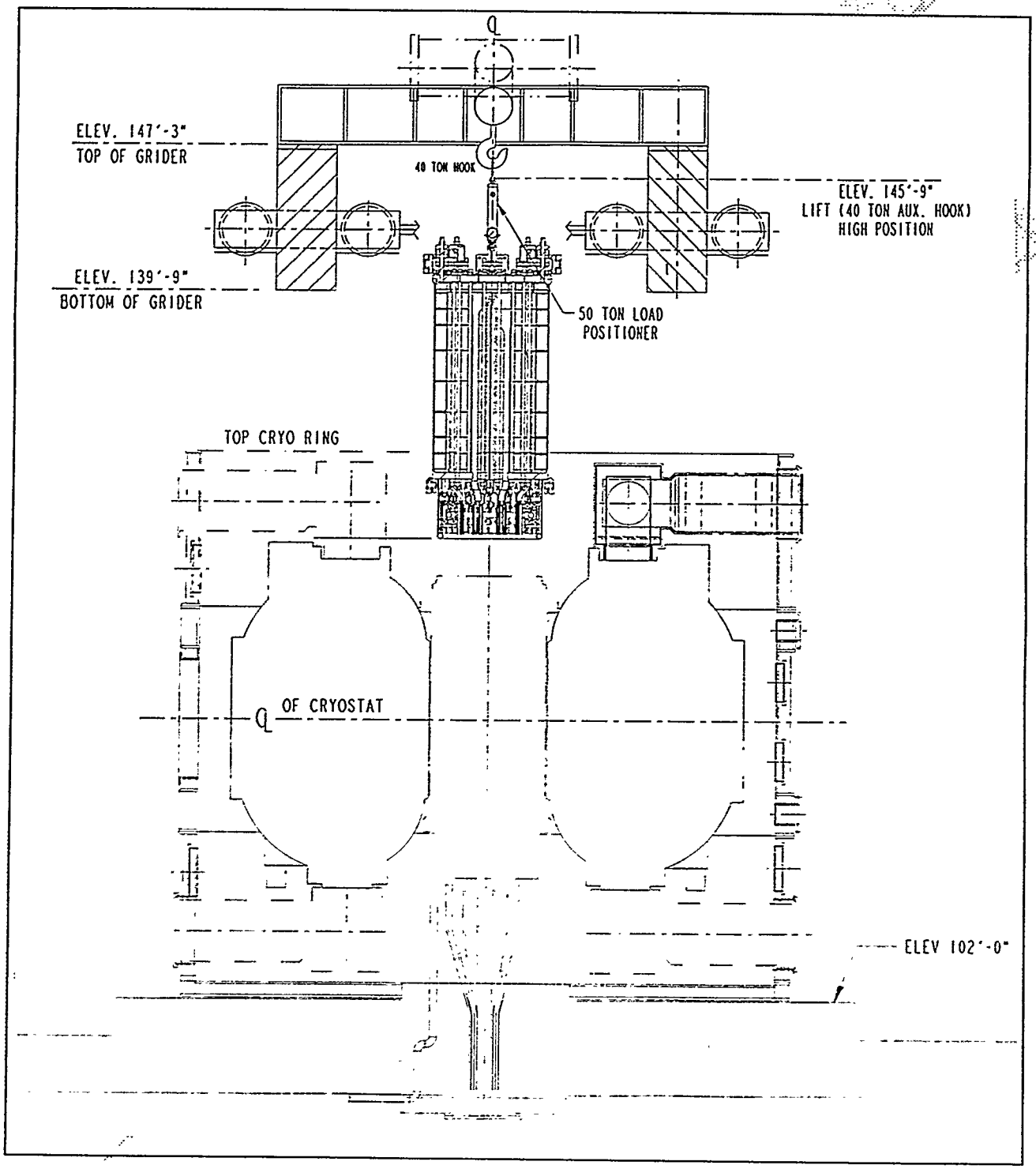

Figure 24. Central Solenoid installation and removal..

Unintentionally left blank.

4.4.3 PF 6 and 7 Installation and Removal

The fixture to install/remove PF 6U, 6L, 7U and 7L is a strongback similar to that used for the PF5 coils. The large cryostat lid must be removed during installation and removal of any of the outer PF coils. PF6U and PF7U can be installed or removed independent of the other PF and TF coils. PF7L must be installed before PF7U, and the sequence is reversed during the removal of PF7U. PF6L will be fixtured temporary at a lower location during the installation of the TF magnets and then raised to its final location. The removal of PF6L requires that the upper PF coils, the CS coils, and all of the TF magnets be removed first, making this a difficult and costly process.

4.4.4 Leak Detection

Leak detection will be accomplished using standard leak detection practices. Prior to filling the coils helium can be used as a tracer gas. For nitrogen components helium can be used as necessary.

Once the cryogenics system has been in operation alternate gasses will be routinely used. Alternate gasses are an excellent method to regain leak detection sensitivity when the helium background is too high. Possible confusion can also result when there are simultaneous leaks with nitrogen and helium sources. Residual Gas Analyzers (RGA) will be used to distinguish leak origins, whether air, nitrogen or helium.

5. MAINTENANCE

5.1 Failure Modes, Effects, and Criticality Analysis (FMECA)

Potential failures in the PF coils and coil components have been identified and assessed. The methodology and results are documented in the FMECA Report[14] 14-950705-WEC-HCalvin-01.

- A SEVERITY CLASSIFICATION is assigned to each failure mode according to its effect on the system or major components. The failure mode SEVERITY CLASSIFICATIONS are defined as follows:

Category	Classification	Description
I	Catastrophic	A failure that may cause death, fatal cryogenic exposure or loss of TPX., i.e. damaged beyond repair.
II	Critical	A failure that may cause severe injury, major TPX or site damage that will result in TPX downtime of approximately one year or greater.
III	Marginal	A failure that may cause minor injury, minor TPX or site damage that will/may result in system downtime of approximately a month

Category	Classification	Description
		or more and/or limit TPX functions.
IV	Minor	A failure that is not serious enough to cause injury, or TPX or site damage, but will result in system downtime (at convenience) or have a minor impact on TPX functions.
V	No Effect	A failure that has no impact on TPX operation and does not result in downtime.

The purpose of the Criticality Analysis (CA) is to rank each potential failure mode according to the combined influence of the severity classification and it PROBABILITY OF OCCURRENCE. The qualitative CA approach in accordance with MIL-STD-1629 was undertaken since specific failure rate data and failure probabilities were not available for most of the subsystems or components.

- The PROBABILITY OF OCCURRENCE of the failure mode during the operating time interval of ten years is qualitatively estimated as follows:

  Level A - Frequent. A high probability of occurrence during the item operating time interval; equivalent to a single failure mode probability greater than 0.01.

  Level B - Reasonably Probable. A moderate probability of occurrence during the item operating time interval; equivalent to a single failure mode probability greater than 0.001 but less than 0.01 during the item operating time interval.

  Level C - Occasional. An occasional probability of occurrence during the item operating time interval; equivalent to a single failure mode probability greater than 0.0001 but less than 0.001 during the item operating time interval.

  Level D - Remote. A remote probability of occurrence during the item operating time interval; equivalent to a single failure mode probability greater than 0.00001 but less than 0.0001 during the item operating time interval.

  Level E - Extremely Unlikely. An extremely unlikely probability of occurrence during the item operating time interval (essentially zero); equivalent to a single failure mode probability less than 0.00001 during the item operating time interval.

The most significant FMECA findings are those failure modes which are classified as catastrophic or critical (Categories I or II) and which have a "frequent" or "reasonably probable" probability of occurrence (Level A or B). There were no failure modes that fell into this category.

There were no Severity Category I failure modes. The Severity Category II failure modes are summarized in Table 37.

Table 37. Item Failure Modes with Severity Category II Effects.

Indenture Level	Description	Probability of Occurrence
A.x.1.1 / A.1.x.1.1 CICC.	Spontaneous normal zone propogation before attaining full field/current.	C
A.1.(1-4).1.2, A.(2-4).1.2 Insulation (Winding Pack)	Decrease in coil inductance resulting from layer-layer short	D
A.1.(1-4).1.2, A.(2-4).1.2 Insulation (Leads)	Fault due to short between leads resulting from insulation breakdown due to fatigue/stress cracking.	D
A.3.1.1.1.1 Plated SC Strand	RRR too low	D
A.3.1.1.3 Sheath	Leaks helium into cryostat	D
B.1.1-2 Quench detection voltage taps	Short-circuit across voltage tap pair	D
B.1.1-2 Quench detection voltage taps	Short-circuit of magnet double pancake by conventional voltage tap	D
B.1.1-2 Quench detection voltage taps	Short-circuit to ground	D
B.4 DAS	REAL Quench not interpreted as such	D
B.4 DAS	REAL Quench indication is not propagated to the protection system	D
C.1 VCL	Loss or reduction of helium flow	D
A.1.(1-4).1.2, A.(2-4).1.2 Insulation (Leads)	Power supply load changes due to terminal to terminal short circuit	E
A.3.1.1.1.1 Plated SC Strand	Poor plating: too rough or falls off	E

Indenture Level	Description	Probability of Occurrence
A.3.1.1.1 Cable	Reduced flow	E
A.3.1.1.3 Sheath	Blocked helium flow passage	E
A.3.1.1.3 Sheath	Conduit lacks mechanical strength	E
A.1.(1-4).1.5, A.(2-4).1.5 Joints	Low flow - blockage in CICC (near joint)	E
A.1.(1-4).1.5, A.(2-4).1.5 Joints	Low I_c	E

For each of these important failure modes listed in the table, we have developed mitigation plans that include inspection, design, test, and historical perspectives.

5.2 Scheduled Maintenance Activities

Minimal scheduled maintenance is envisioned at this time for the TPX PF magnet system. In general, it will probably be limited to bolt tightening on the PF5-7 structural supports, on the pre-load bolts on the central solenoid, and on the cooling-line and power-lead supports. The splice joints between each of the PF coils and the buswork may require repair or replacement.

The following items will require routine inspection:

1. The annular space between the nose of the TF coil and the central solenoid (CS). This area should be visually inspected to monitor movement of the TF coil and to ensure that there is no contact between the TF and CS stack.
2. The helium manifolds at the bottom of the central solenoid. These manifolds should be visually inspected to look for leaks and damage to the tubes, isolators, filters, insulation, and instrumentation.
3. The helium cooling lines to PF5-7. These lines should be inspected for leaks, damage to the tubes, isolators, filters, insulation, and instrumentation.
4. The joints between the coil conductor and the bus. The joint temperatures and voltage drops will be monitored, and the joint will be disassembled and/or replaced when it is suspected of malfunction.

5.3 Maintenance Equipment Lists

There is no special maintenance equipment required for the PF coils.

5.4 Remote Maintenance Category I and II Equipment Lists

There is no required remote maintenance for the PF coils themselves. The plan is to have the bolts and resistive joints between the PF coils and the TF structure disconnected without the requirement of radiation protection.

6. REFERENCES

6.1 Drawing Tree

The Drawing Tree for the Phase 1 PF Magnet System drawings is TPX-D-1431099.SHTBD.P00. There are TBD sheets.

6.2 Reference Documents

[1] TPX-SPEC-14-0001, Rev. 0, TPX PF Magnet System Specification, 28 July 1995.
[2] ITER Documentation Series No. 26, ITER Magnet System, IAEA, Vienna, 1990.
[3] The NET Team, "Concept definition and analysis of the NET Model Coils, N/R/0221/1/E, 22.1.1991
[4] M.M. Steeves et al, "Test results from the Nb3Sn US-Demonstration Poloidal Coil", CEC-ICMC Conf, Huntsville, AL, June 1991
[5] R. Hoard and D. Stevens "A Comparison of Fatigue Properties of Incoloy-908 and 316-LN Steels", Lawrence Livermore Nat. Lab., February 26, 1993
[6] ASME, "1986 ASME Boiler and Pressure Vessel Code", July 1, 1986
[7] J.W. Ekin " Thermal expansion of several Incoloy Alloys," Final Report, NIST, 1986
[8] I.S. Hwang, et al., "Mechanical Properties of Incoloy 908 - An update," paper BZ-8, ICMC, 1991
[9] R.L. Tobler, et al., "Long-crack Fatigue Thresholds and Short-crack Simulation at Liquid Helium Temperature," paper XX, ICMC, 1991
[10] National Bureau of Standards, "Materials for Superconducting Magnet Systems", 1982
[11] W. Reiersen, ed., "TPX General Requirements Document", Feb 2, 1993
[12] R. D. Pillsbury, Jr. and P. W. Wang, "Start-up Simulations for TPX," Internal Memorandum, Ref: 14-930222MIT
[13] TPX-PLAN-14-0001, The Integrated PF Magnet Plan, dated 18 September 1995.
[14] Failure Modes, Effects, and Criticality Analysis Report, TPX-14-950705-WEC-HCalvin-01.

DISCLAIMER

This document was prepared as an account of work sponsored by an agency of the United States Government. Neither the United States Government nor the University of California nor any of their employees, makes any warranty, express or implied, or assumes any legal liability or responsibility for the accuracy, completeness, or usefulness of any information, apparatus, product, or process disclosed, or represents that its use would not infringe privately owned rights. Reference herein to any specific commercial product, process, or service by trade name, trademark, manufacturer, or otherwise, does not necessarily constitute or imply its endorsement, recommendation, or favoring by the United States Government or the University of California. The views and opinions of authors expressed herein do not necessarily state or reflect those of the United States Government or the University of California, and shall not be used for advertising or product endorsement purposes.

This report has been reproduced
directly from the best available copy.

Available to DOE and DOE contractors from the
Office of Scientific and Technical Information
P.O. Box 62, Oak Ridge, TN 37831
Prices available from (615) 576-8401, FTS 626-8401

Available to the public from the
National Technical Information Service
U.S. Department of Commerce
5285 Port Royal Rd.,
Springfield, VA 22161

Work performed under the auspices of the U.S. Department of Energy by Lawrence Livermore National Laboratory under Contract W-7405-ENG-48.